

**TAILORING FLUORESCENT MOLECULES
FOR BIOLOGICAL APPLICATIONS**

by

Luke Daniel Lavis

**A dissertation submitted in partial fulfillment
of the requirements for the degree of**

**Doctor of Philosophy
(Chemistry)**

at the

UNIVERSITY OF WISCONSIN–MADISON

2008

A dissertation entitled

TAILORING FLUORESCENT MOLECULES FOR BIOLOGICAL APPLICATIONS

submitted to the Graduate School of the
University of Wisconsin-Madison
in partial fulfillment of the requirements for the
Degree of Doctor of Philosophy

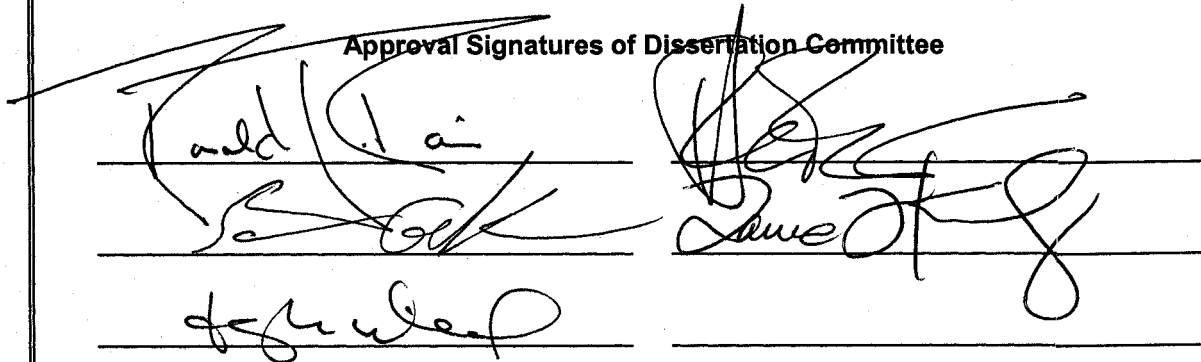
by

LUKE DANIEL LAVIS

Date of Final Oral Examination: January 15, 2008

Month & Year Degree to be awarded: **December** **May 2008** **August**

Approval Signatures of Dissertation Committee

The block contains three handwritten signatures of the Dissertation Committee members, each written over a horizontal line. The signatures are in cursive and appear to be 'L. Davis', 'J. Smith', and 'J. Wilson'.

Signature, Dean of Graduate School

The block contains a handwritten signature of the Dean of Graduate School, 'Martin Cadwallader/EH', written over a horizontal line.

TAILORING FLUORESCENT MOLECULES FOR BIOLOGICAL APPLICATIONS

Luke Daniel Lavis

Under the supervision of Professor Ronald T. Raines

At the University of Wisconsin–Madison

Fluorescent molecules are critical tools for biochemistry and biology. The utility of such probes is far reaching, spanning simple *in vitro* biochemical assays, to *in vivo* imaging. This dissertation describes research that involves building small-molecule probes to study biological processes by “tailoring” established fluorescent molecules through chemical synthesis. Chapter One is a survey of the small-molecule fluorophores used in bioresearch. The photophysical properties of a collection of commonly used fluorophores are described along with useful molecular probes built from these dye structures. This review highlights a key concept in the design of fluorophore-based tools for bioresearch—that of modularity.

Chapter Two is our initial foray into tailoring fluorescent molecules. We build on previous work in the Raines lab where a fluorophore is appended with the “trimethyl lock” moiety to create hyperstable enzyme substrates. In this effort we demonstrate that disparate classes of dyes can be masked using this strategy. Fluorophores with blue and red emission wavelengths are used to make esterase substrates that are useful *in vitro* and *in cellulo*.

Chapter Three also involves the creation of masked fluorophores using the trimethyl lock strategy. In this work we developed a “fluorogenic label” to investigate the

internalization of a cationic protein (bovine pancreatic ribonuclease) by cells. In contrast to a traditional fluorescent label, our fluorogenic label became fluorescent only upon cellular internalization of the conjugate. We utilized a monosubstituted urea-rhodamine dye as the core of our label. The urea substitution preserved fluorescence emission intensity, improved enzyme kinetics over a bis(trimethyl lock)rhodamine substrate, and facilitated synthesis of a reactive moiety for bioconjugation. This label allowed imaging of cells without intermediate washing steps, culminating in a continuous imaging of endocytosis.

Chapter Four describes the design and synthesis of another fluorogenic label. We envisioned using a non-native enzyme–substrate pair to visualize the endosomal escape of ribonucleases into the cytosol. As a first-generation approach, we sought to install bacterial β -galactosidase in the cytosol of cultured cells and label the ribonucleases with a complementary substrate. Synthesis of the desired fluorogenic label was accomplished using a reversible Diels–Alder reaction to protect the thiol-reactive maleimide group. Initial experiments showed encouraging results, demonstrating the use of a non-native substrate as a fluorogenic label holds promise as a useful tool in cell biology.

Chapter Five describes another strategy to prepare stable fluorogenic substrates. Here an acetoxymethyl (AM) ether serves as a surrogate for the typical acetate ester group in esterase substrates based on fluorescein and resorufin fluorophores. We explore different synthetic conditions to prepare such masked fluorophores and then test their properties *in vitro* and *in cellulo*.

Chapter Six deviates from the previous chapters. Instead of making fluorogenic enzyme substrates, here a fluorescent label is tailored to optimize a binding assay.

Previous work in the Raines lab described a binding assay based on a slight decrease in fluorescence intensity of a fluorescein-labeled ribonuclease variant upon binding to its cognate inhibitor protein *in vitro*. We determined this change is not due to a fluorescence quenching phenomenon, but is caused by a shift in the phenolic pK_a of the fluorescein label due to the change in environment. We then hypothesized that “tuning” the pK_a of fluorescein to a higher value could improve the dynamic range of the assay. Accordingly, we synthesized a diethylfluorescein derivative which gave a greater dynamic range in our assay, allowing miniaturization ultimately to a microplate format.

The final Chapter Seven details the future directions of these projects, and is followed by several appendices describing disparate peripheral projects, involving different aspects of fluorescence and tailoring fluorescent small-molecules. Overall, this work demonstrates the power of organic chemistry. Simple, sometimes antique, synthetic molecules are elaborated in a rational manner to produce new tools for illuminating biological systems.

ACKNOWLEDGEMENTS

The fingerprints of many individuals are on this dissertation. Most importantly, my wife, Kristina Lavis, has been a constant source of inspiration and support over my graduate career. I also acknowledge my current mentor, Ron Raines, for teaching me how to do good science and for giving me the freedom, resources, and encouragement to pursue some of my own ideas during my tenure in Madison. I am also grateful to Zhenjun “Jack” Diwu, my former mentor in industry and good friend for being an ever-available resource for questions regarding fluorescence.

It has been a pleasure to work closely with talented graduate students in Ron’s group and come away with publications. In particular, Tzu-Yuan “Cindy” Chao lent her microscopy expertise to several projects, and I am thankful for her diligence and tenacity in all our collaborative efforts. Jeremy Johnson was a great collaborator and our mutual respect and desire to do good science grew into a lasting friendship. Tom Rutkoski served as an invaluable sounding board for ideas, one of which grew into a joint paper, and another that became a (rejected) letter to the editor of the *New England Journal of Medicine*.

Good science is a collaborative effort and other partnerships with lab mates and other graduate students are either in progress or simply never realized. Together with Annie Tam and Matt Soellner, we thought up and tried a variety of interesting things—none of which worked. Greg Ellis elaborated the RI–ribonuclease binding assay, making a system that would function in a high-throughput screening format, and together we developed a red-shifted version of the assay. In collaboration with John Denu’s lab, Brian Smith and I

designed substrates for deacetylases and the synthesis of these compounds is underway. With Vanessa Kung, I prepared some novel HaloTag ligands that are being tested by Rex Watkins. Bryan Smith used the fluorescein–folate conjugates I prepared. Other people I have had the pleasure of collaborating with include Kim Dickson, Sunil Chandran, Christine Schilling, Jeet Kalia, Rebecca Turcotte, Margie Borra, and many other past and present graduate students and postdocs.

I am also grateful to the many other friends we have made here in Wisconsin both in and out of the lab. In particular, the “Anti-Faculty Lunch Group”: Laura Wysocki, Kris Kolonko, and Brian Smith have facilitated great discussions about our specific projects, organic chemistry, and science in general. My committee has also proven extremely helpful, especially Professors Sam Gellman and Laura Kiessling. I appreciate the support of the NIH Biotechnology Training Program, the helpful advice of its director Professor Tim Donahue, and the practical help of Beth Holden. My work was also sponsored by Genentech through an American Chemical Society Division of Organic Chemistry Fellowship, for which I am very grateful.

TABLE OF CONTENTS

Abstract.....	i
Acknowledgements.....	iv
Table of Contents.....	vi
List of Figures	xiv
List of Schemes.....	xvii
List of Tables	xix
List of Abbreviations	xx
Chapter 1	
Fluorescent Dyes: Tools for Biochemistry and Biology.....	1
Abstract.....	2
1.1 Introduction.....	3
1.2 Brief History	4
1.3 Overview of Fluorescence	5
1.4 Classes of Fluorescent Dyes	10
1.4.1 Endogenous Fluorophores	10
1.4.2 Polycyclic Aromatics	11
1.4.3 Coumarins	12
1.4.4 Quinolines	14
1.4.5 Indoles and Imidizoles	14
1.4.6 NBD	15

1.4.7 Other UV-Excited Fluorophores	15
1.4.8 Fluorescein	16
1.4.9 Rhodamine	18
1.4.10 Naphthoxanthene Dyes	20
1.4.11 Phenanthridines	21
1.4.12 BODIPY	21
1.4.13 Cyanines	22
1.4.14 Phthalocyanines	24
1.4.15 Oxazines	24
1.5 Conclusions	25
1.6 Acknowledgments	25

Chapter 2

Latent Blue and Red Fluorophores Based on the Trimethyl Lock	26
2.1 Introduction	27
2.2 Results and Discussion	28
2.2.1 Coumarin-Based Latent Fluorophore	28
2.2.2 Cresyl Violet-Based Latent Fluorophore	34
2.3 Conclusions	35
2.4 Acknowledgements	35
2.5 Experimental Section	39
2.5.1 General Experimental	39
2.5.2 Synthesis of Compounds 2.2 and 2.4	39

2.5.3 Fluorescence Spectroscopy	41
2.5.4 Cell Preparation and Imaging	42
2.4.5 NMR Spectra	43
 Chapter 3	
Fluorogenic Label for Biomolecular Imaging	47
Abstract	48
3.1 Introduction	49
3.2 Results and Discussion	51
3.2.1 Synthesis of Model Compounds	51
3.2.2 Fluorescence Properties of Model Compounds	51
3.2.3 Synthesis of Urea–Rhodamine Trimethyl Lock	58
3.2.4 Chemical Stability	58
3.2.5 Enzymatic Reactivity	62
3.2.6 Cellular Imaging	62
3.2.7 Fluorogenic Label	67
3.2.8 Bioconjugation	68
3.2.9 Cellular Imaging with a Bioconjugate	69
3.3 Envoi	75
3.4 Acknowledgments	76
3.5 Experimental Section	78
3.5.1 General Experimental: Chemical Synthesis	78
3.5.2 Synthesis of Compounds 3.1–3.6 and 3.8–3.13	79

3.5.3 General Spectroscopic Methods	87
3.5.4 Ultraviolet–Visible and Fluorescence Spectroscopy	88
3.5.5 Protein Purification and Labeling	88
3.5.6 Cell Preparation	89
3.5.7 Cell Imaging.....	90
3.5.8 NMR Spectra	91

Chapter 4

Fluorogenic Label Unmasked by β -Galactosidase	115
4.1 Introduction.....	116
4.2 Results and Discussion	118
4.2.1 Choice of Fluorogenic Label System.....	118
4.2.2 Synthesis of Fluorogenic Label	123
4.2.3 Bioconjugation.....	126
4.2.4 Cell Preparation and Preliminary Imaging	126
4.3 Conclusions.....	129
4.4 Acknowledgements.....	129
4.5 Experimental Section	130
4.5.1 Materials and Methods: Chemical Synthesis.....	130
4.5.2 Synthesis of Compounds 4.2 , 4.5 , and 4.7–4.9	131
4.5.3 Protein Conjugation	135
4.5.4 Cell Preparation	135
4.5.5 Cell Imaging.....	136

4.5.6 NMR Spectra and Analytical HPLC Chromatograms	137
---	-----

Chapter 5

Acetoxymethyl Ethers as Fluorophore Ester Surrogates	144
5.1 Introduction.....	145
5.2 Results and Discussion	149
5.2.1 Fluorescein-Based Profluorophores.....	149
5.2.2 Synthesis of Fluorescein AM Ethers.....	152
5.2.3 Chemical Stability of AM Ethers.....	156
5.2.4 Enzyme-Catalyzed Hydrolysis of AM Ethers.....	158
5.2.5 Cellular Imaging Studies.....	158
5.3 Conclusions.....	162
5.3.1 Optimizing Reaction Conditions for Fluorescein AM Ether Synthesis.....	162
5.3.2 Other Fluorophore AM Ethers	162
5.3.3 Envoi.....	164
5.4 Acknowledgements.....	168
5.5 Experimental Section	168
5.5.1 Materials and Methods: Chemical Synthesis.....	168
5.5.2 Synthesis of Compounds 5.5 , 5.6 , 5.8 , 5.10 , and 5.12	169
5.5.3 Materials and Methods: Biochemistry	173
5.5.4 Cell Preparation and Imaging	174
5.5.5 NMR Spectra	175

Chapter 6

Tuning the pK_a of Fluorescein to Optimize Binding Assays	185
Abstract	186
6.1 Introduction	187
6.2 Results and Discussion	192
6.2.1 pK_a Values of Bound and Free Fluorescein-Labeled RNase A	192
6.2.2 Design and Synthesis of 2',7'-Diethylfluorescein	196
6.2.3 Spectral Properties of 2',7'-Diethylfluorescein	197
6.2.4 Synthesis of 2',7'-Diethylfluorescein-5-iodoacetamide (DEFIA)	203
6.2.5 pK_a Values of Free and RI-Bound DEF-Labeled A19C/G88R RNase A	206
6.2.6 Assay Comparison	206
6.2.7 Microplate-Based Determination of K_d Values	207
6.3 Conclusions	213
6.4 Acknowledgments	213
6.5 Experimental Section	214
6.5.1 General Experimental: Chemical Synthesis	214
6.5.2 Synthesis of Compounds 6.6 , 6.7 , and 6.10–6.14	215
6.5.3 General Experimental: Biochemistry and Spectroscopy	221
6.5.4 Preparation of Ribonuclease Inhibitor and Labeled Ribonucleases	222
6.5.5 UV–Visible and Fluorescence Spectroscopy	222
6.5.6 Determination of pK_a Values	223
6.5.7 Spectral Properties of Free Dyes	224
6.5.8 Assay Comparison and Z' -factor Determination	225

6.5.9 Determination of K_d Values	226
6.5.10 NMR Spectra and HPLC Chromatograms.....	228
 Chapter 7	
Future Directions	243
7.1 Latent Fluorophores Based on the Trimethyl Lock	244
7.2 Bioorthogonal Fluorogenic Labels	245
7.3 Fluorophore Acetoxymethyl (AM) Ethers.....	246
7.4 Tuning the pK_a of Fluorophore Labels	247
 Appendix A	
Fluorogenic Histone Deacetylase Substrates with Improved Specificity	248
A.1 Introduction	249
A.2 Results and Discussion.....	253
A.3 Conclusions and Future Directions	253
A.4 Acknowledgements	254
A.5 Experimental Section	256
A.5.1 General Experimental	256
A.5.2 Synthesis of compounds A.8–A.13	257
A.5.3 NMR Spectra.....	261
 Appendix B	
Light-Controlled Staudinger Ligation.....	267

	xiii
B.1 Introduction	268
B.2 Results and Discussion.....	272
B.3 Conclusions and Future Directions	276
B.4 Acknowledgements	277
B.5 Experimental Section	279
B.5.1 General Experimental.....	279
B.5.2 Photoinduced Oxidation Experiments.....	279
Appendix C	
Letter to the Editor of the New England Journal of Medicine.....	280
Letter to the Editor	281
References.....	284

LIST OF FIGURES

Figure 1.1	Jablonski diagram	7
Figure 1.2	Fluorophore brightness vs. absorption maxima	8
Figure 2.1	Normalized fluorescent excitation–emission spectra of profluorophore 2.2 and AMC.....	31
Figure 2.2	Kinetic traces and Michaelis–Menten plots for the hydrolysis of profluorophores 2.2 and 2.4	32
Figure 2.3	Stability of profluorophore 2.2 and methylumbelliferyl acetate 2.3	33
Figure 2.4	Unwashed mammalian cells incubated with profluorophore 2.4	37
Figure 2.5	Modules in trimethyl lock latent fluorophores.....	38
Figure 3.1	Spectra of Rh ₁₁₀ and its derivatives	55
Figure 3.2	Effect of pH on the fluorescence of Rh ₁₁₀ , urea 3.1 , and amide 3.2	56
Figure 3.3	Hammett plot	57
Figure 3.4	Stability of profluorophore 3.8 and fluorescein diacetate in aqueous solution.....	61
Figure 3.5	Kinetic traces and Michaelis–Menten plot for the hydrolysis of profluorophore 3.8	64
Figure 3.6	Unmasking of profluorophore 3.8 in live human cells	65
Figure 3.7	Unwashed HeLa cells incubated with diurea 3.3	66
Figure 3.8	Live-cell imaging experiments with protein conjugates.....	72

Figure 3.9	Antibody counterstaining experiments	74
Figure 4.1	Pathway of cytotoxic ribonucleases	121
Figure 4.2	Imaging of transfected HeLa cells incubated with RNase conjugate	128
Figure 5.1	Time course of the generation of fluorescence of esterase substrates	157
Figure 5.2	Kinetic traces and Michaelis–Menten plot for the hydrolysis of esterase substrates by PLE.....	160
Figure 5.3	HeLa cells incubated with esterase substrates 5.2 , 5.5 , and 5.6	161
Figure 5.4	Live cell imaging experiments with profluorophores 5.5 and 5.8	166
Figure 5.5	Live cell imaging experiments with profluorophores 5.10 and 5.12	167
Figure 6.1	Effect of pH on the fluorescence of fluorophore-labeled RNase A in the absence or presence of RI	195
Figure 6.2	pH-Dependence of the fluorescence of fluorescein and 2',7'- diethylfluorescein.....	201
Figure 6.3	Normalized absorption and emission spectra of fluorescein and 2',7'- diethylfluorescein.....	202
Figure 6.4	Comparison of the fluorescence change of FI–RNase and DEF–RNase upon addition of RI	209
Figure 6.5	<i>Z'</i> -factor determination	210
Figure 6.6	Data from microplate assays for determination of the K_d values of RI-ribonuclease complexes	211

Figure A.1	Fluorescent histone deacetylase assay	251
Figure A.2	Disparate histone deacetylase mechanisms	252
Figure B.1	Proposed mechanism for oxidation of phosphinothiol B.2	271
Figure B.2	Photoinduced oxidation experiments.....	275
Figure B.3	Proposed photopatterning via light-induced oxidation.....	278
Figure C.1	Fluorescence of solutions under long-wave UV illumination	282
Figure C.2	Response to letter to the editor submission.....	283

LIST OF SCHEMES

Scheme 2.1	Route for the synthesis of profluorophore 2.2 , and the chemical structure of 4-methylumbelliferyl acetate (2.3)	30
Scheme 2.2	Route for the synthesis of profluorophore 2.4	36
Scheme 3.1	Synthetic route to profluorophore 3.8	60
Scheme 3.2	Synthetic route to fluorogenic label 3.13	71
Scheme 3.3	Modules in fluorogenic label 3.13	77
Scheme 4.1	Structures of FDG (4.1) and fluorogenic label 4.2	122
Scheme 4.2	Synthesis of fluorogenic label 4.2	125
Scheme 5.1	Unmasking of acetoxymethyl groups by esterase.....	148
Scheme 5.2	Equilibrium forms of fluorescein (5.1) and the structure of fluorescein diacetate (5.2).....	151
Scheme 5.3	Synthesis of AM ether profluorophores 5.5 and 5.6	155
Scheme 5.4	Syntheses of acetoxymethyl ether substrates based on Tokyo Green and resorufin	165
Scheme 6.1	Prototropic forms of fluorescein and corresponding photophysical values..	189
Scheme 6.2	Synthesis of 2',7'-diethylfluorescein	199

Scheme 6.3	Synthesis of 2',7'-diethylfluorescein-5-iodoacetamide (DEFIA).....	205
Scheme A.1	Synthesis of intermediates A.8–13	255
Scheme B.1	The Raines–Kiessling–Staudinger ligation.....	269
Scheme B.2	Attempted synthesis of fluorescein–phosphinothioester B.2.....	270
Scheme B.3	Photoinduced oxidation experiments.....	274

LIST OF TABLES

Table 1.1	Photophysical properties of fluorophores 1.1–1.30	9
Table 3.1	Spectroscopic properties of Rh₁₁₀ and its derivatives	54
Table 6.1	Spectroscopic parameters of fluorescein and DEF	200
Table 6.2	Values of K_d for RI-ribonuclease complexes	212

LIST OF ABBREVIATIONS

Ala (A)	alanine
AM	acetoxymethyl
AMC	7-amino-4-methylcoumarin
Arg (R)	arginine
Asp (D)	aspartic acid
Asn (N)	asparagine
AU	arbitrary units
BCA	bicinchoninic acid
BHT	butylated hydroxytoluene
Boc (<i>t</i> -Boc)	<i>tert</i> -butoxycarbonyl
BODIPY	boron difluoride dipyrromethene
BSA	bovine serum albumin
CHO	Chinese hamster ovary
Cys (C)	cysteine
CV	cresyl violet
DABCO	1,4-diazabicyclo[2.2.2]octane
DAPI	4',6-diamidino-2-phenylindole
DEF	2',7'-diethylfluorescein
DEFIA	2',7'-diethylfluorescein-5-iodoacetamide
DFFDA	2',7'-difluorofluorescein diacetate
DIPEA	diisopropylethylamine (Hünig's base)

DMAP	4-dimethylaminopyridine
DMEM	Dulbecco's modified Eagle's medium
DMF	<i>N,N</i> -dimethylformamide
DMSO	dimethylsulfoxide
DNA	deoxyribonucleic acid
DPBS	Dulbecco's phosphate-buffered saline
DTNB	5,5'-dithiobis(2-nitrobenzoic acid)
DTT	dithiothreitol
EDANS	5-((2-aminoethyl)amino)naphthalene-1-sulfonic acid
EDC	1-ethyl-3-(3-dimethylaminopropyl)carbodiimide hydrochloride
EDPP	ethyldiphenylphosphine
EDTA	ethylenediaminetetraacetic acid
ELISA	enzyme-linked immunosorbent assay
ESIMS	electrospray ionization mass spectrometry
EtOAc	ethyl acetate
5-FAM SE	5-carboxyfluorescein succinimidyl ester
FBS	fetal bovine serum
FDA	fluorescein diacetate
FDG	fluorescein di- β -D-galactopyranoside
FDP	fluorescein diphosphate
FTTC	fluorescein isothiocyanate
FMN	flavin mononucleotide
Fmoc	9-fluorenylmethoxycarbonyl

FP	fluorescence polarization
FRET	Förster (fluorescence) resonance energy transfer
Gly (G)	glycine
GSH	glutathione (reduced)
GSSG	glutathione (oxidized)
HDAC	histone deacetylase
HeNe	helium–neon
HEPES	2[4-(2-hydroxyethyl)-1-piperazinyl]ethanesulfonic acid
HPLC	high performance (pressure) liquid chromatography
HRMS	high-resolution mass spectrometry
HTS	high-throughput screening
ITC	intersystem crossing
λ_{max}	absorption or excitation maximum
λ_{em}	emission maximum
Lys (K)	lysine
MALDI	matrix-assisted laser desorption ionization
MES	2-(<i>N</i> -morpholino)ethanesulfonic acid
MOPS	3-(<i>N</i> -morpholino)propanesulfonic acid
mRFP	monomeric red fluorescent protein
MS	molecular sieves
4-MU	4-methylumbelliferone
NAD ⁺	nicotinamide adenine dinucleotide (oxidized form)
NADH	nicotinamide adenine dinucleotide (reduced form)

NBD	7-nitrobenz-2-oxa-1,3-diazole
NBS	non-binding surface
NHS	<i>N</i> -hydroxysuccinimide
NMR	nuclear magnetic resonance
$^1\text{O}_2$	singlet molecular oxygen
$^3\text{O}_2$	triplet molecular oxygen
OD	optical density
PBS	phosphate-buffered saline
PeT	photoinduced electron transfer
Phe (F)	phenylalanine
PLE	porcine (pig) liver esterase
Pro (P)	proline
Rh ₁₁₀	rhodamine 110
R6G	rhodamine 6G
RI	ribonuclease inhibitor protein
RNA	ribonucleic acid
RNase A	bovine pancreatic ribonuclease (ribonuclease A)
RT	room temperature
S ₀	singlet ground state
S ₁	singlet first-excited state
S ₂	singlet second-excited state
SNARF	seminaphtharhodafluor
SNAFL	seminaphthofluorescein

SRh ₁₀₁	sulforhodamine 101
T ₁	triplet first-excited state
TCEP	<i>tris</i> -(2-carboxyethyl)phosphine
TFA	trifluoroacetic acid
THF	tetrahydrofuran
TLC	thin-layer chromatography
TML	trimethyl lock
TMR	tetramethylrhodamine
TNB	5-thio-2-nitrobenzoic acid
TRIS	<i>tris</i> -(hydroxymethyl)aminomethane
UV	ultraviolet

CHAPTER 1*

FLUORESCENT DYES: TOOLS FOR BIOCHEMISTRY AND BIOLOGY

Contribution: Composition of entire manuscript, including collection and organization of references, writing text, and preparing figure drafts.

***This chapter will be published, in part, as an invited review. Reference: Lavis, L. D., and Raines, R. T. (2008). Bright ideas for chemical biology. *ACS Chem. Biol.* in press.**

Abstract: Small-molecule fluorescent probes embody an essential facet of chemical biology. Although numerous compounds are known, the ensemble of fluorescent probes is based on a modest collection of modular “core” dyes. The elaboration of these dyes with diverse chemical moieties is enabling the precise interrogation of biochemical and biological systems. The importance of fluorescence-based technologies in chemical biology elicits a necessity to understand the major classes of small-molecule fluorophores. Here, we examine the chemical and photophysical properties of oft-used fluorophores, and highlight classic and contemporary examples in which utility has been built upon these scaffolds.

1.1 Introduction

Small-molecule fluorescent molecules are indispensable tools for chemical biology, being ubiquitous as biomolecular labels, enzyme substrates, environmental indicators, and cellular staining agents (Petit *et al.*, 1993; Johnson, 1998; Boonacker and Van Noorden, 2001; Valeur, 2002; Zhang *et al.*, 2002; Frangioni, 2003; Goddard and Reymond, 2004a; Giepmans *et al.*, 2006; Lakowicz, 2006; Waggoner, 2006; Johnsson and Johnsson, 2007; Sadaghiani *et al.*, 2007). Choosing a suitable probe to visualize a biochemical or biological process can be daunting, given the countless molecules available either commercially (Haugland *et al.*, 2005) or through *de novo* design and synthesis. Fortunately, the plethora of fluorescent probes has an inherent modularity. Attachment of various reactive groups, substrate moieties, chelating components, and other chemical entities to a small number of “core” fluorophores gives rise to the ensemble of extant probes. Overall, these core fluorophores are well-established (Giepmans *et al.*, 2006; Waggoner, 2006), consisting of molecules with excellent spectral characteristics, high photo- and chemical stabilities, as well as facile syntheses. Probe selection and design can, therefore, be simplified by understanding the properties of these foundational fluorescent compounds.

In this review, we trek along the electromagnetic spectrum and discuss the properties of the main classes of fluorescent molecules used in bioresearch. We also give examples of tools constructed from these fluorophores. We believe comprehension of the strengths, weaknesses, and common uses of each dye class will equip the chemical biologist for expeditions to reveal new biochemical and biological phenomena.

1.2 Brief History

The first well-defined small-molecule fluorophore was the natural product quinine (**1.1**), an important compound for both medicinal and organic chemistry (Kaufman and Rúveda, 2005). The visible emission from an aqueous quinine solution was reported by Herschel in 1845 (Herschel, 1845). Stokes showed this phenomenon was due to absorption of light by quinine followed by emission, and coined the term “fluorescence” to describe this process (Stokes, 1852). The importance of quinine as an antimalarial would later lead to an attempted synthesis by Perkin, starting from aniline derivatives. Of course, the total synthesis of quinine would tarry for many decades, realized in essence by Woodward and Doering, and in practice by Stork (Seeman, 2007). Instead, Perkin’s fated synthetic route produced the first synthetic textile dye, mauvine, in 1865. Perkin’s success in the commercialization of mauvine and other “aniline dyes” is often considered to be the birth of the modern chemical industry (Garfield, 2001; Kaufman and Rúveda, 2005). This achievement foreshadowed the discovery of many useful dye molecules, fluorescent and otherwise (Christie, 2001). These colored synthetic molecules were fodder for new biological experiments, and many found diagnostic or even clinical utility (Wainwright, 2003).

The intrinsic fluorescence of quinine (**1.1**) also motivated the development of the fluorometer, which was needed to prepare antimalarial drug cocktails during World War II (Lakowicz, 2006). The commercialization of such instrumentation in the 1950’s allowed increased use of fluorescence-based bioanalytical techniques (Udenfriend, 1995). In the 1960’s, the advent of the dye laser spurred much interest in the synthesis of novel or improved fluorescent molecules with desirable photophysical properties (Drexhage,

1977). Indeed, many fluorophores used in bioresearch today can trace their lineage back to laser dyes.

1.3 Overview of Fluorescence

The process of fluorescence is illustrated in the Jablonski diagram shown in Figure 1.1 (Lakowicz, 2006). Although this review is focused on single-photon excitation processes, multiphoton excitation is also an important and vibrant field (Svoboda and Yasuda, 2006). The fluorescence process begins when a molecule in a singlet electronic ground state (S_0) absorbs a photon of suitable energy. This promotes an electron to higher energy orbitals, which relaxes quickly to the first singlet excited state (S_1). The decay of the excited state can occur with photon emission (*i.e.*, fluorescence) or in a non-radiative (NR) fashion. This non-radiative “quenching” of the fluorophore excited state can occur through one of a variety of processes, including bond rotation or vibration, molecular collision (Zelent *et al.*, 1998), and photoinduced electron transfer (PeT) (de Silva *et al.*, 1997). The excited state can also undergo forbidden intersystem crossing (ITC) to the triplet excited state (T_1) and subsequent relaxation either by photon emission (*i.e.*, phosphorescence) or NR decay. ITC efficiency is increased by substitution with, or proximity to, atoms with high atomic number due to spin-orbit coupling—a phenomenon commonly termed the “heavy atom effect” (McGlynn *et al.*, 1963). Another important pathway for decay of the singlet excited state involves Förster resonance energy transfer (FRET) to an acceptor molecule. This process is distance dependent, and can be used as a “spectroscopic ruler” to measure the proximity of labeled entities (Sapsford *et al.*, 2006).

There are several attributes that are critical for evaluating a fluorophore. The maximal absorption (λ_{max}) is related to the energy difference between the S_0 and the higher energy levels. The absorptivity of a molecule at λ_{max} is given by the extinction coefficient (ϵ), defined by the Beer–Lambert–Bouguer law. The maximal emission wavelength (λ_{em}) is longer (*i.e.*, lower in energy) than λ_{max} due to energy losses by solvent reorganization or other processes (Valeur, 2002). Stokes demonstrated this phenomenon by using a rudimentary filter set consisting of a stained glass window and a goblet of wine (Stokes, 1852). The difference between λ_{max} and λ_{em} is therefore termed the “Stokes shift”. Fluorophores with small Stokes shifts are susceptible to self-quenching via energy transfer, therefore limiting the number of labels that can be attached to a biomolecule (Hemmilä, 1991). The lifetime of the excited state (τ) can range from 0.1 to >100 ns, and is an important parameter for time-resolved measurements (Bright and Munson, 2003) and fluorescence polarization applications (Owicki, 2000). Another critical property of a fluorophore is the quantum yield or quantum efficiency (Φ)—essentially the ratio of photons fluoresced to those absorbed.

The product of the extinction coefficient and the quantum yield ($\epsilon \times \Phi$) is a highly useful parameter for comparing different fluorescent molecules. This term is directly proportional to the brightness of the dye, accounting for both the amount of light absorbed and the quantum efficiency of the fluorophore. Accurate comparisons between dye molecules must include both these parameters. Figure 1.2 plots the major classes of biologically significant fluorescent dyes as $\epsilon \times \Phi$ against λ_{max} . A more detailed table of the properties of these fluorophores can be found in Table 1.1.

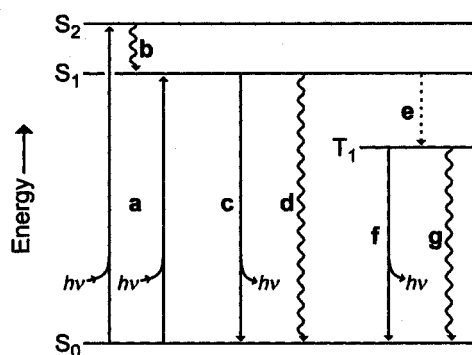


Figure 1.1 Jablonski diagram. (a) Absorption of a photon gives an excited state. (b) Internal conversion to S_1 . (c) Fluorescence. (d) Non-radiative decay. (e) Intersystem crossing to T_1 . (f) Phosphorescence. (g) Non-radiative decay.

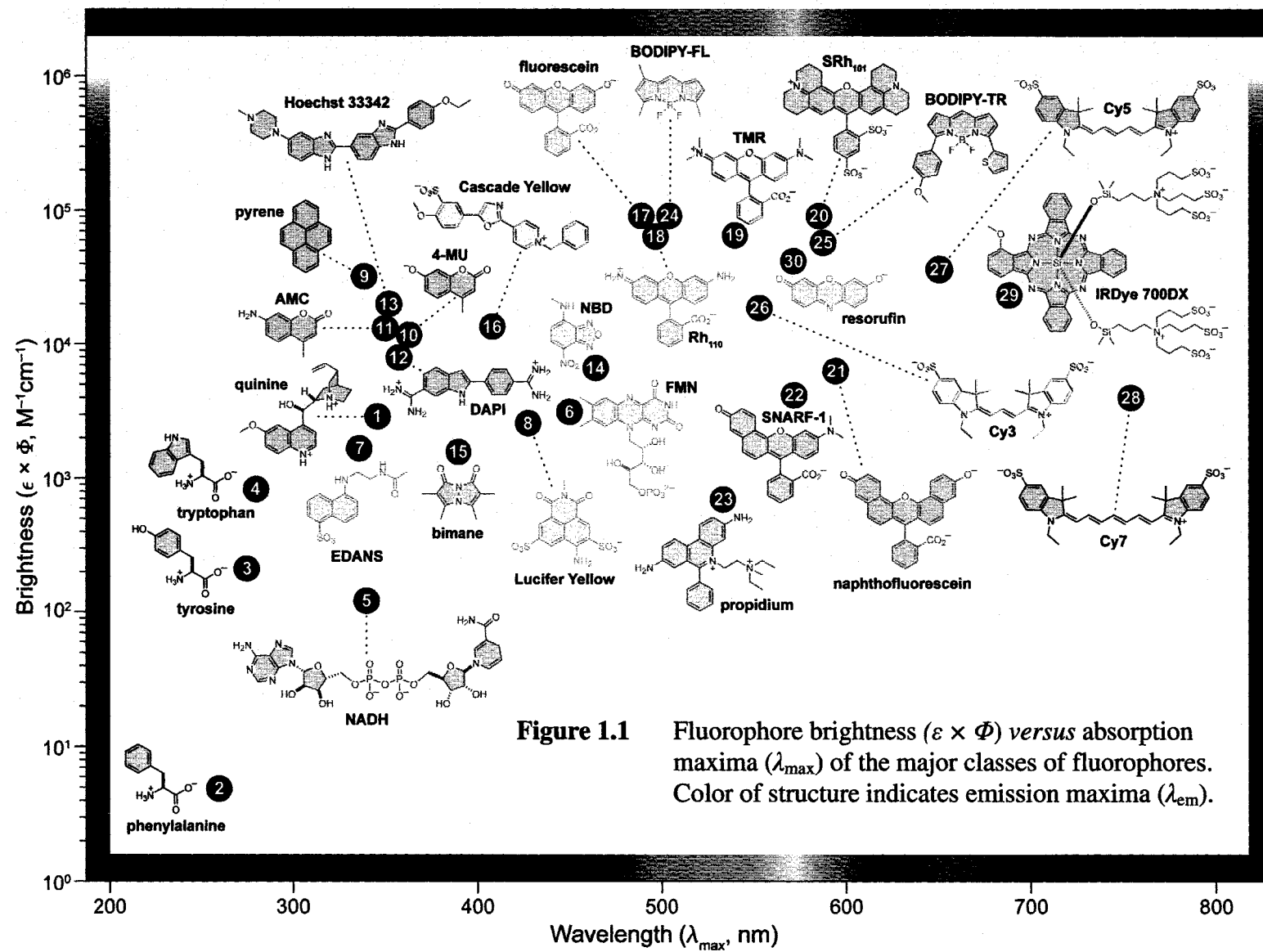


Table 1.1 Photophysical properties of fluorophores 1.1–1.30

Fluorophore	Solvent	λ_{max} (nm)	ϵ ($\text{M}^{-1}\text{cm}^{-1}$)	λ_{em} (nm)	Φ	$\epsilon \times \Phi$ ($\text{M}^{-1}\text{cm}^{-1}$)	Reference
quinine 1.1	pH 2	347	5 400	448	0.55	3 000	(Schulman <i>et al.</i> , 1974)
phenylalanine 1.2	H ₂ O	260	200	282	0.024	5	(Wolfbeis, 1985; Lakowicz, 2006)
tyrosine 1.3	H ₂ O	275	1 500	303	0.14	210	(Wolfbeis, 1985; Lakowicz, 2006)
tryptophan 1.4	H ₂ O	280	6 300	348	0.13	820	(Wolfbeis, 1985; Lakowicz, 2006)
NADH 1.5	H ₂ O	340	6 200	435	0.019	120	(Horecker and Kornberg, 1948; Wolfbeis, 1985)
FMN 1.6	H ₂ O	450	12 200	530	0.25	3 100	(Whitby, 1953; Wolfbeis, 1985)
EDANS 1.7	H ₂ O	336	6 100	520	0.27	1 600	(Hudson and Weber, 1973)
Lucifer Yellow 1.8	H ₂ O	428	12 300	535	0.21	2 600	(Stewart, 1981)
pyrene 1.9	MeOH	340	43 000	376	0.75	32 000	(Karpovich and Blanchard, 1995; Haugland <i>et al.</i> , 2005)
4-MU 1.10	pH 10	360	17 000	450	0.63	11 000	(Sun <i>et al.</i> , 1998)
AMC 1.11	MeOH	351	18 000	430	0.75	14 000	(Johnson, 1998)
DAPI 1.12	H ₂ O/DNA	358	21 000	461	0.34	7 100	(Cosa <i>et al.</i> , 2001; Haugland <i>et al.</i> , 2005)
Hoechst 33342 1.13	H ₂ O/DNA	350	45 000	461	0.38	17 000	(Cosa <i>et al.</i> , 2001; Haugland <i>et al.</i> , 2005)
NBD 1.14	MeOH	465	22 000	535	0.3	7 000	(Haugland <i>et al.</i> , 2005)
bimane 1.15	pH 7.4	390	5 300	482	0.3	2 000	(Kosower <i>et al.</i> , 1979)
Cascade Yellow 1.16	MeOH	409	24 000	558	0.56	13 000	(Anderson <i>et al.</i> , 1998; Haugland <i>et al.</i> , 2005)
fluorescein 1.17	pH 9	490	93 000	514	0.95	88 000	(Haugland <i>et al.</i> , 2005; Lakowicz, 2006)
Rh ₁₁₀ 1.18	pH 7.5	496	74 000	517	0.92	68 000	(Lavis <i>et al.</i> , 2006a)
TMR 1.19	MeOH	540	95 000	565	0.68	65 000	(Johnson, 1998)
SRh ₁₀₁ 1.20	pH 7	586	108 000	605	0.77	83 000	(Johnson, 1998; Haugland <i>et al.</i> , 2005)
naphthofluorescein 1.21	pH 9.5	595	44 000	660	0.14	6 200	(Lee <i>et al.</i> , 1989b)
SNARF-1 1.22	pH 10	573	44 000	631	0.092	4 100	(Whitaker <i>et al.</i> , 1991b)
propidium 1.23	H ₂ O/DNA	535	5 400	617	0.13	700	(Cosa <i>et al.</i> , 2001; Haugland <i>et al.</i> , 2005)
BODIPY-FL 1.24	MeOH	505	91 000	511	0.94	86 000	(Johnson, 1998)
BODIPY-TR 1.25	MeOH	588	68 000	616	0.84	57 000	(Johnson, 1998)
Cy3 1.26	pH 7	554	130 000	568	0.14	18 000	(Waggoner and Kenneth, 1995)
Cy5 1.27	pH 7	652	200 000	672	0.18	36 000	(Waggoner and Kenneth, 1995)
Cy7 1.28	pH 7	755	200 000	778	0.02	4 000	(Waggoner and Kenneth, 1995)
IRDye 700DX 1.29	H ₂ O	689	165 000	700	0.14	23 000	(Peng <i>et al.</i> , 2006)
resorufin 1.30	pH 9.5	572	56 000	585	0.74	41 000	(Bueno <i>et al.</i> , 2002)

1.4 Classes of Fluorescent Dyes

1.4.1 Endogenous Fluorophores

Like quinine (**1.1**), many naturally occurring compounds exhibit measurable fluorescence (Wolfbeis, 1985). These include the aromatic amino acids, whose fluorescence properties were first described by Weber (Teale and Weber, 1957). Phenylalanine (**1.2**) and tyrosine (**1.3**) exhibit weak fluorescence under UV excitation wavelengths. Tryptophan (**1.4**) is the most fluorescent natural amino acid, with a λ_{max} of 280 nm, λ_{em} of 353 nm, extinction coefficient of $5.6 \times 10^3 \text{ M}^{-1}\text{cm}^{-1}$, and a quantum yield of 0.13 (Demchenko, 1986). Tryptophan fluorescence is environmentally-sensitive and has been used as an index for a variety of processes, including protein folding and ligand binding (Beechem and Brand, 1985). Tryptophan can also be used in FRET applications (Sapsford *et al.*, 2006), or serve as a quencher for a variety of fluorophores by PeT (Marmé *et al.*, 2004).

Other naturally-occurring fluorophores include reduced nicotinamide cofactors (*e.g.*, NADH; **1.5**) that show measurable fluorescence with $\lambda_{\text{max}}/\lambda_{\text{em}} = 340/435 \text{ nm}$ (Weber, 1957). Flavins are also very important intrinsic fluorophores, with flavin mononucleotide (FMN; **1.6**) showing significant fluorescence with $\lambda_{\text{max}} = 450 \text{ nm}$, $\lambda_{\text{em}} = 540 \text{ nm}$, $\epsilon = 1.25 \times 10^4 \text{ M}^{-1}\text{cm}^{-1}$, and $\Phi = 0.25$ (Whitby, 1953; Wolfbeis, 1985). Other native moieties are fluorescent, including porphyrins and pyridoxal derivatives (Wolfbeis, 1985). Collectively, endogenous fluorophores can give rise to “autofluorescence”, which can obfuscate desired signals from labeled entities in imaging and other *in cellulo* or *in vivo* experiments (Aubin, 1979). Red-shifted dyes can circumvent this background problem, while allowing deeper tissue penetration (Ballou *et al.*, 2005). Long-wavelength

excitation is also gentle to DNA, as nucleobase moieties absorb at $\lambda_{\text{max}} \approx 260$ nm with $\epsilon \approx 7\text{--}15 \times 10^3 \text{ M}^{-1}\text{cm}^{-1}$ (Cavaluzzi and Borer, 2004).

1.4.2 Polycyclic Aromatics

Polycyclic aromatic compounds are a widely-used subset of fluorescent dyes. In general, spectral properties correlate to size, and substitution on the abundant open valencies affords a variety of useful probes. A classic category of synthetic biomolecule labels are naphthalene derivatives. These include the amine-reactive 5-dimethylaminonaphthalene-1-sulfonyl (dansyl) chloride (Weber, 1952), and other associated fluorophores (Daniel and Weber, 1966; Weber and Farris, 1979). Another related naphthalene derivative is 5-((2-aminoethyl)amino)naphthalene-1-sulfonic acid (EDANS). Derivatives of this fluorophore, such as compound **1.7**, exhibit a λ_{max} of 336 nm, λ_{em} of 520 nm, extinction coefficient of $6.1 \times 10^3 \text{ M}^{-1}\text{cm}^{-1}$, and a quantum yield of 0.27 in water (Hudson and Weber, 1973). This label remains in wide use, particularly in FRET-based experiments (Maggiora *et al.*, 1992; Tyagi and Kramer, 1996). Naphthalene can be further elaborated to give 4-amino-3,6-disulfonylnaphthalimides (*e.g.*, compound **1.8**) that absorb at 428 nm (Stewart, 1981). These fluorophores bear the moniker “Lucifer Yellow”, and are useful polar tracers that can be loaded into cells for long-term tracking and other experiments (Haugland *et al.*, 2005).

Pyrene-derived molecules also find use as probes. Derivatives of pyrene (**1.9**) show $\lambda_{\text{max}}/\lambda_{\text{em}}$ of 340/376 nm, $\epsilon = 4.3 \times 10^4 \text{ M}^{-1}\text{cm}^{-1}$, and $\Phi = 0.53$ (Dawson and Windsor, 1968; Haugland *et al.*, 2005). The environmental sensitivity of this fluorophore can be used to report on RNA folding (Smalley and Silverman, 2006). Pyrene also exhibits a

long-lived excited state ($\tau > 100$ ns). This long lifetime allows an excited pyrene molecule to associate with a pyrene in the ground state. The resulting excimer exhibits a bathochromic (*i.e.*, red) shift in fluorescence intensity ($\lambda_{\text{em}} \approx 490$ nm). This process can be used to measure important biomolecular processes, such as protein conformation (Sahoo *et al.*, 2000). Sulfonation of pyrene elicits a bathochromic shift, affording useful compounds that are excited at > 390 nm. These compounds include the pH probe 8-hydroxy-1,3,6-pyrenetrisulfonate (HPTS or pyranine) (Kano and Fendler, 1978), and useful sulfonated pyrene labels with good water solubility (Whitaker *et al.*, 1991a; Haugland *et al.*, 2005).

Other polycyclic aromatic molecules are also sometimes used to construct fluorescent tools. Anthracene has been elaborated to prepare sensors for anions such as pyrophosphate (Gunnlaugsson *et al.*, 2006). Perylene derivatives constitute another intriguing class of fluorophores that exhibit very high quantum yields in organic solvents (Süßmeier and Langhals, 2001), but require significant structural elaboration to become useful in water (Kohl *et al.*, 2004). Still another functional scaffold is coronene, which exhibits a long lifetime ($\tau \approx 200$ ns) that is useful in some time-resolved experiments (Davenport *et al.*, 2001).

1.4.3 Coumarins

Coumarins represent a broad class of natural products, pharmaceuticals, and fluorophores. Heteroatom substitution at position 7 of coumarin gives fluorescent molecules with UV or near-UV excitation wavelengths. A common example is 7-hydroxy-4-methylcoumarin (*i.e.*, 4-methylumbelliferone; 4-MU; **1.10**). Under basic

conditions, the phenolate form of 4-MU ($pK_a = 7.8$) exhibits $\lambda_{\text{max}} = 360$ nm, $\lambda_{\text{em}} = 450$ nm, $\epsilon = 1.7 \times 10^3 \text{ M}^{-1}\text{cm}^{-1}$, and $\Phi = 0.63$ (Sun *et al.*, 1998). The related 7-amino-4-methylcoumarin (AMC; **1.11**) shows similar spectral properties that are constant above pH 5 (Haugland *et al.*, 2005). The large Stokes shift of coumarins is due in part to the significant change in dipole upon excitation and subsequent loss in energy by solvent reorganization (Valeur, 2002).

Molecular probes built on the coumarin scaffold include useful biomolecular labels. Different reactive groups are compatible with this fluorophore, and are typically attached at the 3 or 4 position of coumarin (Haugland *et al.*, 2005). The spectral characteristics of AMC can be tuned through different nitrogen substitution patterns (Grandberg *et al.*, 1987). Still other substitutions (*e.g.*, fluoronation or sulfonation) can yield coumarin dyes with desirable chemical properties, such as higher solubility in aqueous solution and lower sensitivity to pH (Sun *et al.*, 1998; Panchuk-Voloshina *et al.*, 1999).

Coumarins are also useful for assembling enzyme substrates. Various derivatives of 7-hydroxycoumarin can be used to assay an assortment of hydrolases (Gee *et al.*, 1999; Leroy *et al.*, 2003; Babiak and Reymond, 2005; Hyatt *et al.*, 2005), and dealkylases (Yamazaki *et al.*, 1996). Peptidyl derivatives of AMC are widely used to measure protease activity (Zimmerman *et al.*, 1976; Morita *et al.*, 1977; Zimmerman *et al.*, 1977). Microarrays of coumarin substrates have been built to examine protease specificities (Salisbury *et al.*, 2002). AMC has also been elaborated to prepare substrates for other enzymes including deacetylases (Wegener *et al.*, 2003) and esterases (Lavis *et al.*, 2006b).

1.4.4 Quinolines

The archetypal fluorophore quinine (**1.1**), is still employed as a fluorescence standard (Eaton, 1988). The 6-methoxyquinoline moiety can be alkylated and the resulting quinolinium species is quenched collisionally by halide ions in solution. Several quinolinium compounds find use as indicators for chloride ion (Jayaraman and Verkman, 2000). The chelating properties of hydroxyquinoline derivatives have been exploited to create useful fluorescence-based kinase substrates (Shults *et al.*, 2006) and fluorescent ion indicators (Tsien, 1980).

1.4.5 Indoles and Imidizoles

The indole fluorophore has been elaborated beyond tryptophan to construct useful tools such as the calcium indicator “Indo-1” (Grynkiewicz *et al.*, 1985). Another notable indole-based probe is 4',6-diamidino-2-phenylindole (DAPI; **1.12**), which binds in the minor groove of DNA (Larsen *et al.*, 1989). As this binding is accompanied by a large increase in fluorescence, this molecule can be used to stain DNA for cellular imaging or other experiments (Crissman and Hirons, 1994).

The dibenzimidazole dyes originally developed by Hoechst AG are useful DNA-binding probes. Like DAPI, the Hoechst dyes bind in the minor groove of DNA and can be used for fluorescence microscopy and flow cytometry (Petit *et al.*, 1993). Hoechst 33342 (**1.13**) is sufficiently cell-permeable for use in live cells (Crissman and Hirons, 1994). Unlike DAPI, the Hoechst dyes are quenched upon binding to DNA containing 5-bromo-2-deoxyuridine due to the heavy atom effect, thereby allowing cell-cycle analyses (Mozdziak *et al.*, 2000).

1.4.6 NBD

Another notable example of a small heterocyclic fluorophore is 7-nitrobenz-2-oxa-1,3-diazole (NBD) and other related benzoxadiazole compounds. Examples include the amine- or thiol-reactive NBD-Cl (Ghosh and Whitehouse, 1968) and the thiol-reactive 7-chlorobenz-2-oxa-1,3-diazole-4-sulfonate (SBD-Cl) (Andrews *et al.*, 1982). Primary amine adducts of NBD-Cl (*e.g.*, compound **1.14**) exhibit photophysical properties that belie the size of the molecule. Such derivatives emit in the green portion of the electromagnetic spectrum, with a $\lambda_{\text{max}} = 465 \text{ nm}$, $\lambda_{\text{em}} = 535 \text{ nm}$, $\epsilon = 2.2 \times 10^4 \text{ M}^{-1}\text{cm}^{-1}$, and $\Phi = 0.3$ in MeOH (Haugland *et al.*, 2005). This lightweight fluorophore allows conjugates with small molecules, such as sugars, to retain biological relevance (Levi *et al.*, 2007). The environmentally-sensitive fluorescence (Lin and Struve, 1991), of NBD derivatives can be exploited in a variety of ways, including the preparation of lipid probes (Chattopadhyay, 1990) and novel kinase substrates (Yeh *et al.*, 2002; Dai *et al.*, 2007).

1.4.7 Other UV-Excited Fluorophores

There are numerous examples of other small heterocyclic molecules as useful fluorescent probes. These include the 1,5-diazabicyclo[3.3.0]octa-3,6-diene-2,8-dione (*i.e.*, bimeane) structure (**1.15**) that exhibits moderate fluorescence with a $\lambda_{\text{max}} = 390 \text{ nm}$, $\lambda_{\text{em}} = 482 \text{ nm}$, and $\Phi = 0.30$ in water (Kosower *et al.*, 1979). Halogenated versions of these fluorophores are useful thiol-reactive labels, and can be used as fluorescent cross-linkers (Kim and Raines, 1995). Additional significant core dyes include the diaryloxazole structure which can exhibit large Stokes shifts (Diwu *et al.*, 2000). This

structure can be elaborated to yield useful organelle stains (Diwu *et al.*, 1999) and fluorescent labels (Anderson *et al.*, 1998). An example is the “Cascade Yellow” fluorophore (CY; **1.16**), which exhibits near UV excitation ($\lambda_{\text{max}} = 409 \text{ nm}$) with $\lambda_{\text{em}} = 558 \text{ nm}$, $\varepsilon = 2.4 \times 10^4 \text{ M}^{-1}\text{cm}^{-1}$, and $\Phi = 0.50$ (Anderson *et al.*, 1998).

1.4.8 Fluorescein

The well known xanthene dye fluorescein (**1.17**) was first synthesized by Baeyer in 1871 (Baeyer, 1871). Despite its antiquity, fluorescein remains one of the most widely utilized fluorophores in modern biological, biochemical, and medicinal research. Fluorescein exhibits several interesting (and underappreciated) properties in aqueous solution. For example, fluorescein can exist in seven prototropic forms, with the most biologically-relevant molecular forms being the monoanion and the dianion that interchange with a $\text{p}K_{\text{a}} \approx 6.4$ (Lavis *et al.*, 2007). The dianion is the most fluorescent form with a λ_{max} of 490 nm, λ_{em} of 514 nm, extinction coefficient of $9.3 \times 10^4 \text{ M}^{-1}\text{cm}^{-1}$, and a quantum yield of 0.95 (Haugland *et al.*, 2005; Lakowicz, 2006).

Fluorescein is an extremely versatile core dye. Fluorescein can be appended with reactive groups to yield important biomolecule labels (Brinkley, 1992). The structure of fluorescein can be modified further to tune properties such as $\text{p}K_{\text{a}}$ or wavelength. For example, 2',7'-difluorofluorescein (*i.e.*, Oregon Green) is less basic than fluorescein ($\text{p}K_{\text{a}} = 4.6$), maintains fluorescein-like wavelengths, and exhibits increased photostability relative to fluorescein (Sun *et al.*, 1997). Addition of other substituents, such as chloro groups, affect not only pH sensitivity (Mchedlov-Petrosyan *et al.*, 1992), but also elicits bathochromic shifts in excitation wavelength. Examples include the traditional automated

DNA sequencing dye 2',4,7,7'-tetrachlorofluorescein (TET), which exhibits a $\lambda_{\text{max}}/\lambda_{\text{em}}$ of 521/536 nm (Haugland *et al.*, 2005). Fluoresceins containing bromine or iodine substituents also have red-shifted spectra and exhibit significant intersystem crossing due to the heavy atom effect (Fleming *et al.*, 1977).

Fluorescein also serves as a scaffold for preparing indicator molecules. In particular, the pH sensitivity of fluorescein has been exploited to prepare small-molecule pH sensors (Graber *et al.*, 1986). Changes in the pK_a of fluorescein can be used as an index to report on the status of fluorescein-labeled biomolecules (Lavis *et al.*, 2007). Appending fluorescein with various chelating moieties affords sensors for biologically important ions. A noteworthy example is the calcium indicator Fluo-3 developed by Tsien and co-workers (Minta *et al.*, 1989). This compound can be used to measure calcium ion fluxes in live cells and is employed widely in high-throughput screening (Inglese *et al.*, 2007). Other notable examples of fluorescein-based indicators are compounds for measuring sodium (Martin *et al.*, 2005), zinc (Kikuchi *et al.*, 2004), palladium (Song *et al.*, 2007), mercury(II) (Yoon *et al.*, 2007), and fluoride (Yang *et al.*, 2007) ions, as well as clever nitric oxide sensors based on copper(II) chelates (Lim and Lippard, 2007).

Fluorescein exists in equilibrium between an “open” quinoid and a “closed” lactone form. Acylation or alkylation of the phenolic groups locks the molecule into the nonfluorescent lactone in an aqueous environment, and serves as the basis for a variety of fluorogenic substrates for esterases, phosphatases, glycosylases, and other enzymes (Rotman *et al.*, 1963; Rotman and Papermaster, 1966; Huang *et al.*, 1999; Zaikova *et al.*, 2001). Fluorescein can also be “caged” with photolabile groups and unmasked by distinct wavelengths of light (Mitchison *et al.*, 1998). Other substitutions can confer redox

sensitivity to the fluorescein molecule (Miller *et al.*, 2007). Appending fluorescein derivatives with electron-donating substituents on the pendant phenyl ring allows the construction of enzyme substrates with only one substrate moiety. These “Tokyo Green” substrates show improved enzyme kinetics relative to disubstituted fluorescein substrates (Urano *et al.*, 2005), and can be used for *in vivo* imaging (Kamiya *et al.*, 2007).

1.4.9 Rhodamine

Isologues of fluorescein, the rhodamines are used widely as fluorophores. Some key characteristics of this dye class include low pH sensitivity and tunable spectral properties. Different *N*-alkyl substitution patterns on the rhodamine core can modify spectral characteristics. The simplest member of this class, rhodamine 110 (Rh₁₁₀; **1.18**), exhibits fluorescein-like spectral properties in the green portion of the spectrum with $\lambda_{\text{max}} = 496 \text{ nm}$, $\lambda_{\text{em}} = 517 \text{ nm}$, $\epsilon = 7.4 \times 10^4 \text{ M}^{-1}\text{cm}^{-1}$, and $\Phi = 0.92$ in aqueous solution (Lavis *et al.*, 2006a). Substitution to tetramethylrhodamine (TMR; **1.19**) gives longer excitation and emission wavelengths ($\lambda_{\text{max}}/\lambda_{\text{em}} = 540/565 \text{ nm}$) but a lower quantum yield. ($\Phi = 0.68$) (Johnson, 1998). This lower quantum yield is likely due to decay of the excited state via rotation around the C–N bond (Drexhage, 1977). This undesirable decay process can be circumvented by freezing the C–N bond via appropriate substitution. Rhodamines containing rigid julolidine ring systems show higher quantum yields than do the unrestricted dyes (Karstens and Kobs, 1980), and exhibit longer excitation and emission wavelengths (Haugland *et al.*, 2005). Sulforhodamine 101 (SRh₁₀₁; **1.20**) is a julolidine-based dye that is common in bioresearch. Amine-reactive sulfonyl chloride derivatives of SRh₁₀₁ are sold under the trademark “Texas Red” (Haugland *et al.*, 2005).

Other substitutions of the rhodamine structure can be used to prepare dyes with still longer excitation and emission wavelengths (Panchuk-Voloshina *et al.*, 1999; Liu *et al.*, 2003).

Rhodamine labels are often paired with fluorescein derivatives for FRET-based experiments due to efficient energy transfer between these xanthene compounds (Haugland *et al.*, 2005). Dye constructs containing both fluorescein and rhodamine moieties have proven useful for DNA sequencing. The fluorescein donor of these “BigDye” fluorophores can be excited by a single-wavelength light source, and the emission is dictated by the specific rhodamine derivative that serves as the FRET acceptor (Lee *et al.*, 1997).

Rhodamines can also be used to assemble enzyme substrates. Acyl substitution of both the amino groups of a rhodamine locks the molecule into a nonfluorescent lactone form. As with fluorescein, this property can be exploited to prepare caged compounds (Mitchison *et al.*, 1998), or fluorogenic molecules for enzymatic studies. Substrates based on Rh₁₁₀ for simple proteases were first described by Mangel in 1983 (Leytus *et al.*, 1983b). More recent developments have centered on using Rh₁₁₀ to build useful caspase substrates to assay apoptosis (Liu *et al.*, 1999). Rh₁₁₀-based substrates have also been developed for phosphatases (Kupcho *et al.*, 2004), esterases (Lavis *et al.*, 2006a), and metal-ion catalysis in a cellular context (Streu and Meggers, 2006).

Rhodamines have also been used to build indicators for ions such as sodium (Martin *et al.*, 2004) and calcium (Minta *et al.*, 1989). Other rhodamine derivatives have been assembled to detect reactive oxygen species in cells (Koide *et al.*, 2007). Hybrid structures between fluorescein and rhodamine (*i.e.*, xanthene dyes with one oxygen and

one nitrogen substituent) are termed “rhodols” and exhibit interesting spectral properties (Whitaker *et al.*, 1992). The unique properties of these rhodol fluorophores can be harnessed to build interesting probes such as ion indicators (Burdette and Lippard, 2002).

1.4.10 Naphthoxanthene Dyes

A notable modification to the fluorescein and rhodamine dyes is the introduction of a fused benzo ring into the xanthene structure. This modification elicits a severe bathochromic shift in excitation and emission wavelengths. A classic example is naphthofluorescein (NF; **1.21**), which exhibits much longer wavelengths than does fluorescein ($\lambda_{\text{max}}/\lambda_{\text{em}} = 595/660 \text{ nm}$) (Lee *et al.*, 1989b). Unfortunately, the advantageous bathochromic shift is countered by an undesirable $\text{p}K_{\text{a}} = 8.0$, and a lower extinction coefficient ($\epsilon = 4.4 \times 10^4 \text{ M}^{-1}\text{cm}^{-1}$) and quantum yield ($\Phi = 0.14$) (Lee *et al.*, 1989b). The poor fluorescence properties of naphthofluorescein limits the utility of this scaffold, though some useful derivatives have been reported (Lee *et al.*, 1989b; Sarpara *et al.*, 1999; Xu *et al.*, 2005).

Xanthene dyes that bear only one fused benzo ring display interesting spectral properties. Unlike the symmetrical fluoresceins and rhodamines, the resonance forms of these seminaphtho dyes are not equivalent, and therefore exhibit dissimilar spectral properties. Thus, the asymmetry of the dye can be yoked to construct ratiometric fluorescent indicators. Probes from the seminaphthofluorescein (SNAFL) core include pH sensors (Whitaker *et al.*, 1991b) and other ion indicators (Chang *et al.*, 2004). Rhodol-type seminaphthoxanthenes are also useful pH indicators (Liu *et al.*, 2001). One example is ratiometric pH sensor **1.22**, which bears the common name

“seminaphtharhodafluor-1” (SNARF-1) This compound displays a $\lambda_{\text{max}} = 573 \text{ nm}$, $\lambda_{\text{em}} = 631 \text{ nm}$, $\varepsilon = 4.4 \times 10^4 \text{ M}^{-1}\text{cm}^{-1}$, and $\Phi = 0.092$ at high pH values (Whitaker *et al.*, 1991b; Johnson, 1998). Derivatives of dye **1.22** boast useful pK_{a} values around 7.5, that can be tuned to lower values by fluorine substitution (Liu *et al.*, 2001).

1.4.11 Phenanthridines

Phenanthridine derivatives are widely used DNA intercalators that exhibit higher fluorescence intensity upon binding to nucleic acids. Examples include the cationic dyes ethidium and propidium (**1.23**). In the presence of DNA, propidium has a $\lambda_{\text{max}} = 534 \text{ nm}$, $\lambda_{\text{em}} = 617 \text{ nm}$, $\varepsilon = 5.4 \times 10^3 \text{ M}^{-1}\text{cm}^{-1}$, and $\Phi = 0.13$ (Cosa *et al.*, 2001). These values constitute a 20–30-fold increase in fluorescence relative to the free dye. The fixed ionic character of compound **1.23** limits passive diffusion through the intact membranes of living cells. Thus, propidium can be used to identify dead cells with compromised membranes (Darzynkiewicz *et al.*, 1992).

1.4.12 BODIPY

The boron difluoride dipyrromethene (BODIPY) dye structure has been used to build a variety of useful fluorescent labels and other probes. Key features of this dye class are the insensitivity of the spectral properties to environment, the small Stokes shift, and the overall lipophilicity of the dye (Karolin *et al.*, 1994; Haugland *et al.*, 2005). The core structure of BODIPY is somewhat base sensitive, limiting its use in applications such as solid-phase peptide synthesis (Lumbierres *et al.*, 2005). The simplest BODIPY fluorophore **1.24** shows fluorescein-like parameters with $\lambda_{\text{max}} = 505 \text{ nm}$, $\lambda_{\text{em}} = 511 \text{ nm}$,

$\epsilon = 9.1 \times 10^4 \text{ M}^{-1}\text{cm}^{-1}$, and $\Phi = 0.94$ and bears the common name “BODIPY-FL” (Johnson, 1998; Haugland *et al.*, 2005). Another important property of this class of dyes is the tunability of wavelength through appropriate substitution. BODIPY dyes can thus serve as surrogates for traditional dyes such as fluorescein, tetramethylrhodamine, and many others. One example is the “BODIPY-TR” fluorophore (**1.25**) which exhibits spectral properties similar to those of Texas Red (i.e., SRh₁₀₁; **1.20**; (Johnson, 1998; Haugland *et al.*, 2005)).

The ensemble of probes built on the BODIPY scaffold are centered largely on fluorescent labels, but some indicators for ions and other molecules have been reported (Gabe *et al.*, 2004; Martin *et al.*, 2005). These fluorophores are particularly useful labels for fluorescence polarization techniques (Banks *et al.*, 2000). The nonpolar character of BODIPY allows incorporation into lipophilic probes (Karolin *et al.*, 1994). Moreover, the small Stokes shift of BODIPY dyes causes efficient self-quenching of overlabeled biomolecules. This phenomenon can be utilized to create useful protease substrates, as proteolysis of densely labeled proteins leads to an increase in fluorescence intensity (Thompson *et al.*, 2000).

1.4.13 Cyanines

The term “cyanine dye” denotes a dye system with a polymethine chain between two nitrogens (i.e., $\text{R}_2\text{N}-(\text{CH}=\text{CH})_n-\text{CH}=\text{N}^+\text{R}_2$). This dye system, which resembles the retinaldimine visual pigment of rhodopsin (Nathans, 1987), has been the subject of many seminal studies on the molecular basis of color (Lewis and Calvin, 1939). Numerous cyanines and associated polymethine structures are useful as labels (Buschmann *et al.*,

2003), DNA stains (Cosa *et al.*, 2001), and membrane potential sensors (Smith, 1990; Plasek and Sigler, 1996). Perhaps the most well-known cyanine dyes in modern bioresearch are the “CyDye” fluorophores, which are based on a sulfoindocyanine structure (Mujumdar *et al.*, 1993). These compounds are given common names according to the number of carbon atoms between the dihydroindole units. Cy3 (**1.26**) shows spectral characteristics that are comparable to TMR with $\lambda_{\text{max}} = 554$ nm, $\lambda_{\text{em}} = 568$ nm, $\epsilon = 1.3 \times 10^5 \text{ M}^{-1} \text{ cm}^{-1}$, and $\Phi = 0.14$ in water. Cy5 (**1.27**) exhibits longer wavelengths with $\lambda_{\text{max}} = 652$ nm, $\lambda_{\text{em}} = 672$ nm, $\epsilon = 2.0 \times 10^5 \text{ M}^{-1} \text{ cm}^{-1}$, and $\Phi = 0.18$. Longer cyanine constructs, such as Cy7 (**1.28**), exhibit $\lambda_{\text{max}}/\lambda_{\text{em}} = 755/788$ nm, albeit with a lower quantum yield ($\Phi = 0.02$) (Waggoner and Kenneth, 1995). Further elaboration of the cyanine core can provide control over wavelength. For example, introduction of a fused benzo ring in the dihydroindole moieties elicits a bathochromic shift of ~20–30 nm (Mujumdar *et al.*, 1996). This structural modification is designated with a “.5” suffix (*e.g.*, Cy5.5).

The CyDyes are useful biomolecular labels and are now the standard fluorophores for microarrays and many other analyses (Waggoner, 2006). CyDye pairs are also often used for FRET experiments (Schobel *et al.*, 1999), and can be utilized as photo-switchable probes for ultrahigh-resolution imaging (Bates *et al.*, 2007). One significant drawback to these cyanine labels is the severe dependence of the fluorescence of their bioconjugates on the number of fluorophores per biomolecule. This phenomenon likely has several causes, and can limit the utility of CyDye conjugates in some applications (Gruber *et al.*, 2000). Newer (albeit structurally mysterious) sulfonated cyanine dyes reportedly overcome this problem (Berlier *et al.*, 2003).

1.4.14 Phthalocyanines

The phthalocyanine structure serves as a scaffold for a variety of interesting compounds, from pigments to photosensitizers. Wavelength absorption and other properties can be tuned by structural modification or through substitution of metal centers (Christie, 2001). To prevent dye aggregation and facilitate water solubility, inclusion of numerous ionic substituents is necessary (Liu *et al.*, 2005). A successful example of a phthalocyanine fluorescent label is IRDye 700DX (**1.29**), which shows $\lambda_{\text{max}} = 689 \text{ nm}$, $\lambda_{\text{em}} = 700 \text{ nm}$, $\epsilon = 1.7 \times 10^5 \text{ M}^{-1}\text{cm}^{-1}$, $\Phi = 0.14$ and excellent photostability (Peng *et al.*, 2006).

1.4.15 Oxazines

Substituted oxazine compounds are useful fluorophores. Of particular importance is resorufin (**1.30**), the anion of which exhibits $\lambda_{\text{max}} = 572 \text{ nm}$, $\lambda_{\text{em}} = 585 \text{ nm}$, $\epsilon = 5.6 \times 10^4 \text{ M}^{-1}\text{cm}^{-1}$, and quantum yield = 0.74. These attributes have some sensitivity to pH, as resorufin has a pK_a of 5.8 (Bueno *et al.*, 2002). Use of the resorufin scaffold to prepare fluorescent labels has been limited (Christoph and Meyer-Almes, 2003), though this dye has been used to construct molecules that are unmasked by various hydrolases (Hofmann and Sernetz, 1984; Kitson, 1996; Gao *et al.*, 2003) and cytochrome P450 enzymes (Burke *et al.*, 1994).

Resorufin exhibits interesting redox properties. Oxidation to the *N*-oxide yields resazurin, which is only weakly fluorescent. Resazurin can be reduced to resorufin by biological reducing equivalents, and thus has been used to assay cell viability (O'Brien *et al.*, 2000). In addition, reduced versions of resorufin are nonfluorescent, but can be

oxidized to resorufin by H_2O_2 in the presence of horseradish peroxidase. These compounds are useful for the ELISA and other assays (Zhou *et al.*, 1997).

Other important oxazine dyes include cresyl violet, which can be elaborated to give substrates for proteases (Van Noorden *et al.*, 1997; Boonacker *et al.*, 2003; Lee *et al.*, 2003) and esterases (Lavis *et al.*, 2006b). A key property of several oxazine fluorophores is their environmental sensitivity. These compounds can be used to prepare useful compounds, such as labels to report on protein conformation (Cohen *et al.*, 2005).

1.5 Conclusions

Known small-molecule fluorophores have a wide range of spectral and chemical properties. Elaboration of these core structures has provided numerous probes for assaying biological systems. Nonetheless, extraordinary opportunities remain, as delving deeper into biochemical and biological phenomena will require ever more sophisticated and tailored probes. Scientists who straddle the fields of chemistry and biology are best equipped to fashion these tools, and then wield them to illuminate otherwise inscrutable life processes.

1.6 Acknowledgments

We are grateful to Z.J. Diwu. and T.J. Rutkoski for contributive discussions and to H.A. Steinberg for assistance with Figure 1.2. L.D.L was supported by Biotechnology Training Grant 08349 (NIH) and an ACS Division of Organic Chemistry Graduate Fellowship sponsored by The Genentech Foundation. Related work in our laboratory was supported by grant CA73808 (NIH).

CHAPTER 2*

LATENT BLUE AND RED FLUOROPHORES BASED ON THE TRIMETHYL LOCK

Contribution: Chemical synthesis, *in vitro* enzyme assays, stability studies, composition of manuscript, and preparation of figure drafts. Cellular imaging was performed by T.-Y. Chao.

***This chapter has been published, in part, under the same title. Reference:** Lavis, L. D., Chao, T.-Y., and Raines, R. T. (2006). *ChemBioChem* **7**, 1151–1154.

2.1 Introduction

Fluorescent molecules are indispensable tools in modern biochemical and biological research, being used as labels for biomolecules, indicators for ions, stains for organelles, and substrates for enzymes (Haugland *et al.*, 2005). The major targets of this last class are hydrolases that catalyze the removal of a masking moiety, thereby modulating fluorescence (Johnson, 1998). A critical property of fluorogenic hydrolase substrates is their chemical stability in aqueous solution, as spontaneous hydrolysis can compete deleteriously with enzymatic activity. New substrate classes that exhibit increased stability while maintaining enzymatic reactivity would be highly desirable.

Our laboratory recently reported on the use of the “trimethyl lock” strategy in the design of a latent fluorophore (Chandran *et al.*, 2005). This latent fluorophore consists of a trimethyl lock component inserted between a dye and enzyme-reactive group. The trimethyl lock is an *o*-hydroxycinnamic acid derivative in which unfavorable steric interactions between three methyl groups encourage rapid lactonization to form a hydrocoumarin and release a leaving group (Borchardt and Cohen, 1972a; Borchardt and Cohen, 1972b; Milstein and Cohen, 1972). Our initial latent fluorophore exhibited remarkable stability in aqueous solution, but released a xanthene dye (rhodamine 110) upon hydrolytic cleavage by an esterase. Here, we explore the modularity of our design, probing its applicability to unrelated dyes that absorb at short (blue) and long (red) wavelengths.

2.2 Results and Discussion

2.2.1 Coumarin-Based Latent Fluorophore

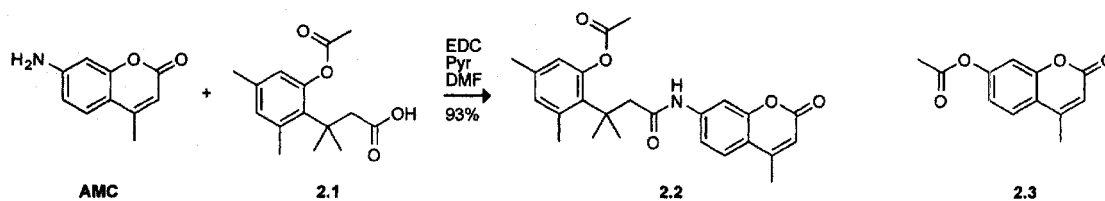
Coumarin-based compounds comprise an important class of blue dyes possessing UV or near-UV excitation wavelengths (Valeur, 2002). Acyl esters and acyloxymethyl ethers of 7-hydroxycoumarin (*i.e.*, umbelliferone) can be substrates for esterases (Leroy *et al.*, 2003; Babiak and Reymond, 2005; Hyatt *et al.*, 2005). 7-Amino-4-methylcoumarin (AMC) is used widely as the basis for protease substrates (Zimmerman *et al.*, 1976; Morita *et al.*, 1977; Zimmerman *et al.*, 1977). Upon amidation, the excitation and emission wavelengths of AMC are shifted to shorter wavelengths with concomitant reduction in quantum yield (Zimmerman *et al.*, 1976).

We reasoned that AMC could be subjected to our latent fluorophore strategy. Accordingly, we condensed AMC with acetylated trimethyl lock **2.1** (Amsberry *et al.*, 1991) to give profluorophore **2.2** (Scheme 2.1), which displayed the expected hypsochromic shift of excitation and emission spectra relative to free AMC (Figure 2.1). The hydrolysis of profluorophore **2.2** was catalyzed by porcine liver esterase (PLE) with $k_{\text{cat}}/K_{\text{M}} = 2.5 \times 10^5 \text{ M}^{-1}\text{s}^{-1}$ and $K_{\text{M}} = 8.2 \text{ }\mu\text{M}$ (Figure 2.2a). This $k_{\text{cat}}/K_{\text{M}}$ value is 10^2 -fold greater than the apparent $k_{\text{cat}}/K_{\text{M}}$ value for the latent fluorophore based on rhodamine 110 (Chandran *et al.*, 2005). (We use the term “apparent” because full fluorescence manifestation requires the lactonization of two trimethyl lock moieties. (Chandran *et al.*, 2005))

To evaluate the relative stability of profluorophore **2.2**, we monitored the accretion of fluorescence in phosphate-buffered saline (PBS) containing bovine serum albumin (BSA; 1.0 mg/mL) and either profluorophore **2.2** or 4-methylumbelliferyl acetate (**2.3**, which is

a common esterase substrate (Hyatt *et al.*, 2005)). Profluorophore **2.2** proved to be highly stable compared to 4-methylumbelliferyl acetate (Figure 2.3). An additional advantage of profluorophore **2.2** is that the product of its hydrolysis, AMC, shows little change in fluorescence at $\text{pH} \geq 5$ (Haugland *et al.*, 2005). In contrast, the fluorescence of 4-methylumbelliferone is highly variable due to its $\text{pK}_a = 7.40$ (Graber *et al.*, 1986) being near the physiological pH.

Scheme 2.1 Route for the synthesis of profluorophore **2.2**, and the chemical structure of 4-methylumbelliferyl acetate (**2.3**)



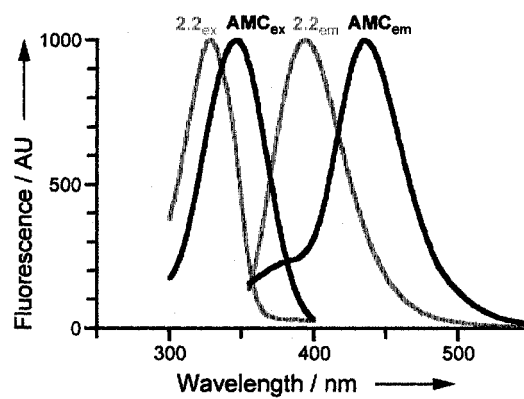


Figure 2.1 Normalized fluorescent excitation–emission spectra of profluorophore 2.2 and AMC.

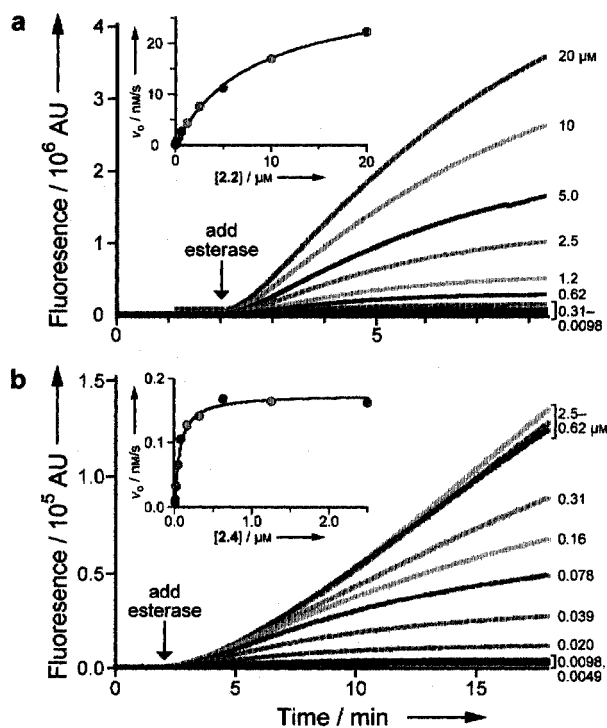


Figure 2.2 (a) Kinetic traces (λ_{ex} 365 nm, λ_{em} 460 nm) and Michaelis–Menten plot (inset) for the hydrolysis of profluorophore **2.2** (20 μM \rightarrow 9.8 nm) by PLE (2.5 $\mu\text{g/mL}$); $k_{\text{cat}}/K_{\text{M}} = 2.5 \times 10^5 \text{ M}^{-1}\text{s}^{-1}$ and $K_{\text{M}} = 8.2 \mu\text{M}$. (b) Kinetic traces (λ_{ex} 586 nm, λ_{em} 620 nm) and Michaelis–Menten plot (inset) for the hydrolysis of profluorophore **2.4** (2.5 μM \rightarrow 4.9 nm) by PLE (2.5 $\mu\text{g/mL}$); apparent $k_{\text{cat}}/K_{\text{M}} = 1.2 \times 10^5 \text{ M}^{-1}\text{s}^{-1}$ and apparent $K_{\text{M}} = 0.14 \mu\text{M}$.

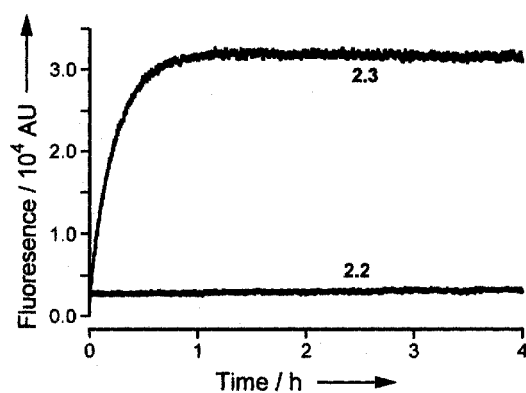


Figure 2.3 Time course of the generation of fluorescence (λ_{ex} 365 nm, λ_{em} 460 nm) from profluorophore **2.2** (50 nm) or methylumbelliferyl acetate **2.3** (50 nm) in PBS containing BSA (1 mg/mL).

2.2.2 Cresyl Violet-Based Latent Fluorophore

To access longer wavelengths, we turned to the oxazine class of red dyes. One such dye, cresyl violet (CV) has been used for decades to stain tissues (Banny and Clark, 1950; Culling *et al.*, 1985) and as a laser dye (Gacoin and Flamant, 1972). Although CV has a maximal absorbance at 586 nm, its fused benzo ring broadens its absorption spectrum (Drexhage, 1977). and thereby allows excitation with a variety of light sources. Diamide derivatives of CV are virtually nonfluorescent and thus useful in the production of fluorogenic protease substrates (Van Noorden *et al.*, 1997; Boonacker *et al.*, 2003; Lee *et al.*, 2003).

The attributes of CV make this dye an attractive candidate for our latent fluorophore strategy. Accordingly, we condensed CV with acetylated trimethyl lock **2.1** (Amsberry *et al.*, 1991) to give profluorophore **2.4** (Scheme 2.2). Although profluorophore **2.4** was stable in PBS containing BSA (data not shown), its hydrolysis was catalyzed by PLE with apparent kinetic parameters of $k_{cat}/K_M = 1.2 \times 10^5 \text{ M}^{-1}\text{s}^{-1}$ and $K_M = 0.14 \text{ }\mu\text{M}$ (Figure 2.2b). The k_{cat}/K_M value for the hydrolysis of profluorophore **2.4** is similar to that of profluorophore **2.2**; the K_M value is, however, 10-fold lower than that of profluorophore **2.2**.

Profluorophore **2.4** serves as a probe for esterase activity in live mammalian cells. The broad excitation peak allowed confocal microscopy experiments using excitation at 543 nm and emission at 605 nm. Profluorophore **2.4** was hydrolyzed by esterases endogenous in the cells of a rodent (Figure 2.4a) or human (Figure 2.4b) to give a red-stained cytosol within minutes. The somewhat enhanced fluorescence observed in the human cells could be indicative of more efficient internalization or hydrolysis of the latent fluorophore.

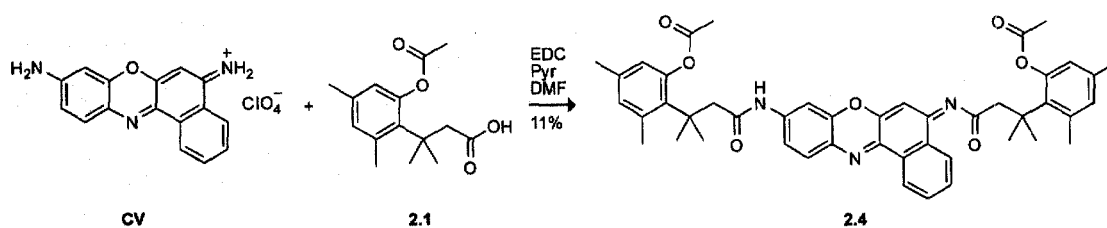
After longer incubation, the liberated CV became further localized in subcellular compartments (data not shown), which is consistent with previous reports (Lee *et al.*, 2003). To date, there have been few reports of long-wavelength esterase substrates that are useful in cell biology (Haugland *et al.*, 2005). Its evident stability, optical properties, and fast intracellular education make profluorophore **2.4** useful in a wide variety of biological applications, especially in assays involving fluorophores of different wavelengths.

2.3 Conclusions

In conclusion, we have established that one component of our latent fluorophores—the dye—is modular (Figure 2.5). Specifically, we have now prepared useful latent fluorophores from three dyes (blue, green (Chandran *et al.*, 2005), and red), all linked by a trimethyl lock moiety to an esterase-reactive group. In future work, we shall explore the modularity of the other component—the enzyme-reactive group. We anticipate that the end result will be a broad spectrum of stable latent fluorophores with numerous applications in biochemical and biological research.

2.4 Acknowledgements

We are grateful to S.S. Chandran and Z. Diwu for contributive discussions. L.D.L. was supported by Biotechnology Training Grant 08349 (NIH). This research was supported by grant CA73808 (NIH). NMRFAM was supported by grant P41RR02301 (NIH).

Scheme 2.2 Route for the synthesis of profluorophore **2.4**.

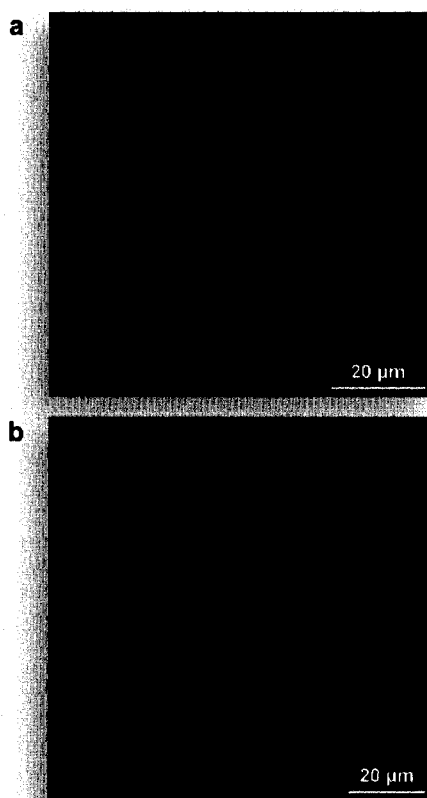


Figure 2.4 Unwashed mammalian cells incubated for 15 min with profluorophore **2.4** (10 μ M) at 37 °C in DMEM and counter-stained with Hoechst 33342 (5% v/v CO₂(g), 100% humidity). (a) CHO K1 cells. (b) HeLa cells.

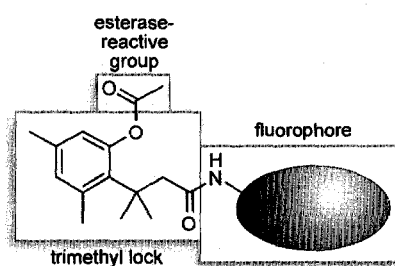


Figure 2.5 Modules in the latent fluorophores described in this work.

2.5 Experimental Section

2.5.1 General Experimental: Chemical Synthesis

AMC (*i.e.*, Coumarin 440) and CV·HClO₄ (*i.e.*, Cresyl Violet 670 Perchlorate) were from Exciton (Dayton, OH). Dimethylformamide was drawn from a Baker CYCLE-TAINER solvent delivery system. All other reagents were from Aldrich Chemical (Milwaukee, WI) or Fisher Scientific (Hanover Park, IL) and used without further purification.

PBS contained (in 1.00 L at pH 7.4) KCl (0.20 g), KH₂PO₄ (0.20 g), NaCl (8.0 g), and Na₂HPO₄·7H₂O (2.16 g).

Thin-layer chromatography was performed using aluminum-backed plates coated with silica gel containing F₂₅₄ phosphor and visualized by UV illumination or developed with I₂, ceric ammonium molybdate, or phosphomolybdic acid stain. Flash chromatography was performed on open columns with silica gel-60 (230–400 mesh), or on a FlashMaster Solo system (Argonaut, Redwood City, CA) with Isolute Flash Si II columns (International Sorbent Technology, Hengoed, Mid Glamorgan, UK).

NMR spectra were obtained with a Bruker DMX-400 Avance spectrometer at the National Magnetic Resonance Facility at Madison (NMRFAM). Mass spectrometry was performed with a Micromass LCT (electrospray ionization, ESI) mass spectrometer in the Mass Spectrometry Facility in the Department of Chemistry.

2.5.2 Synthesis of Compounds 2.2 and 2.4

7-Amino-4-methylcoumarin Trimethyl Lock (2.2). AMC (53 mg, 0.304 mmol) was dissolved in anhydrous DMF (2.0 mL) and anhydrous pyridine (1.0 mL). 3-(2'-Acetoxy-

4',6'-dimethylphenyl)-3,3-dimethylpropanoic acid (Amsberry *et al.*, 1991) (**2.1**, 100 mg, 0.378 mmol) and EDC (117 mg, 0.609 mmol) were added, and the reaction mixture was stirred at ambient temperature for 48 h. Solvent was removed under reduced pressure, and the residue was purified by column chromatography (silica gel, 0% to 40% v/v gradient of EtOAc in hexanes). Compound **2.2** was isolated as an off-white crystalline solid (119 mg, 93%). ^1H NMR (400 MHz, CDCl_3) δ (ppm): 7.66 (bs, 1H), 7.39 (d, $J = 8.6$ Hz, 1H), 7.21 (m, 2H), 6.76 (s, 1H), 6.65 (s, 1H), 6.15 (d, $J = 1.3$ Hz, 1H), 2.55 (s, 2H), 2.41 (s, 3H), 2.39 (s, 3H), 2.36 (d, $J = 1.2$ Hz, 3H), 2.25 (s, 3H), 1.71 (s, 6H). ^{13}C NMR (100 MHz, CDCl_3) δ (ppm): 172.51, 169.96, 161.13, 154.08, 152.17, 150.16, 141.56, 139.13, 137.40, 133.15, 132.82, 124.82, 123.46, 115.68, 115.27, 113.06, 106.65, 51.11, 40.53, 32.25 (2C), 25.49, 21.95, 20.15, 18.51. HRMS (ESI): m/z 444.1797 (MNa^+ [$\text{C}_{25}\text{H}_{27}\text{NO}_5\text{Na}$] = 444.1787).

Cresyl Violet Bis(trimethyl lock) (2.4). CV·HClO₄ (250 mg, 0.691 mmol) was dissolved in anhydrous DMF (2.0 mL) and anhydrous pyridine (2.0 mL). 3-(2'-Acetoxy-4',6'-dimethylphenyl)-3,3-dimethylpropanoic acid (Amsberry *et al.*, 1991) (**2.1**, 394 mg, 1.38 mmol) and EDC (265 mg, 1.38 mmol) were added, and the reaction mixture was stirred at ambient temperature for 24 h. Solvent was removed under reduced pressure, and the residue was partitioned between CH_2Cl_2 and 5% v/v HCl(aq). The layers were separated, and the aqueous layer extracted with CH_2Cl_2 . The combined organic layers were washed with H_2O and saturated brine, and dried over anhydrous $\text{MgSO}_4(\text{s})$. Removal of solvent gave a brown solid that was purified by column chromatography (silica gel, 30% v/v EtOAc in hexanes). Compound **2.4** was isolated as a red-brown solid (55 mg, 11%). ^1H NMR (400 MHz, CDCl_3) δ (ppm): 8.57 (dd, $J = 7.9, 1.1$ Hz, 1H), 8.12

(dd, $J = 8.0, 1.2$ Hz, 1H), 7.72 (bs, 1H), 7.65 (ddd, $J = 8.0, 7.2, 1.4$ Hz, 1H), 7.59 (ddd, $J = 7.9, 7.2, 1.4$ Hz, 1H), 7.50 (d, $J = 8.6$ Hz, 1H), 7.46 (d, $J = 2.1$ Hz, 1H), 6.85 (dd, 8.6, 2.4 Hz, 1H), 6.77 (m, 1H), 6.66 (m, 2H), 6.47 (m, 1H), 5.98 (s, 1H), 3.19 (s, 2H), 2.54 (s, 2H), 2.51 (s, 3H), 2.43 (s, 3H), 2.41 (s, 3H), 2.26 (s, 3H), 2.25 (s, 3H), 2.05 (s, 3H), 1.73 (s, 6H), 1.66 (s, 6H). ^{13}C NMR (100 MHz, CDCl_3) δ (ppm): 188.04, 172.79, 169.95, 169.91, 154.02, 150.21, 149.40, 147.92, 145.84, 144.77, 140.86, 139.24, 138.20, 137.37, 136.13, 133.48, 133.23, 132.88, 132.47, 132.13, 131.07, 130.77, 130.74, 129.49, 129.40, 125.56, 124.240, 123.41, 123.12, 115.63, 105.51, 101.12, 52.88, 51.15, 40.64, 39.34, 32.28 (2C), 32.06 (2C), 25.55, 25.33, 21.99, 21.88, 20.17, 20.10. HRMS (ESI): m/z 754.3471 (MH^+ [$\text{C}_{46}\text{H}_{48}\text{N}_3\text{O}_7$] = 754.3492).

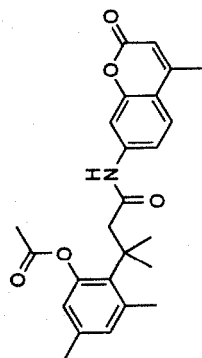
2.5.3 Fluorescence Spectroscopy

Fluorometric measurements were made with a QuantaMaster1 photon-counting spectrofluorometer from Photon Technology International (South Brunswick, NJ) equipped with sample stirring, and fluorescence grade quartz or glass cuvettes from Starna Cells (Atascadero, CA). All measurements were recorded at ambient temperature (23 ± 2 °C). Compounds were prepared as stock solutions in DMSO and diluted such that the DMSO concentration did not exceed 1% v/v. PLE (MW = 163 kDa (Horgan *et al.*, 1969)) was from Sigma Chemical (St. Louis, MO; product number E2884) as a suspension in 3.2 M $(\text{NH}_4)_2\text{SO}_4$, and was diluted to appropriate concentrations in PBS before use. Kinetic parameters were calculated with Microsoft Excel 2003 and GraphPad Prism 4.

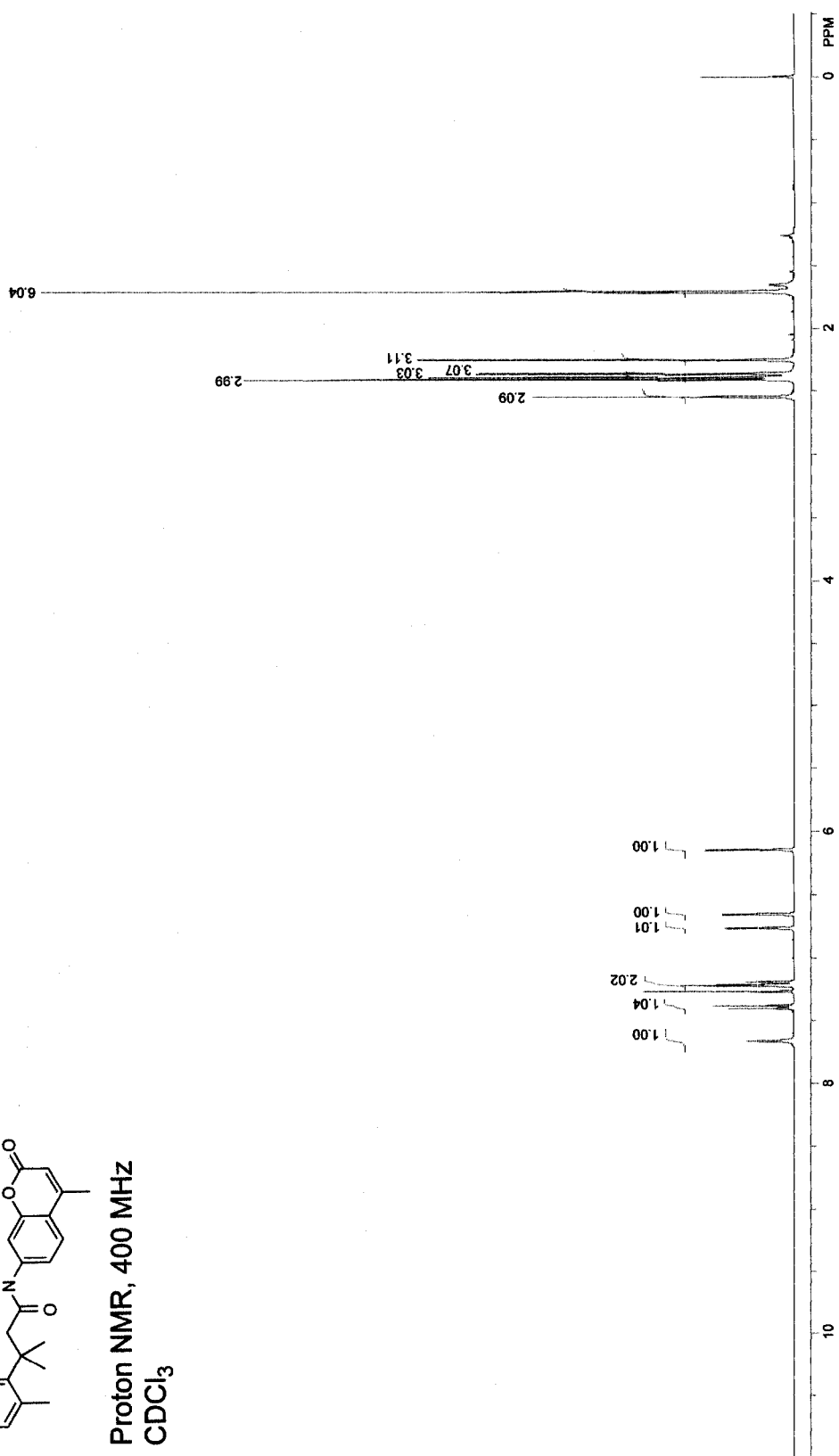
2.5.4 Cell Preparation and Imaging

CHO K1 or HeLa cells were plated on Nunc Lab-Tek II 8-well Chamber Coverglass (Fisher Scientific, Hanover Park, IL) and grown to 70% confluence at 37 °C in Dulbecco's modified Eagle's medium (Invitrogen, Carlsbad, CA) containing FBS (10% v/v). Cells were then incubated with profluorophore **2.4** (10 μ M) for 15 min at 37 °C and imaged immediately. Nuclear staining was accomplished by addition of Hoechst 33342 (2 μ g/mL) for the final 5 min of incubation.

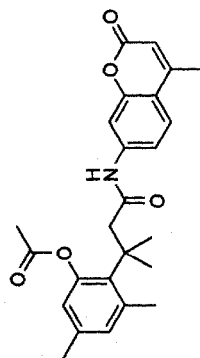
Cells were imaged with a Nikon Eclipse TE2000-U confocal microscope equipped with a Zeiss AxioCam digital camera. Excitation at 408 nm was provided by a blue-diode laser, and emission light was passed through a filter centered at 450 nm with a 35-nm band-pass. Excitation at 543 nm was provided by a HeNe laser, and emission light was passed through a filter centered at 605 nm with a 75-nm band-pass.

2.2

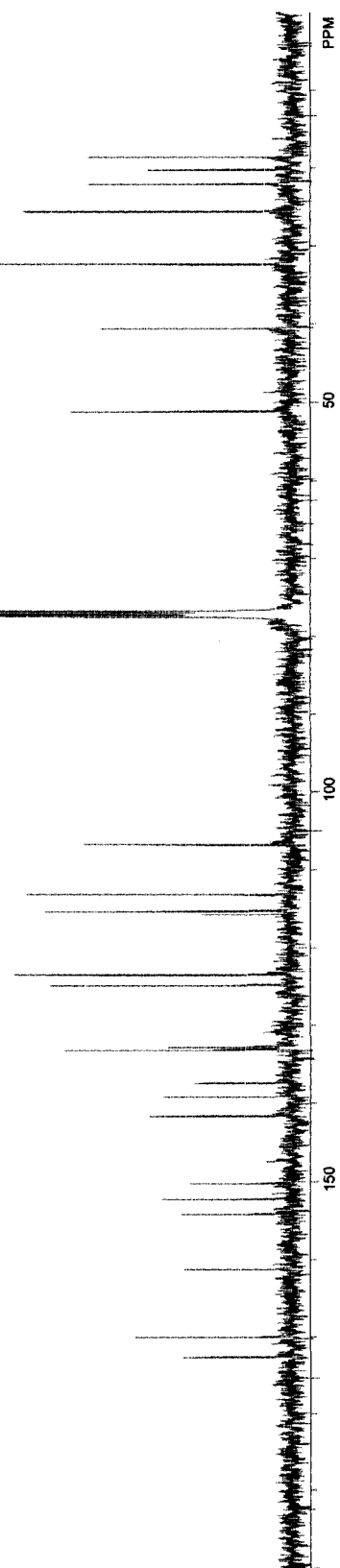
Proton NMR, 400 MHz
CDCl₃

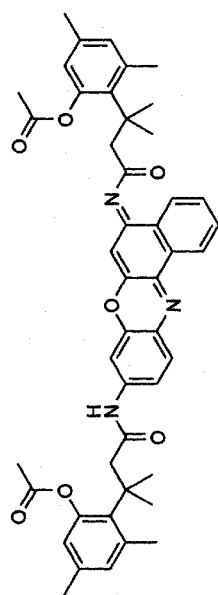


2.2

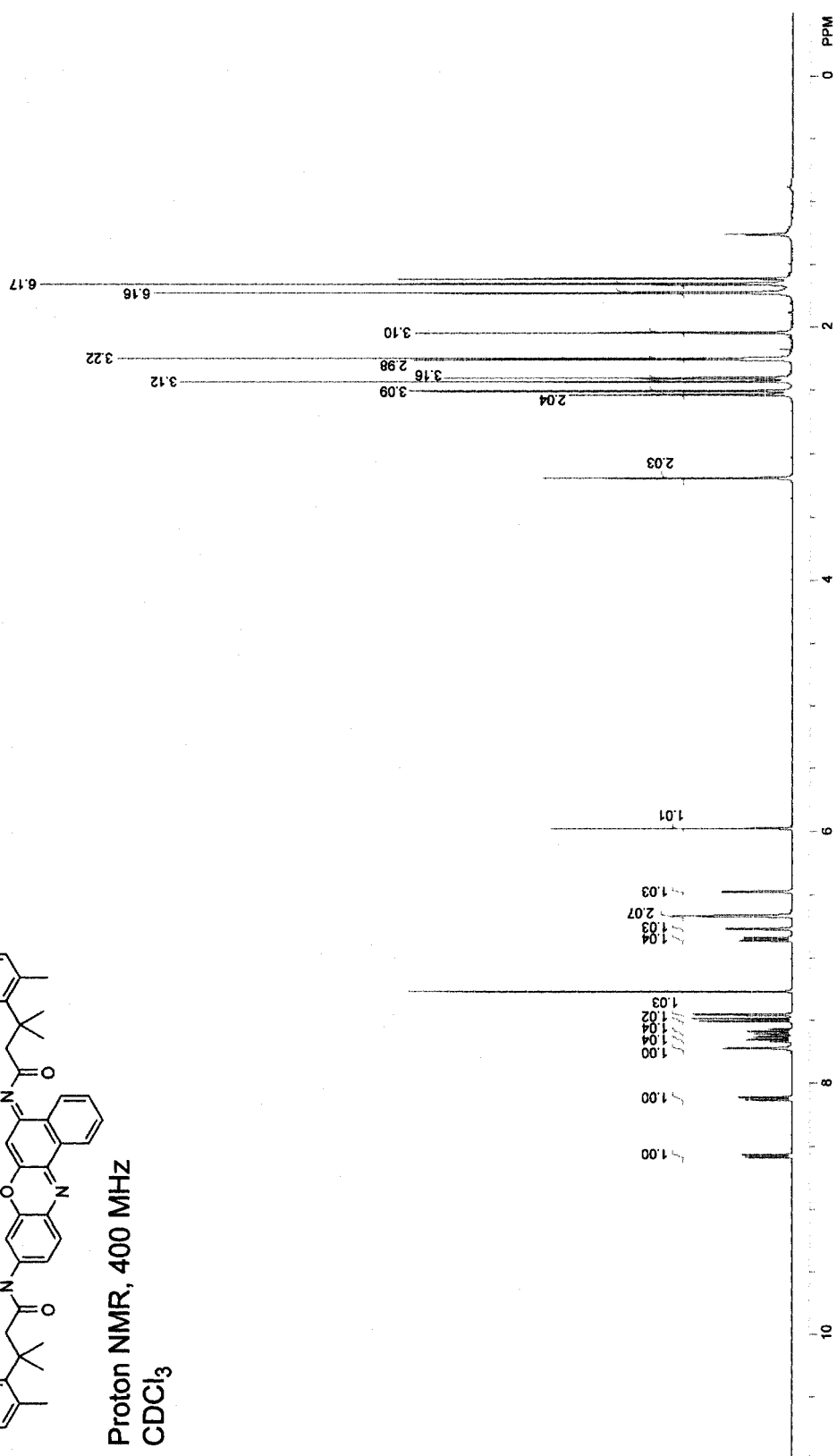


Carbon-13 NMR, 100 MHz
CDCl₃

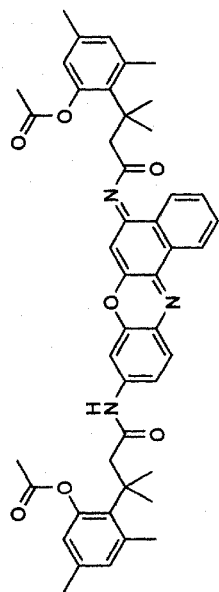


2.4

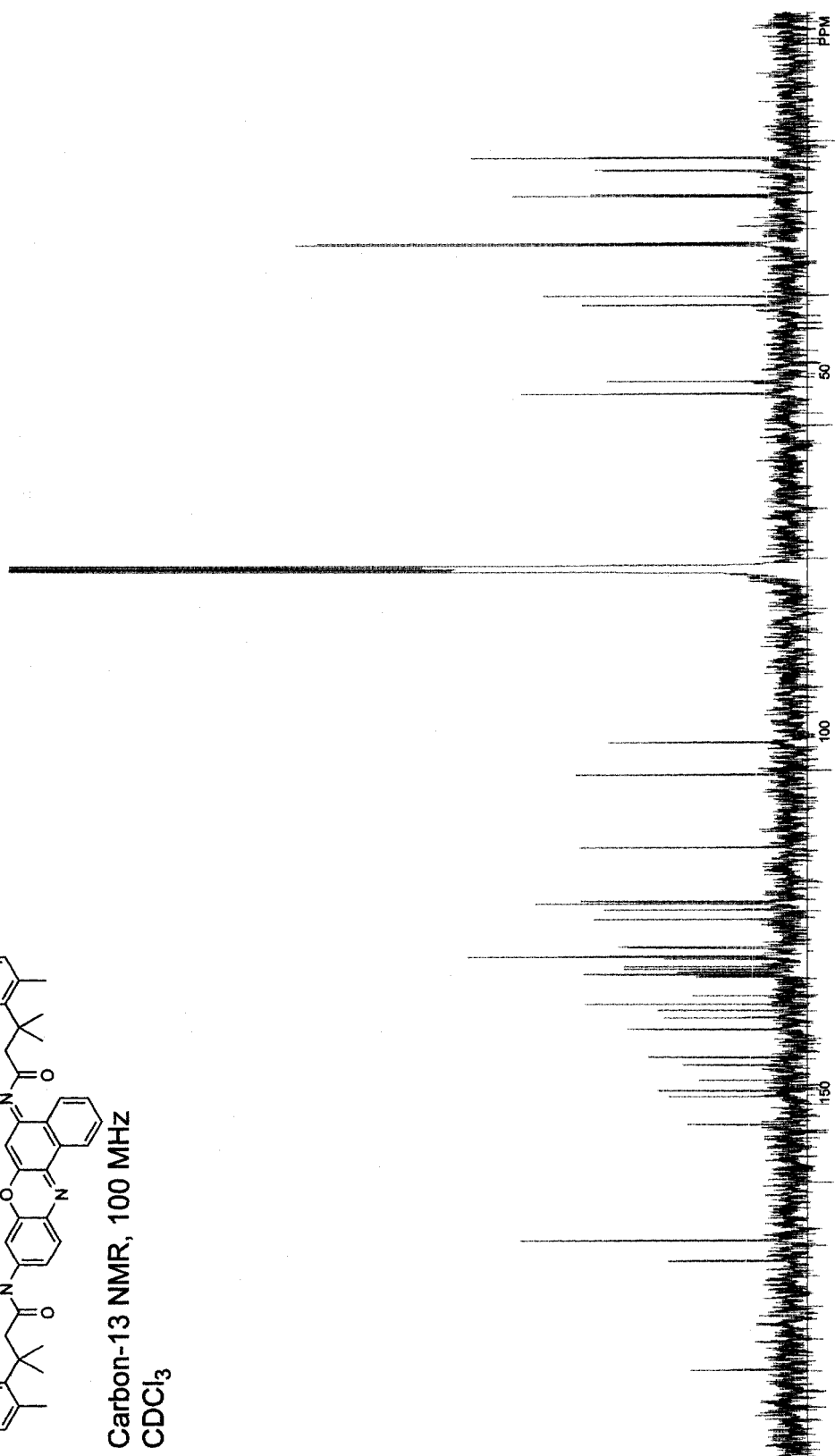
Proton NMR, 400 MHz
CDCl₃



2.4



Carbon-13 NMR, 100 MHz
CDCl₃



CHAPTER 3*

FLUOROGENIC LABEL FOR BIOMOLECULAR IMAGING

Contribution: Chemical synthesis and characterization, determination of fluorescent properties, *in vitro* enzyme assays, stability studies, composition of manuscript, and preparation of figure drafts. Protein conjugation and cellular imaging was performed by T.-Y. Chao.

***This chapter has been published, in part, under the same title. Reference:** Lavis, L. D., Chao, T.-Y., and Raines, R. T. (2006). *ACS Chem. Biol.* **1**, 252–260.

Abstract: Traditional small-molecule fluorophores are always fluorescent. That attribute can obscure valuable information in biological experiments. Here, we report on a versatile “latent” fluorophore that overcomes this limitation. At the core of the latent fluorophore is a derivative of rhodamine in which one nitrogen is modified as a urea. That modification enables rhodamine to retain half of its fluorescence while facilitating conjugation to a target molecule. The other nitrogen of rhodamine is modified with a “trimethyl lock”, which enables fluorescence to be unmasked fully by a single user-designated chemical reaction. An esterase-reactive latent fluorophore was synthesized in high yield and attached covalently to a cationic protein. The resulting conjugate was not fluorescent in the absence of esterases. The enzymatic activity of esterases in endocytic vesicles and the cytosol induced fluorescence, enabling the time-lapse imaging of endocytosis into live human cells and thus providing unprecedented spatiotemporal resolution of this process. The modular design of this “fluorogenic label” enables the facile synthesis of an ensemble of small-molecule probes for the illumination of numerous biochemical and cell biological processes.

3.1 Introduction

Fluorescent molecules are critical tools in the study of biochemical and cell biological processes (Haugland *et al.*, 2005). In many studies, however, only few of the fluorescent molecules experience a phenomenon of interest. Because traditional fluorophores, such as rhodamine and fluorescein, are always fluorescent, bulk fluorescence can obscure valuable information. To overcome this limitation, molecules can be designed such that a chemical reaction elicits a change in their fluorescence. Such “latent” fluorophores are at the core of common methods, including the enzyme linked immunosorbent assay (ELISA), high-throughput screening of enzyme inhibitors, detection of reporter genes, and evaluation of cell viability (Haugland *et al.*, 2005). We reasoned that the use of a latent fluorophore as a “fluorogenic label” could overcome limitations of traditional fluorescent labels and thereby improve the spatial and temporal resolution of bioimaging.

Recently, our laboratory reported on a new class of latent fluorophores based on the “trimethyl lock” (Chandran *et al.*, 2005; Lavis *et al.*, 2006b). The rapid lactonization (Borchardt and Cohen, 1972a; Borchardt and Cohen, 1972b; Milstein and Cohen, 1972) of the trimethyl lock had been exploited previously to prepare stable prodrugs that were unmasked by an enzyme-catalyzed reaction (Shan *et al.*, 1997; Testa and Mayer, 2003). We first used the trimethyl lock to shroud the fluorescence of a xanthene dye, rhodamine 110 (Rh₁₁₀) (Chandran *et al.*, 2005), and then an oxazine dye, cresyl violet (Lavis *et al.*, 2006b). This approach afforded highly stable bis(trimethyl lock) “profluorophores” that were labile to esterase catalysis *in vitro* and *in cellulo*.

Our bis(trimethyl lock) profluorophores had two problematic attributes. First, two chemical reactions were necessary to unveil the vast majority of their fluorescence,

decreasing the rate of fluorescence manifestation and limiting the linear range of assays (Fiering *et al.*, 1991; Urano *et al.*, 2005). Analogous fluorogenic protease substrates based on a rhodamine diamide display complex hydrolysis kinetics (Leytus *et al.*, 1983a; Leytus *et al.*, 1983b; Liu *et al.*, 1999), as we observed with our bis(trimethyl lock) profluorophores (Chandran *et al.*, 2005; Lavis *et al.*, 2006b). The second problematic attribute was the absence of a handle for target-molecule conjugation. Such a handle is available in derivatives, such as 5- or 6-carboxyrhodamine, that are accessible only from low-yielding synthetic routes.

We suspected that we could solve both problems by capping one of the amino groups of Rh₁₁₀. The capping of rhodamine dyes with an amide (Guzikowski *et al.*, 2000; Lorey *et al.*, 2002; Zhang *et al.*, 2003), carbamate (Cai *et al.*, 2001), or urea (Wang *et al.*, 2005) can preserve much of their fluorescence. We were especially intrigued by the attributes of urea–rhodamine, which according to recent reports in the scientific (Wang *et al.*, 2005) and patent (Zhang *et al.*, 2000; Diwu *et al.*, 2003) literature appears to retain significant fluorescence intensity relative to Rh₁₁₀.

Here, we report on a versatile fluorogenic label for biomolecular imaging. First, we describe the synthesis of a complete set of ureated and amidated derivatives of Rh₁₁₀, as well as a characterization of their fluorescent properties. Then, we show that imposing our trimethyl lock strategy upon a urea–rhodamine yields a stable latent fluorophore with a high rate of enzymatic hydrolysis. Finally, we demonstrate the power of our modular approach by using the urea moiety as a handle for protein conjugation and subsequent continuous imaging of endocytosis by live human cells.

3.2 Results and Discussion

3.2.1 Synthesis of Model Compounds

To gain a comprehensive understanding of the urea and amide derivatives of rhodamine, we undertook the synthesis of compounds **3.1–3.5** (Table 3.1). Rhodamine itself and these five derivatives encompass the ensemble of possible ureated and amidated derivatives. We were especially interested in those properties of **3.1–3.5** with biological implications, such as the extinction coefficient and quantum yield in aqueous solution. Previous reports (Ioffe and Otten, 1965a; Leytus *et al.*, 1983a; Leytus *et al.*, 1983b; Zhang *et al.*, 2000; Diwu *et al.*, 2003; Wang *et al.*, 2005) of similar derivatives did not provide a complete listing of relevant fluorescent characteristics.

Installation of the urea moiety to produce urea **3.1** proved to be surprisingly difficult. In our hands, the reported conditions (Wang *et al.*, 2005) involving the reaction of Rh₁₁₀ with a carbamoyl chloride using Hünig's base gave an intractable mixture of products. In contrast, we found that Rh₁₁₀ was deprotonated effectively with NaH, and that the resulting anion reacted with dimethylcarbamyl chloride to yield the desired urea **3.1**. This deprotonation strategy also proved useful for the synthesis of amide **3.2** and diurea **3.3**. The additional acetamide group in urea–amide **3.4** and diamide **3.5** were installed by reaction with acetyl chloride in the presence of a base.

3.2.2 Fluorescence Properties of Model Compounds

The absorbance and fluorescence spectra of Rh₁₁₀ and each derivative are shown in Figure 3.1. The corresponding values of λ_{max} , extinction coefficient at λ_{max} (ϵ), λ_{em} , and quantum yield (Φ) are listed in Table 3.1. We determined the relative fluorescence

intensity of these compounds by calculating the product of extinction coefficient and quantum yield and then normalizing these values to those of Rh₁₁₀. In our measurement, urea **3.1** retained 35% of the fluorescence intensity of Rh₁₁₀ with a quantum yield value of 0.49. Amide **3.2** is only 12% as fluorescent as Rh₁₁₀, which is consistent with earlier reports (Leytus *et al.*, 1983a; Leytus *et al.*, 1983b). The fluorescence of the bis-substituted dyes was largely quenched in aqueous solution. Diurea **3.3** did, however, possess significant absorbance and fluorescence compared to the urea–amide **3.4** or diamide **3.5**. These latter two rhodamine derivatives are essentially nonfluorescent.

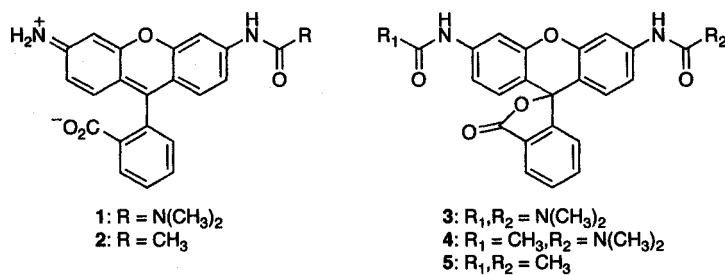
We also determined the pH-dependence of the fluorescence of urea **3.1** and amide **3.2**. The fluorescence of Rh₁₁₀ is relatively insensitive to pH values between 4 and 10 (Haugland *et al.*, 2005). This property is beneficial in biological assays, where unknown variations in pH can hamper quantitative measurements. Like Rh₁₁₀, urea **3.1** and amide **3.2** show no significant spectral change between pH values of 4 and 10 (see: Figure 3.1).

Substituent effects on the fluorescent properties of rhodamine dyes are challenging to predict or interpret due to the complexity of the rhodamine system (López Arbeloa *et al.*, 1991). In solution, rhodamine derivatives exist in equilibrium between a zwitterion that absorbs visible light and is fluorescent and a lactone that is colorless and nonfluorescent. Substitution on nitrogen can affect both this open–closed equilibrium and the spectral characteristics of the fluorescent zwitterions (Ioffe and Otten, 1965b; López Arbeloa *et al.*, 1989). We suspected that the differences in optical properties seen in compounds **3.1**–**3.5** could be rationalized, in part, through examination of the electron-donation capability of the different nitrogen substituents. According to this reasoning, weakly donating substituents would favor the colorless lactone as well as decrease the intrinsic

absorptivity of the zwitterions and, hence, the extinction coefficient. Weakly donating substituents could also reduce the quantum yield by decreasing the C–N bond-order and thereby enhancing nonradiative decay of the excited state through vibrational relaxation processes (Vogel *et al.*, 1988; López Arbeloa *et al.*, 1992).

We explored the relationship between the values of extinction coefficient and quantum yield and the Hammett σ_p substituent constants (Hansch *et al.*, 1991). An unprotonated amino group is a good electron donor ($\sigma_p = -0.66$), whereas an amide group is a relatively poor donor ($\sigma_p = 0.00$), due to amidic resonance. A urea group is peculiar—its carbonyl group is cross-conjugated and both of its nitrogens participate in amidic resonance. This cross-conjugation attenuates its electron-donating ability, as reflected in an intermediate Hammett constant ($\sigma_p = -0.26$). A plot of both extinction coefficient and quantum yield versus σ_p substituent constant for Rh₁₁₀ and monosubstituted rhodamines **3.1** and **3.2** are shown in Figure 3.3. The correlation indicates that both spectral properties are affected by electron donation from the nitrogens. A similar trend in quantum yields has been observed in substituted phenoxazinone dyes (Descalzo *et al.*, 2005).

The moderate electron-donating character of the urea moiety provides an explanation for the advantageous properties of urea **3.1**. Substitution with the cross-conjugated urea suppresses the fluorescence intensity of urea **3.1** relative to Rh₁₁₀. This decrease is not, however, as severe as seen in amide **3.2**, due to the greater electron-donating properties of the urea moiety. Still, the attenuated electron-donation allows complete suppression of fluorescence upon amidation of the remaining nitrogen in urea–amide **3.4**. Finally, the effects of electron-rich substituents on the rhodamine system are apparent again in the fluorescence of diurea **3.3** being greater than that of diamide **3.5**.

Table 3.1 Spectroscopic properties of Rh₁₁₀ and its derivatives

Dye	λ_{\max} (nm)	ϵ ($M^{-1}cm^{-1}$)	λ_{em} (nm)	Φ	$\epsilon \times \Phi$ (rel)
Rh₁₁₀	496	74,000	517	0.92	100%
3.1	492	48,600	518	0.49	35%
3.2	489	30,200	522	0.28	12%
3.3	482	3300	517	0.01	0.05%
3.4	475	400	—	—	—
3.5	~469	≤ 200	—	—	—

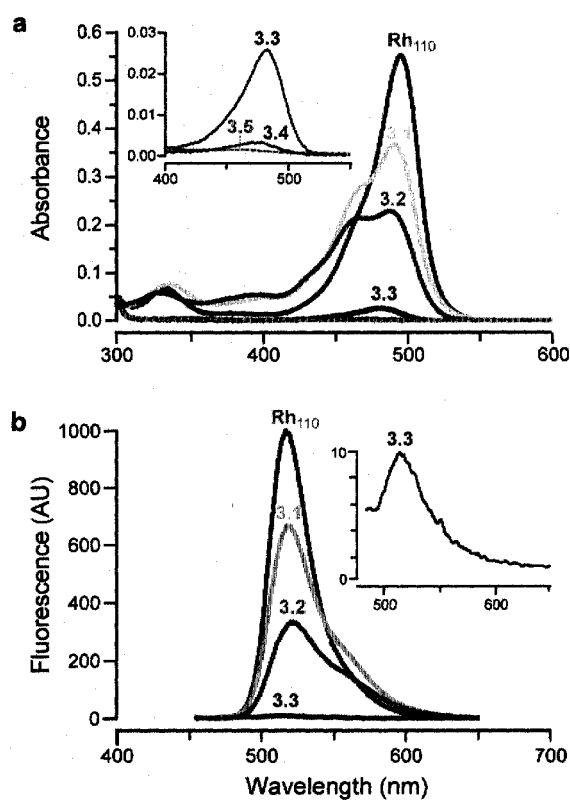


Figure 3.1 Spectra of Rh₁₁₀ and its derivatives. (a) Absorption spectra of Rh₁₁₀ and derivatives 3.1–3.5 (7.5 μ M). (b) Fluorescent emission spectra of Rh₁₁₀ and 3.1–3.3 ($\lambda_{\text{ex}} = 450$ nm, not to scale).

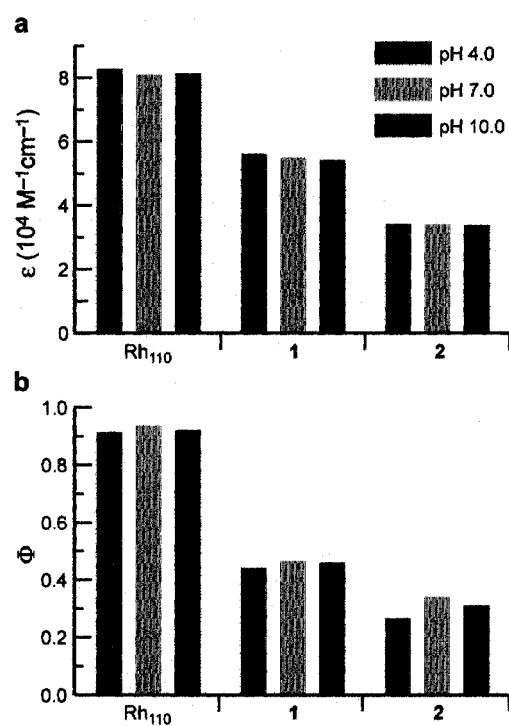


Figure 3.2 (a) Effect of pH on the extinction coefficient of Rh₁₁₀, urea 3.1, and amide 3.2. (b) Effect of pH on the quantum yield of Rh₁₁₀, urea 3.1, and amide 3.2.

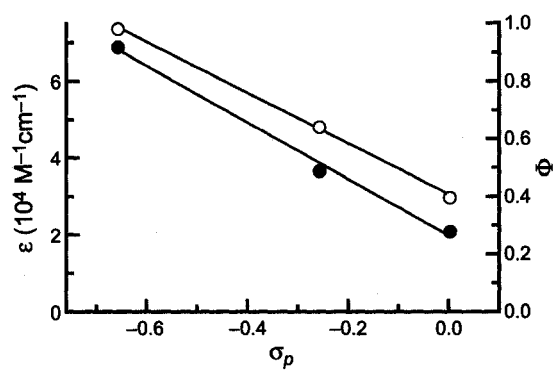


Figure 3.3 Hammett plot of extinction coefficient (\circ) and quantum yield (\bullet) versus σ_p for Rh₁₁₀, urea **3.1**, and amide **3.2**.

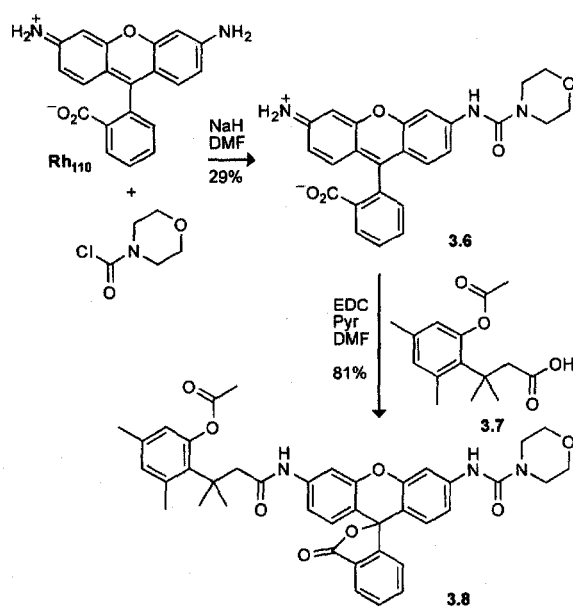
3.2.3 Synthesis of Urea–Rhodamine Trimethyl Lock

Having affirmed the desirable properties of urea–rhodamine, we next sought to apply our trimethyl lock strategy to this dye. The synthetic route to the fluorogenic substrate, which employs rhodamine morpholino-urea **3.6** (Wang *et al.*, 2005), is shown in Scheme 3.1. Again, we found that the use of Hünig's base in the synthesis afforded a mixture of products. Deprotonation of Rh₁₁₀ with NaH followed by dropwise addition of 4-morpholinecarbonyl chloride furnished rhodamine morpholino-urea **3.6**. This compound exhibited similar fluorescent characteristics to urea **3.1** (Table 3.1), having an extinction coefficient of 51,700 M⁻¹cm⁻¹ and quantum yield of 0.44. Carbodiimide coupling of rhodamine morpholino-urea **3.6** with acid **3.7** (Amsberry *et al.*, 1991) afforded the desired profluorophore **3.8**.

3.2.4 Chemical Stability

Profluorophore **3.8** must be stable in aqueous solution to be useful in biological assays. Such stability can be problematic for hydrolase substrates, as spontaneous hydrolysis can compete effectively with enzymatic activity and raise background levels. As shown in Figure 3.4, profluorophore **3.8** showed remarkable stability in both phosphate-buffered saline (PBS) and Dulbecco's modified Eagle's medium (DMEM) supplemented with 10% v/v fetal bovine serum (FBS). In contrast, fluorescein diacetate, which is a widely used esterase substrate (Rotman and Papermaster, 1966), suffered relatively rapid hydrolysis in both solutions. This dramatic increase in stability arises from the large difference in pK_a values between the conjugate acids of the two leaving groups. Specifically, fluorescein (pK_a 6.32 (Goldberg and Baldwin, 1998a)) is a much

better leaving group than is the electron-rich trimethyl-lock phenol (*o*-methylphenol has pK_a 10.28 (Fickling *et al.*, 1959)).

Scheme 3.1 Synthetic route to profluorophore **3.8**

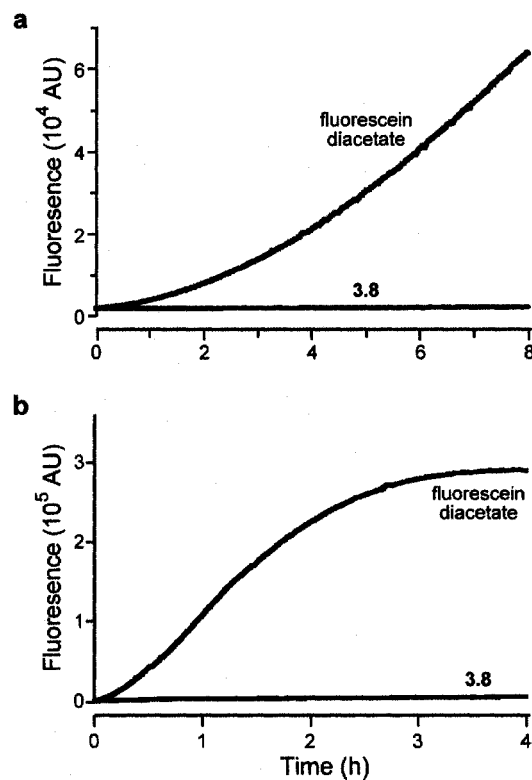


Figure 3.4 Stability of profluorophore **3.8** and fluorescein diacetate in aqueous solution. (a) Time course for the generation of fluorescence (λ_{ex} 496 nm, λ_{em} 520 nm) of profluorophore **3.8** (25 nM) and fluorescein diacetate (25 nM) in PBS. (b) Time course of the generation of fluorescence (λ_{ex} 496 nm, λ_{em} 520 nm) of profluorophore **3.8** (25 nM) and fluorescein diacetate (25 nM) in DMEM containing FBS (10% v/v).

3.2.5 Enzymatic Reactivity

An objective in the design of profluorophore **3.8** was to improve its reactivity as an esterase substrate relative to the original bis(trimethyl lock) rhodamine substrate. The appearance of fluorescence upon reaction of porcine liver esterase (PLE) with profluorophore **3.8** was indicative of single-hit kinetics (Figure 3.5). The kinetic constants were calculated to be $k_{\text{cat}}/K_{\text{M}} = 8.2 \times 10^5 \text{ M}^{-1}\text{s}^{-1}$ and $K_{\text{M}} = 0.10 \text{ }\mu\text{M}$. Comparison with the apparent kinetic constants from the original bis(trimethyl lock) rhodamine substrate (Chandran *et al.*, 2005) ($k_{\text{cat}}/K_{\text{M}} = 1.9 \times 10^3 \text{ M}^{-1}\text{s}^{-1}$ and $K_{\text{M}} = 0.47 \text{ }\mu\text{M}$) shows a 430-fold increase in $k_{\text{cat}}/K_{\text{M}}$ value. A more appropriate comparison takes into account the expected 65% decrease in fluorescence of urea **3.6** (Table 3.1), which is the hydrolysis product of profluorophore **3.8**, relative to Rh₁₁₀. After this adjustment, latent fluorophore performance is still enhanced by 150-fold.

The substantial increase in catalytic efficiency is likely due to the change from the double-hit kinetics observed for the bis-substituted substrate to the single-hit kinetics of profluorophore **3.8**. Hydrolysis of the bis-substituted fluorogenic substrate progresses from diamide to free Rh₁₁₀ via a monoamide intermediate, with the unmasking of the second amino group producing the majority (<90%) of the fluorescence (Leytus *et al.*, 1983a; Leytus *et al.*, 1983b). In contrast, the urea–rhodamine substrate requires only a single cleavage event for the complete manifestation of fluorescence.

3.2.6 Cellular Imaging

Having established the high chemical stability and enzymatic reactivity of profluorophore **3.8**, we next evaluated the behavior of this compound in live human cells.

Profluorophore **3.8** was incubated with HeLa cells and imaged using confocal fluorescence microscopy. As shown in Figure 3.6a, the substrate was activated *in cellulo* by endogenous esterases to produce diffuse green cytosolic staining. Importantly, the high chemical stability of the fluorogenic probe allowed for its imaging in the cytosol without an intermediate washing step. Counter-staining with LysoTracker Red showed significant but incomplete colocalization, suggesting that after hydrolysis, a portion of the free urea–rhodamine localized in acidic vesicles (yellow color in Figure 3.6b). To ensure that the fluorescence increase was due to trimethyl lock activation and not hydrolysis of the urea moiety, we incubated HeLa cells with the relatively non-fluorescent diurea-rhodamine **3.5**. In these experiments we observed virtually no intracellular fluorescence (see: Figure 3.7).

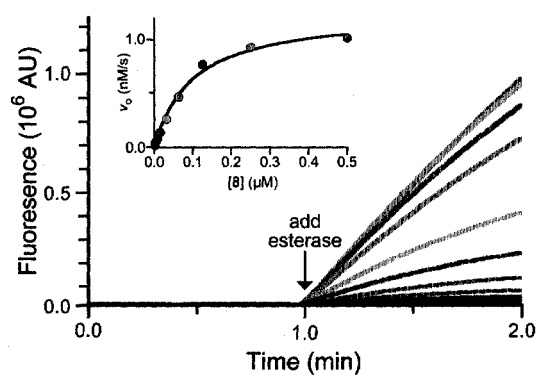


Figure 3.5 Kinetic traces (λ_{ex} 496 nm, λ_{em} 520 nm) and Michaelis–Menten plot (inset) of a serial dilution of profluorophore **3.8** (0.5 μ M \rightarrow 2 nM) with PLE (2.5 μ g/mL).

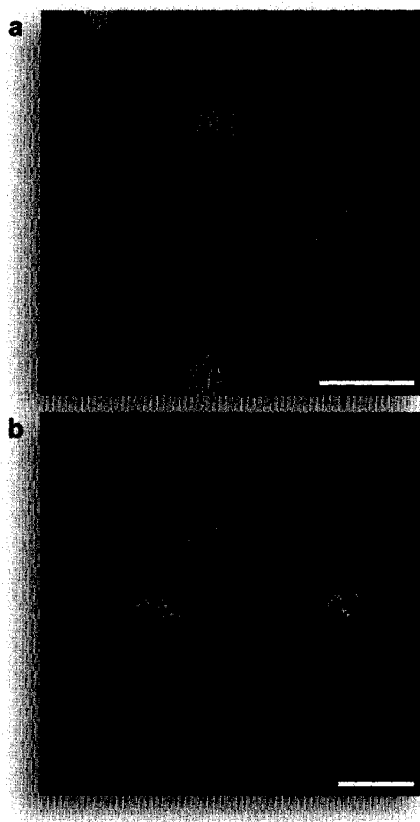


Figure 3.6 Unmasking of profluorophore **3.8** in live human cells. (a) Unwashed HeLa cells incubated for 1 h with profluorophore **3.8** (10 μ M) at 37 °C in DMEM and counter-stained with Hoechst 33342. (b) Washed HeLa cells incubated for 1 h with profluorophore **3.8** (10 μ M) at 37 °C in DMEM and counter-stained with Hoechst 33342 and LysoTracker Red (5% v/v CO₂(g), 100% humidity). Scale bar: 20 μ m.



Figure 3.7 Unwashed HeLa cells incubated for 1 h with diurea **3.3** (10 μ M) at 37 °C in DMEM (5% v/v CO₂(g), 100% humidity) and counter-stained with Hoechst 33342. Scale bar: 20 μ m.

3.2.7 Fluorogenic Label

The high chemical stability and rapid *in cellulo* unmasking of profluorophore **3.8** prompted us to develop a derivative for bioconjugation. We reasoned that such a fluorogenic label would be stable enough to survive conjugation and purification protocols while still providing a strong signal for continuous biological experiments. It is noteworthy that simple fluorescein diesters have found only limited use as fluorogenic labels (Laurent *et al.*, 1997; Bergsdorf *et al.*, 2003; Drobni *et al.*, 2003; Kamal *et al.*, 2004), as fluorescein diesters suffer from low chemical stability in aqueous solution (Figure 3.4).

Developing profluorophore **3.8** into a fluorogenic label requires the installation of a functional group with selective reactivity. We chose to install the maleimide functionality (Ji, 1983; Aslam and Dent, 1998), which react rapidly with thiol groups (Bednar, 1990). The resulting conjugates are stable (Yoshitake *et al.*, 1979), even after the slow hydrolysis of the nascent sulfosuccinimidyl ring (Ishii and Lehrer, 1986).

Traditionally, reactive groups are attached to the pendant carboxyphenyl ring of rhodamine and fluorescein dyes (Haugland *et al.*, 2005). Synthesis of these compounds requires difficult chromatographic steps to obtain isomerically pure compounds (Jiao *et al.*, 2003). We envisioned a facile and economical alternative involving the attachment of a maleimide derivative via the desirable urea functionality. Although uncommon, bioconjugation via the amino groups of rhodamines has been used previously (Corrie *et al.*, 1998; Lorey *et al.*, 2002; Meunier and Wilkinson, 2002). This strategy allows for the use of commercially available (and relatively inexpensive) Rh₁₁₀ as the starting material for the synthesis of maleimidourea–rhodamine trimethyl lock **3.13**, as shown in

Scheme 3.2. Desymmetrization of Rh₁₁₀ was accomplished by its deprotonation with NaH and reaction with Boc₂O to give *t*-Boc–rhodamine **3.9**. An isocyanate was generated *in situ* from maleimide **3.10** by a Curtius rearrangement (Curtius, 1890; Curtius, 1894), and that isocyanate was reacted with *t*-Boc–rhodamine **3.9** to generate a urea (Scriven and Turnbull, 1988; Bräse *et al.*, 2005). Deprotection of maleimidourea–rhodamine–*t*-Boc **3.11** with TFA afforded fluorescent urea–rhodamine **3.12**. Condensation with **3.7** using EDC gave thiol-reactive fluorogenic label **3.13**.

3.2.8 Bioconjugation

To test the utility of fluorogenic label **3.13** in a biological experiment, we attached it to a thiol-containing variant of bovine pancreatic ribonuclease (RNase A (Raines, 1998)). RNase A is a cationic protein that is internalized by mammalian cells via endocytosis (Haigis and Raines, 2003). This internalization is critical to the action of cytotoxic RNase A variants and homologs (Haigis *et al.*, 2003). Fluorogenic label **3.13** reacted cleanly with the A19C variant of RNase A to give a mono-substituted conjugate as determined by MALDI mass spectrometry. This protein conjugate was stable to purification by cation-exchange chromatography at pH 5.0 and showed a 1200-fold increase in fluorescence upon incubation with PLE (data not shown).

At physiological pH, the protein conjugate was less stable than unconjugated profluorophore **3.8**. Spontaneous hydrolysis of the acetate ester was slow but significant in PBS, presumably because conjugation to the protein places the probe in close proximity to nucleophilic functional groups of the protein. Storage at pH 5.0 did,

however, extend the stability of the conjugate, allowing multiple experiments to be performed with one preparation.

3.2.9 Cellular Imaging with a Bioconjugate

Fluorescently labeled biomolecules have been used to image endocytotic events (Watson *et al.*, 2005). We sought to determine the efficacy of our fluorogenic label approach by comparing endocytosis of HeLa cells incubated with Oregon Green-labeled RNase A (Haigis and Raines, 2003) to that of cells incubated with the protein conjugated with fluorogenic label **3.13**. As shown in Figure 3.8a, the Oregon Green conjugate showed intense extracellular background signal that obscures the fluorescence from endocytosed material. This background could be eliminated only with many vigorous washing steps (Figure 3.8b). In contrast, the profluorophore conjugate allowed imaging without intermediate washing steps. As shown in Figure 3.8c, unwashed HeLa cells incubated with the RNase A conjugate have bright, punctate staining, indicative of the conjugate being localized in small vesicles. Counterstaining with LysoTracker Red shows a large degree of colocalization (Figure 3.8d), suggesting that the latent conjugate is internalized via endocytosis and activated by endosomal or lysosomal esterases (Leinweber, 1987; Runquist and Havel, 1991; Hornick *et al.*, 1992). Images with the protein conjugate (Figure 3.8c) are less diffuse and more punctate than are images with free profluorophore **3.8** (Figure 3.6), which has much more ready access to the cytosol. To ensure that the signal in Figure 3.8c is due to unmasked fluorophore attached to RNase A, we fixed cells incubated with our latent conjugate and counterstained them with a primary antibody to RNase A and a secondary antibody labeled with

AlexaFluor 594. In a fluorescence microscopy image, we observed a significant overlap of the green and red fluorescent signals to produce a yellow signal, indicating that the unmasked RNase A conjugate is largely intact (see: Figure 3.9).

The high chemical stability and low background fluorescence of the fluorogenic label conjugate allowed for the time-lapse imaging of its endocytosis. Cells were incubated with the fluorogenic label **3.13**–RNase A conjugate at room temperature, and images were recorded without washing during the next 90 min. The compilation of these images into a movie revealed that internalization of the conjugate occurred continuously and that vesicular fluorescence increased monotonically (data not shown).

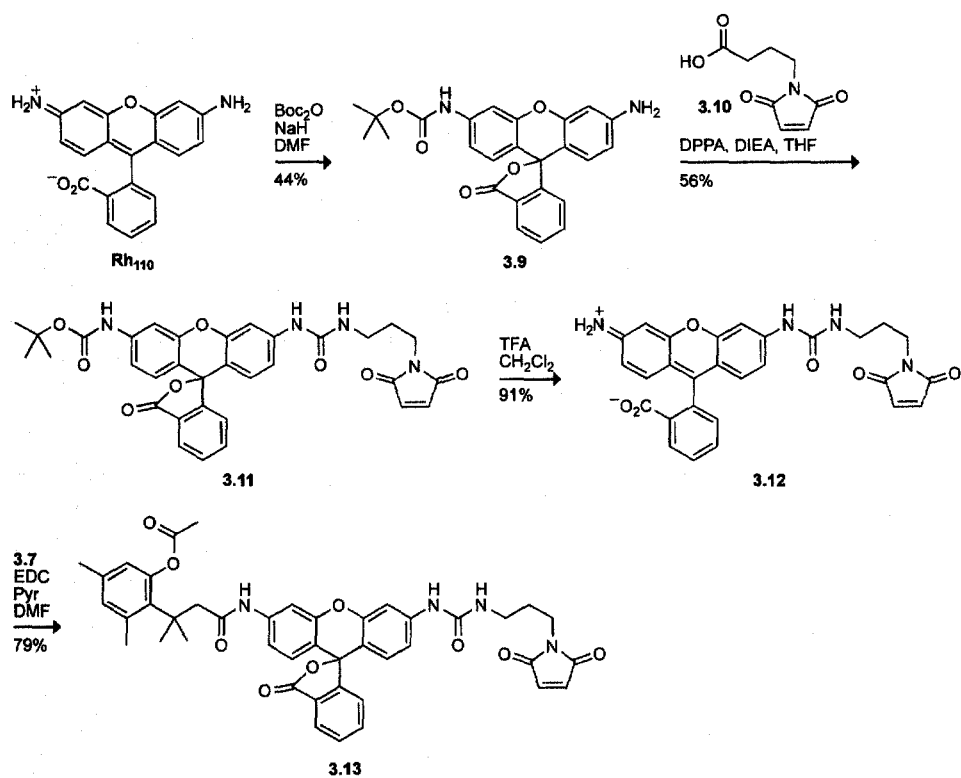
Scheme 3.2 Synthetic route to fluorogenic label **3.13**

Figure 3.8 Live-cell imaging experiments with protein conjugates. (a) Unwashed HeLa cells incubated for 1 h with Oregon Green–RNase A conjugate (10 μ M) at 37 °C in DPBS and counter-stained with Hoechst 33342. (b) Washed HeLa cells incubated for 1 h with Oregon Green–RNase A conjugate (10 μ M) at 37 °C in DPBS and counter-stained with Hoechst 33342. (c) Unwashed HeLa cells incubated for 1 h with fluorogenic label **3.13**–RNase A conjugate (10 μ M) at 37 °C in DPBS and counter-stained with Hoechst 33342. (d) Washed HeLa cells incubated for 1 h with fluorogenic label **3.13**–RNase A conjugate (10 μ M) at 37 °C in DPBS and counter-stained with Hoechst 33342 and LysoTracker Red (5% v/v CO₂(g), 100% humidity). Scale bar: 20 μ m.

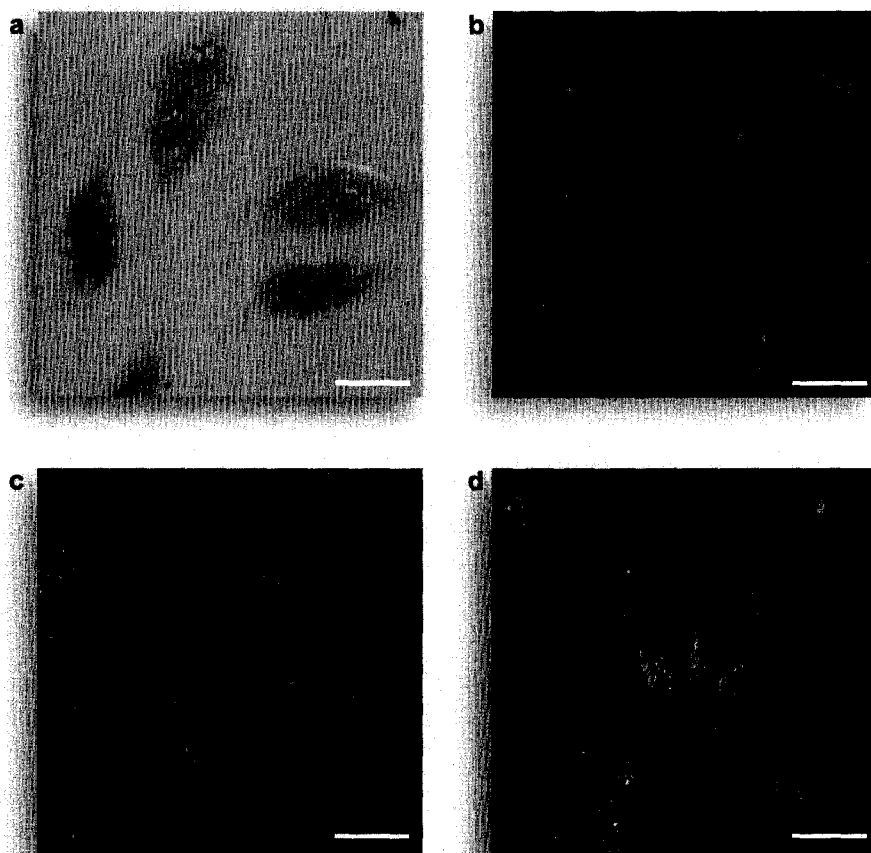




Figure 3.9 HeLa cells incubated for 1 h with the fluorogenic label **3.13**–RNase A conjugate (10 μ M) at 37°C in DMEM (5% v/v CO₂(g), 100% humidity). Cells were fixed with 4% paraformaldehyde, washed extensively, and counter-stained with a primary antibody to RNase A and secondary antibody labeled with AlexaFluor 594. Cells were imaged on a Nikon Eclipse E800 fluorescence microscope (Melville, NY) equipped with a Photometrics CoolSnap HQ cooled CCD camera (Roper Scientific, Tucson, AZ). Excitation light was provided by a mercury lamp. Scale bar: 20 μ m.

3.3 Envoi

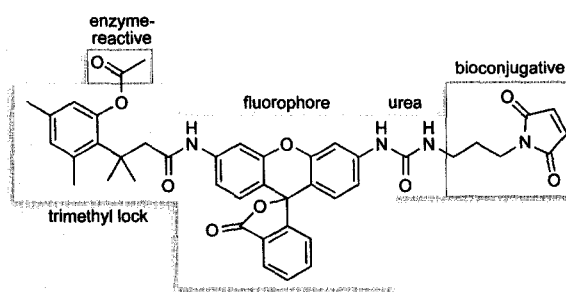
We have demonstrated how a common fluorophore, Rh₁₁₀, can be elaborated into a powerful new tool for biochemistry and cell biology. The use of a trimethyl lock provides a latent fluorophore with high chemical stability while maintaining enzymatic reactivity (Chandran *et al.*, 2005; Lavis *et al.*, 2006b). The use of a urea group (rather than a second trimethyl lock) improves enzymatic reactivity markedly while preserving desirable fluorescence properties, as in profluorophore **3.8**. The elaboration of the urea to include an electrophile outfits the latent fluorophore for conjugation, as in fluorogenic label **3.13**. Conjugation of this fluorogenic label to a target molecule enables, for example, the continuous imaging of the endocytosis of a target molecule by live human cells.

We note that the urea–rhodamine–trimethyl lock probe can be tailored to suit a variety of applications (Scheme 3.3). For example, modification of the enzyme-reactive group on the trimethyl lock could be used to detect the entry of a conjugate into a particular compartment within a cell. Alteration of the bioconjugative group on the urea moiety could be used to change conjugation chemistry, enhance cellular internalization, or target a conjugate to a specific subcellular location. In addition, the fluorogenic label strategy could transcend cultured cells and allow continuous imaging in tissues or *in vivo*. These goals are facilitated by inventories of the enzymes in various organs and organelles (Foster *et al.*, 2006; Kislinger *et al.*, 2006). This versatility will enable the development of specific probes for biological experiments of ever-increasing sophistication.

3.4 Acknowledgments

We are grateful to K.A. Dickson for preliminary bioimaging experiments and S.S. Chandran, Z. Diwu, and M.B. Soellner for contributive discussions. L.D.L was supported by Biotechnology Training Grant 08349 (NIH). This work was supported by Grant CA73808 (NIH). The University of Wisconsin–Madison Biophysics Instrumentation Facility was established with grants BIR-9512577 (NSF) and RR13790 (NIH). NMRFAM was supported by grant P41RR02301 (NIH).

Scheme 3.3 Modules in fluorogenic label **3.13**



3.5 Experimental Section

3.5.1 General Experimental: Chemical Synthesis

Rh₁₁₀ (sold as Rhodamine 560) was obtained from Exciton (Dayton, OH). Dimethylformamide, tetrahydrofuran, and dichloromethane were drawn from a Baker CYCLE-TAINER solvent delivery system. All other reagents were obtained from Aldrich Chemical (Milwaukee, WI) or Fisher Scientific (Hanover Park, IL) and used without further purification. Thin-layer chromatography was performed using aluminum-backed plates coated with silica gel containing F₂₅₄ phosphor and visualized by UV illumination or developed with I₂, ceric ammonium molybdate, or phosphomolybdic acid stain. Flash chromatography was performed using open columns with silica gel-60 (230–400 mesh), or on a FlashMaster Solo system (Argonaut Inc., Redwood City, CA) with Isolute Flash Si II columns (International Sorbent Technology Ltd., Hengoed, Mid Glamorgan, UK).

NMR spectra were obtained with a Bruker DMX-400 Avance spectrometer at the National Magnetic Resonance Facility at Madison (NMRFAM). Mass spectrometry was performed with a Micromass LCT (electrospray ionization, ESI) mass spectrometer at the Mass Spectrometry Facility in the Department of Chemistry or with a Perkin–Elmer Voyager (matrix assisted laser desorption ionization, MALDI) mass spectrometer in the Biophysics Instrumentation Facility.

3.5.2 Synthesis of Compounds 3.1–3.6 and 3.8–3.13

Dimethylurea-Rh₁₁₀ (3.1). Rh₁₁₀ (500 mg, 1.363 mmol) was dissolved in anhydrous DMF (50 mL) under Ar(g). NaH (98 mg, 4.089 mmol) was added slowly, and the resulting purple solution was stirred at ambient temperature for 1 h. Dimethylcarbamyl chloride (138 μ L, 1.499 mmol) was added dropwise, and the reaction mixture was stirred at ambient temperature for 24 h. The reaction was quenched with a few drops of glacial acetic acid and solvent was removed under reduced pressure. The residue was partially purified by flash chromatography (silica gel, 0–6% v/v gradient of MeOH in CH₂Cl₂). The partially pure compound was recrystallized from MeOH to yield compound **3.1** as a red powder (93 mg, 17%). ¹H NMR (400 MHz, DMSO-*d*₆) δ (ppm): 8.54 (bs, 1H), 7.97 (d, *J* = 7.5 Hz, 1H), 7.78 (td, *J* = 7.5, 1.1 Hz, 1H), 7.70 (td, *J* = 7.5, 0.7 Hz, 1H), 7.63 (d, *J* = 2.1 Hz, 1H), 7.25 (d, *J* = 7.6 Hz, 1H), 7.12 (dd, *J* = 8.9, 2.1 Hz, 1H), 6.56 (d, *J* = 8.9 Hz, 1H), 6.44 (d, *J* = 1.8 Hz, 1H), 6.36 (d, *J* = 8.5 Hz, 1H), 6.32 (dd, *J* = 8.5, 1.9 Hz, 1H), 5.64 (bs, 2H), 2.93 (s, 6H). ¹³C NMR (100 MHz, DMSO-*d*₆) δ (ppm): 168.85, 155.35, 152.53, 152.08, 151.32, 151.18, 142.92, 135.45, 129.89, 128.49, 127.63, 126.44, 124.49, 124.01, 115.12, 111.82, 111.10, 105.96, 105.35, 99.14, 83.83, 36.25 (2C). HRMS (ESI): *m/z* 402.1440 (MH⁺ [C₂₃H₂₀N₃O₄] = 402.1454).

Monoacetamide-Rh₁₁₀ (3.2). Rh₁₁₀ (500 mg, 1.363 mmol) was dissolved in anhydrous DMF (15 mL) under Ar(g). NaH (65 mg, 2.73 mmol) was added slowly, and the resulting brown solution was stirred at ambient temperature for 1 h. Acetic anhydride (107 μ L, 1.136 mmol) was added dropwise in anhydrous DMF (1.0 mL), and the reaction mixture was stirred for 24 h. The reaction was quenched with a few drops of glacial acetic acid and the solvent was removed under reduced pressure. The residue was

partially purified by flash chromatography (silica gel, 0–5% v/v gradient of MeOH in CH₂Cl₂). This crude compound was further purified by flash chromatography (silica gel, 5% v/v MeOH in CH₂Cl₂). Compound **3.2** was isolated as an orange solid (188 mg, 44%). ¹H NMR (400 MHz, DMSO-*d*₆) δ (ppm): 10.20 (bs, 1H), 7.98 (d, *J* = 7.7 Hz, 1H), 7.79 (m, 2H), 7.70 (td, *J* = 7.4, 0.8 Hz, 1H), 7.26 (d, *J* = 7.6 Hz, 1H), 7.07 (dd, *J* = 8.6, 2.2 Hz, 1H), 6.64 (d, *J* = 8.6 Hz, 1H), 6.45 (d, *J* = 1.8 Hz, 1H), 6.37 (d, *J* = 8.5 Hz, 1H), 6.33 (dd, *J* = 8.6, 2.0 Hz, 1H), 5.67 (bs, 2H), 2.06 (s, 3H). ¹³C NMR (100 MHz, DMSO-*d*₆) δ (ppm): 168.87, 168.78, 152.47, 151.95, 151.36, 151.16, 141.15, 135.50, 129.99, 128.50, 128.25, 126.33, 124.55, 123.99, 114.64, 113.41, 111.25, 106.00, 105.18, 99.11, 83.49, 24.10. HRMS (ESI): *m/z* 373.1177 (MH⁺ [C₂₂H₁₇N₂O₄] = 373.1188).

Bis(dimethylurea)–Rh₁₁₀ (3.3). Rh₁₁₀ (500 mg, 1.363 mmol) was dissolved in anhydrous DMF (50 mL) under Ar(g). NaH (134 mg, 5.589 mmol) was added slowly, and the resulting brown solution was stirred at ambient temperature for 1 h. Dimethylcarbamyl chloride (250 μ L, 2.73 mmol) was added dropwise and the mixture was stirred at ambient temperature for 24 h. The reaction was quenched with a few drops of glacial acetic acid and solvent was removed under reduced pressure. The residue was purified by flash chromatography (silica gel, EtOAc). Compound **3.3** was isolated as an off-white solid (359 mg, 56%). ¹H NMR (400 MHz, DMSO-*d*₆) δ (ppm): 8.58 (bs, 2H), 8.01 (d, *J* = 7.4 Hz, 1H), 7.79 (td, *J* = 7.4, 1.3 Hz, 1H), 7.72 (td, *J* = 7.5, 0.9 Hz, 1H), 7.66 (d, *J* = 2.3 Hz, 2H), 7.28 (d, *J* = 7.6 Hz, 1H), 7.18 (dd, *J* = 8.8, 2.1 Hz, 2H), 6.62 (d, *J* = 8.8 Hz, 2H), 2.93 (s, 12H). ¹³C NMR (100 MHz, DMSO-*d*₆) δ (ppm): 168.79, 155.33 (2C), 152.63, 150.89 (2C), 143.14 (2C), 135.65, 130.10, 127.75 (2C), 125.97, 124.69,

123.97, 115.44 (2C), 111.36 (2C), 105.95 (2C), 82.65, 36.24 (4C). HRMS (ESI): m/z 473.1831 (MH^+ [$C_{26}H_{25}N_4O_5$] = 473.1825).

Monoacetamide-Monourea-Rh₁₁₀ (3.4). Dimethylurea-Rh₁₁₀ **3.1** (66 mg, 0.164 mmol) was dissolved in anhydrous DMF (1.0 mL) and anhydrous pyridine (1.0 mL) under Ar(g). Acetyl chloride (94 μ L, 1.32 mmol) was added, and the reaction mixture was stirred at ambient temperature for 5 h. Solvent was removed under reduced pressure, and the residue dissolved in CH_2Cl_2 . This solution was washed with 5% HCl and saturated brine. The organic layer was then dried over anhydrous $MgSO_4(s)$, and the solvent was removed under reduced pressure. The residue was purified by flash chromatography (silica gel, EtOAc) to give the compound **3.4** as a pale yellow solid (43 mg, 59%). 1H NMR (400 MHz, $CDCl_3$) δ (ppm): 8.59 (bs, 1H), 7.95 (d, J = 6.7 Hz, 1H), 7.58 (m, 2H), 7.31 (d, J = 1.4 Hz, 1H), 7.28 (d, J = 1.9 Hz, 1H), 7.19 (d, J = 8.6 Hz, 1H), 7.07 (bs, 1H), 7.03 (dd, J = 8.8, 2.1 Hz, 1H), 6.98 (d, J = 7.2 Hz, 1H), 6.61 (d, J = 8.7 Hz, 1H), 6.58 (d, J = 8.8 Hz, 1H), 3.00 (s, 6H), 2.08 (s, 3H). ^{13}C NMR (100 MHz, $CDCl_3$) δ (ppm): 170.11, 169.29, 155.72, 153.09, 151.55, 151.46, 141.68, 140.36, 135.35, 129.81, 128.12, 128.00, 126.15, 124.83, 124.13, 116.07, 115.58, 113.66, 112.49, 107.88, 107.60, 83.45, 36.51 (2C), 24.34. HRMS (ESI): m/z 466.1398 (MNa^+ [$C_{25}H_{21}N_3O_5Na$] = 466.1379).

Diacetamide-Rh₁₁₀ (3.5). Rh₁₁₀ (200 mg, 0.545 mmol) was dissolved in anhydrous DMF (2.0 mL) and anhydrous pyridine (2.0 mL) under Ar(g). Acetyl chloride (0.311 mL, 4.36 mmol) was added dropwise, and the reaction mixture was stirred at ambient temperature for 24 h. The solution was poured into ice water containing 5% v/v HCl and the pale pink precipitate was collected by filtration. The crude product was purified by

flash chromatography (silica gel, EtOAc). Compound **3.5** was isolated as an off-white solid (135 mg, 60%). ^1H NMR (400 MHz, $\text{DMSO-}d_6$) δ (ppm): 10.24 (bs, 2H), 8.02 (d, $J = 7.5$ Hz, 1H), 7.84 (d, $J = 1.9$ Hz, 2H), 7.79 (td, $J = 7.4, 1.3$ Hz, 1H), 7.73 (td, $J = 7.5, 0.9$ Hz, 1H), 7.28 (d, $J = 7.4$ Hz, 1H), 7.14 (dd, $J = 8.7, 2.2$ Hz, 2H), 6.72 (d, $J = 8.7$ Hz, 2H), 2.07 (s, 6H). ^{13}C NMR (100 MHz, $\text{DMSO-}d_6$) δ (ppm): 168.91 (2C), 168.66, 152.53, 150.82 (2C), 141.41 (2C), 135.76, 130.21, 128.36 (2C), 125.71, 124.75, 123.98, 115.13 (2C), 112.84 (2C), 106.04 (2C), 81.97, 24.09 (2C). HRMS (ESI): m/z 437.1127 (MNa^+ [$\text{C}_{24}\text{H}_{18}\text{N}_2\text{O}_5\text{Na}$] = 437.1113).

Morpholinourea-Rh₁₁₀ (3.6). Rh₁₁₀ (500 mg, 1.36 mmol) was dissolved in anhydrous DMF (50 mL) under Ar(g). NaH (67 mg, 2.86 mmol) was added portion-wise, and the resulting purple-brown solution was stirred at ambient temperature for 1 h. 4-Morpholinecarbonyl chloride (0.156 mL, 1.36 mmol) was added dropwise and the mixture was stirred for 24 h. Solvent was removed under reduced pressure and the residue was purified by flash chromatography (silica gel, 100:7:1 v/v/v CHCl_3 :MeOH:AcOH). The purification gave compound **3.6** as a red-orange crystalline solid (176 mg, 29%). ^1H NMR (400 MHz, $\text{DMSO-}d_6$) δ (ppm): 8.80 (bs, 1H), 7.97 (d, $J = 7.9$ Hz, 1H), 7.78 (td, $J = 7.4, 1.4$ Hz, 1H), 7.70 (td, $J = 7.5, 0.6$ Hz, 1H), 7.62 (d, $J = 2.6$ Hz, 1H), 7.25 (d, $J = 7.4$ Hz, 1H), 7.09 (dd, $J = 8.6, 1.8$ Hz, 1H), 6.58 (d, $J = 9.1$ Hz, 1H), 6.44 (d, $J = 2.0$ Hz, 1H), 6.36 (d, $J = 8.2$ Hz, 1H), 6.32 (dd, $J = 8.5, 2.2$ Hz, 1H), 5.65 (bs, 2H), 3.60 (m, 4H), 3.43 (m, 4H). ^{13}C NMR (100 MHz, $\text{DMSO-}d_6$) δ (ppm): 168.86, 154.78, 152.55, 152.06, 151.31, 151.12, 142.64, 135.46, 129.94, 128.50, 127.81, 126.42, 124.52, 124.02, 115.01, 112.08, 111.14, 105.97, 105.33, 99.15, 83.74, 65.95 (2C), 44.17 (2C). HRMS (ESI): m/z 444.1570 (MH^+ [$\text{C}_{25}\text{H}_{22}\text{N}_3\text{O}_5$] = 444.1559).

Morpholinourea-Rh₁₁₀ Trimethyl Lock (3.8). Compound **3.6** (54 mg, 0.122 mmol) was dissolved in a mixture of anhydrous DMF (0.9 mL) and anhydrous pyridine (0.6 mL) under Ar(g). To this solution was added EDC (47 mg, 0.244 mmol) and 3-(2'-acetoxy-4',6'-dimethylphenyl)-3,3-dimethylpropanoic acid **3.7** (Amsberry *et al.*, 1991) (64 mg, 0.244 mmol). The resulting solution was stirred for 48 h at ambient temperature. Solvent was removed under reduced pressure, and the residue was taken up in CH₂Cl₂. This solution was washed with 5% HCl and saturated brine. The organic layer was dried over anhydrous MgSO₄(s), and the solvent was removed under reduced pressure. The pale orange residue was purified by flash chromatography (silica gel, 2:1 EtOAc:hexanes) to give compound **3.8** as a pale yellow solid (68 mg, 81%). ¹H NMR (400 MHz, CDCl₃) δ (ppm): 7.97 (m, 1H), 7.63 (td, *J* = 7.4, 1.3 Hz, 1H), 7.58 (td, *J* = 7.4, 1.2 Hz, 1H), 7.55 (bs, 1H), 7.39 (d, *J* = 2.2 Hz, 1H), 7.36 (d, *J* = 2.0 Hz, 1H), 7.08 (m, 2H), 6.94 (dd, *J* = 8.6, 1.9 Hz, 1H), 6.90 (bs, 1H), 6.79 (d, *J* = 1.4 Hz, 1H), 6.65 (dd, *J* = 8.6, 2.1 Hz, 1H), 6.63 (d, *J* = 1.5 Hz, 1H), 6.57 (d, *J* = 8.7 Hz, 1H), 6.55 (d, *J* = 8.6 Hz, 1H), 3.69 (m, 4H), 3.48 (m, 4H), 2.59 (ABq, *J* = 13.4 Hz, 2H), 2.42 (s, 3H), 2.37 (s, 3H), 2.23 (s, 3H), 1.68 (s, 3H), 1.67 (s, 3H). ¹³C NMR (100 MHz, CDCl₃) δ (ppm): 172.11, 169.96, 169.89, 154.74, 153.22, 151.66, 151.59, 150.05, 141.34, 140.08, 139.02, 137.28, 135.17, 133.19, 132.87, 129.71, 128.15, 128.09, 126.24, 124.87, 124.06, 123.45, 115.52, 115.16, 113.68, 112.76, 107.43 (2C), 83.25, 66.47 (2C), 51.03, 44.27 (2C), 40.35, 32.16, 32.11, 25.51, 21.94, 20.17. HRMS (ESI): *m/z* 712.2657 (MNa⁺ [C₄₀H₃₉N₃O₈Na] = 712.2635).

***t*-Boc-Rh₁₁₀ (3.9).** Rh₁₁₀ (403 mg, 1.10 mmol) was dissolved in anhydrous DMF (15 mL) under Ar(g). NaH (53 mg, 2.20 mmol) was added slowly, and the resulting brown solution was stirred for 1 h. Di-*tert*-butyl dicarbonate (200 mg, 0.916 mmol) was

added, and the reaction mixture was stirred at ambient temperature for 24 h. The reaction was quenched with a few drops of glacial acetic acid and the solvent was removed under reduced pressure. The orange solid was taken up into 80 mL of CH₂Cl₂:MeOH (1:1 v/v) and filtered to remove unreacted Rh₁₁₀ (98 mg). The mother liquor was concentrated under reduced pressure and the residue was purified by flash chromatography (silica gel, 5:3:2 v/v/v hexanes:CH₂Cl₂:EtOAc). *t*-Boc-Rh₁₁₀ was isolated as an orange powder (171 mg, 43%). ¹H NMR (400 MHz, DMSO-*d*₆) δ (ppm): 9.65 (bs, 1H), 7.97 (d, *J* = 8.1 Hz, 1H), 7.78 (td, *J* = 7.4, 1.5 Hz, 1H), 7.70 (td, *J* = 7.5, 0.7 Hz, 1H), 7.52 (d, *J* = 1.8 Hz, 1H), 7.24 (d, *J* = 7.9 Hz, 1H), 7.09 (dd, *J* = 8.8, 2.5 Hz, 1H), 6.59 (d, *J* = 8.8 Hz, 1H), 6.43 (d, *J* = 1.9 Hz, 1H), 6.36 (d, *J* = 8.5 Hz, 1H), 6.32 (dd, *J* = 8.5, 2.4 Hz, 1H), 5.66 (bs, 2H), 1.48 (s, 9H). ¹³C NMR (100 MHz, DMSO-*d*₆) δ (ppm): 168.84, 152.64, 152.52, 151.98, 151.36, 151.30, 141.61, 135.46, 129.93, 128.49, 128.22, 126.34, 124.54, 124.00, 113.93, 112.55, 111.21, 105.26, 104.93, 99.08, 83.55, 79.64, 28.03 (3C). HRMS (ESI): *m/z* 431.1593 (MH⁺ [C₂₅H₂₃N₂O₅] = 431.1607).

4-Maleimidobutyric Acid (3.10). 4-Aminobutyric acid (20.0 g, 194 mmol) was dissolved in glacial acetic acid (250 mL). Maleic anhydride (19.0 g, 194 mmol) was added, and the mixture was heated at reflux for 4 h with removal of the condenser for the final 20 min to allow escape of H₂O. The reaction mixture was concentrated under reduced pressure, and residual acetic acid was removed by its azeotrope with toluene. Purification by flash chromatography (silica gel, CH₂Cl₂) gave the compound **3.10** as a white crystalline solid (12.6 g, 35%). ¹H NMR (400 MHz, DMSO-*d*₆) δ (ppm): 7.00 (s, 2H), 3.42 (t, *J* = 6.8 Hz, 2H), 2.20 (t, *J* = 7.3 Hz, 2H), 1.71 (p, *J* = 7.0 Hz, 2H). ¹³C NMR

(100 MHz, DMSO- d_6) δ (ppm): 173.82, 171.17 (2C), 134.50 (2C), 36.58, 30.84, 23.41.

HRMS (ESI): m/z 182.0456 (M-H [$C_8H_8NO_4$] = 182.0453).

Maleimidourea-Rh₁₁₀-*t*-Boc (3.11). 4-Maleimidobutyric acid **3.10** (162 mg, 0.885 mmol) was dissolved in anhydrous THF (2.0 mL) under Ar(g). Hünig's base (0.206 mL, 1.180 mmol) was added followed by diphenylphosphoryl azide (244 mg, 0.885 mmol). The resulting solution was stirred at ambient temperature for 4 h, and the reaction mixture was then heated at reflux for 1 h. *t*-Boc-Rh₁₁₀ **3.9** (127 mg, 0.295 mmol) was then added in anhydrous THF (2.0 mL), and the reaction mixture was heated at reflux for 18 h. Solvent was removed under reduced pressure, and the residue was purified by flash chromatography (silica gel, 60% v/v EtOAc in hexanes). The purification gave compound **3.11** as a pale yellow crystalline solid (101 mg, 56%). 1H NMR (400 MHz, CDCl₃) δ (ppm): 7.99 (d, J = 7.0 Hz, 1H), 7.68 (bs, 1H), 7.63 (td, J = 7.4, 1.3 Hz, 1H), 7.58 (td, J = 7.4, 1.1 Hz, 1H), 7.36 (d, J = 1.8 Hz, 1H), 7.17 (bs, 1H), 7.13 (d, J = 1.7 Hz, 1H), 7.05 (m, 2H), 6.94 (dd, J = 8.8, 2.0 Hz, 1H), 6.64 (d, J = 8.8 Hz, 1H), 6.63 (s, 2H), 6.53 (d, J = 8.5 Hz, 1H), 5.87 (t, J = 5.8 Hz, 1H), 3.52 (t, J = 6.6 Hz, 2H), 3.17 (m, 2H), 1.75 (p, J = 6.6 Hz, 2H), 1.51 (s, 9H). ^{13}C NMR (100 MHz, CDCl₃) δ (ppm): 170.91 (2C), 170.36, 155.44, 153.15, 152.66, 151.77, 151.54, 141.71, 140.83, 135.41, 134.04 (2C), 129.78, 128.47, 128.13, 126.16, 124.91, 124.08, 114.98, 114.18, 112.59, 111.69, 106.32, 106.19, 84.03, 80.95, 37.07, 35.07, 28.86, 28.30 (3C). HRMS (ESI): m/z 611.2147 (MH⁺ [$C_{33}H_{31}N_4O_8$] = 611.2142).

Maleimidourea-Rh₁₁₀ (3.12). Maleimidourea-Rh₁₁₀-*t*-Boc **3.11** (123 mg, 0.201 mmol) was dissolved in a mixture of CH₂Cl₂ (8 mL) and TFA (2 mL). The resulting solution was stirred at 0°C for 10 min and ambient temperature for 90 min. Solvent was

removed under reduced pressure, and the residue was purified by flash chromatography (silica gel, 5% v/v MeOH in CH₂Cl₂). Compound **3.12** was isolated as an orange crystalline solid (94 mg, 91%). ¹H NMR (400 MHz, DMSO-*d*₆) δ (ppm): 8.89 (bs, 1H), 7.97 (d, *J* = 7.8 Hz, 1H), 7.78 (td, *J* = 7.5, 1.2 Hz, 1H), 7.70 (td, *J* = 7.5, 0.9 Hz, 1H), 7.63 (d, *J* = 1.9 Hz, 1H), 7.25 (d, *J* = 7.6 Hz, 1H), 7.02 (s, 2H), 6.86 (dd, *J* = 8.9, 2.2 Hz, 1H), 6.54 (d, *J* = 8.7 Hz, 1H), 6.43 (d, *J* = 2.2 Hz, 1H), 6.36 (d, *J* = 8.3 Hz, 1H), 6.32 (dd, *J* = 8.6, 2.0 Hz, 1H), 6.26 (t, *J* = 5.9 Hz, 1H), 5.65 (bs, 2H), 3.44 (t, *J* = 7.0 Hz, 2H), 3.06 (q, *J* = 6.4 Hz, 2H), 1.66 (p, *J* = 6.9 Hz, 2H). ¹³C NMR (100 MHz, DMSO-*d*₆) δ (ppm): 171.18 (2C), 168.83, 154.92, 152.52, 152.09, 151.40, 151.31, 142.58, 135.42, 134.53 (2C), 129.90, 128.47, 128.10, 126.44, 124.46, 124.03, 113.56, 111.36, 111.10, 105.31, 104.23, 99.14, 83.86, 36.63, 34.92, 28.80. HRMS (ESI): *m/z* 511.1605 (MH⁺ [C₂₈H₂₃N₄O₆] = 511.1617).

Maleimidourea–Rh₁₁₀ Trimethyl Lock (3.13). Maleimidourea–Rh₁₁₀ **3.12** (24 mg, 0.047 mmol) was dissolved in a mixture of anhydrous DMF (1.0 mL) and anhydrous pyridine (1.0 mL) under Ar(g). EDC (18 mg, 0.094 mmol) and 3-(2'-acetoxy-4',6'-dimethylphenyl)-3,3-dimethylpropanoic acid **3.7** (Amsberry *et al.*, 1991) (15 mg, 0.094 mmol) were added, and the reaction mixture was stirred at ambient temperature for 24 h. Solvent was removed under reduced pressure, and the pale orange residue was purified by flash chromatography (silica gel, 0–30% v/v gradient of EtOAc in hexanes). Compound **3.13** was isolated as an off-white crystalline solid (28 mg, 79%). ¹H NMR (400 MHz, CDCl₃) δ (ppm): 8.00 (d, *J* = 6.9 Hz, 1H), 7.68 (bs, 1H), 7.64 (td, *J* = 7.4, 1.3 Hz, 1H), 7.60 (td, *J* = 7.5, 1.0 Hz, 1H), 7.38 (d, *J* = 1.9 Hz, 1H), 7.29 (bs, 1H), 7.12 (d, *J* = 2.2 Hz, 1H), 7.07 (d, *J* = 7.2 Hz, 1H), 7.04 (dd, *J* = 8.7, 2.2 Hz, 1H), 6.81 (d, *J* = 1.8

Hz, 1H), 6.69 (s, 2H), 6.69 (dd, $J = 8.6, 2.2$ Hz, 1H), 6.64 (d, $J = 1.6$ Hz, 1H), 6.58 (d, $J = 8.6$ Hz, 1H), 6.57 (d, $J = 8.7$ Hz, 1H), 5.66 (t, $J = 5.9$ Hz, 1H), 3.60 (t, $J = 6.5$ Hz, 2H), 3.21 (q, $J = 6.3$ Hz, 2H), 2.64 (ABq, $J = 13.5$ Hz, 2H), 2.45 (s, 3H), 2.39 (s, 3H), 2.24 (s, 3H), 1.81 (p, $J = 6.5$ Hz, 2H), 1.70 (s, 3H), 1.69 (s, 3H). ^{13}C NMR (100 MHz, CDCl_3) δ (ppm): 172.02, 170.98 (2C), 170.20, 170.12, 155.02, 153.18, 151.56, 151.51, 149.99, 141.63, 139.97, 138.94, 137.25, 135.22, 134.14 (2C), 133.16, 132.90, 129.72, 128.23 (2C), 126.24, 124.93, 124.08, 123.43, 115.20, 114.98, 113.72, 111.94, 107.55, 106.39, 83.58, 50.95, 40.31, 36.93, 35.03, 32.09, 32.06, 28.85, 25.55, 21.92, 20.16. HRMS (ESI): m/z 779.2715 (MNa^+ [$\text{C}_{43}\text{H}_{40}\text{N}_4\text{O}_9\text{Na}$] = 779.2693).

3.5.3 General Spectroscopic Methods

HEPES (2[4-(2-hydroxyethyl)-1-piperazinyl]ethanesulfonic acid) was from Research Products International. Fluorescein (reference standard grade) was from Molecular Probes. Other reagents were from Sigma–Aldrich or Fisher Scientific. Phosphate-buffered saline, pH 7.4 (PBS) contained (in 1.00 liter) KCl (0.20 g), KH_2PO_4 (0.20 g), NaCl (8.0 g), and $\text{Na}_2\text{HPO}_4 \cdot 7\text{H}_2\text{O}$ (2.16 g). All measurements were recorded at ambient temperature (23 ± 2 °C) and buffers were not degassed prior to measurements. Compounds were prepared as stock solutions in DMSO and diluted such that the DMSO concentration did not exceed 1% v/v. Porcine liver esterase (PLE; MW = 163 kDa (Horgan *et al.*, 1969)) was obtained from Sigma Chemical (product number E2884) as a suspension in 3.2 M $(\text{NH}_4)_2\text{SO}_4$, and was diluted to appropriate concentrations in PBS before use. In pH-dependency studies, the pH of PBS was adjusted by additions of 1.0 M HCl or 1.0 M NaOH and measured using a Beckmann glass electrode that was calibrated

prior to each use. Graphs were manipulated and parameters were calculated with Microsoft Excel 2003 and GraphPad Prism 4.

3.5.4 Ultraviolet–Visible and Fluorescence Spectroscopy

Absorption spectra were recorded in 1-cm path length cuvettes having a volume of 1.0 or 3.5 mL on a Cary Model 50 spectrometer from Varian. The extinction coefficients were measured in 10 mM HEPES–NaOH buffer, pH 7.5. Fluorometric measurements were made using fluorescence grade quartz or glass cuvettes from Starna Cells and a QuantaMaster1 photon-counting spectrofluorometer from Photon Technology International equipped with sample stirring. The quantum yields of Rh₁₁₀ and compounds **3.1–3.5** were measured with dilute samples ($A \leq 0.1$) in 10 mM HEPES–NaOH buffer, pH 7.5. These values were obtained by the comparison of the integrated area of the emission spectrum of the samples with that of fluorescein in 0.1 M NaOH, which has a quantum efficiency of 0.95 (Lakowicz, 1999). The concentration of the fluorescein reference was adjusted to match the absorbance of the test sample at the excitation wavelength. Under these conditions, quantum yields were calculated by using eq 3.1.

$$\Phi_{\text{sample}} = \Phi_{\text{standard}} (\int F_{\text{em, sample}} / \int F_{\text{em, standard}}) \quad (3.1)$$

3.5.5 Protein Purification and Labeling

The TNB-protected A19C variant of RNase A and the Oregon Green-labeled RNase A conjugate were prepared as described previously (Haigis and Raines, 2003). The TNB-protected protein was deprotected with a three-fold molar excess of dithiothreitol (DTT)

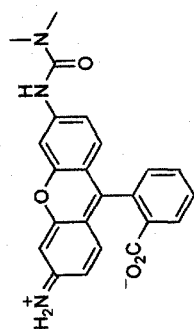
and desalted by chromatography using a HiTrap Desalting column (Amersham). The protein conjugate then was prepared by reaction with ten-fold molar excess of thiol-reactive maleimide **3.13** for 16 h at 4 °C. Purification by chromatography using a HiTrap HP SP column (Amersham) afforded the desired conjugate (MS (MALDI): m/z 14,468 (expected: 14,475)). Protein concentration was determined by using a bicinchoninic acid (BCA) assay kit from Pierce with wild-type RNase A as a standard.

3.5.6 Cell Preparation

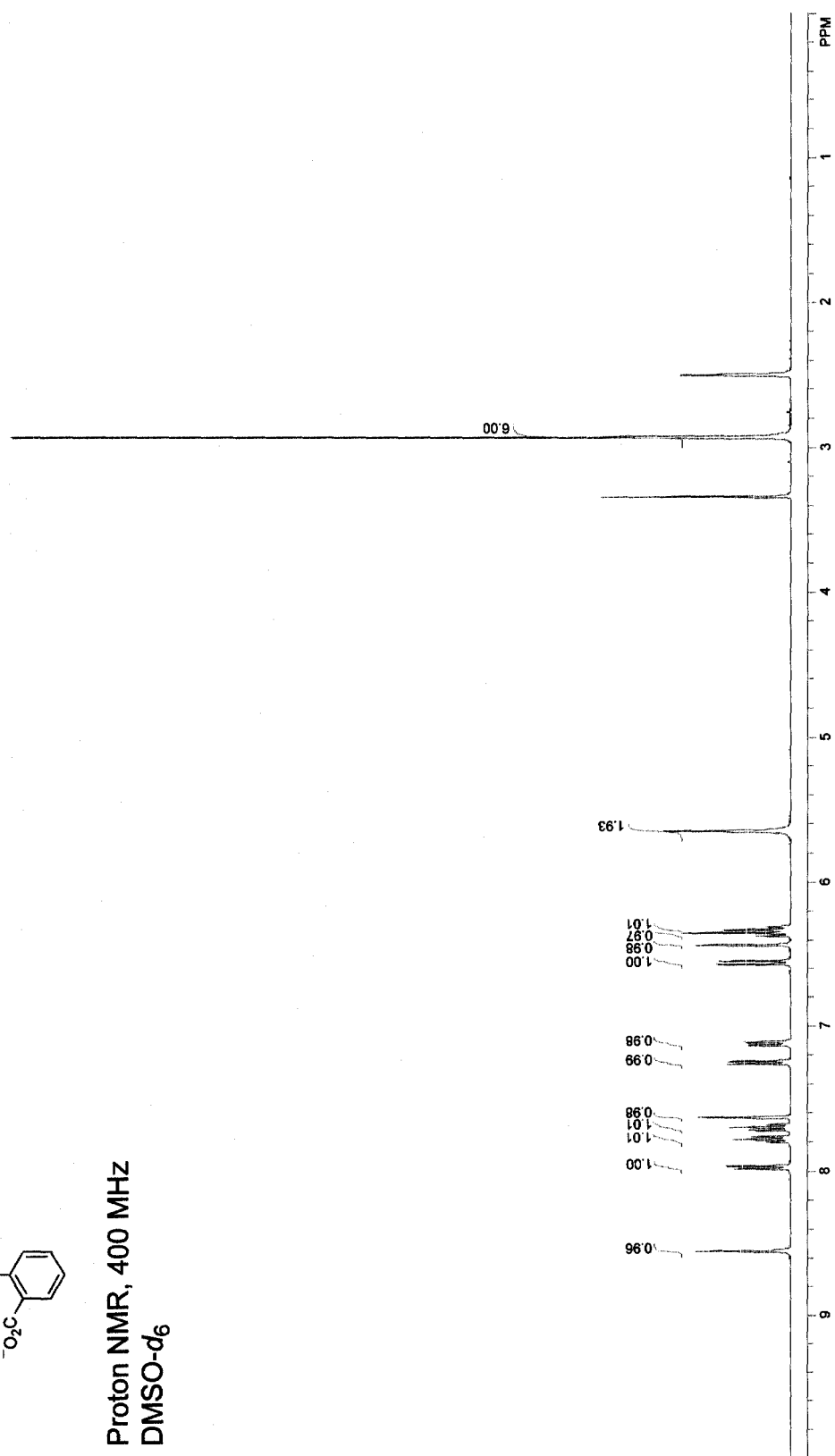
HeLa cells were plated on Nunc Lab-Tek II 8-well Chamber Coverglass (Fisher Scientific) and grown to 70–80% confluence at 37 °C in DMEM (Invitrogen) containing FBS (10% v/v). For static imaging, cells were first washed with Dulbecco's phosphate-buffered saline (DPBS, Invitrogen). Cells were then incubated with profluorophore **3.8** (10 μ M), RNase A conjugated to maleimide **3.13** (10 μ M), or Oregon Green-labeled RNase A (10 μ M) for 1 h at 37 °C prior to imaging. Nuclear staining was accomplished by addition of Hoechst 33342 (2 μ g/mL) for the final 5 min of incubation. Lysosomal staining involved washing the cells with DPBS followed by incubation with 100 nM LysoTracker Red (Molecular Probes) in DPBS for 1 min at ambient temperature. For dynamic imaging, cells were incubated with Hoechst 33342 (2 μ g/mL) for 5 min at 37 °C, and then washed twice with DPBS. Profluorophore **3.13**–RNase A conjugate (10 μ M) was added to the cells at ambient temperature (23 \pm 2 °C). Imaging of endocytosis started within 1 min after the addition of the conjugate.

3.5.7 Cell Imaging

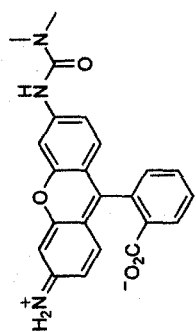
Cells were imaged on a Nikon Eclipse TE2000-U confocal microscope equipped with a Zeiss AxioCam digital camera, unless indicated otherwise. Excitation at 408 nm was provided by a blue-diode laser, and emission light was passed through a filter centered at 450 nm with a 35-nm band-pass. Excitation at 488 nm was provided by an argon-ion laser and emission light was passed through a filter centered at 515 nm with a 40-nm band-pass. Excitation at 543 nm was provided by a HeNe laser, and emission light was passed through a filter centered at 605 nm with a 75-nm band-pass. For time-lapse imaging, 1 image/min was recorded during the first 30 min of incubation, 2 images/min were recorded during the next 10 min, and 5 images/min were recorded during the last 50 min. The resulting movie condenses these 300 images recorded over 90 min into 40 s. Brightfield images indicated that the cells were alive and appeared to have normal physiology, both before and after the time-lapse imaging.

3.1

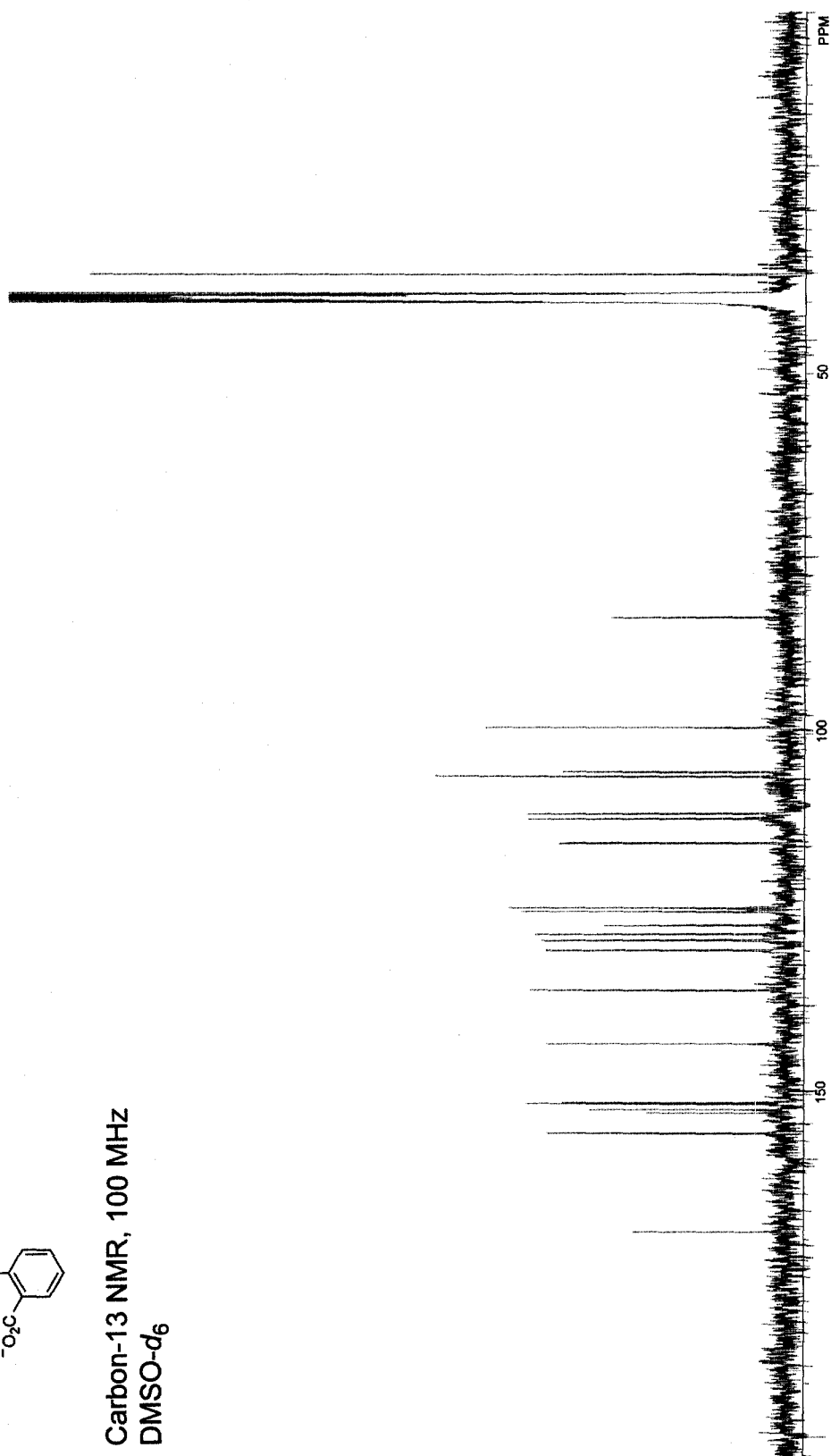
Proton NMR, 400 MHz
DMSO- d_6



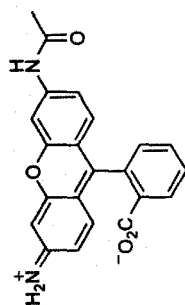
3.1



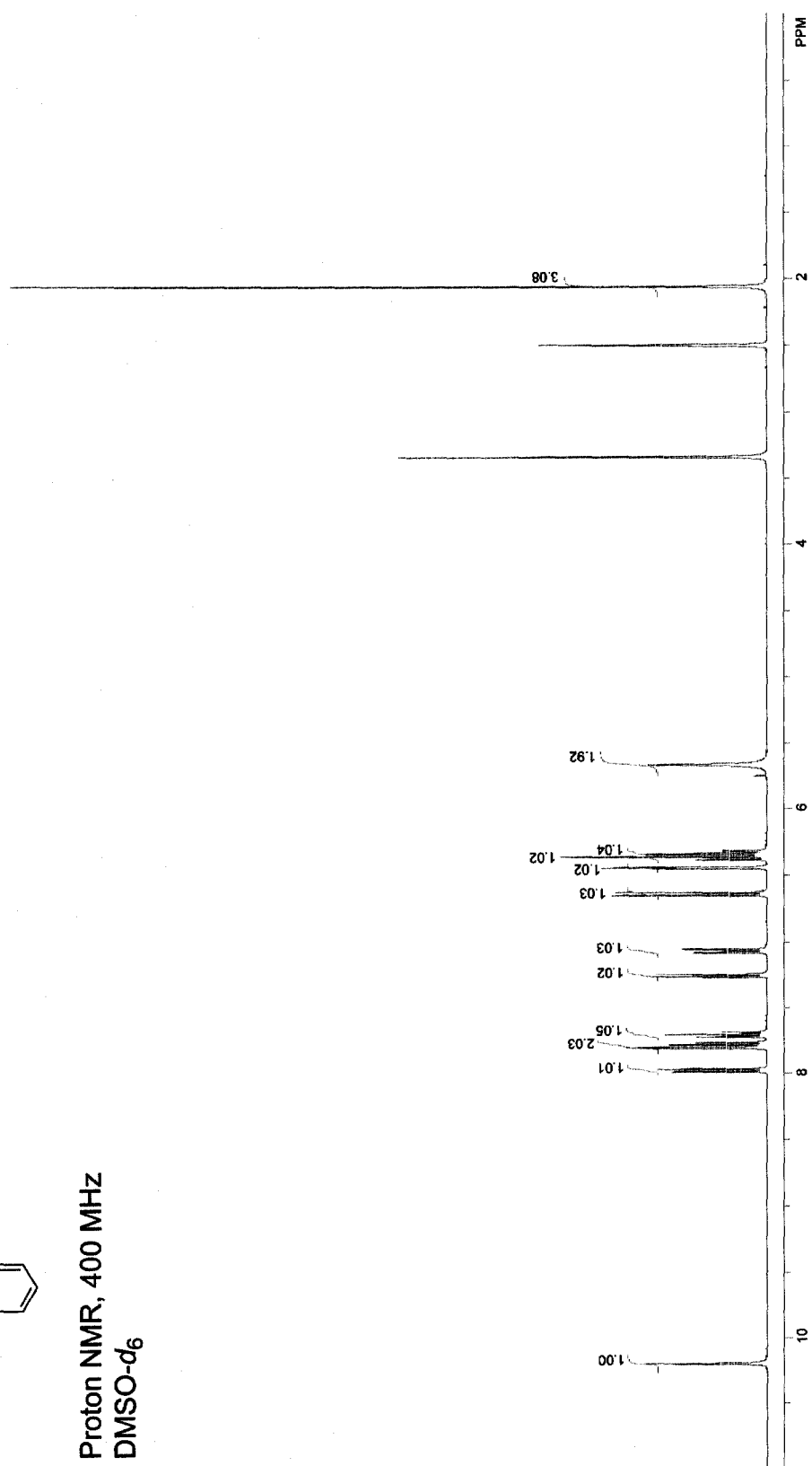
Carbon-13 NMR, 100 MHz
DMSO-*d*₆



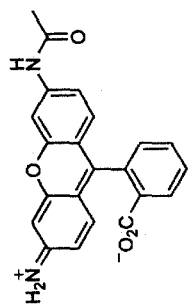
3.2



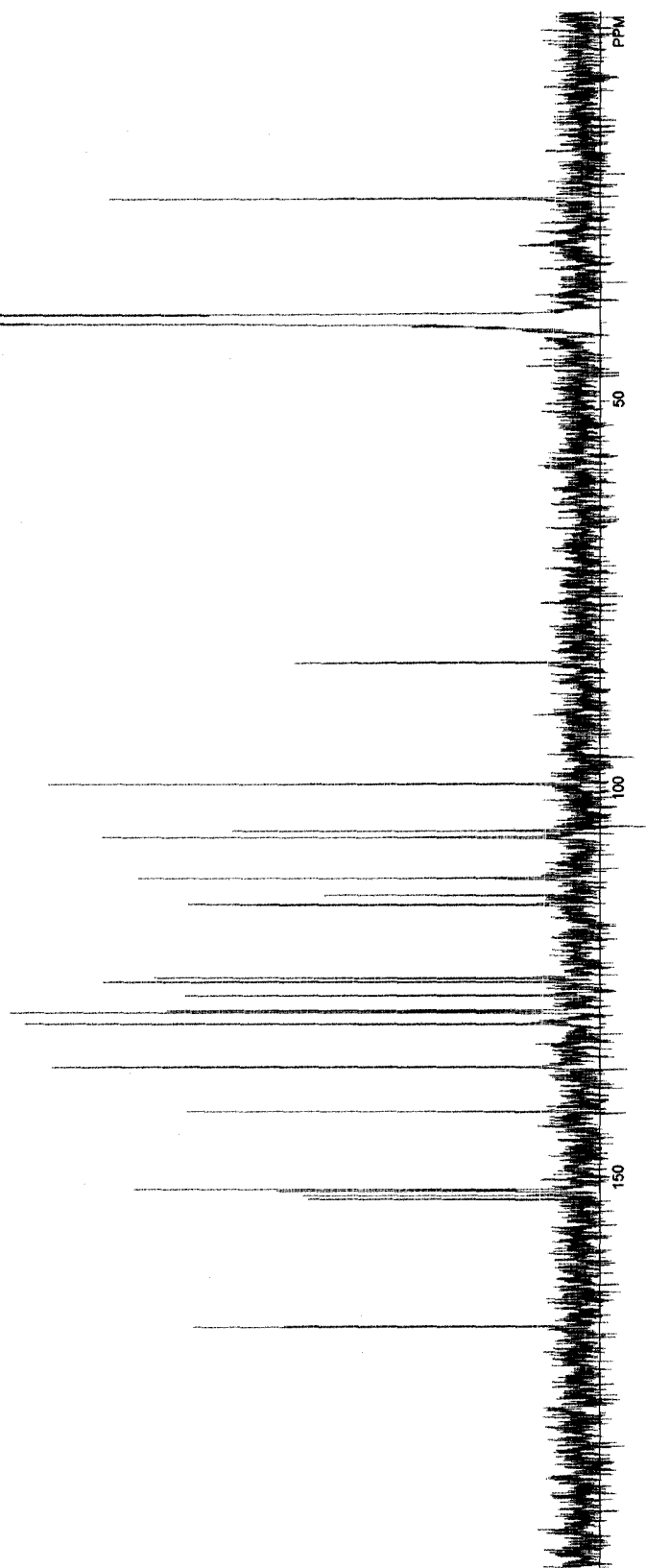
Proton NMR, 400 MHz
DMSO-*d*₆



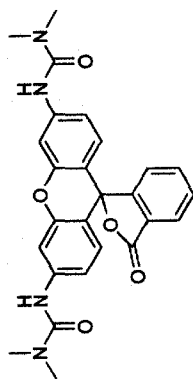
3.2



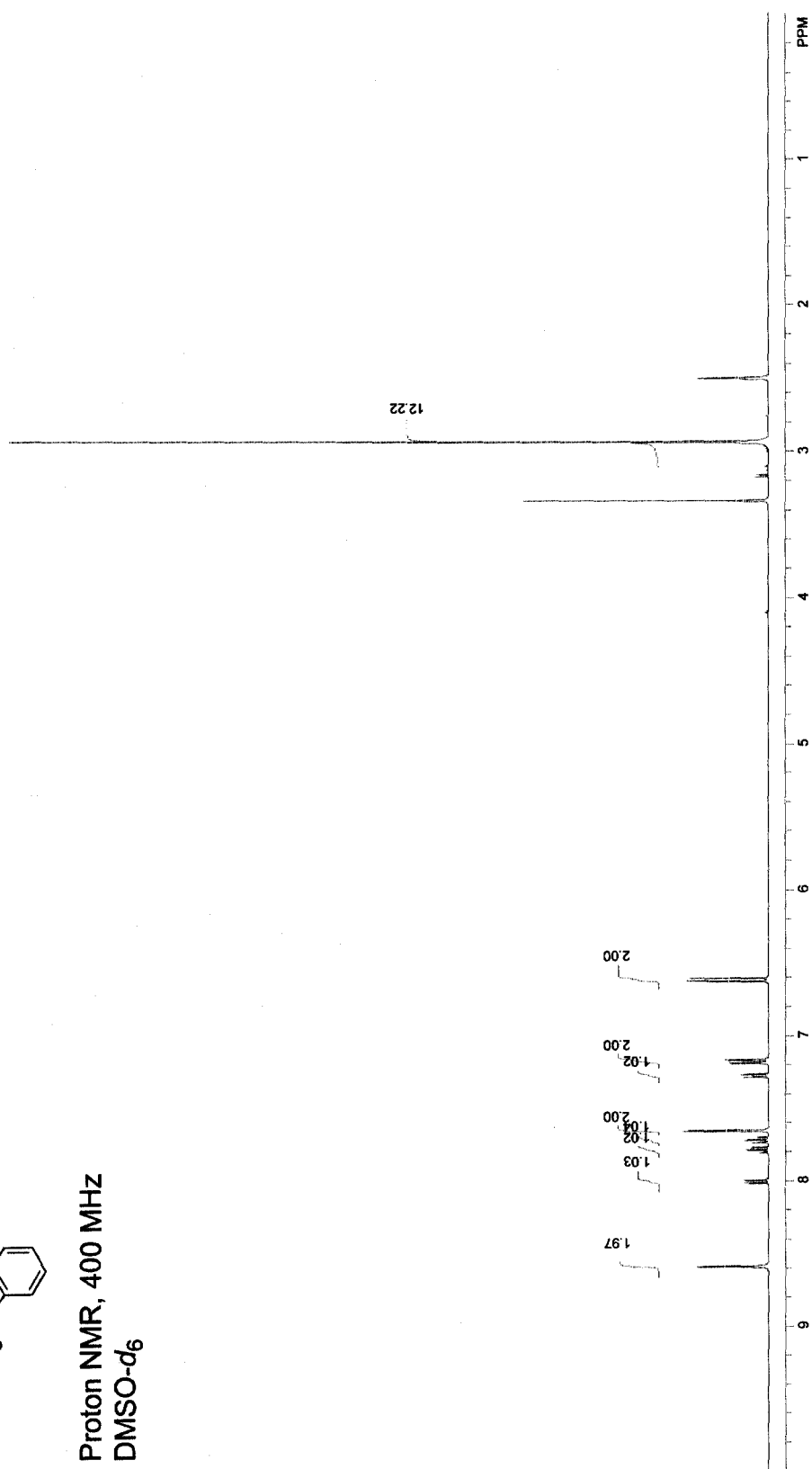
Carbon-13 NMR, 100 MHz
DMSO-*d*₆



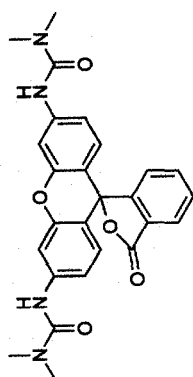
3.3



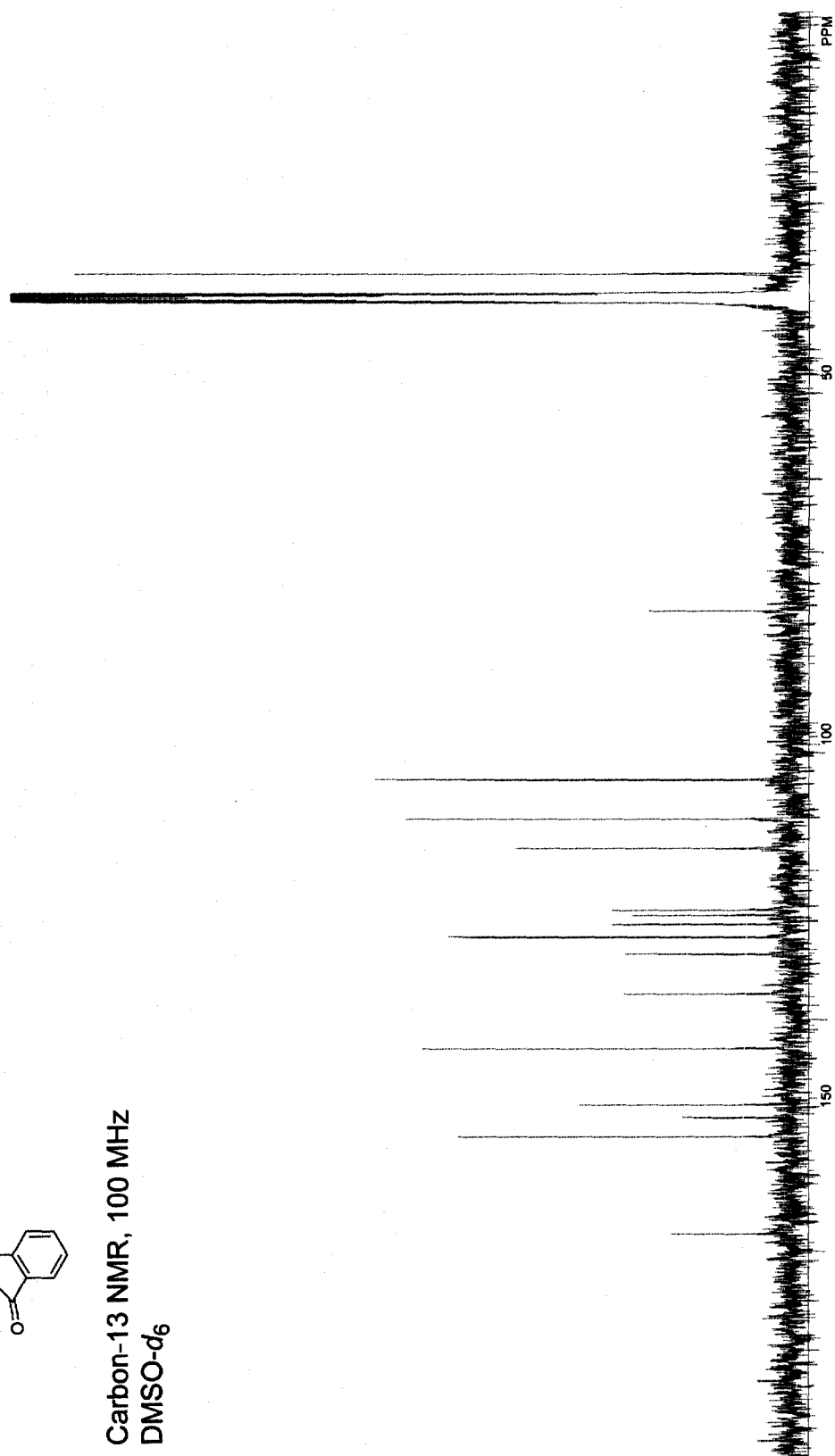
Proton NMR, 400 MHz
DMSO- d_6



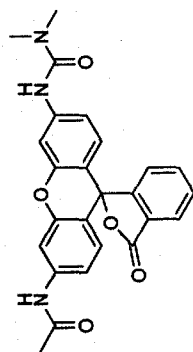
3.3



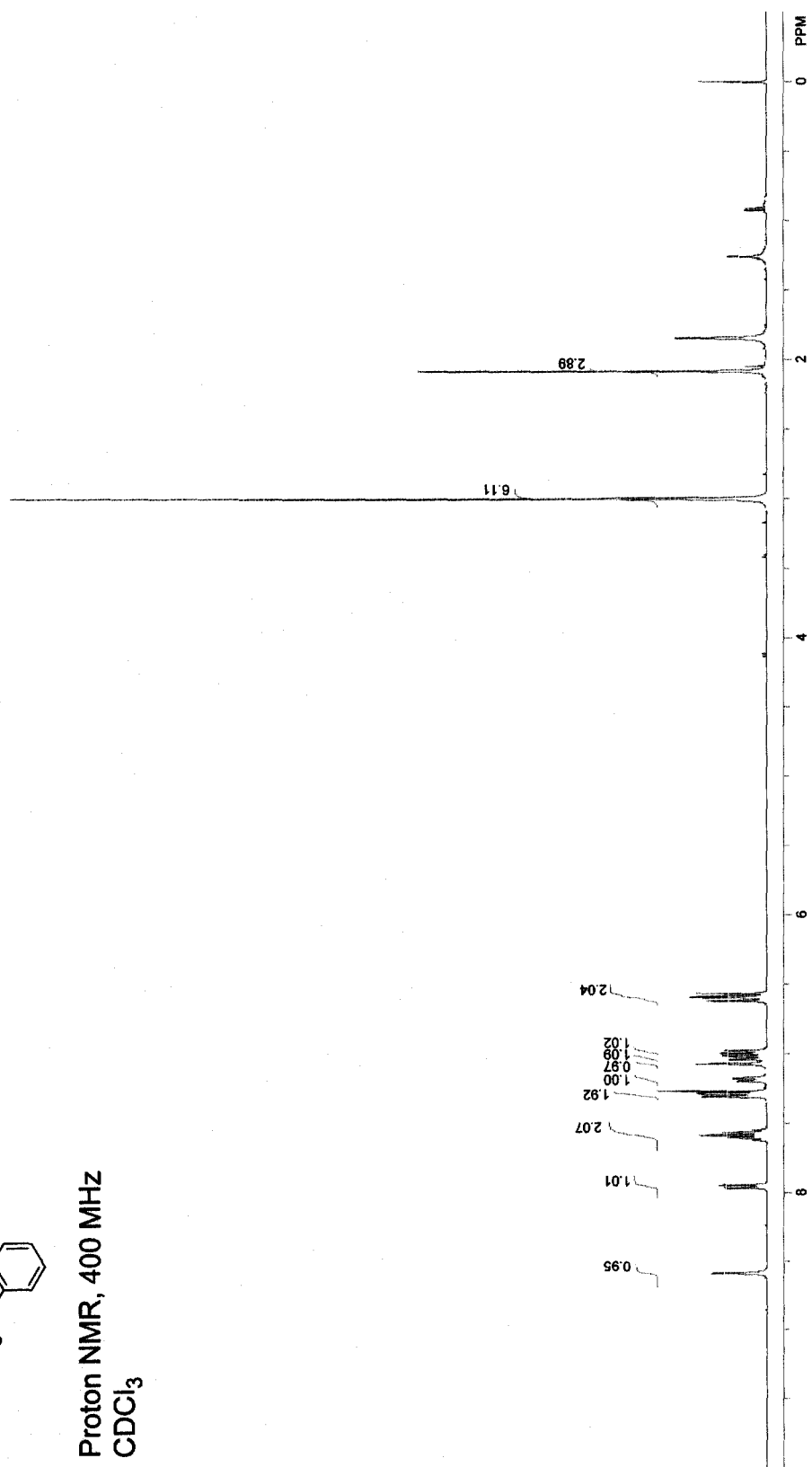
Carbon-13 NMR, 100 MHz
DMSO- d_6



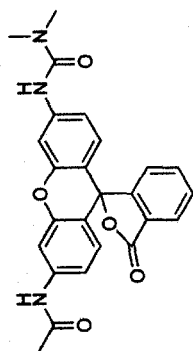
3.4



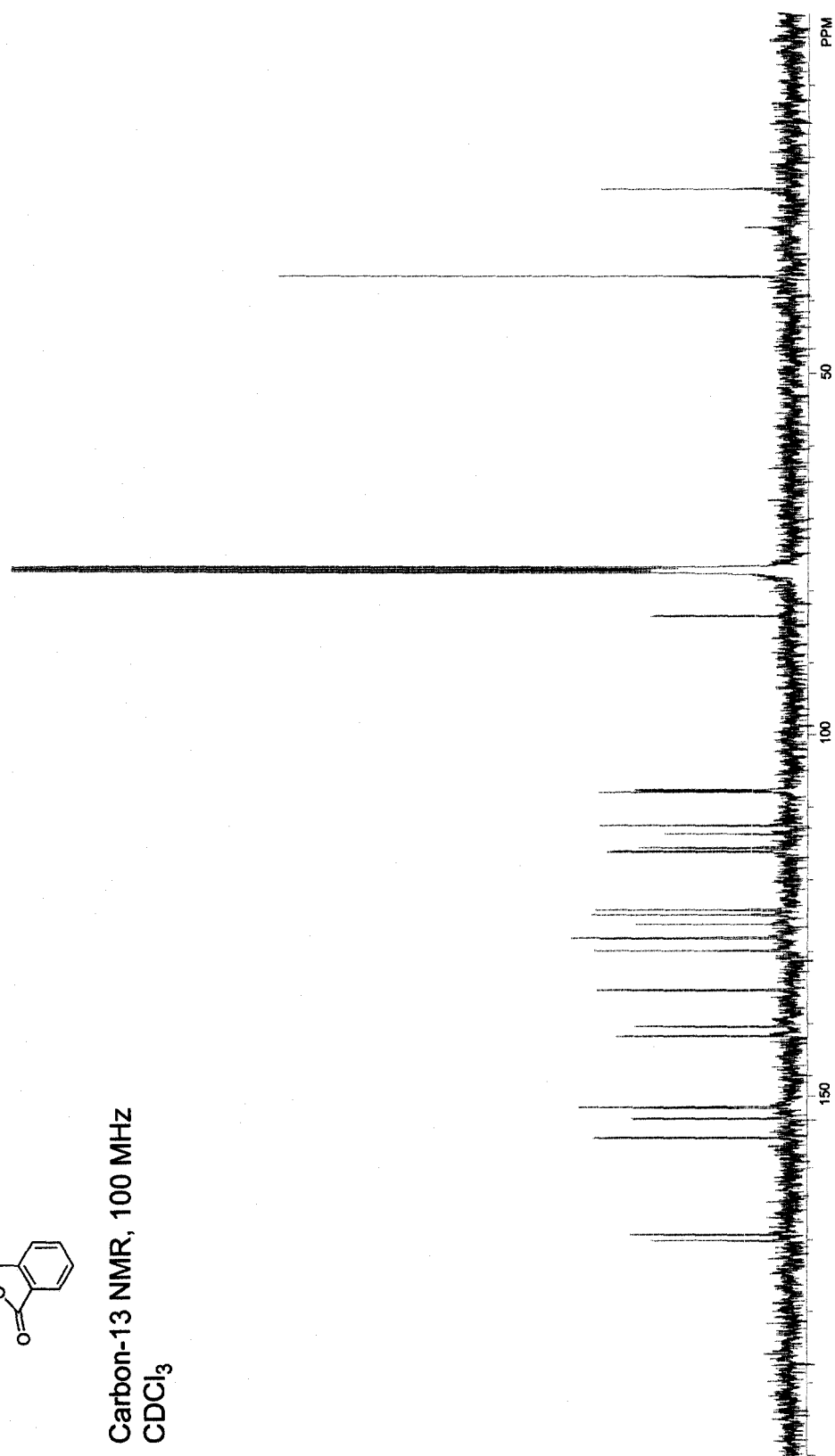
Proton NMR, 400 MHz
CDCl₃



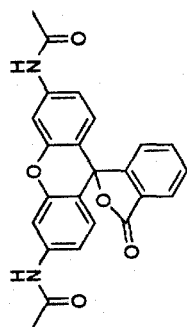
3.4



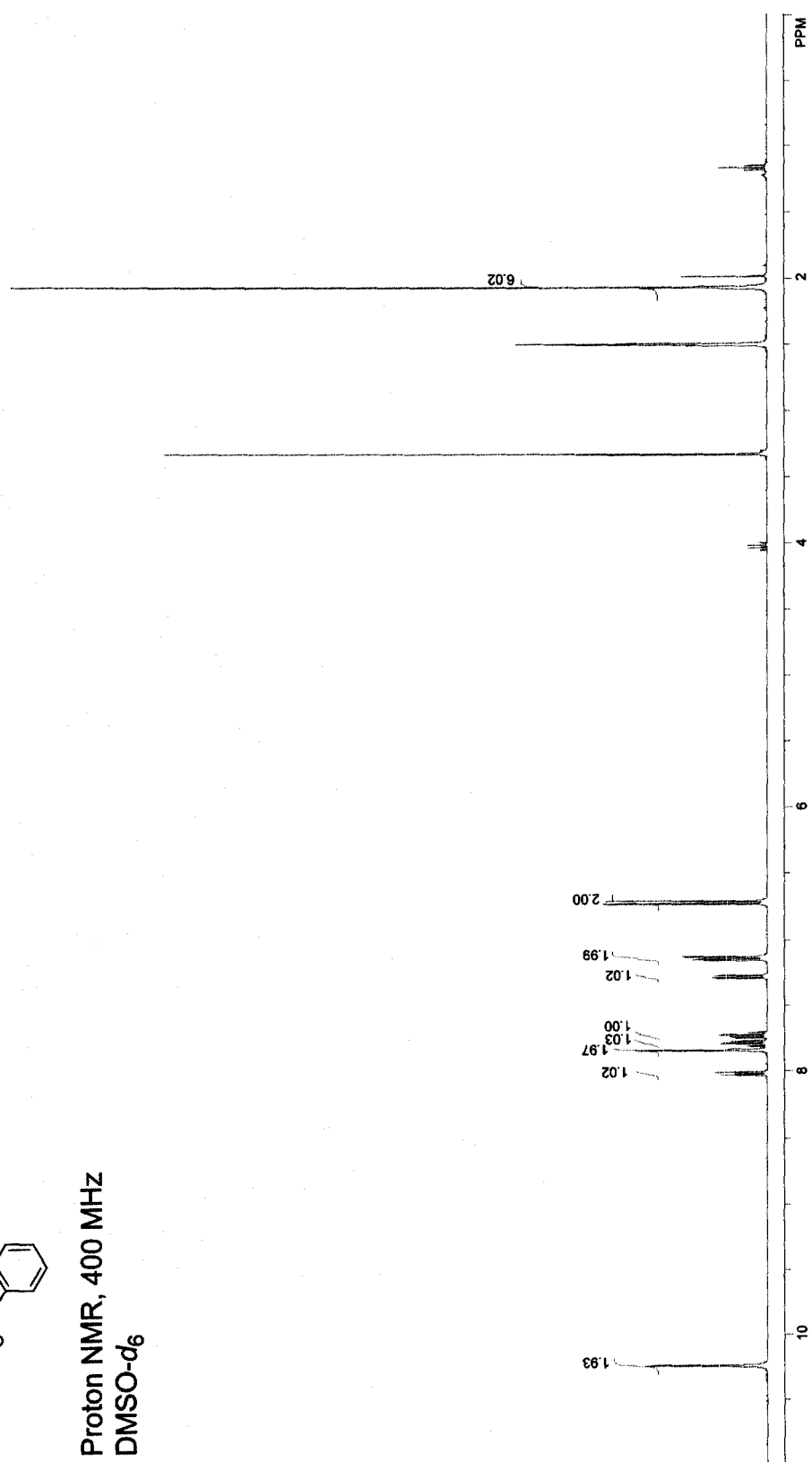
Carbon-13 NMR, 100 MHz
CDCl₃



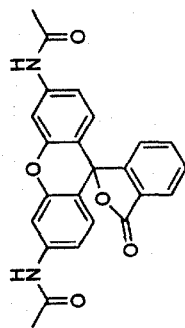
3.5



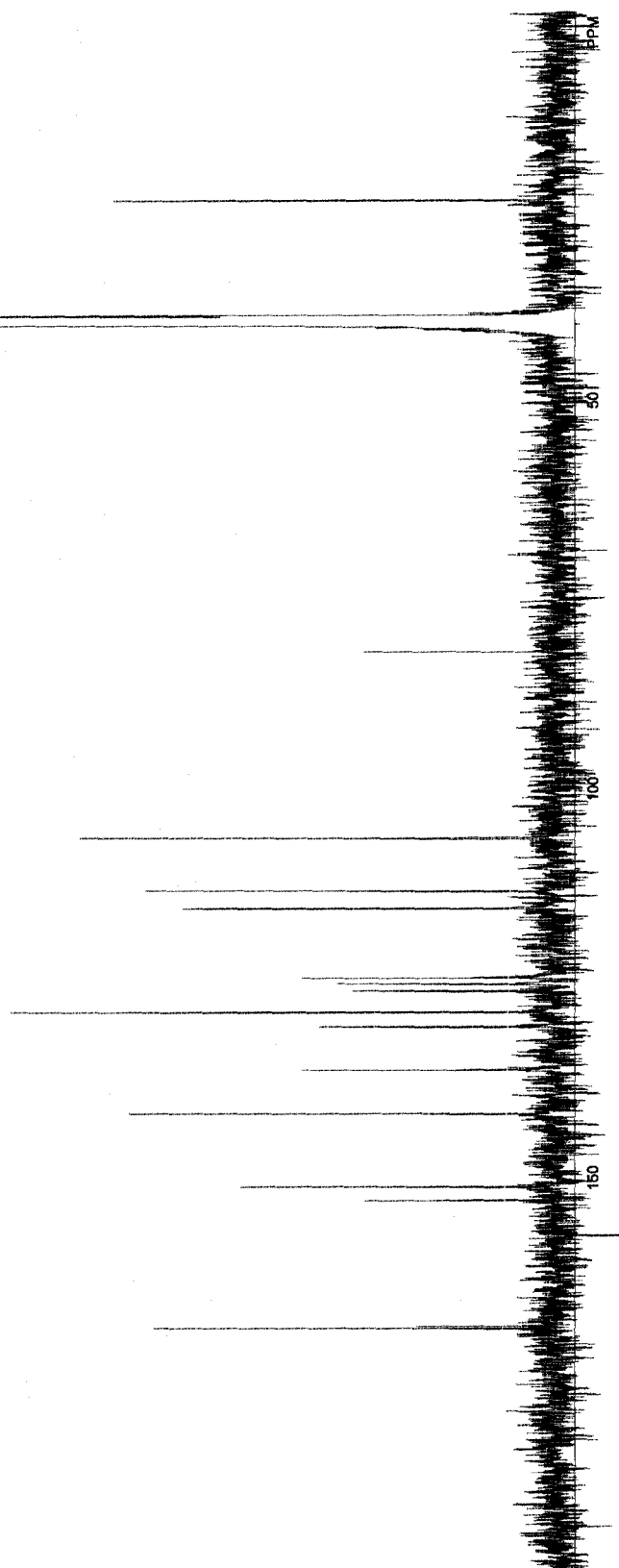
Proton NMR, 400 MHz
DMSO- d_6



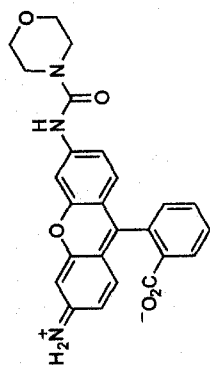
3.5



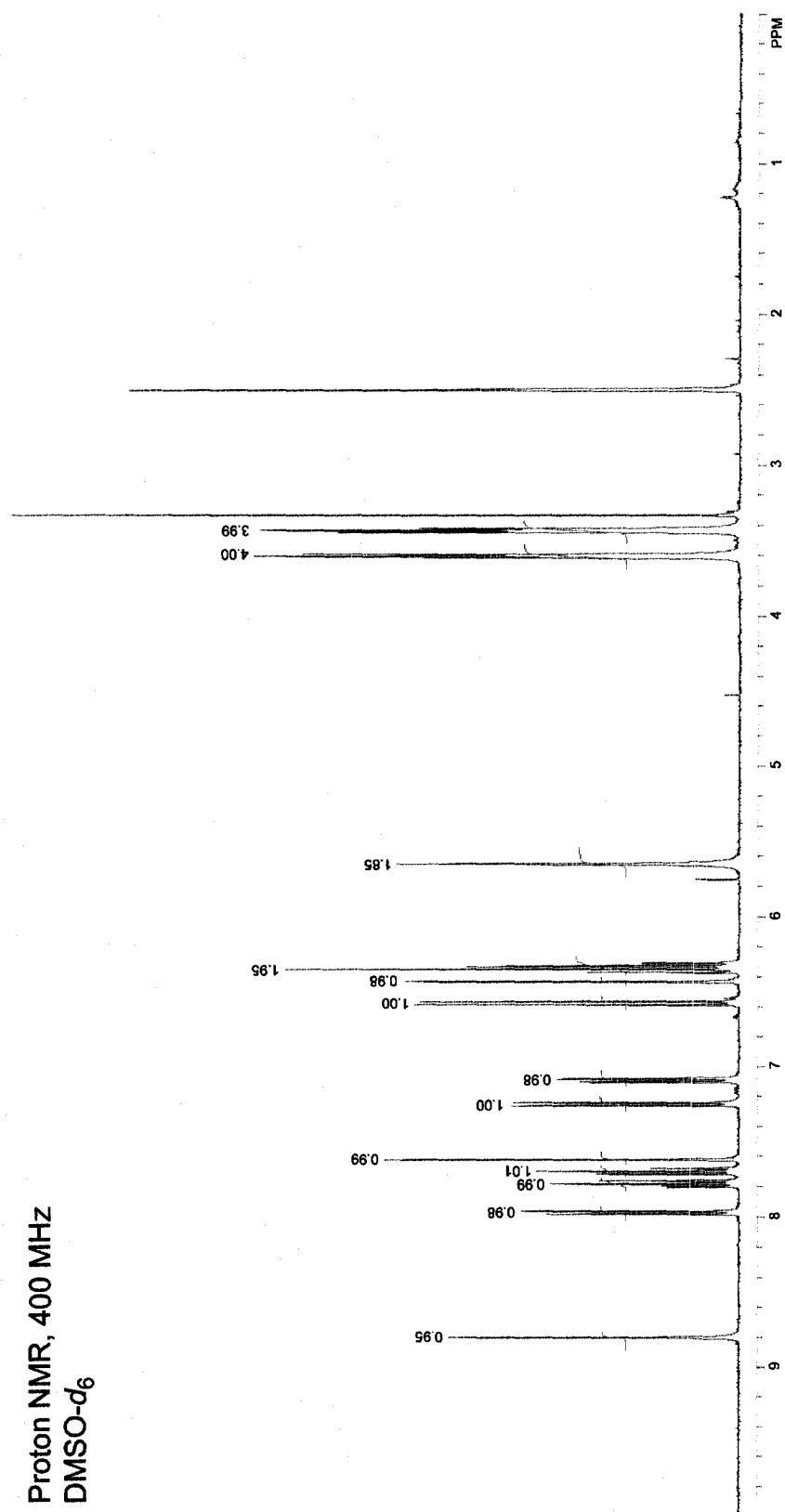
Carbon-13 NMR, 100 MHz
DMSO- d_6



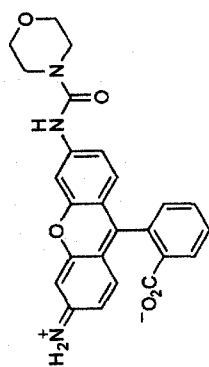
3.6



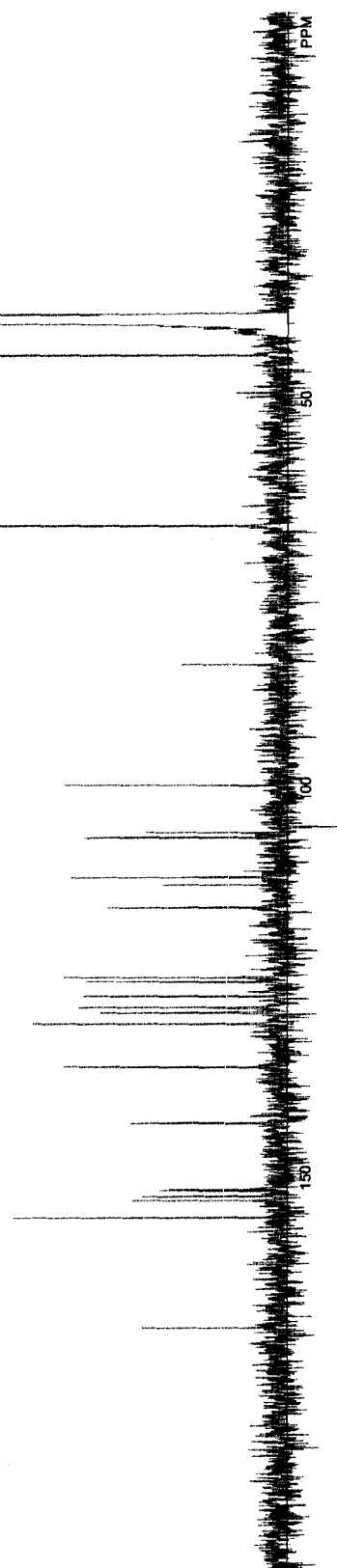
Proton NMR, 400 MHz
DMSO- d_6

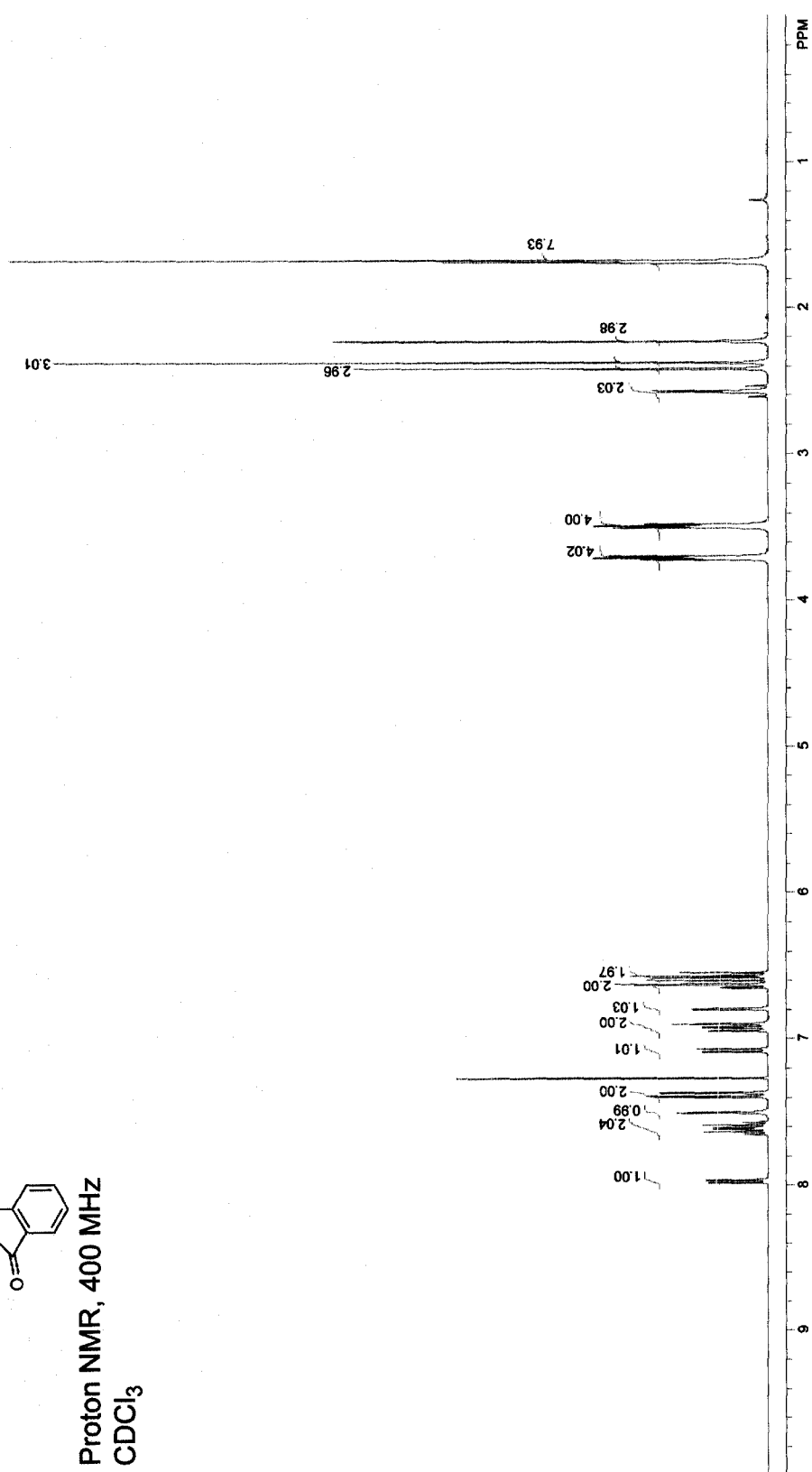
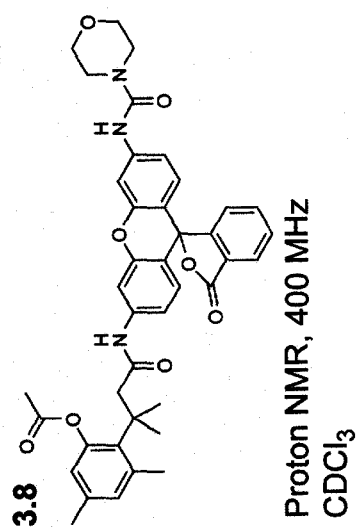


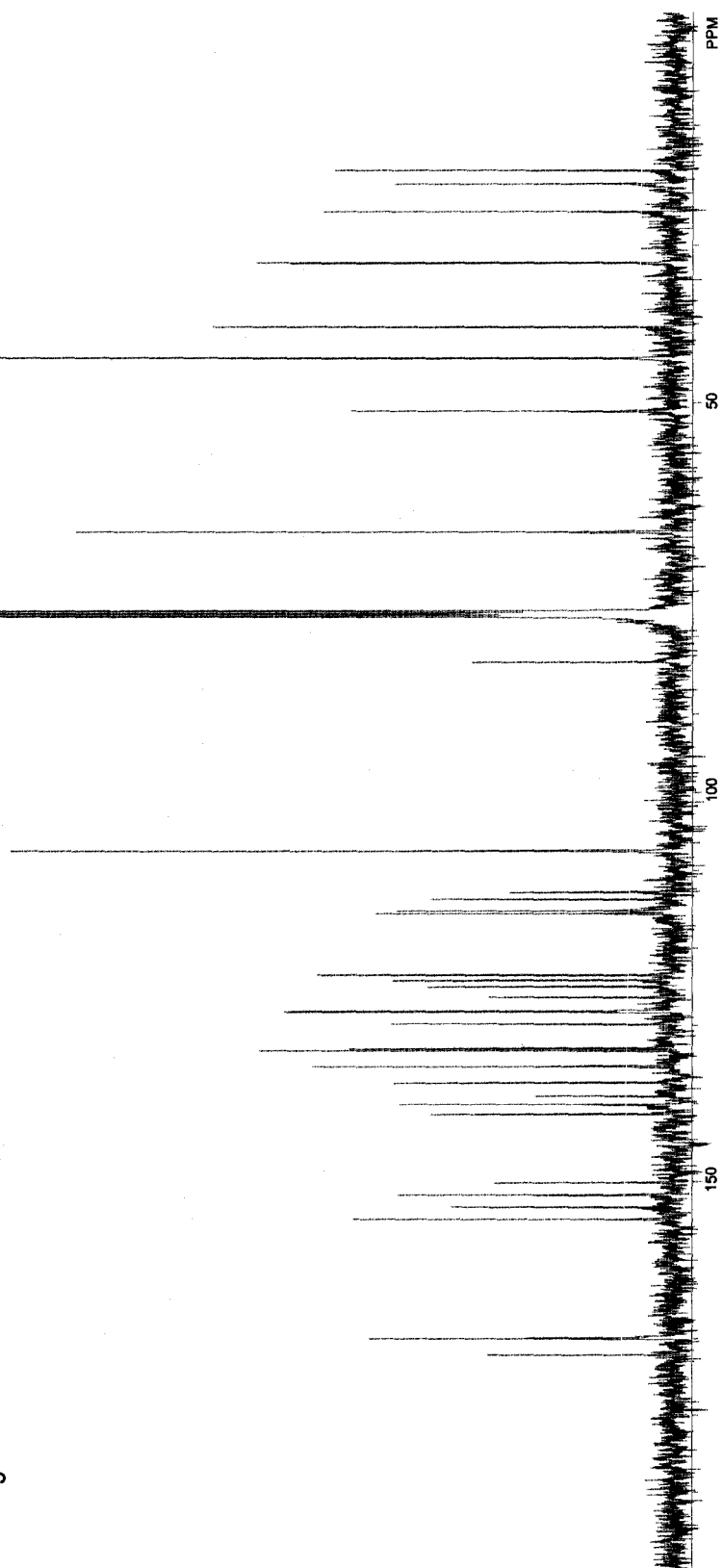
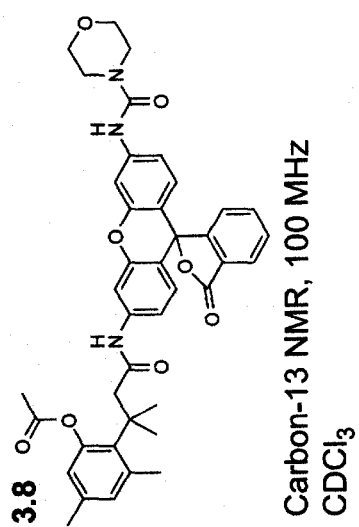
3.6

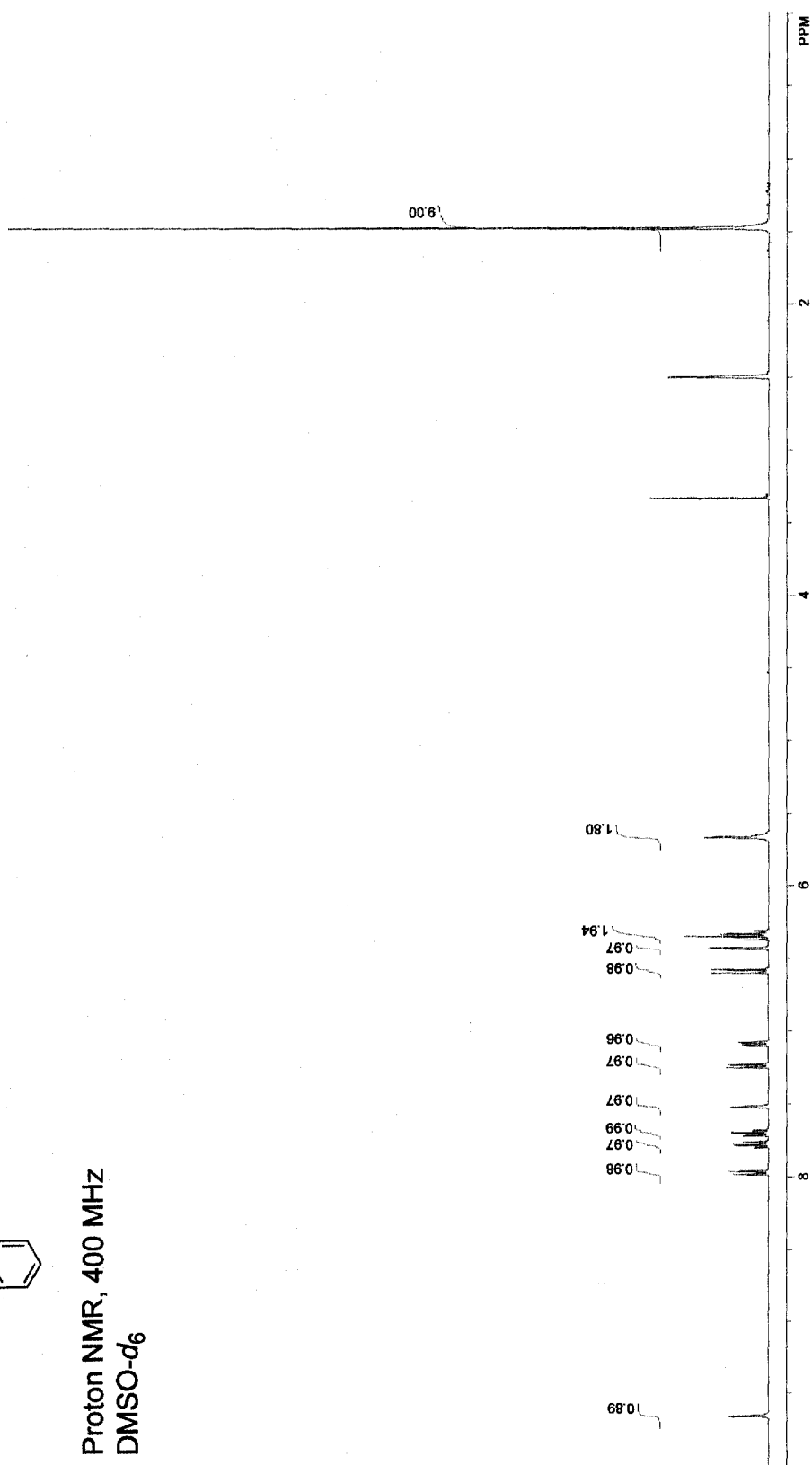
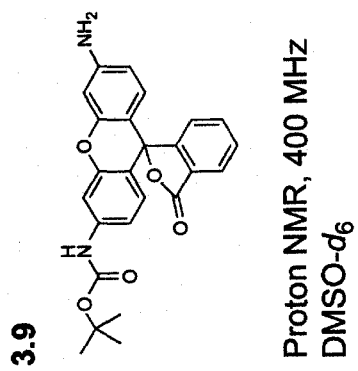


Carbon-13 NMR, 100 MHz
DMSO- d_6

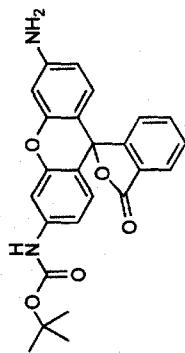




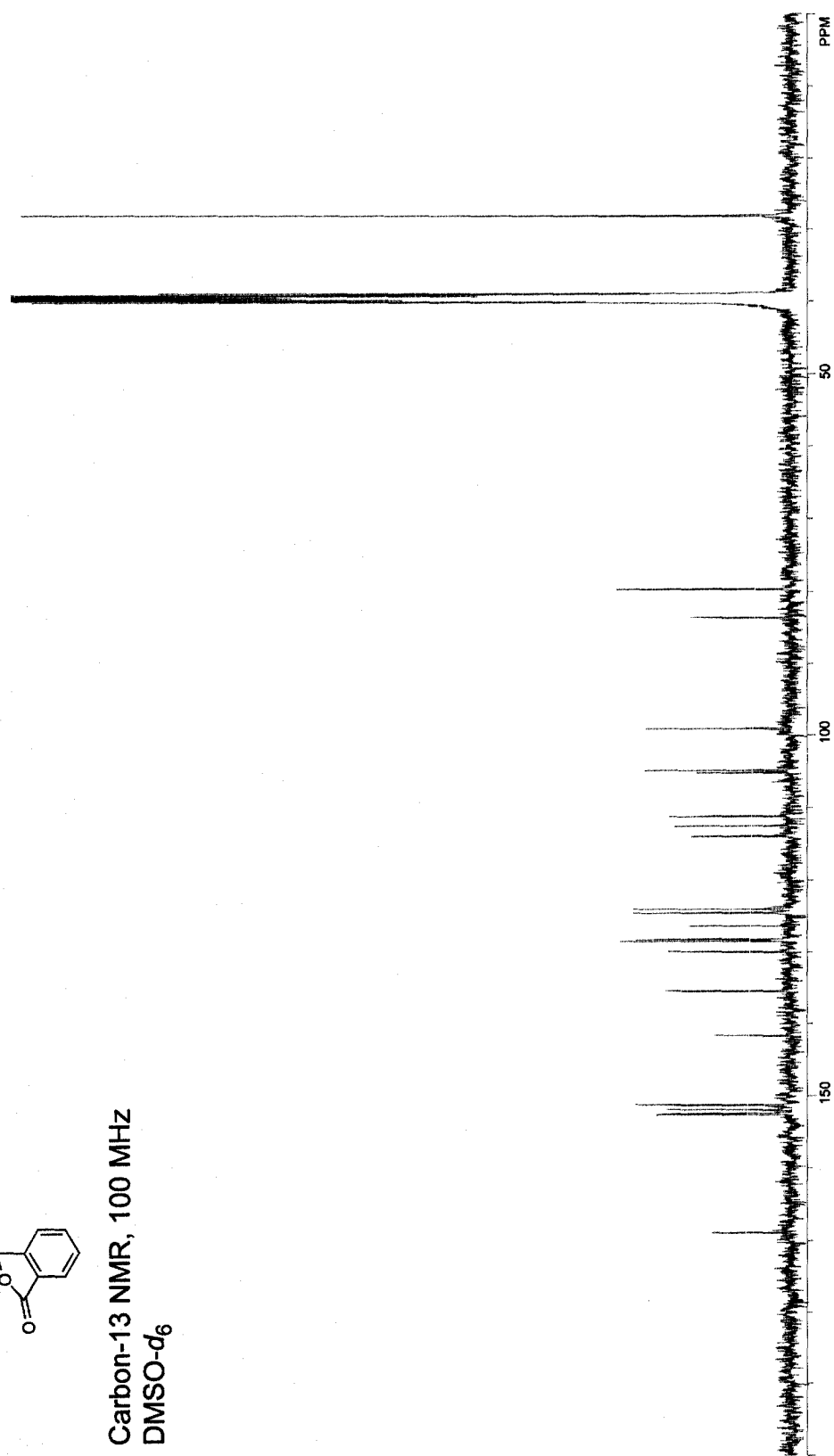


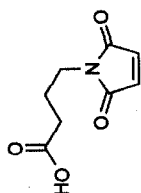


3.9

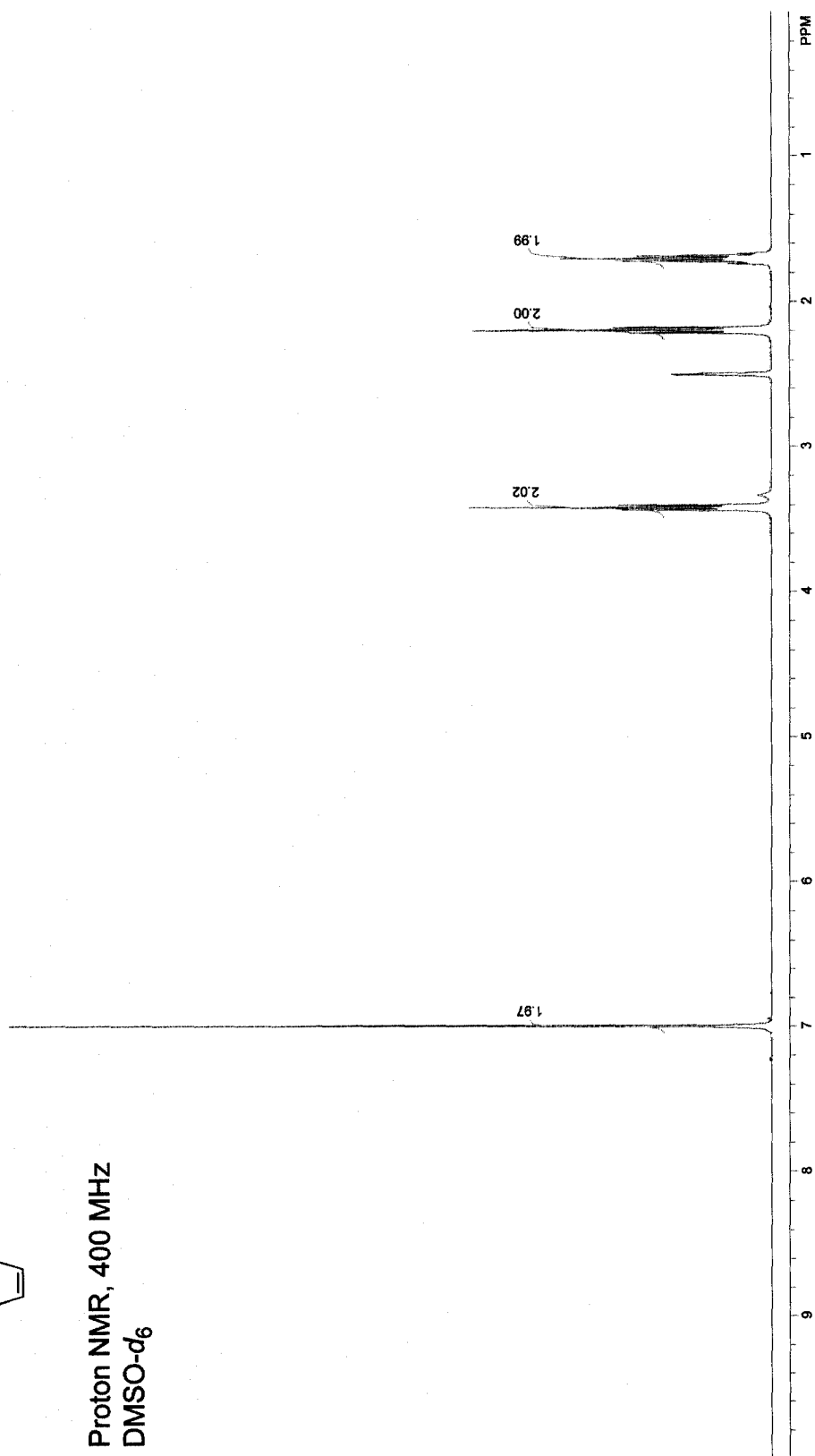


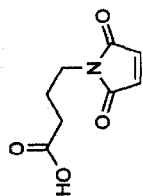
Carbon-13 NMR, 100 MHz
DMSO- d_6



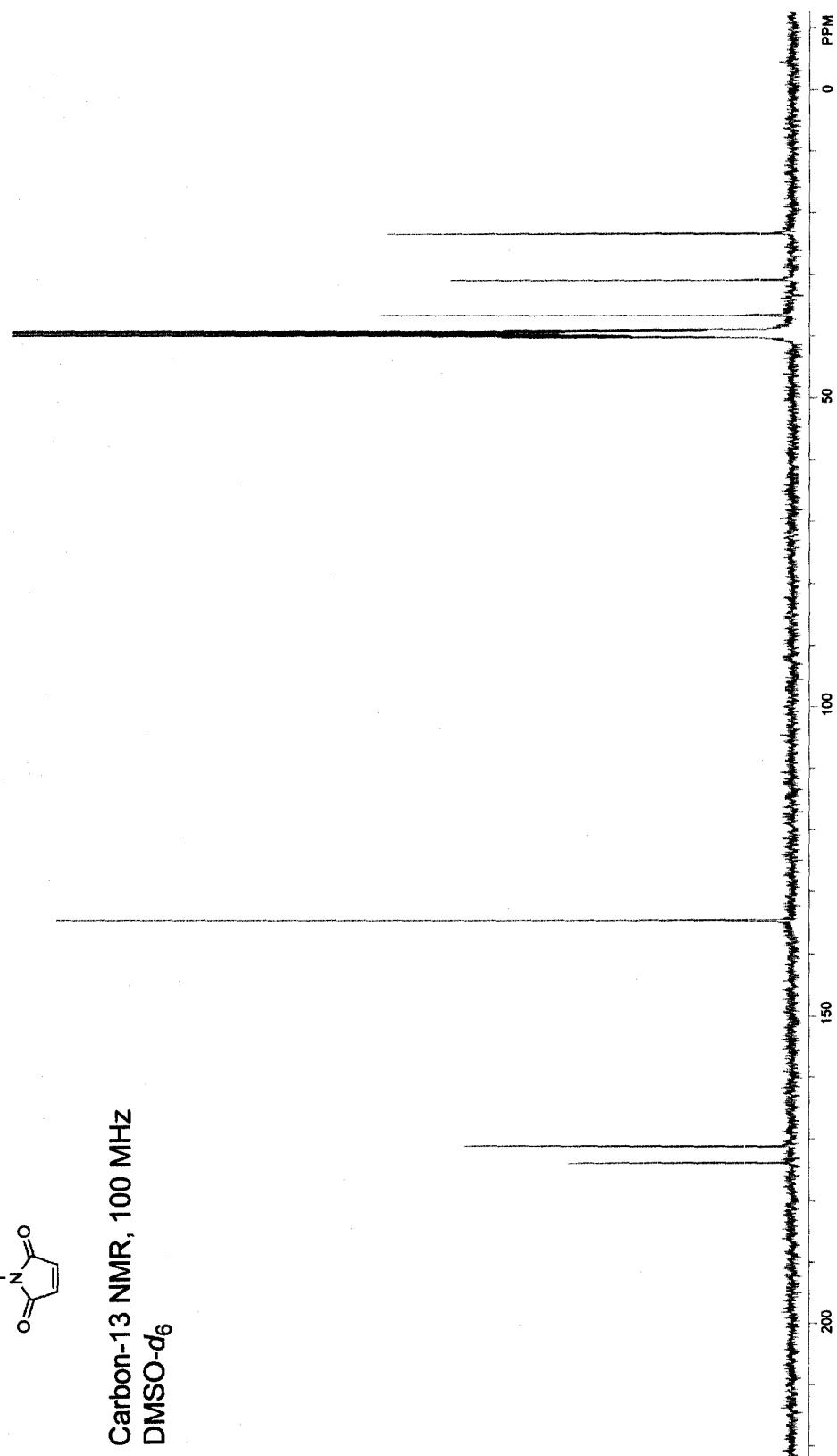
3.10

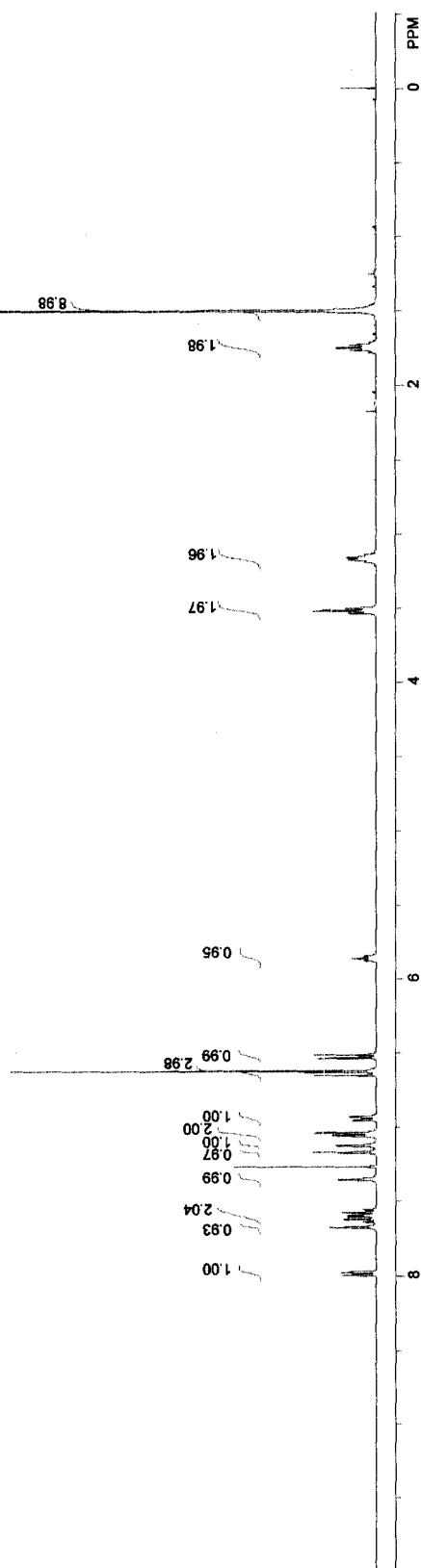
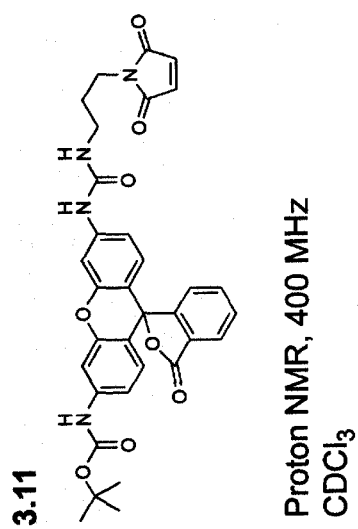
Proton NMR, 400 MHz
DMSO-*d*₆

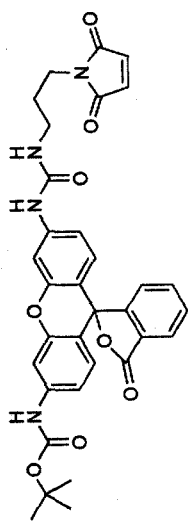


3.10

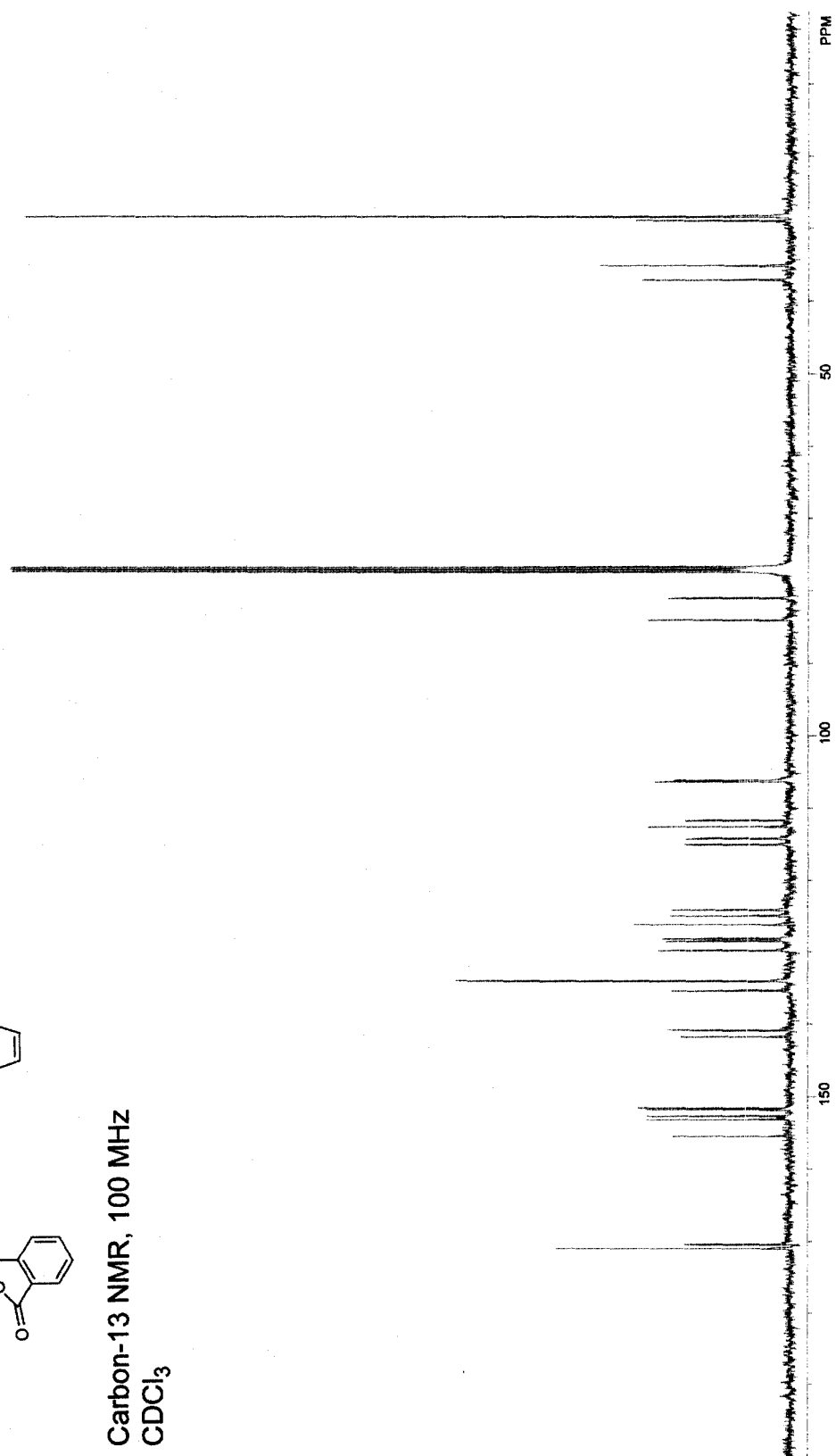
Carbon-13 NMR, 100 MHz
DMSO-*d*₆

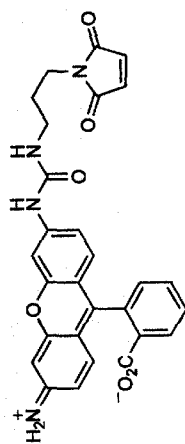




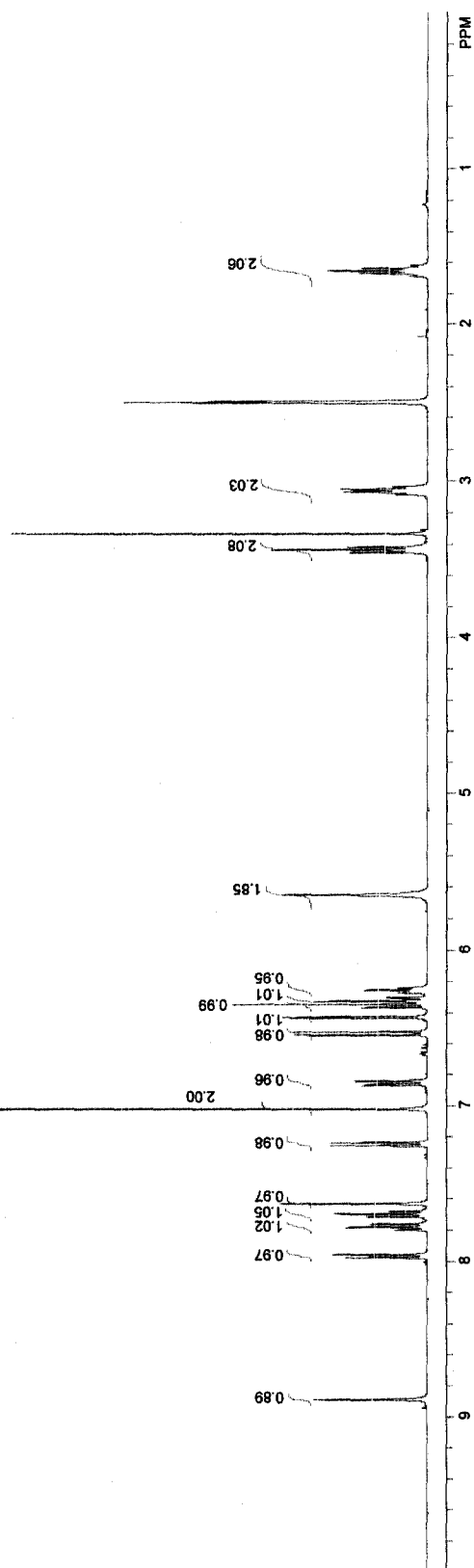
3.11

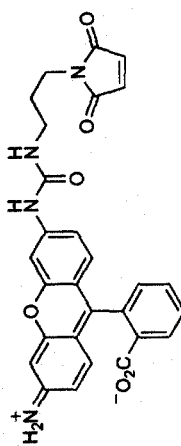
Carbon-13 NMR, 100 MHz
CDCl₃



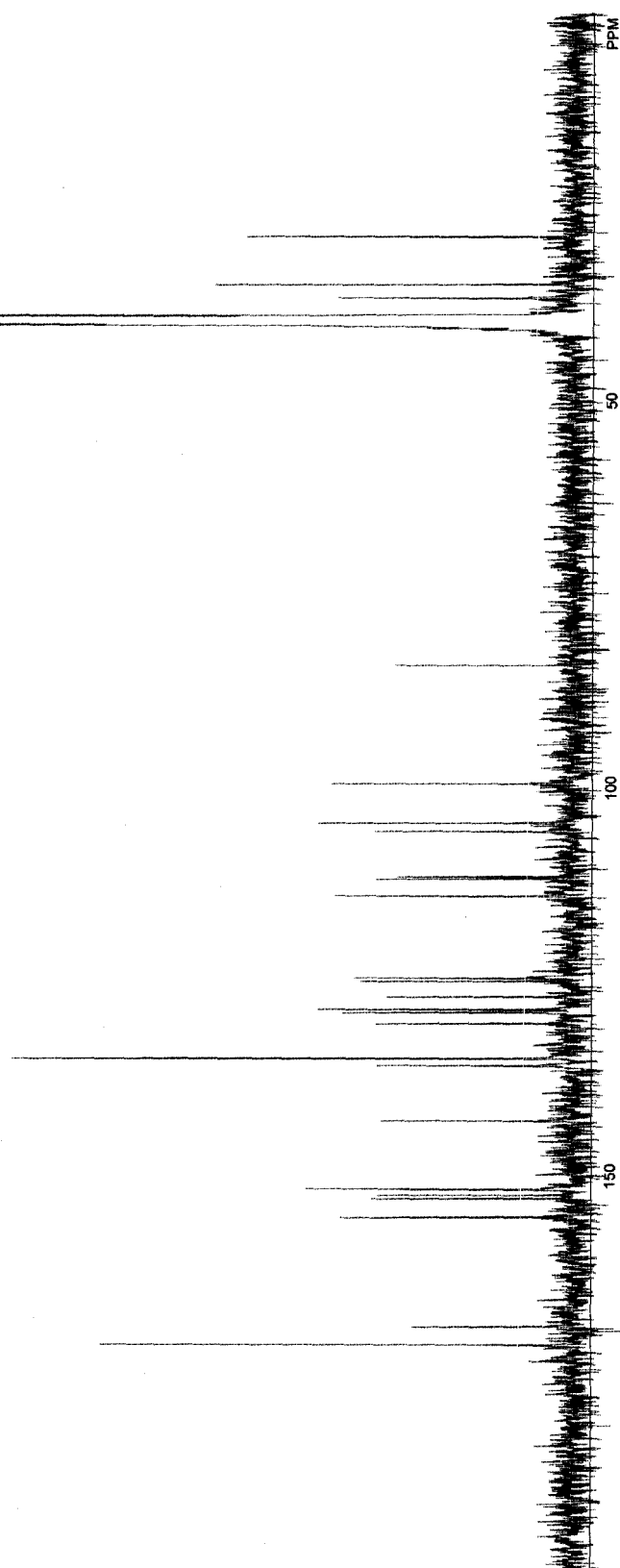
3.12

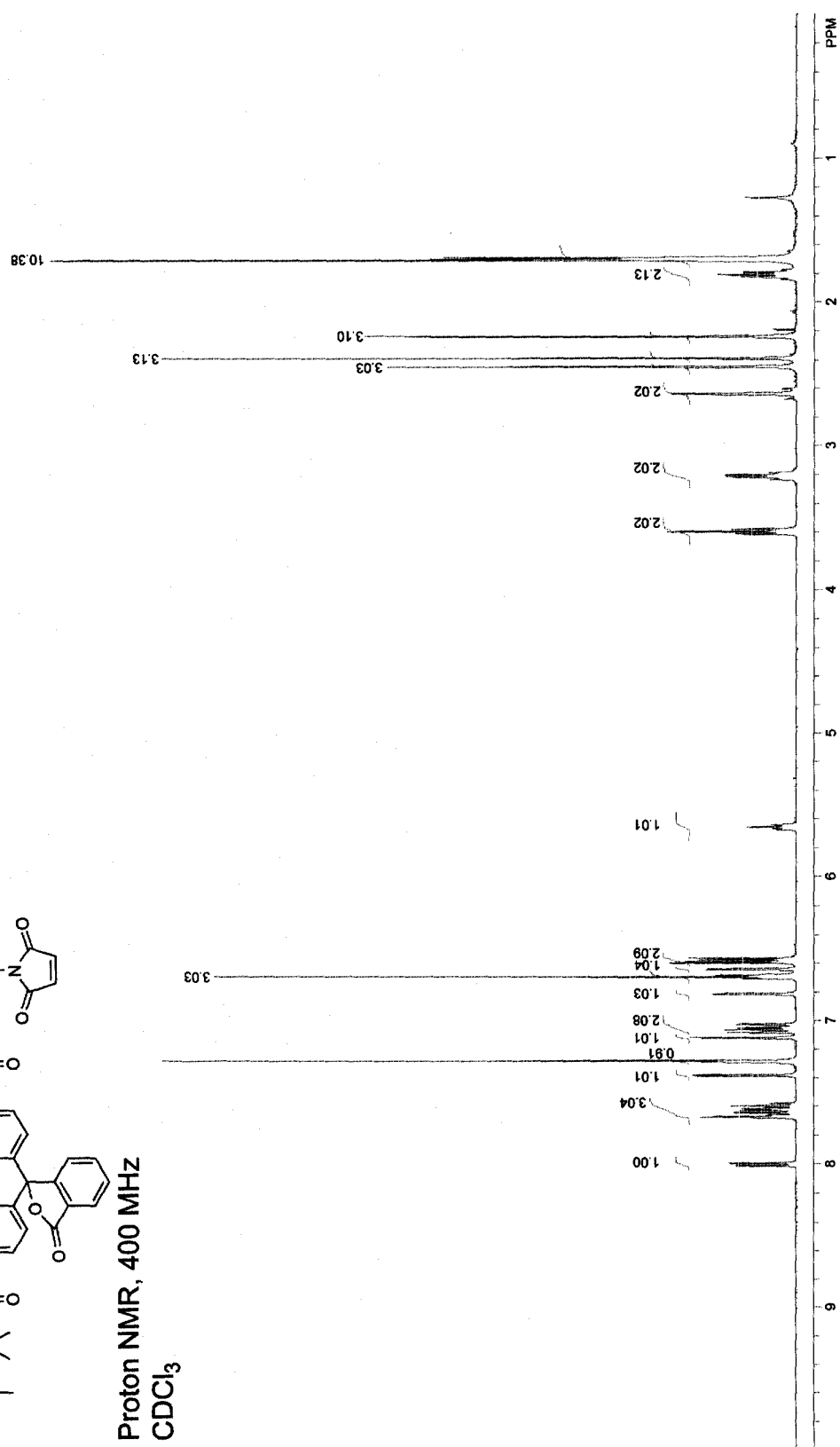
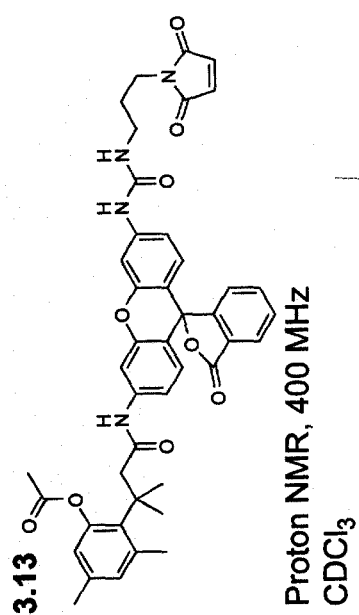
Proton NMR, 400 MHz
DMSO- d_6

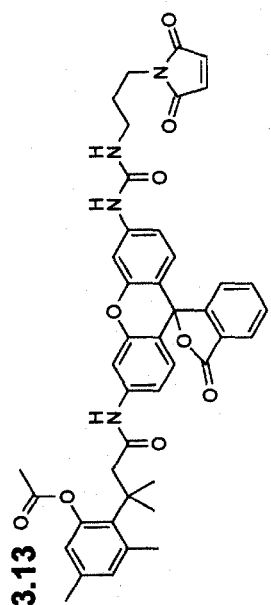


3.12

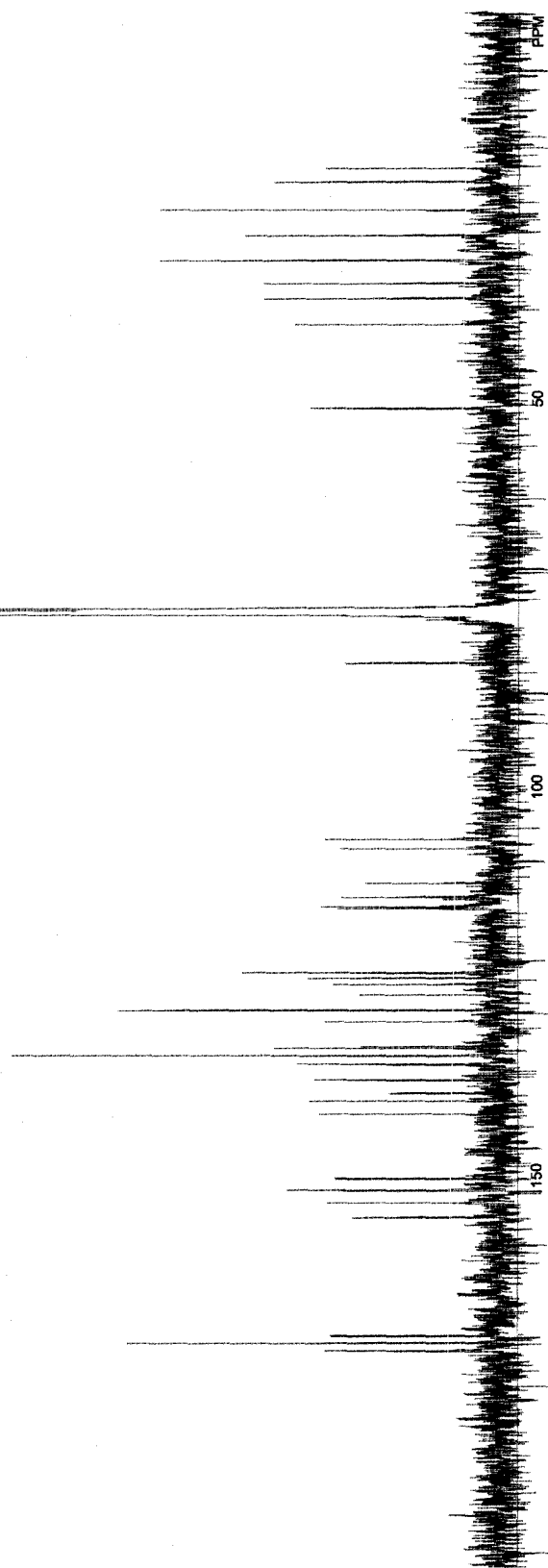
Carbon-13 NMR, 100 MHz
DMSO-*d*₆







Carbon-13 NMR, 100 MHz
CDCl₃



CHAPTER 4

FLUOROGENIC LABEL UNMASKED BY β -GALACTOSIDASE

Contribution: Design and synthesis of fluorogenic label, composition of chapter, and preparation of figure drafts. Protein conjugation and cellular studies were performed by T.-Y. Chao.

4.1 Introduction

Fluorogenic molecules are used extensively to assay enzyme activity *in vitro* and *in vivo*. Enzyme-catalyzed hydrolysis of these “latent” fluorophores can be exploited to create a portfolio of substrates that are unmasked by specific enzymes. These substrates are used in many biochemical and biological applications, including assessment of cell viability, visualizing reporter gene activity, the enzyme-linked immunosorbent assay (ELISA), and high-throughput screening (Johnson, 1998; Goddard and Reymond, 2004b; Haugland *et al.*, 2005).

Another intriguing use for fluorogenic molecules is the preparation of bioconjugates containing a fluorophore-based enzyme substrate. Attachment of such a “fluorogenic label” to a biomolecule renders the conjugate invisible until unmasking catalyzed by a specific and user-designated enzyme. This strategy facilitates sophisticated biomolecular imaging experiments to measure cellular trafficking of different molecular entities (Laurent *et al.*, 1997; Bergsdorf *et al.*, 2003; Drobni *et al.*, 2003; Kamal *et al.*, 2004; Lavis *et al.*, 2006a).

Chemical stability of the fluorogenic label is a critical property, as spontaneous hydrolysis can raise fluorescence background levels in imaging or other experiments. Previous work in our lab involved the development of a new class of hyperstable latent fluorophores based on the trimethyl lock chemical system (Chandran *et al.*, 2005; Lavis *et al.*, 2006b). Our strategy was furthered to prepare a useful esterase-reactive fluorogenic label (Lavis *et al.*, 2006a). This label allowed visualization of the endocytosis of labeled bovine pancreatic ribonuclease (RNase A (Raines, 1998)) variants and homologues in

both bioimaging (Lavis *et al.*, 2006a) and flow cytometry experiments (Johnson *et al.*, 2007).

Our interest in ribonuclease internalization stems from a longstanding investigation of the cytotoxic action of variants and homologues of RNase A towards cancer cells (Rutkoski *et al.*, 2005). These proteins hold potential as chemotherapeutic agents (Leland and Raines, 2001), and one such protein, Onconase, is currently in phase IIIb clinical trials for the treatment of malignant mesothelioma (Mikulski *et al.*, 2002). The putative pathway for a cytotoxic ribonuclease is shown in Figure 4.1 (Johnson *et al.*, 2007).

Ribonucleases bind to the cell surface, and are internalized by endocytosis, after which a portion of the protein translocates to the cytosol (Haigis and Raines, 2003). The majority of ribonuclease material likely remains in the endosomal/lysosomal pathway (Bosch *et al.*, 2004). If the cytosolic portion evades the ubiquitous ribonuclease inhibitor (RI (Dickson *et al.*, 2005)), it can cleave cellular RNA, resulting in cell death. The basis for selectivity towards cancerous cells is not well-understood, and examination of this biological process could augment our understanding of cancer cell biology, while providing insight for the development of better therapeutic agents.

We designed our first generation fluorogenic label to be unmasked by endogenous esterases (Lavis *et al.*, 2006a), allowing measurement of the internalization of ribonucleases (Johnson *et al.*, 2007). To measure the endosomal translocation event, we envisioned designing a label that remains quiescent until entry to the cytosol. We reasoned the use of a non-native enzyme–substrate pair could limit background hydrolysis and allow exquisite control over the location of unmasking within a cell. Here, we investigate the utility of the oft-used enzyme–substrate system: bacterial

β -galactosidase and fluorescein di- β -D-galactopyranoside (FDG; **4.1**; Scheme 4.1) (Rotman *et al.*, 1963; Hofmann and Sernetz, 1983; Nolan *et al.*, 1988; Fiering *et al.*, 1991; MacGregor *et al.*, 1991; Johnson, 1998; Rakhmanova and MacDonald, 1998; Rondelez *et al.*, 2005). We first develop chemistry to allow facile preparation of a thiol-reactive fluorogenic label based on FDG. We then conjugate this molecule to a variant of RNase A and examine the utility of this fluorogenic label strategy in live human cells. These experiments show promising preliminary results, illustrating the utility of fluorogenic labels in cell biology.

4.2 Results and Discussion

4.2.1 Choice of Fluorogenic Label System

The imaging of only the cytosolic portion of internalized ribonuclease is an audacious goal. With the majority of protein remaining in the endosomal/lysosomal pathway (Bosch *et al.*, 2004), very low fluorescence background is required for successful imaging experiments. We chose to construct a label based on FDG (**4.1**; Scheme 4.1). Appending sugar groups to the fluorescein fluorophore secure the molecule in a lactone form, which lacks visible absorption and is essentially nonfluorescent (Rotman *et al.*, 1963; Johnson, 1998).

Another important consideration for a useful fluorogenic label is chemical stability. Spontaneous hydrolysis of hydrolase substrates can compete deleteriously with enzyme activity and raise background levels. Other fluorescein-based substrates such as fluorescein diacetate exhibit poor stability in aqueous solution (Chandran *et al.*, 2005; Lavis *et al.*, 2006a). In an initial assessment of compound **4.1**, however, the acetal groups

in FDG proved reasonably stable in aqueous solution for hours, even at pH 4.0 (data not shown). Another advantage of compound **4.1** as a fluorogenic label is the hydrophilicity of the sugar moieties in FDG that render the molecule cell-impermeant (Urano *et al.*, 2005) without the addition of charge. The net molecular charge can affect greatly the internalization of a biomolecule (Johnson *et al.*, 2007). Thus, bioconjugation with an FDG derivative could preserve the native propensity for cellular internalization of a molecule and maintain biofidelity in bioconjugate trafficking measurements.

FDG and its derivatives are widely used fluorogenic enzyme substrates (Zhang *et al.*, 1991; Johnson, 1998; Haugland *et al.*, 2005). The unmasking of FDG molecule is catalyzed by bacterial β -galactosidase, the product of the *lacZ* gene. This gene is a common transcription reporter (Silhavy and Beckwith, 1985; Fiering *et al.*, 1991; MacGregor *et al.*, 1991; Lampson *et al.*, 1993; Brustugun *et al.*, 1995; Poot and Arttamangkul, 1997; Rakhmanova and MacDonald, 1998; Kamiya *et al.*, 2007), and the use of transfected cell lines in imaging or flow cytometry experiments would ensure abundant cytosolic enzyme to unmask the fluorogenic ribonuclease conjugate in an orthogonal fashion.

Endogenous glycosidases that are able to catalyze the hydrolysis of the β -galactoside moieties on FDG could prove problematic in our experiment. Such enzymatic activity exists within the endosomal pathway within acidic vesicles and has maximal activity at low pH (Hoogeveen *et al.*, 1983; Morreau *et al.*, 1989; Fiering *et al.*, 1991). Some reports detailing related fluorogenic substrates for β -galactosidase make no mention of any background problems resulting from native activity in mammalian cells (Urano *et al.*, 2005; Koide *et al.*, 2007), while others state the activity differs between cell types

(Fiering *et al.*, 1991). We postulated that our fluorescein-based strategy takes advantage of the native acidity within the endosomal/lysosomal pathway. Fluorescein possesses a pK_a of approximately 6.4 (Lavis *et al.*, 2007), and thus any FDG conjugate unmasked in the endosomes (pH ~6) or lysosomes (pH ~5) would exhibit lower fluorescence relative to the fluorescein-labeled protein in the neutral cytosol (Maxfield and McGraw, 2004). This could overcome, to a degree, the background from any native glycohydrolase activity encountered by the conjugate.

Another critical element of a fluorogenic label is the conjugation strategy. We envisioned installation of a thiol-reactive moiety to allow site-specific labeling of ribonuclease variants containing engineered cysteine residues (Lavis *et al.*, 2006a). We chose to incorporate the maleimide functionality which is thiol-specific and provides very stable linkages (Ji, 1983). We therefore sought the synthesis of 5-carboxamid fluorescein, C₂-maleimide, di- β -galactopyranoside (**4.2**; Scheme 4.1) as our target fluorogenic label.

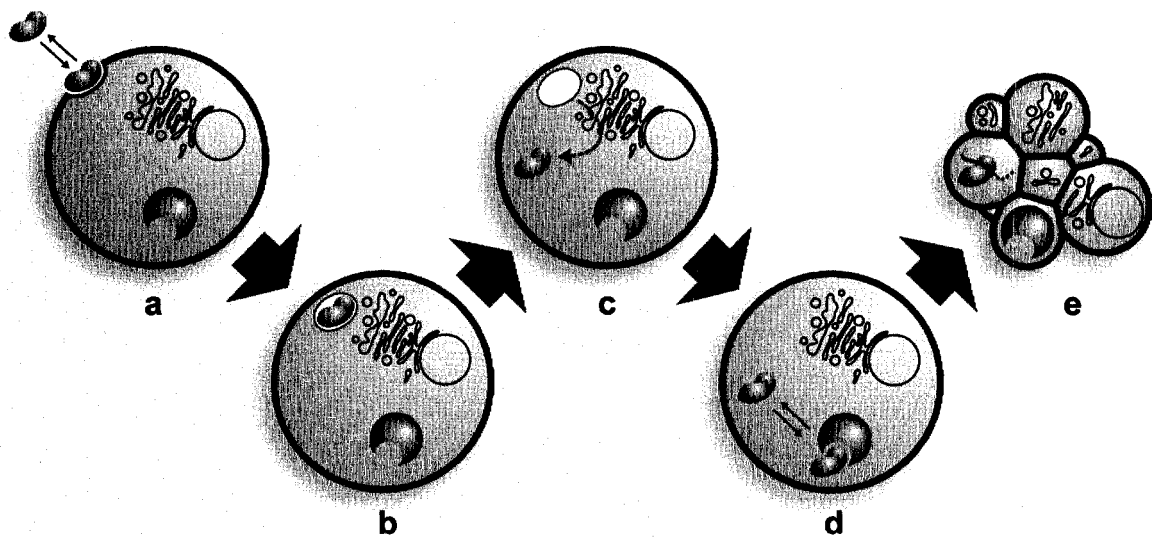
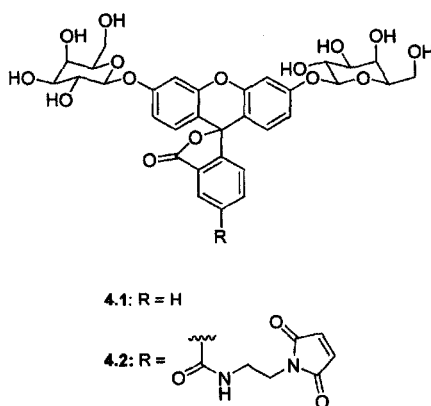


Figure 4.1 Pathway of cytotoxic ribonucleases. (a) Binding of ribonucleases (blue) to the cell surface. (b) Uptake by endocytosis. (c) Translocation to the cytosol. (d) Evasion of RI (red). (e) Degradation of RNA leading to cell death.

Scheme 4.1 Structures of FDG (4.1) and fluorogenic label 4.2



4.2.2 Synthesis of Fluorogenic Label

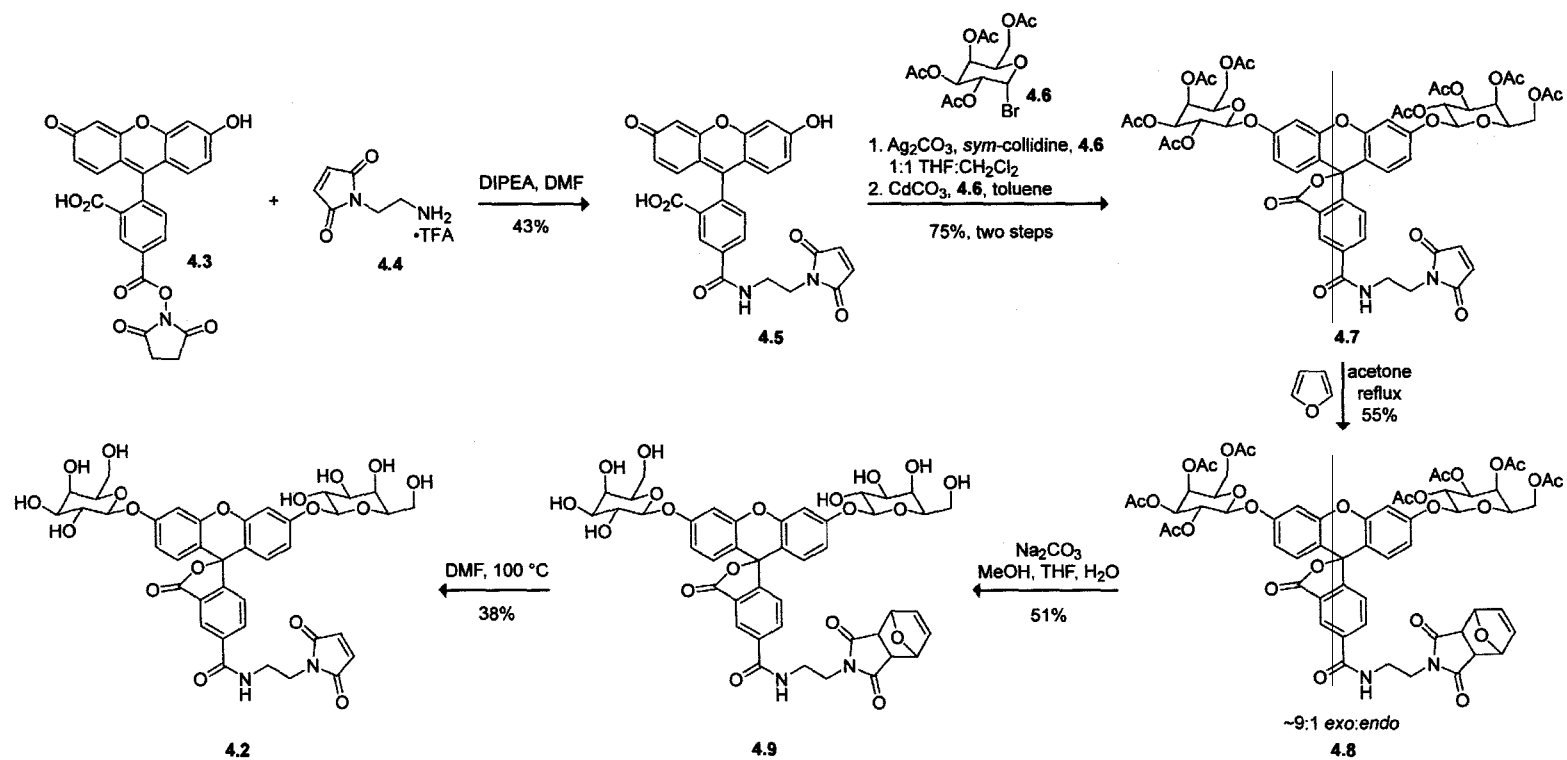
A pivotal issue in the synthetic design of compound **4.2** is the incorporation of the maleimide moiety in the presence of the sugar hydroxyls. Thus, the choice of sugar hydroxyl protecting groups is an important consideration. Benzyl protecting groups seemed an imperfect choice on the basis that both the lactone form of fluorescein (Zaikova *et al.*, 2001) and the maleimide moiety (Verschueren *et al.*, 2005) can be reduced under the catalytic hydrogenation conditions used for benzyl group removal. We therefore utilized acetate groups for sugar protection which are removed with nucleophilic reagents (Herzig *et al.*, 1986; Kasai *et al.*, 1993).

Such nucleophiles proved incompatible with the maleimide group and a protection strategy for this electrophilic moiety was the next hurdle in our synthetic plan. We envisaged installing the maleimide early in the synthesis, and protecting this electrophilic moiety during sugar deprotection using a reversible Diels–Alder reaction with furan (Kwart and King, 1968). This was inspired, in part, by the use of the Diels–Alder reaction between maleimides and furanyl moieties to prepare thermosensitive molecules (McElhanon and Wheeler, 2001; McElhanon *et al.*, 2005; Szalai *et al.*, 2007) and to tether molecules to solid supports (Pontrello *et al.*, 2005). The retro Diels–Alder has also been utilized in the synthesis of thiol-reactive moieties for bioconjugation (Mantovani *et al.*, 2005). Such maleimide–furan Diels–Alder adducts are stable in a variety of conditions (McElhanon *et al.*, 2005) and provide a general means to protect the widely-used maleimide functionality in biomolecule label synthesis.

The synthesis of 5-carboxamid fluorescein, C₂-maleimide, di- β -galactoside (**4.2**) is shown in Scheme 4.2. 5-Carboxyfluorescein, succinimidyl ester **4.3** (Adamczyk *et al.*,

1997) reacted with maleimide-amine **4.4** (Arano *et al.*, 1996) to give 5-carboxamid fluorescein, C₂-maleimide (**4.5**). This dye was glycosylated using Koenigs–Knorr chemistry (Koenigs and Knorr, 1901; Chilvers *et al.*, 2001) with α -bromogalactose derivative **4.6** to give a monogalactoside. A second sugar was installed using cadmium carbonate under Dean–Stark conditions (Bernstein and Conrow, 1971) to give the protected di- β -galactoside **4.7**.

Reaction of maleimide **4.7** in neat furan at reflux provided the Diels–Alder adduct **4.8** in high yield as a mixture of ~9:1 *exo:endo* isomers. Removal of the acetate groups under basic conditions (Kasai *et al.*, 1993) afforded the deprotected di- β -galactoside **4.9** which was purified by preparative HPLC. Heating in DMF overnight at 100 °C effected the retro Diels–Alder reaction giving the desired maleimide **4.2**.



Scheme 4.2 Synthesis of fluorogenic label **4.2**

4.2.3 Bioconjugation

Fluorogenic label **4.2** reacted cleanly with the A19C variant of RNase A to give a singly-labeled conjugate. The conjugate was purified by cationic-exchange chromatography and exhibited low background fluorescence intensity. Incubation of the labeled ribonuclease with purified bacterial β -galactosidase *in vitro* showed significant increase in fluorescence. The rate of unmasking, however, was slower than with free substrate **4.1** (data not shown). This is likely a result of the tetrameric structure of β -galactosidase (Juers *et al.*, 2000). We suspect that small-molecule substrates are able to access the active site easily, while the steric bulk of the fluorogenic label–ribonuclease conjugate slows enzymatic catalysis. Long incubation times would be required to measure the translocation process, however, and render the decrease in catalysis rate immaterial.

4.2.4 Cell Preparation and Preliminary Imaging

HeLa cells were transiently transfected with a single vector containing both *lacZ* to produce β -galactosidase and the sequence to produce monomeric red fluorescent protein (mRFP). This endowed successfully transfected cells with red fluorescence, allowing identification of this subpopulation of cells in both imaging and flow cytometry experiments. Transfected HeLa cells were incubated with ribonuclease conjugate from label **4.2** for 24 h after which they were imaged by confocal microscopy. Preliminary images are shown in Figure 4.2.

We expect cells successfully transfected with the *lacZ* gene should show diffuse green staining from unmasked ribonuclease conjugate labeled with compound **4.2**. These cells

should also exhibit bright red fluorescence from expressed mRFP. Indeed, the cell that shows diffuse green staining (Figure 4.2a) also exhibits a bright red signal from mRFP (Figure 4.2b). Green punctuate staining is evident in all cells, however, presumably due to glycohydrolase hydrolase activity within the endosomal/lysosomal pathway (Hoogeveen *et al.*, 1983; Fiering *et al.*, 1991). Preliminary flow cytometry experiments show a significant (albeit small) difference between transfected cells lines (data not shown). Background fluorescence remains a significant problem in these flow cytometry experiments and precludes rigorous quantitative assessment of the translocation process to the cytosol.

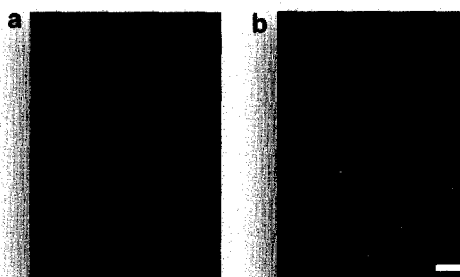


Figure 4.2 Transfected, live HeLa cells incubated with fluorogenic label 4.2–RNase A conjugate (10 μ M) for 24 h (5% v/v CO₂(g), 100% humidity). (a) Green channel only showing diffuse cytosolic staining of unmasked conjugate within transfected cell. (b) Merged image showing fluorescence from conjugate (green), mRFP fluorescence (red), and nuclei stained with Hoechst 33342 (blue). Scale bar: 20 μ m.

4.3 Conclusions and Future Directions

In previous work we showed how the use of a fluorogenic label can allow sophisticated biological measurements by suppressing unwanted fluorescence intensity signals (Lavis *et al.*, 2006a). Here, the use of a matched orthogonal enzyme–substrate pair allowed somewhat selective visualization of the population of ribonuclease conjugates within the cytosol. While not ideal, these initial data are promising and portend the construction of other fluorogenic labels to measure biomolecular trafficking in the cell.

Given the wide utility of β -galactosidase as a reporter gene and the straightforward synthesis of FDG derivatives, this enzyme–substrate pair was an obvious initial attempt at a non-native fluorogenic label system. The tantalizing results from this experiment should inspire the synthesis of other truly orthogonal enzyme–substrate pairs to facilitate biomolecular imaging. In particular, the use of the small, monomeric *TEM-1* gene product, β -lactamase, should ensure very low fluorescence background due to absence of any native lactamase activity in mammalian cells. Tsien and coworkers have prepared fluorogenic substrates for β -lactamase (Zlokarnik *et al.*, 1998; Gao *et al.*, 2003) and fluorogenic labels based on such substrates should find wide utility. Overall, the fluorogenic label approach should continue to facilitate sophisticated and exciting experiments in cell biology.

4.4 Acknowledgements

We are grateful to Z. Diwu for contributive discussions. L.D.L was supported by Biotechnology Training Grant 08349 (NIH) and an ACS Division of Organic Chemistry

Fellowship sponsored by the Genentech Foundation. This work was supported by grant CA73808 (NIH). NMRFAM was supported by grant P41 RR02301 (NIH).

4.5 Experimental Section

4.5.1 Materials and Methods: Chemical Synthesis

5-Carboxyfluorescein, succinimidyl ester (5-FAM SE; **4.3**) was synthesized as described previously (Adamczyk *et al.*, 1997). Molecular sieves (3-Å) were dried for 3 h at 320 °C prior to use (Fieser and Fieser, 1967). Furan was purchased as “Furan, 99+%, inhibited with 0.025 wt. % BHT” (Aldrich; Product 185922) and was used as received. Dimethylformamide (DMF), tetrahydrofuran (THF), and dichloromethane (CH₂Cl₂) were drawn from a Baker CYCLE-TAINER solvent delivery system. All other reagents were obtained from Sigma (Saint Louis, MO) or Fisher Scientific (Hanover Park, IL) and used without further purification.

Thin-layer chromatography was performed using aluminum-backed plates coated with silica gel or C-18 silica gel containing F₂₅₄ phosphor and visualized by UV illumination or staining with I₂, ceric ammonium molybdate, or phosphomolybdic acid. Flash chromatography was performed by using open glass columns loaded with silica gel-60 (230–400 mesh), or on a FlashMaster Solo system (Argonaut Inc., Redwood City, CA) with Isolute Flash Si II columns (International Sorbent Technology Ltd., Hengoed, Mid Glamorgan, UK). The term “high vacuum” refers to a vacuum (≤ 1 mm Hg) achieved by a mechanical belt-drive oil pump. The term “concentrated under reduced pressure” refers to the removal of solvents and other volatile materials using a rotary evaporator at water-aspirator pressure (< 20 mm Hg) while maintaining the water-bath

temperature below 40 °C. The term “concentrated under high vacuum” refers to the removal of solvents and other volatile materials using a rotary evaporator at high vacuum while maintaining the water-bath temperature below 40 °C.

NMR spectra were obtained with a Bruker DMX-400 Avance spectrometer at the NMR Facility at Madison (NMRFAM). Mass spectrometry was performed with a Micromass LCT (electrospray ionization, ESI) mass spectrometer in the Mass Spectrometry Facility in the Department of Chemistry. Analytical HPLC was performed on a system from Waters (Milford, MA) with a Microsorb C18 Analytical HPLC column (4.6 × 250 mm; 5 µm) from Varian (Walnut Creek, CA). Analytical HPLC Method: linear gradient of 10% to 20% v/v CH₃CN in H₂O containing 1.0% v/v AcOH over 45 min; flow rate = 1.0 mL/min. Semipreparative HPLC was performed on a system from Waters (Milford, MA) with a SB-C8 Zorbax Semipreparative HPLC column (9.4 × 250 mm; 5 µm) from Agilent (Santa Clara, CA). Preparative HPLC Method: Linear gradient of 10% to 20% v/v CH₃CN in H₂O containing 1% v/v AcOH over 40 min; flow rate = 4.0 mL/min.

4.5.2 Synthesis of Compounds 4.2, 4.5, and 4.7–4.9

5-Carboxamidefluorescein, C₂-Maleimide (4.5). 5-Carboxyfluorescein succinimidyl ester **4.3** (Adamczyk *et al.*, 1997) (1.26 g, 2.66 mmol) was dissolved in anhydrous DMF (20 mL) under Ar(g). Hünig's base (1.85 mL, 10.63 mmol) was added followed by *N*-(2-aminoethyl)maleimide trifluoroacetate (**4.4**, 1.01 g, 3.99 mmol) (Arano *et al.*, 1996), and the reaction was stirred at ambient temperature for 24 h. The reaction mixture was concentrated under reduced pressure and the residue purified via column

chromatography (silica gel, 100:7:1 v/v/v CHCl₃:MeOH:AcOH) to give compound **4.4** as an yellow-orange solid (570 mg, 43%). ¹H NMR (400 MHz, DMSO-*d*₆) δ (ppm): 10.20 (bs, 2H), 8.93 (t, *J* = 5.9 Hz, 1H), 8.33 (s, 1H), 8.14 (dd, *J* = 8.5, 1.7 Hz, 1H), 7.37 (d, *J* = 8.3 Hz, 1H), 7.04 (s, 2H), 6.68 (d, *J* = 2.0 Hz, 2H), 6.57 (m, 4H), 3.63 (t, *J* = 5.9 Hz, 2H), 3.46 (q, *J* = 5.6 Hz, 2H). ¹³C NMR (100 MHz, DMSO-*d*₆) δ (ppm): 171.16, 168.20, 165.06, 159.87, 154.47, 151.89, 136.21, 134.60, 134.50, 129.15, 126.61, 124.38, 123.24, 112.86, 109.10, 102.31, 84.14, 37.90, 37.17. ESIMS [M+Na]⁺ calculated, 521.0961; found, 521.0947.

5-Carboxamid fluorescein, C₂ Maleimide, Di- β -D-Galactoside Octaacetate (4.7).

5-Carboxamid fluorescein, C₂-maleimide **4.4** (200 mg, 0.401 mmol) was dissolved in anhydrous CH₂Cl₂ (9 mL) and anhydrous THF (9 mL) under Ar(g). 2,3,4,6-Tetra-O-acetyl- α -D-galactopyranosyl bromide (**4.6**, 495 mg, 1.20 mmol) and silver carbonate (277 mg, 1.00 mmol) were added followed by 3-Å molecular sieves (500 mg). *sym*-Collidine (133 μ L, 1.00 mmol) was added dropwise and the reaction was stirred at ambient temperature for 96 h, protected from light. The reaction mixture was filtered through celite and rinsed with CHCl₃. The reaction mixture was concentrated under reduced pressure and the residue was dissolved in CHCl₃ and washed with 10% v/v HCl(aq), H₂O, 0.1 M Na₂S₂O₅, saturated NaHCO₃ and saturated brine. The organic layer was dried over anhydrous MgSO₄(s) and the solution was concentrated under reduced pressure to give crude 5-carboxamid fluorescein, C₂ maleimide, mono- β -galactoside tetraacetate as a pale orange solid. This material was dissolved in anhydrous toluene (25 mL) under Ar(g). 2,3,4,6-Tetra-O-acetyl- α -D-galactopyranosyl bromide (**4.6**, 495 mg, 1.20 mmol) and cadmium carbonate (173 mg, 1.00 mmol) were added and the reaction

was heated to reflux for 6 h with removal of water effected by a Dean–Stark apparatus. The reaction was concentrated under reduced pressure and the residue partitioned between EtOAc and H₂O. The layers were separated and the aqueous portion extracted with EtOAc. The combined organics were washed with saturated brine and dried over anhydrous MgSO₄(s). The solution was concentrated under reduced pressure and the crude product was purified via column chromatography (silica gel, 20% to 50% v/v gradient of EtOAc in Hexanes). Compound **4.7** was isolated as a white solid (351 mg, 75%, two steps). ¹H NMR (300 MHz, CDCl₃) δ (ppm): 8.35 (d, *J* = 1.0 Hz, 1H), 8.13 (dd, *J* = 7.9, 1.6 Hz, 1H), 7.23 (d, *J* = 8.1 Hz, 1H), 6.95 (t, *J* = 5.3 Hz, 1H), 6.90 (m, 2H), 6.78 (s, 2H), 6.71 (m, 4H), 5.49 (m, 4H), 5.11 (m, 4H), 4.18 (m, 6H), 3.88 (m, 2H), 3.73 (m, 2H), 2.19 (s, 2H), 2.07 (m, 18H). ¹³C NMR (100 MHz, CDCl₃) δ (ppm): 171.10, 170.35, 170.17, 170.09, 169.33, 168.22, 165.86, 158.40, 155.36, 151.98, 136.50, 134.38, 129.28, 126.85, 124.41, 123.48, 113.81, 113.10, 112.96, 104.70, 104.16, 99.08, 82.34, 71.27, 71.17, 70.68, 68.34, 66.68, 61.37, 61.23, 40.19, 37.49, 20.70, 20.65, 20.57. ESIMS [M+Na]⁺ calculated, 1181.2863; found, 1181.2897.

5-Carboxamid fluorescein, C₂ Maleimide–Furan, Di-β-D-Galactoside

Octaacetate (4.8). 5-Carboxamid fluorescein, C₂-maleimide, di-β-galactoside octaacetate (**4.7**, 40 mg, 0.0346 mmol) was dissolved in acetone (4 mL) and furan (1 mL) and heated a reflux for 48 h. Solvent was removed under reduced pressure and the residue was purified via column chromatography (silica gel, gradient of 1→2% v/v MeOH in CH₂Cl₂). Compound **4.8** was isolated as an off-white solid (23 mg, 55%). ¹H NMR (~9:1 *exo:endo* isomers; 400 MHz, CDCl₃) δ (ppm): 8.37 and 8.31 (s, 1H), 8.13 (m, 1H), 7.24–7.18 (m, 1H), 7.17–6.83 (m, 3H), 6.81–6.62 (m, 4H), 6.51 and 6.35 (s, 2H), 5.59–5.43

(m, 4H), 5.36–5.24 (m, 2H), 5.18–5.04 (m, 4H), 4.49–3.97 (m, 6H), 3.88–3.79 (m, 2H), 3.77–3.64 (m, 2H), 3.57 and 2.93 (m, 2H), 2.27–1.85 (m, 24H). ESIMS $[M+Na]^+$ calculated, 1249.3125; found, 1249.3075.

5-Carboxamidefluorescein, C₂ Maleimide–Furan, Di-β-D-Galactoside (4.9).

5-Carboxamidefluorescein, C₂ maleimide–furan, di-β-galactoside octaacetate (25 mg, 0.0204 mmol) was dissolved in 1:1 v/v/v MeOH:CH₃CN (3.2 mL) and cooled to 0° C. Na₂CO₃ (11 mg, 0.1019 mmol) in H₂O (0.8 mL) was added and the reaction was stirred for 2 h and monitored by TLC (C-18 silica gel, 20% v/v CH₃CN in H₂O, R_f = 0.26). The solution was diluted with MeOH (5 mL) and H₂O (5 mL) and neutralized with Amberlite IRC-50 ion-exchange resin. After filtration, the organics were removed under reduce pressure and the aqueous solution was lyophilized to yield a yellow powder. Purification by semipreparative HPLC afforded compound **4.9** as an off-white powder (9.2 mg, 51%). ESIMS $[M+Na]^+$ calculated, 913.2274; found, 913.2294. Analytical HPLC: >95% purity at λ = 254 nm; retention time 21.3 min.

5-Carboxamidefluorescein, C₂ Maleimide, Di-β-D-Galactoside (4.2).

5-Carboxamidefluorescein, C₂ maleimide–furan, di-β-galactoside (4.6 mg, 0.0052 mmol) was dissolved in anhydrous DMF (2 mL) and heated to 100 °C for 24 h. The reaction was concentrated under high vacuum and the residue taken up into H₂O and lyophilized to yield a pale yellow powder. Purification by semipreparative HPLC afforded compound **4.2** was isolated as an off-white powder (1.6 mg, 38%). ESIMS $[M+Na]^+$ calculated, 845.2017; found, 845.2018. Analytical HPLC: >95% purity at λ = 254 nm; retention time 19.6 min.

4.5.3 Protein Conjugation

The TNB-protected A19C variant of RNase A and the Oregon Green-labeled RNase A conjugate were prepared as described previously (Lavis *et al.*, 2006a). The TNB-protected protein was deprotected with a three-fold molar excess of dithiothreitol (DTT) and desalted by chromatography using a PD10 Desalting column (GE Healthcare). The protein conjugate then was prepared by reaction with two-fold molar excess of thiol-reactive maleimide **4.2** for 6 h at 25 °C. Purification by chromatography using a HiTrap HP SP column (GE Healthcare) afforded the desired conjugate (MS (MALDI-TOF): *m/z* 14535 (expected: 14537)). Protein concentration was determined by using a bicinchoninic acid (BCA) assay kit from Pierce with wild-type RNase A as a standard.

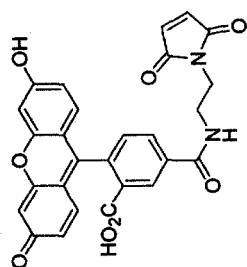
4.5.4 Cell Preparation

HeLa cells were seeded in 35mm glass bottom dishes at a cell density of 1.2×10^5 cells per dish in DMEM containing FBS (10% v/v). After incubation at 37 °C for 24 h, cells were transfected with the plasmid *p3313-LacZ-mRFP* using PolyFect transfection reagent (Qiagen, Valencia, CA). At 24 h post-transfection, cells were first washed three times with Dulbecco's phosphate-buffered saline (DPBS, Invitrogen) and incubated with 800 μ L of DMEM containing 10% v/v FBS and RNase A-maleimide **4.4** conjugate (10 μ M), for 24 h at 37 °C prior to imaging. Nuclear staining was accomplished by addition of Hoechst 33342 (2 μ g/mL) for the final 5 min of incubation.

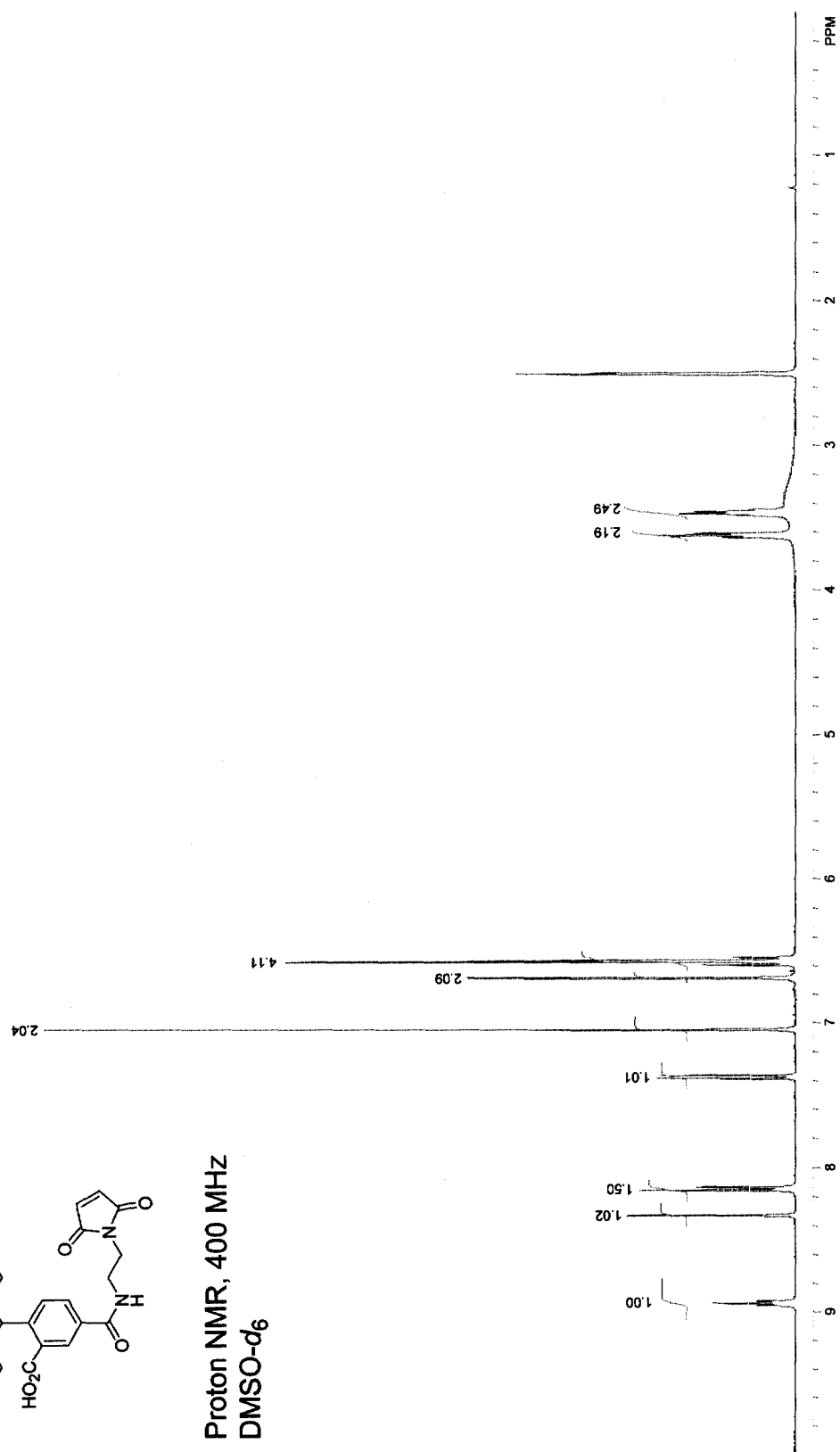
4.5.5 Cell Imaging

Cells were imaged on a Nikon Eclipse TE2000-U confocal microscope equipped with a Zeiss AxioCam digital camera, unless indicated otherwise. Excitation at 408 nm was provided by a blue-diode laser, and emission light was passed through a filter centered at 450 nm with a 35-nm band-pass. Excitation at 488 nm was provided by an argon-ion laser and emission light was passed through a filter centered at 515 nm with a 40-nm band-pass. Excitation at 543 nm was provided by a HeNe laser, and emission light was passed through a filter centered at 605 nm with a 75-nm band-pass.

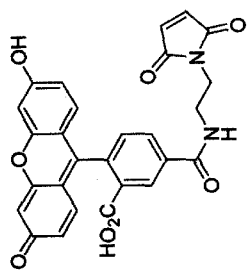
4.5



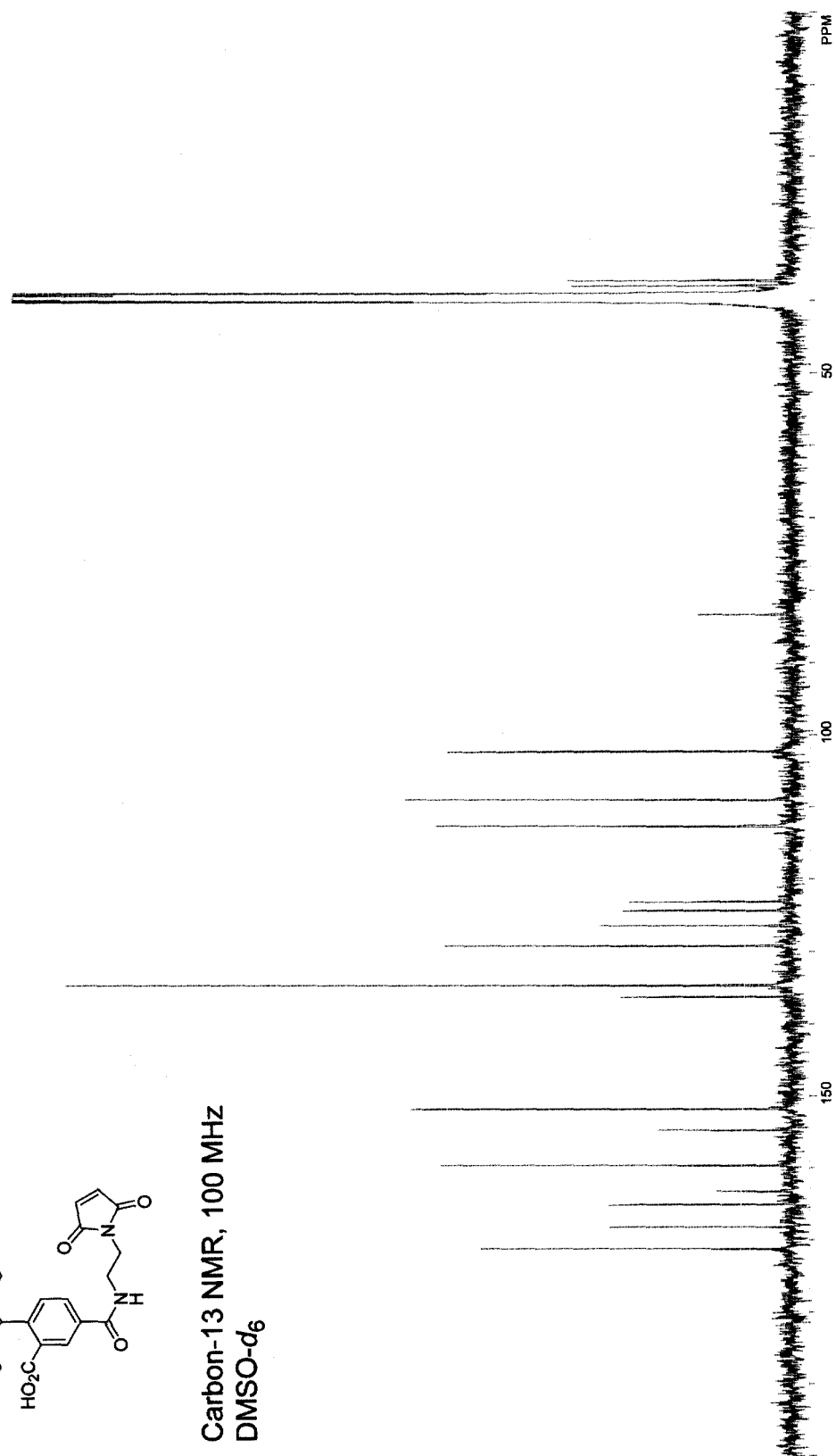
Proton NMR, 400 MHz
DMSO- d_6

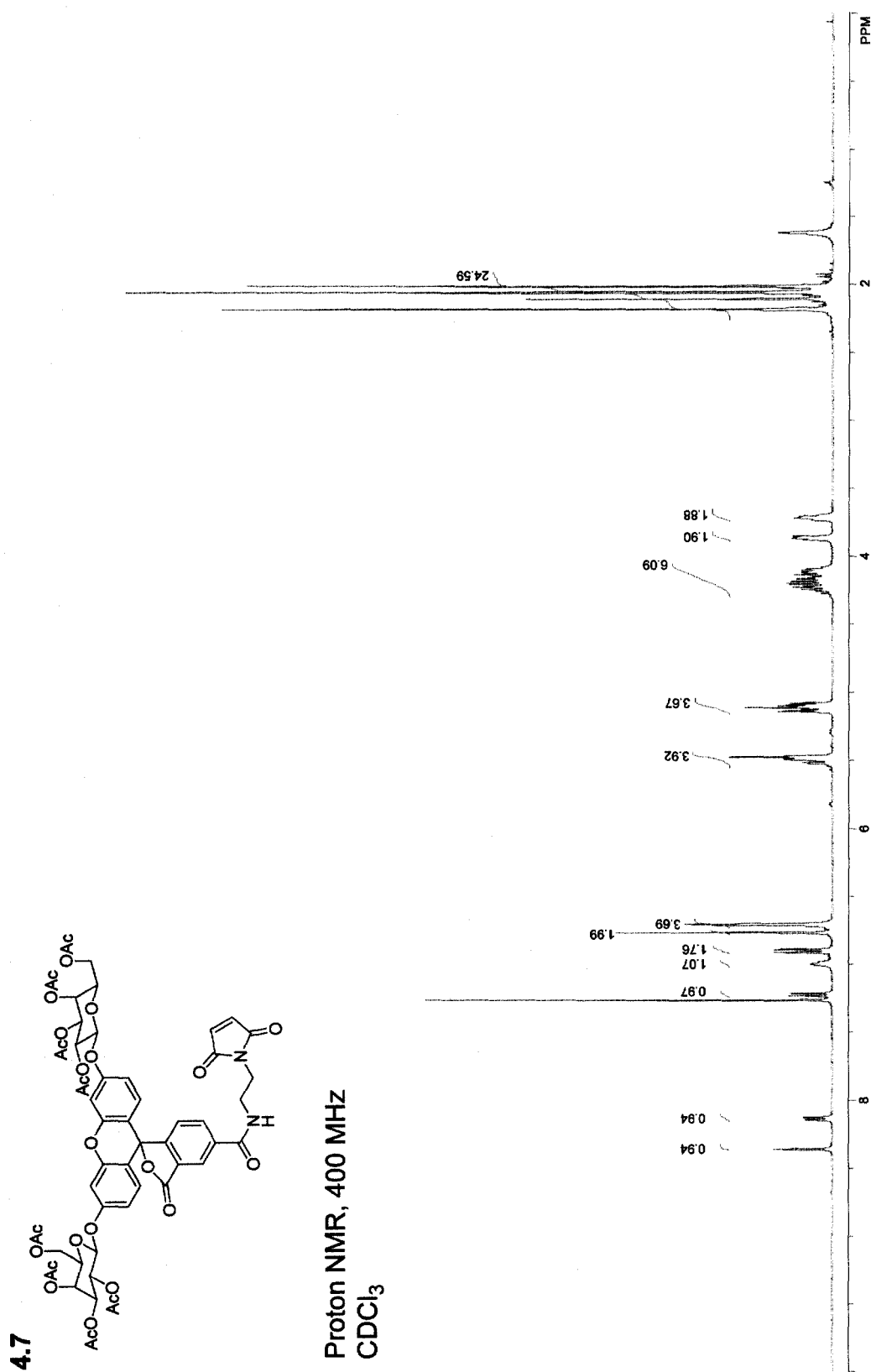


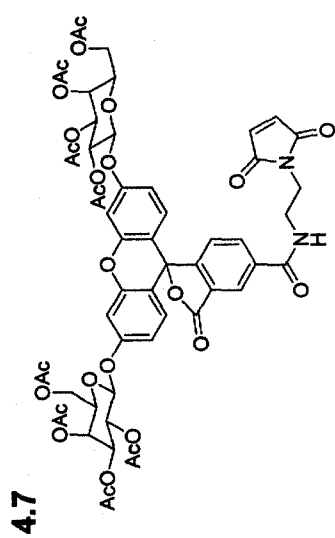
4.5



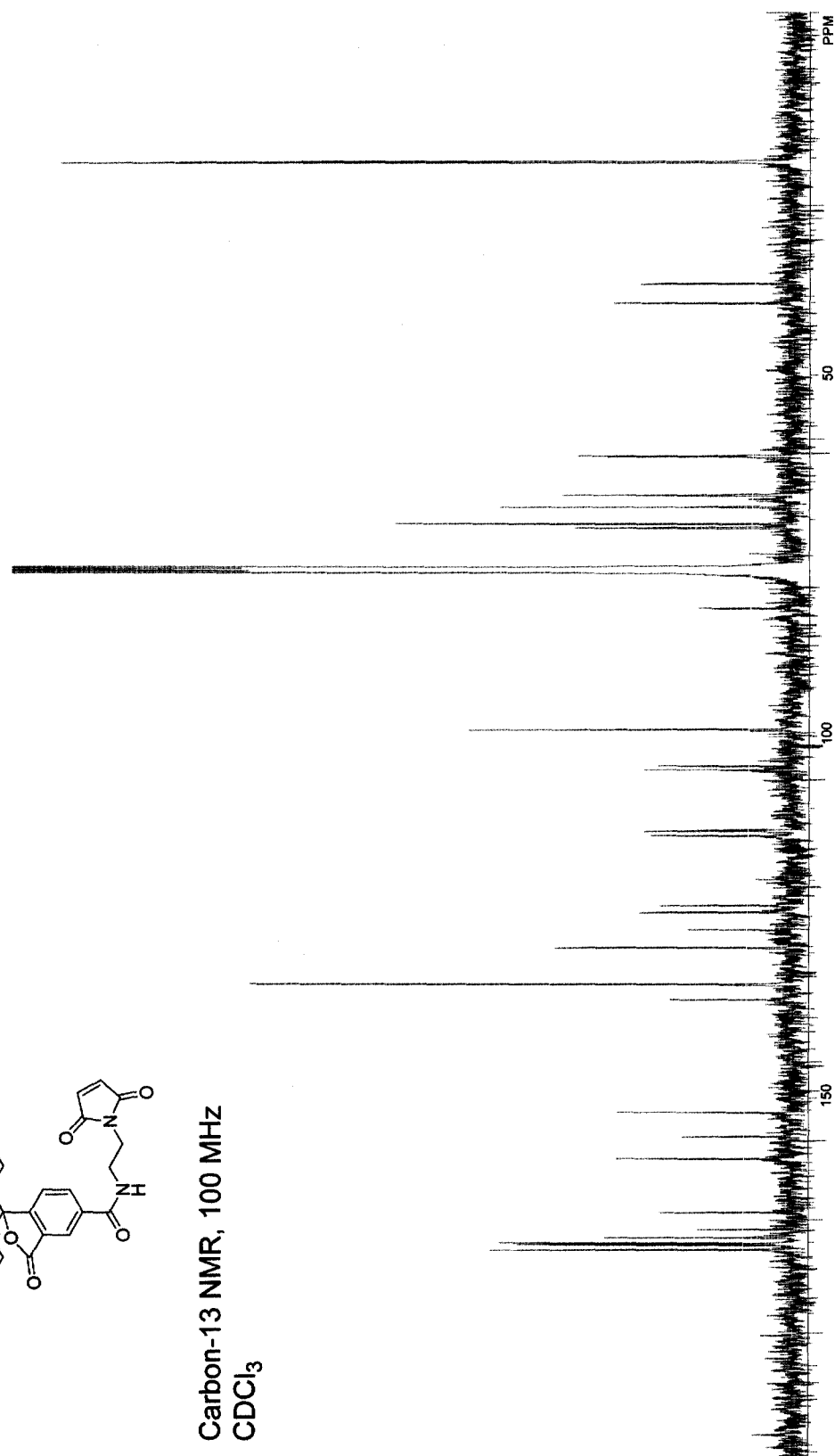
Carbon-13 NMR, 100 MHz
DMSO-*d*₆

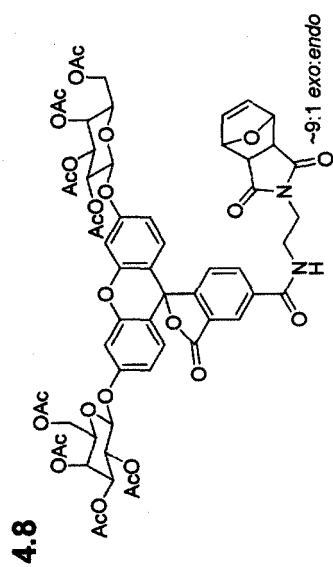




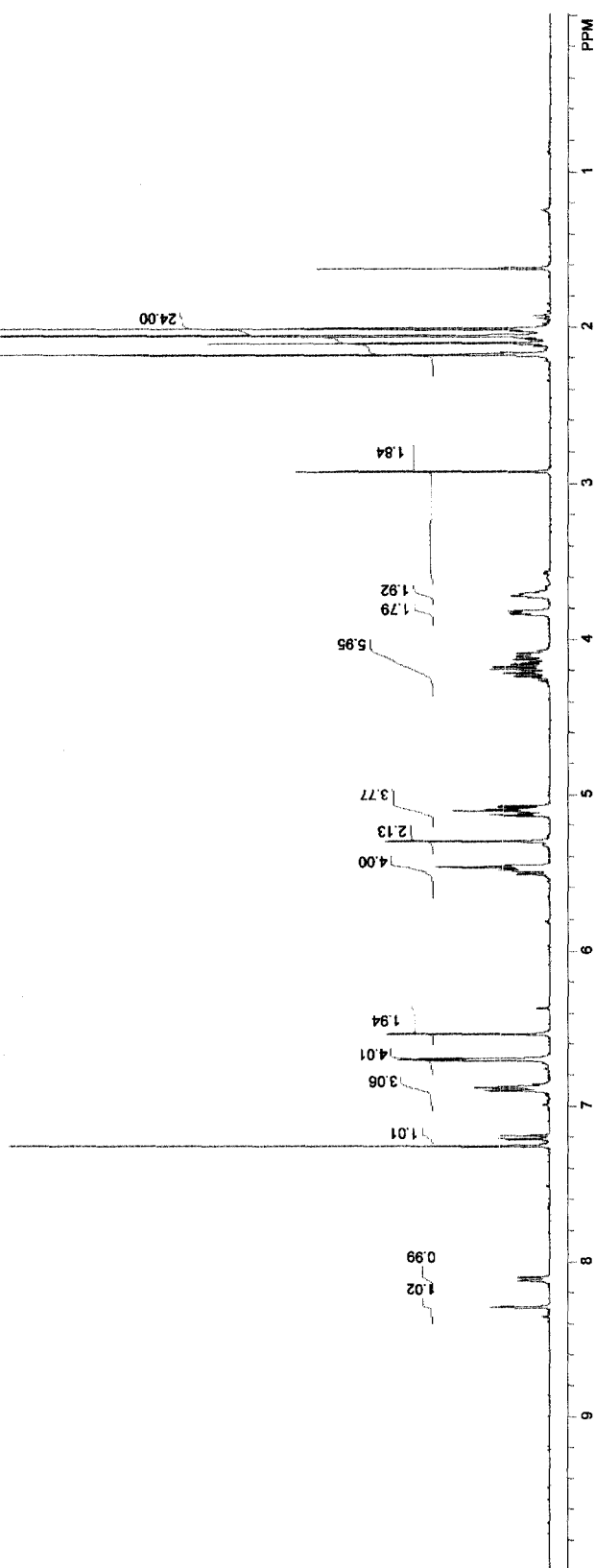


Carbon-13 NMR, 100 MHz
CDCl₃

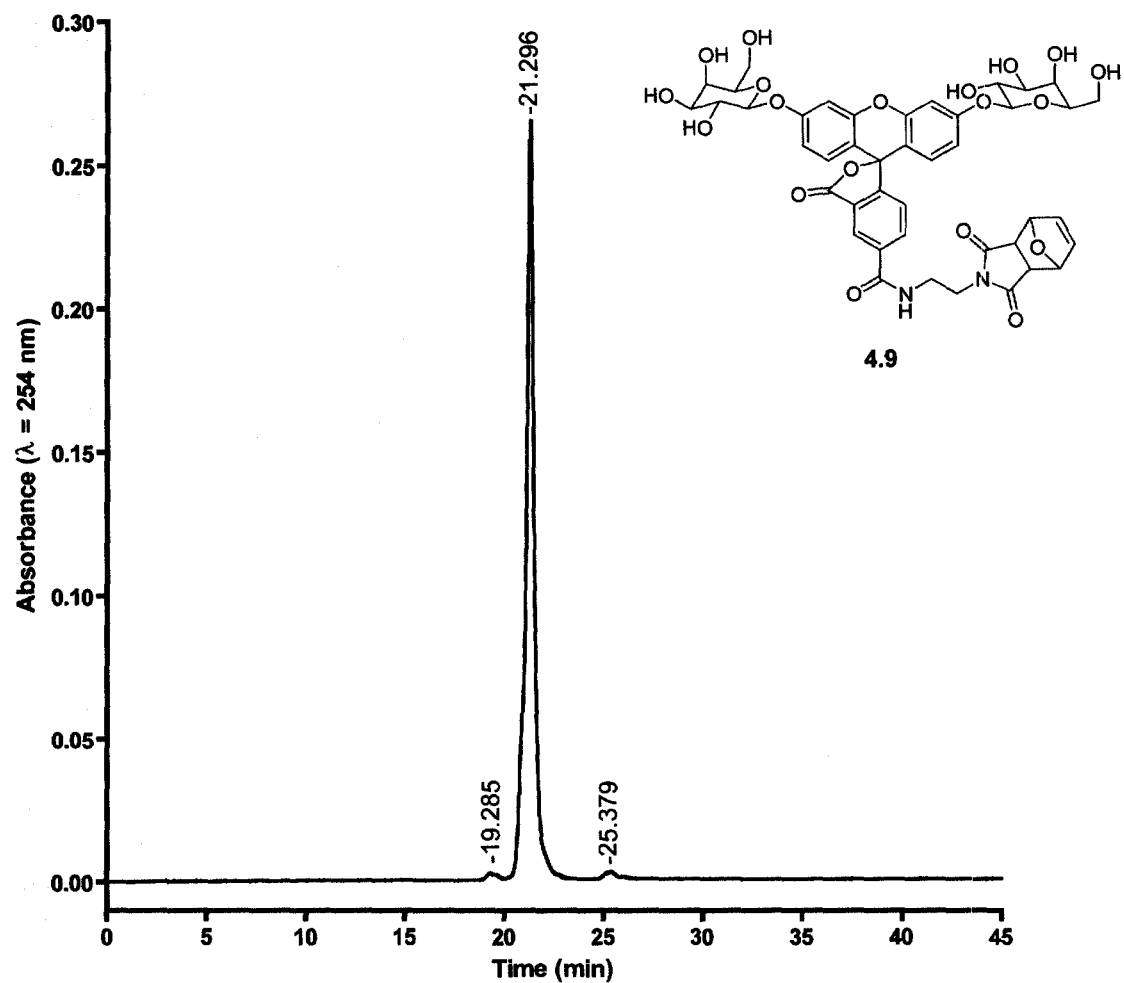




Proton NMR, 400 MHz
CDCl₃

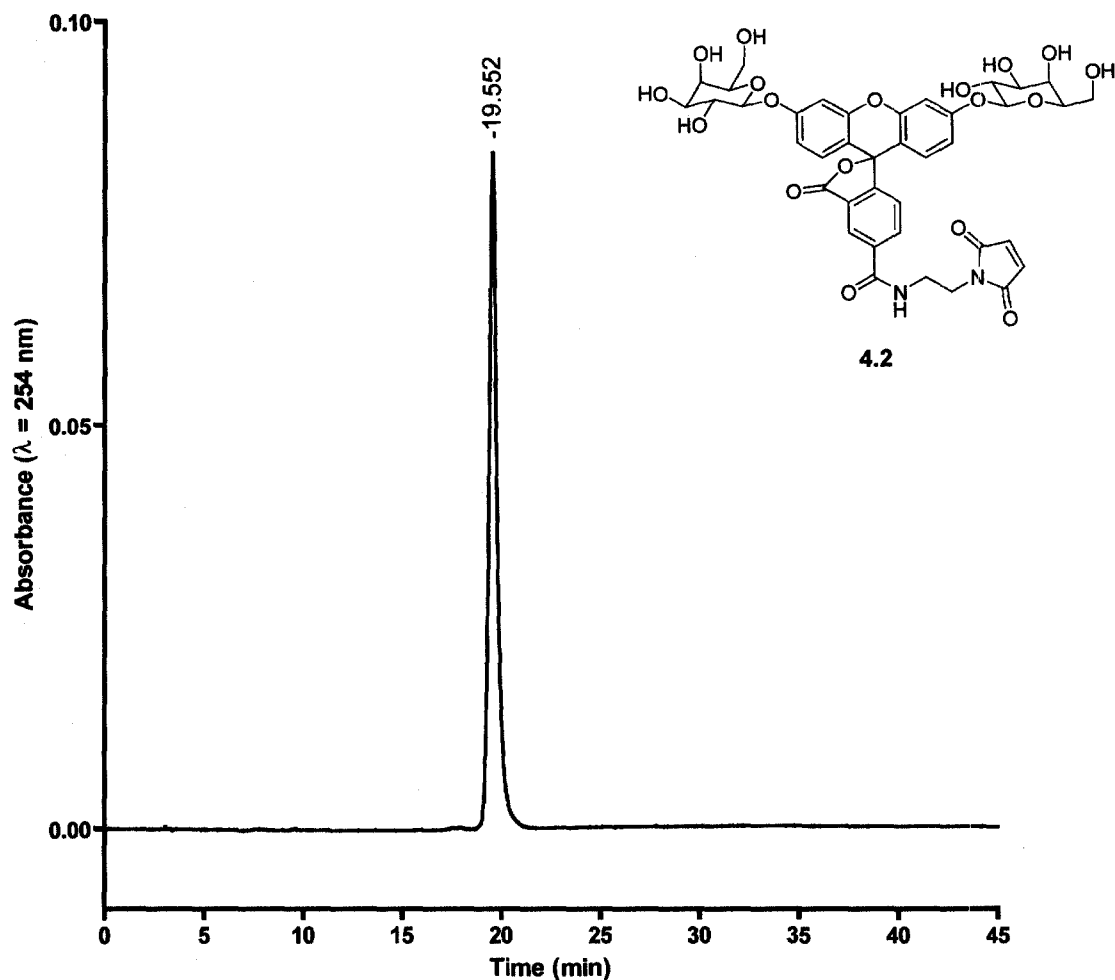


Analytical HPLC Trace
Microsorb C18 Column
10→20% v/v CH₃CN in H₂O with 1% v/v AcOH



Peak	Retention Time	Area	% Area	Height
1	19.285	50898	0.66	1568
2	21.296	7608337	98.43	263508
3	25.379	70809	0.92	1841

Analytical HPLC Trace
Microsorb C18 Column
10→20% v/v CH₃CN in H₂O with 1% v/v AcOH



Peak	Retention Time	Area	% Area	Height
1	19.552	2277767	100.00	82439

CHAPTER 5

ACETOXYMETHYL ETHERS AS FLUOROPHORE ESTER SURROGATES

Contribution: Chemical synthesis, *in vitro* enzyme assays, stability studies, composition of chapter, and preparation of figure drafts. Cellular imaging studies were performed by T.-Y. Chao.

5.1 Introduction

Fluorogenic enzyme substrates are vital tools for bioresearch. Uses for such compounds include the discovery of enzyme inhibitors via high-throughput screening, the enzyme-linked immunosorbent assay (ELISA), quantification of reporter gene activity, and assessment of cell viability (Johnson, 1998; Goddard and Reymond, 2004a; Haugland *et al.*, 2005). In particular, esterase-sensitive functionalities are used widely, as the endogenous, nonspecific, and ubiquitous esterases within eukaryotic cells catalyze the hydrolysis of ester bonds in fluorophores (Rotman and Papermaster, 1966; Thomas *et al.*, 1979; Paradiso *et al.*, 1984). This esterase-sensitive strategy is used not only to mask fluorophoric moieties, but also other polar functionalities to allow efficient diffusion of the compound across cellular membranes (Tsien, 1981; Schultz *et al.*, 1993).

Chemical stability of fluorogenic esterase substrates is paramount, as spontaneous hydrolysis competes deleteriously with enzymatic activity. One strategy to improve the stability of fluorogenic substrates involves insertion of a self-immolative chemical functionality between the fluorophore and the enzyme-reactive moiety (Ho *et al.*, 2007). In this tactic, enzyme action yields an intermediate that undergoes rapid decomposition to release ultimately the free fluorophore. We have used this idea in the synthesis of fluorogenic esterase substrates based on the “trimethyl lock” prodrug strategy to mask amine-containing fluorophores (Chandran *et al.*, 2005; Lavis *et al.*, 2006a; Lavis *et al.*, 2006b). These “profluorophores” possessed high chemical stability, but were unmasked by esterases efficiently both *in vitro* and *in cellulo*.

We used the trimethyl lock system to mask aniline-containing fluorophores such as rhodamine 110 (Chandran *et al.*, 2005) and 7-amino-4-methyl-coumarin (Lavis *et al.*,

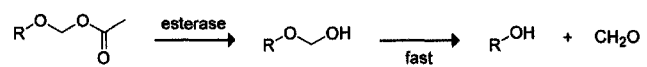
2006b). These compounds were found to have superior chemical stability compared to analogous substrates based on esters of phenolic fluorophores fluorescein and 4-methylumbelliferylone. Indeed, the masking of phenolic-containing fluorophores as esters suffers from two juxtaposed problems. The phenolic fluorophores possess relatively low pK_a values, causing instability of the ester bonds in aqueous solution. These low pK_a values, however, are essential, as the conjugate base of the fluorophore is typically the most fluorescent species (Sun *et al.*, 1998; Lavis *et al.*, 2007). Thus, increasing the stability of a simple fluorophore ester substrate by altering the pK_a of the fluorophore phenolic moiety could have detrimental effects on the fluorescence properties of that fluorophore.

The trimethyl lock strategy was not applicable to phenolic-type fluorophores such as fluorescein. We reasoned that insertion of a simple oxygen–methylene group into a fluorophore acetate ester substrate could “insulate” the reactive group from the dye portion and thus endow the compound with increased stability. Hydrolysis of the enzyme-labile moiety in these acetoxymethyl-containing substrates results in a hemiacetal that decomposes spontaneously to liberate the free oxygen atom (Scheme 5.1).

This strategy has been used before. Acetoxymethyl (AM) esters ($R = \text{carbonyl}$; Scheme 5.1) were first used to increase the cell-permeability of certain antibiotics (Jansen and Russell, 1965; Ferres, 1980) and is now a well-known prodrug strategy (Testa and Mayer, 2003). Tsein later used AM esters as an effective means to deliver carboxylate-containing ion indicators to cells (Tsien, 1981). Acetoxymethyl ethers of phenols ($R = \text{aryl}$; Scheme 5.1) have also been used in prodrug strategies (Bodor *et al.*, 1983;

Ouyang *et al.*, 2002; Thomas and Sloan, 2007) and to create fluorogenic enzyme substrates. Reymond and co-workers established that acyloxymethyl ethers of 4-methylumbelliferylone could be useful profluorophores with improved stability (Leroy *et al.*, 2003). Curiously, reports (Bensel *et al.*, 2001; Yang *et al.*, 2006) from the Reymond lab also detail the synthesis of a monoacyloxymethyl ethers of fluorescein but to our knowledge, no report of a diacyloxymethyl ether of fluorescein exists. Furthermore, this strategy has not been used to shield fluorophores with red-shifted wavelengths. Fluorogenic esterase substrates with red-shifted wavelengths that are useful in cell biology remain surprisingly sparse (Haugland *et al.*, 2005; Lavis *et al.*, 2006b).

Here we use the acetoxymethyl ether system to prepare substrates based on fluorescein and 2',7'-difluorofluorescein, Tokyo Green, and resorufin derivatives. We first investigate experimental conditions to allow efficient synthesis of such compounds from accessible chemical reagents. We then assess the hydrolytic stability, enzyme kinetics, and behavior in live human cells. Our preliminary results show the acetoxymethyl ether profluorophores possess higher chemical stability compared to analogous fluorophore-ester compounds and can be unmasked by esterases *in vitro* and *in cellulo*.

Scheme 5.1 Unmasking of acetoxymethyl (AM) groups by esterase

5.2 Results and Discussion

5.2.1 Fluorescein-Based Profluorophores

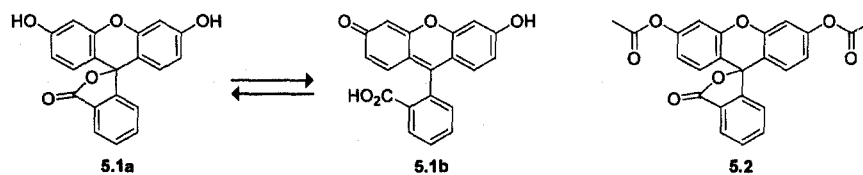
Fluorescein (**5.1**; Scheme 5.2), first synthesized by Baeyer in 1871 (Baeyer, 1871), remains one of the most widely used fluorophores in modern biological and biochemical research. Fluorescein derivatives are used as biomolecule labels, ion indicators, and fluorogenic enzyme substrates (Johnson, 1998; Haugland *et al.*, 2005; Lavis *et al.*, 2007). This latter use exploits the equilibrium between two forms of fluorescein—the colorless lactone **5.1a** and a fluorescent quinoid **5.1b** (Scheme 5.2). Acylation or alkylation of the phenol groups of fluorescein locks the molecule in the nonfluorescent lactone form **5.1a**. Enzymatic activity can liberate the phenolic oxygens in fluorescein, shifting the equilibrium back to the quinoid form **5.1b** with concomitant increase in fluorescence.

The archetype of fluorescein-based enzyme substrates is fluorescein diacetate (FDA; **5.2**). Rotman and coworkers demonstrated that FDA could cross cell membranes and be activated by cellular esterases (Rotman and Papermaster, 1966). This diester strategy has been used to mask a variety of fluorescein derivatives for intracellular delivery (Haugland *et al.*, 2005). Related fluorogenic enzyme substrates include derivatives such as fluorescein diphosphate (FDP) and fluorescein di- β -D-galactopyranoside (FDG). FDP has found wide use as a substrate for alkaline phosphatase (Rotman *et al.*, 1963; Huang *et al.*, 1999) and FDG derivatives are used to visualize β -galactosidase activity, the gene product of *lacZ* (Koide *et al.*, 2007).

Despite the wide use of FDA and its derivatives in biological systems, this substrate suffers from two significant disadvantages. First, FDA exhibits relatively poor stability in aqueous solution as fluorescein is an excellent ester leaving group (Chandran *et al.*, 2005;

Lavis *et al.*, 2006a). Second, the released fluorescein is both pH sensitive (Lavis *et al.*, 2007) and susceptible to photobleaching (Haugland *et al.*, 2005). Thus, new fluorescein-based substrates that exhibit increased stability, maintain enzymatic reactivity, and release fluorescein derivatives with superior properties should find use in a variety of applications.

Scheme 5.2 Equilibrium forms of fluorescein (**5.1**) and the structure of fluorescein diacetate (**5.2**)



5.2.2 Synthesis of Fluorescein AM Ethers

Synthesis of diacetoxymethyl ethers of fluorescein derivatives required finesse. In published reports of acetoxymethyl ethers of fluorophore derivatives, syntheses involve deprotonation of the fluorophore phenolic moiety with NaH followed by addition of a halomethyl ester such as bromomethyl acetate (**5.4**; Scheme 5.3; (Leroy *et al.*, 2003; Yang *et al.*, 2006)). This synthesis of AM ethers is low-yielding (~10%) due to the presence of two electrophilic carbons in the halomethyl ester molecule leading to a mixture of ester and ether products (Ouyang *et al.*, 2002; Yang *et al.*, 2006). Based on the poor yield of monosubstituted fluoresceins using this strategy (Yang *et al.*, 2006), we suspected the preparation of disubstituted AM ether profluorophores would require a different synthetic route.

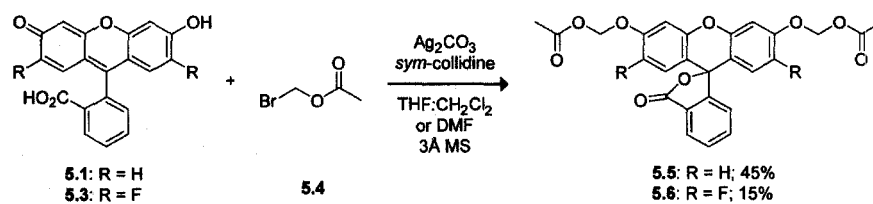
Similar nucleophilic substitution reactions between oxygen nucleophiles and halomethyl esters have used amine bases in DMF (Tsien, 1980), phase-transfer conditions (Thomas and Sloan, 2007), or carbonate salts in polar aprotic solvents (Bodor *et al.*, 1983; Ouyang *et al.*, 2002). These strategies work to prepare AM esters from carboxylic acids and AM ethers from simple phenols. Still, the added complexity of the fluorescein molecule—with the additional carboxyl group and associated equilibrium—allow the formation of an AM ether–AM ester byproduct. These concerns prompted evaluation of different reaction conditions. Initial attempts to synthesize a disubstituted fluorescein using Hünig's base in DMF with bromomethyl acetate (**5.4**) showed poor conversion under ambient conditions. At elevated temperature some reaction progress was observed. The major product proved to be fluorescein diacetate (**5.2**), however, showcasing the bifurcated reactivity of the bromomethyl acetate molecule.

To encourage the desired substitution reaction, we were interested in utilizing silver(I) salts under heterogeneous reaction conditions which can encourage nucleophilic substitution at a halide-bearing carbon (Mislow, 1951; Paulsen, 1982; Krafft *et al.*, 1988). This could partition the reaction toward the desired AM ether product. As an initial test, we subjected the fluorescein molecule to bromomethyl acetate with Ag_2CO_3 in $\text{THF}:\text{CH}_2\text{Cl}_2$ —conditions reserved typically for glycosylation of the fluorescein molecule (Haugland *et al.*, 1990). The reaction gave the desired profluorophore **5.5** in 45% isolated yield (Scheme 5.3).

With this promising initial result, we then applied this strategy to another fluorescein derivative. Substitution of the 2' and 7' position of fluorescein can alter the fluorescent properties of the molecule (Haugland *et al.*, 2005; Lavis *et al.*, 2007). Notably, fluorine substitution at these positions lowers the $\text{p}K_a$ of the molecule giving a dye with diminished pH sensitivity and increased photostability (Sun *et al.*, 1997). Unfortunately, this lower $\text{p}K_a$ also reduces the stability of diester derivatives causing an increase in fluorescence background (Gee, 1999). We reasoned that the acetoxymethyl ether system could insulate the ester functionality from the electron-withdrawing fluoro groups, making it less susceptible to spontaneous hydrolysis.

This hypothesis was tested through the synthesis of 2',7'-difluorofluorescein using an established route (Sun *et al.*, 1997). The material was subjected to similar conditions used to install the AM groups in unsubstituted fluorescein. Due to solubility concerns, DMF was used in place of the $\text{THF}:\text{CH}_2\text{Cl}_2$ mixture. These reaction conditions gave the desired profluorophore **5.6**, albeit in lower yield (Scheme 5.3). The observed difference in reactivity between fluorescein and difluorofluorescein is due likely to several factors. The

difference in nucleophilicity of the phenolic groups due to the fluoro substitution could decrease reaction efficiency. In addition, the open–closed equilibrium could be altered leading to increased byproduct formation. Investigation of other reaction conditions could furnish this compound in improved yield (*vide infra*).

Scheme 5.3 Synthesis of AM ether profluorophores **5.5** and **5.6**

5.2.3 Chemical Stability of AM Ethers

The chemical stability of both fluorescein diacetoxymethyl ether (**5.5**) and 2',7'-difluorofluorescein diacetoxymethyl ether (**5.6**) profluorophores were assessed by incubating these compounds in aqueous solution and monitoring the accretion of fluorescence over time. For reference, fluorescein diacetate (**5.2**) and the analog 2',7'-difluorofluorescein diacetate (DFFDA) were also subjected to the same conditions. The results are shown in Figure 5.1.

As shown in Figure 5.1a each of the compounds showed low initial fluorescence signals in Dulbecco's phosphate-buffered saline (DPBS). This signifies both acylation and alkylation of the phenolic groups in fluorescein locks the molecule into the nonfluorescent lactone form. The diester compounds: DFFDA and **5.2** undergo spontaneous hydrolysis faster than do the AM ether profluorophores **5.5** and **5.6**. This difference in stability is more pronounced in Dulbecco's modified Eagle's medium (DMEM; Figure 5.1b). Here, DFFDA exhibited a half-life of minutes and FDA was hydrolyzed completely in hours. This is in contrast to the higher stability of the acetoxymethyl ether dyes **5.5** and **5.6**, which show only modest hydrolysis over the same time period. The similarity in the chemical stability of the AM ether dyes support the hypothesis that the acetoxymethyl groups insulate the ester bond, and therefore diminish the effect of fluorine substitution on the chemical stability of the substrate. In particular, profluorophore **5.6** realizes our goal of creating a fluorogenic esterase substrate exhibiting higher chemical stability than fluorescein diacetate (**5.2**), but releasing a pH-insensitive dye with increased photostability (Sun *et al.*, 1997).

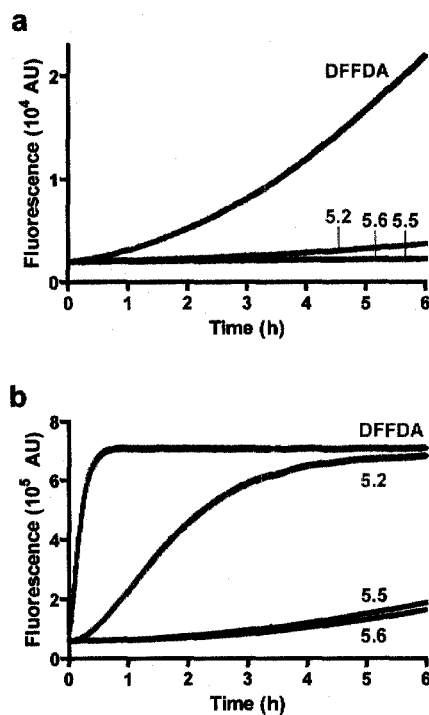


Figure 5.1 Time course of the generation of fluorescence (λ_{ex} 496 nm, λ_{em} 520 nm) of esterase substrates (25 nM). (a) 2',7'-Difluorofluorescein diacetate (DFFDA), fluorescein diacetate (5.2) and profluorophores 5.5 and 5.6 in DPBS. (b) 2',7'-Difluorofluorescein diacetate (DFFDA), fluorescein diacetate (5.2), and profluorophores 5.5 and 5.6 in DMEM containing 10% v/v FBS.

5.2.4 Enzyme-Catalyzed Hydrolysis of AM Ethers

Having established the improved chemical stability of profluorophores **5.5** and **5.6**, we sought to assess the enzymatic reactivity of these potential enzyme substrates *in vitro*. Incubation of both of these compounds with porcine liver esterase (PLE) elicited a rapid increase in fluorescence intensity. Preliminary kinetic traces are shown in Figure 5.2. The substrates behaved similarly, giving approximate kinetic constants of $k_{\text{cat}}/K_{\text{M}} \approx 1.4 \times 10^6 \text{ M}^{-1}\text{s}^{-1}$ and $K_{\text{M}} \approx 1.9 \text{ }\mu\text{M}$ for substrate **5.5** (Figure 5.2a), and $k_{\text{cat}}/K_{\text{M}} \approx 1.0 \times 10^6 \text{ M}^{-1}\text{s}^{-1}$ and $K_{\text{M}} \approx 1.5 \text{ }\mu\text{M}$ for substrate **5.6** (Figure 5.2b). These approximate kinetic constants were similar to those measured for fluorescein diacetate (**5.2**; data not shown), suggesting that enzyme-mediated ester hydrolysis—not decomposition of the nascent hemiacetal—is the slow step in the reaction pathway to fluorophore release. Attempts to better quantify kinetic parameters through the use of higher substrates concentration have met solubility problems. Investigation into conditions utilizing co-solvents such as DMF or DMSO (Yang *et al.*, 2006) are ongoing.

5.2.5 Cellular Imaging Studies

The acetoxymethyl ethers of fluorescein are substrates for purified enzyme *in vitro*. The utility of the AM ether-masked dyes was then assessed in live human cells to test whether these compounds could be unmasked by endogenous esterase activity. Figure 5.3 shows fluorescence microscopy images of live HeLa cells incubated with either fluorescein diacetate (**5.2**; Figure 5.3a), fluorescein diacetoxymethyl ether (**5.5**; Figure 5.3b), 2',7'-difluorofluorescein diacetate (DFFDA; ; Figure 5.3c), or 2',7'-difluorofluorescein diacetoxymethyl ether (**5.6**; Figure 5.3d). All four experiments

show bright cellular staining, indicating the molecule is indeed internalized and unmasked by cellular esterases. Moreover, the extracellular background in Figures 5.3a and 5.3c is much higher than the other images, indicative of the poor relative chemical stability of the fluorescein diacetate derivatives in aqueous solution compared to the AM ether profluorophores.

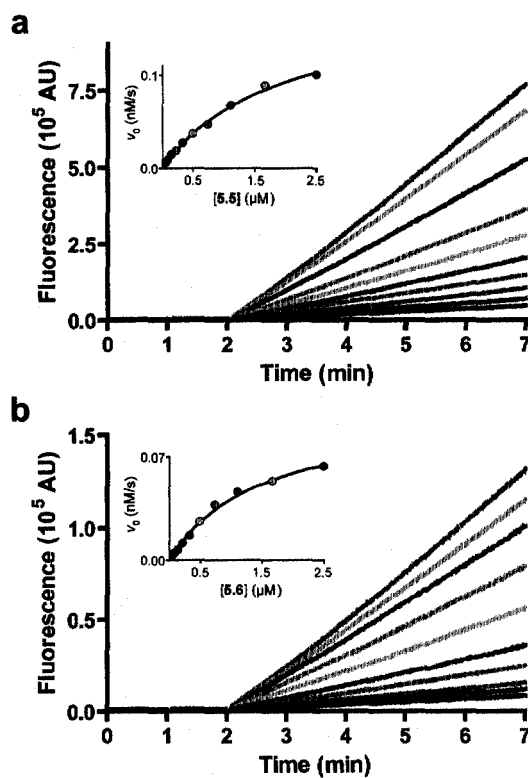


Figure 5.2 Kinetic traces and Michaelis–Menten plot (inset) for the hydrolysis of esterase substrates by PLE (25 ng/mL). (a) Compound **5.5** (2.5 μM→65 nM); $k_{\text{cat}}/K_{\text{M}} \approx 1.4 \times 10^6 \text{ M}^{-1}\text{s}^{-1}$ and $K_{\text{M}} \approx 1.9 \text{ μM}$. (b) Compound **5.6** (2.5 μM→65 nM); $k_{\text{cat}}/K_{\text{M}} \approx 1.0 \times 10^6 \text{ M}^{-1}\text{s}^{-1}$ and $K_{\text{M}} \approx 1.5 \text{ μM}$.

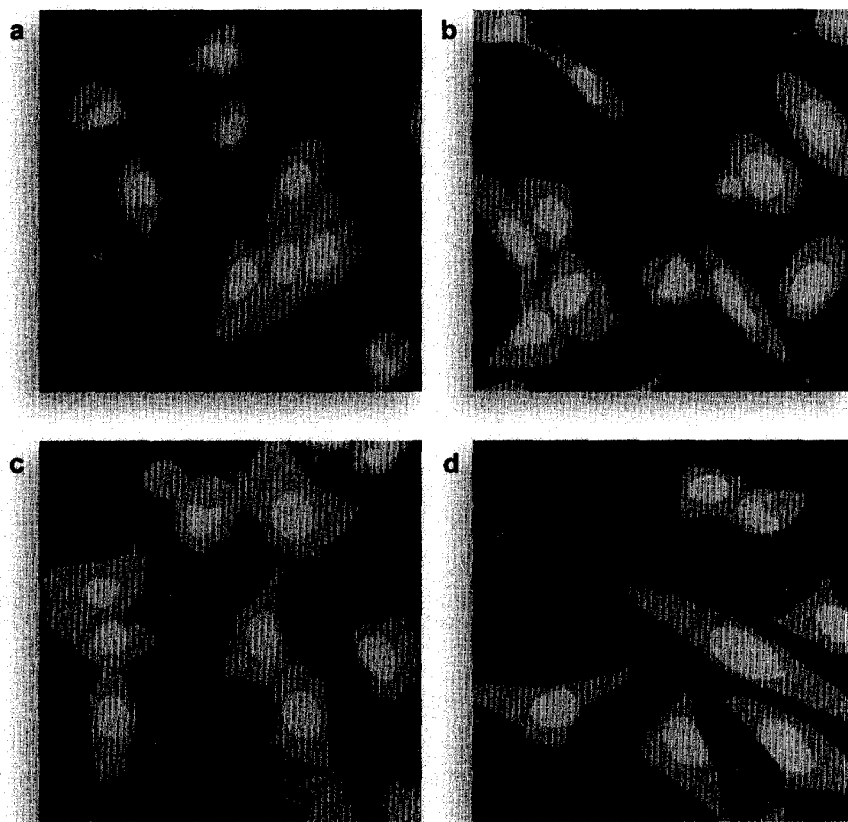


Figure 5.3 Unwashed, live HeLa cells incubated with esterase substrates **5.2**, **5.5**, and **5.6** (10 μ M) for 1 h and counterstained with Hoechst 33342 (5% v/v CO₂(g), 100% humidity). (a) FDA (**5.2**). (b) Profluorophore **5.5**. (c) 2',7'-difluorofluorescein diacetate (DFFDA). (d) Profluorophore **5.6**.

5.3 Future Directions and Conclusions

5.3.1 Optimizing Reaction Conditions for Fluorescein AM Ether Synthesis

In addition to use of Ag_2CO_3 with *sym*-collidine, other reaction conditions hold promise. Initial screening of different bases and solvents to identify other viable reaction conditions has identified Ag_2O in anhydrous CH_3CN as a useful reagent for preparation of these compounds. CH_3CN appears to maintain the “closed” lactone form of fluorescein and has been used in preparation of other fluorescein derivatives (Kasai *et al.*, 1993). In addition, the synthesis of the fluorescein diacetoxymethyl ether (**5.5**) using phase-transfer conditions (Thomas and Sloan, 2007) gave the molecule in 31% isolated yield. These reaction conditions allow higher concentrations and circumvent the use of heterogeneous (and expensive) Ag(I) salts. All of these described reaction conditions constitute a marked improvement over the existing methods to prepare fluorophore AM ethers using NaH (Leroy *et al.*, 2003; Yang *et al.*, 2006).

5.3.2 Other Fluorophore AM Ethers

Based on the promising work from the fluorescein-based AM ether profluorophores, this strategy has been applied to other dyes as shown in Scheme 5.4. Reaction of the phenolic dyes with bromomethyl acetate (**5.4**) in the presence of a base gave the desired substrate molecule with poor to moderate yields. They include substrate **5.8** based on the fluorescein variant with the common name “Tokyo Green” (**5.7**; (Urano *et al.*, 2005)). Here the fluorescein system is modified by substitution of the carboxyl group on the pendant phenyl ring with a simple methyl group, and addition of an electron-donating methoxy group. The electron-rich ring facilitates photoinduced electron transfer (PeT)

that quenches fluorescence when the phenolic portion of the fluorescein is protonated or alkylated (Urano *et al.*, 2005; Kobayashi *et al.*, 2007). We reasoned the acetoxymethyl ether strategy could suppress the fluorescence of this dye, providing a stable substrate that would be unmasked in a single step. Incubation of Tokyo Green (5.7) with bromomethyl acetate (5.4) with Hünig's base afforded the desired compound (5.8) in good yield. Unlike fluorescein, this molecule does not suffer from the complex lactone–quinoid equilibria, resulting in an improved yield. Figure 5.4 shows preliminary live-cell imaging experiments where fluorescein diacetoxymethyl ether (5.5; Figure 5.4a) is compared to profluorophore 5.8 (Figure 5.4b). We observed efficient unmasking of these probes by endogenous cellular esterases and resulting cellular fluorescence is evident. The overall brightness of the fluorescence in cells with profluorophore 5.8 appears lower, due perhaps to protonation of the released Tokyo Green dye, causing diminished fluorescence *in cellulo*.

Resorufin (5.9) exhibits excitation and emission wavelengths that are red-shifted relative to fluorescein ($\lambda_{\text{ex}} = 572 \text{ nm}$, $\lambda_{\text{em}} = 585 \text{ nm}$; (Bueno *et al.*, 2002)). Substitution on the phenolic group of resorufin elicits a hypsochromic shift and a dramatic decrease in quantum yield. Alkylated and glycosylated variants of resorufin are used extensively as enzyme substrates (Hofmann and Sernetz, 1984; Burke *et al.*, 1994). Based on this precedence, resorufin seemed a good candidate for the acetoxymethyl ether strategy. We prepared profluorophore 5.10 through Ag_2O -mediated alkylation of resorufin in DMF. We note the poor solubility of resorufin compounds in several solvents resulted in poor yields. This could be alleviated by using phase transfer conditions (*vide supra*).

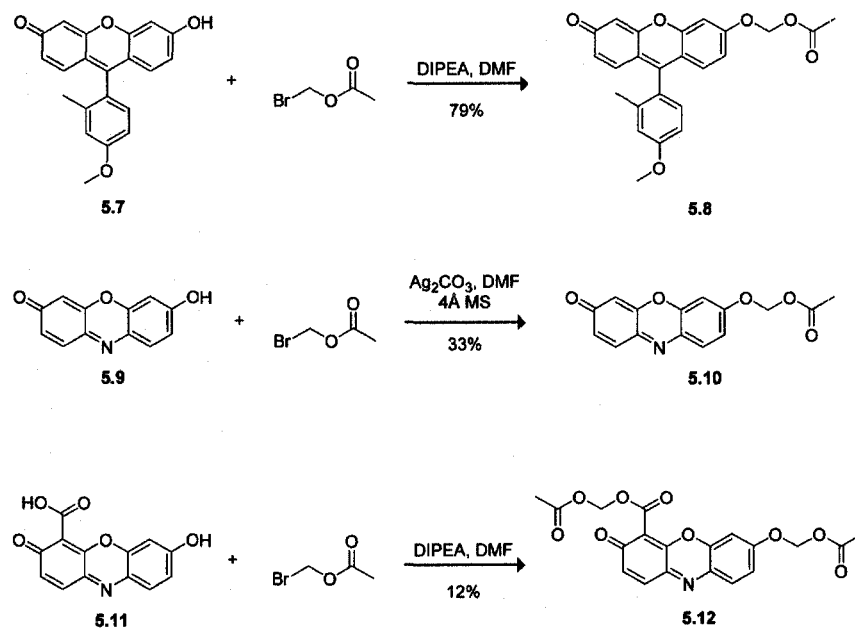
We also prepared profluorophore **5.12** from 4-carboxyresorufin (**5.11**; (Klein *et al.*, 1990)) to examine the effect of an extra carboxyl group on cellular retention. Initial fluorescence microscopy imaging experiments at 2 μ M of substrate **5.10** showed only minor cellular fluorescence with substantial extracellular background (Figure 5.3a). We suspect this background is due to poor retention of simple resorufin **5.9** within the cell. In contrast, incubation with the same concentration of carboxyresorufin derivative **5.12** resulted in bright red cytosolic staining with minimal fluorescence background (Figure 5.3b), showcasing the effect of a carboxylate moiety on the cellular retention of a fluorescent dye.

5.3.3 Envoi

The insertion of a simple oxygen–methylene group into a fluorophore ester endows molecules with high chemical stability, while maintaining enzymatic reactivity *in vitro* and *in cellulo*. We have investigated different reaction conditions, such as the use of silver(I) salts or phase-transfer conditions, allowing the synthesis of difficult disubstituted fluorescein compounds in moderate yields.

Importantly, we have shown this modification insulates the ester moiety from the fluorophore structure, allowing preparation of stable substrates based on dyes with low pK_a values, such as 2',7'-difluorofluorescein. Moreover, this strategy can be used to mask disparate dyes to create a portfolio of substrates with different wavelengths and chemical properties. Overall, this strategy could supplement or replace simple fluorophore acetate esters, allowing sophisticated, facile assays for illuminating biological systems.

Scheme 5.4 Syntheses of acetoxymethyl ether substrates from Tokyo Green and resorufin derivatives



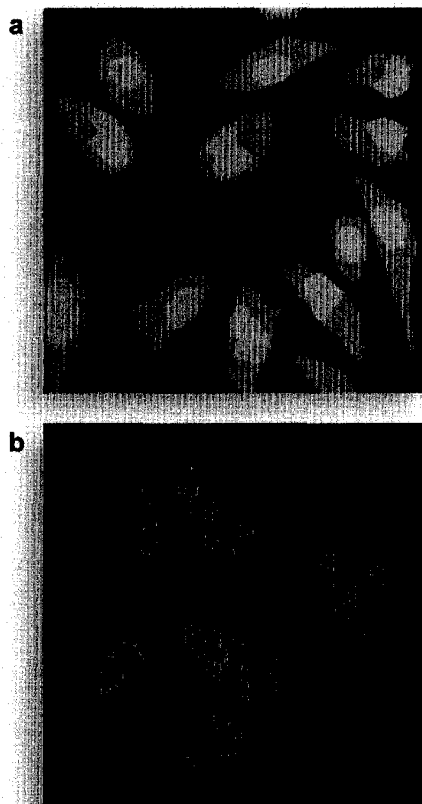


Figure 5.4 Live cell imaging experiments with esterase substrates **5.5**, and **5.8** incubated for 20 min and counterstained with Hoechst 33342 (5% v/v CO₂(g), 100% humidity). (a) Profluorophore **5.5** (10 μM). (b) Profluorophore **5.8** (10 μM).

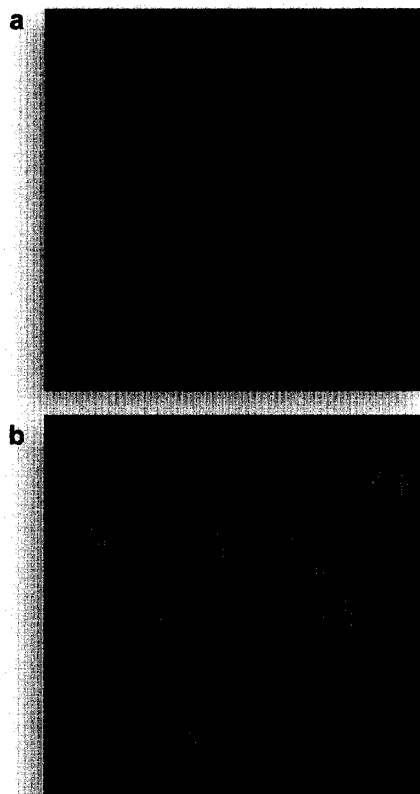


Figure 5.5 Live cell imaging experiments with esterase substrates **5.10**, and **5.12** ($2\ \mu\text{M}$) incubated for 1 h and counterstained with Hoechst 33342 (5% v/v $\text{CO}_2(\text{g})$, 100% humidity). (a) Profluorophore **5.10**. (b) Profluorophore **5.12**.

5.4 Acknowledgments

We are grateful to Z. Diwu and J.B. Binder for contributive discussions. L.D.L was supported by Biotechnology Training Grant 08349 (NIH) and an ACS Division of Organic Chemistry Fellowship sponsored by Genentech. This work was supported by grant CA73808 (NIH). NMRFAM was supported by grant P41 RR02301 (NIH).

5.5 Experimental Section

5.5.1 Materials and Methods: Chemical Synthesis

2',7'-Difluorofluorescein (**5.3**; (Sun *et al.*, 1997)), (Tokyo Green (**5.7**; (Urano *et al.*, 2005)), and 4-carboxyresorufin (**5.11**; (Klein *et al.*, 1990)) were synthesized as previously described. 3-Å Molecular sieves were dried for 3 hours at 320 °C prior to use (Fieser and Fieser, 1967). Preactivated, powdered 4-Å molecular sieves were used as received. Dimethylformamide (DMF), tetrahydrofuran (THF), and dichloromethane (CH₂Cl₂) were drawn from a Baker CYCLE-TAINER solvent delivery system. All other reagents were obtained from Sigma (Saint Louis, MO) or Fisher Scientific (Hanover Park, IL) and used without further purification.

Thin-layer chromatography was performed using aluminum-backed plates coated with silica gel containing F₂₅₄ phosphor and visualized by UV illumination or staining with I₂, ceric ammonium molybdate, or phosphomolybdic acid. Flash chromatography was performed by using open columns loaded with silica gel-60 (230–400 mesh), or on a FlashMaster Solo system (Argonaut Inc., Redwood City, CA) with Isolute Flash Si II columns (International Sorbent Technology Ltd., Hengoed, Mid Glamorgan, UK). The term “high vacuum” refers to a vacuum (≤ 1 mm Hg) achieved by a mechanical belt-drive

oil pump. The term “concentrated under reduced pressure” refers to the removal of solvents and other volatile materials using a rotary evaporator at water-aspirator pressure (<20 mm Hg) while maintaining the water-bath temperature below 40 °C. The term “concentrated under high vacuum” refers to the removal of solvents and other volatile materials using a rotary evaporator at high vacuum while maintaining the water-bath temperature below 40 °C.

NMR spectra were obtained with a Bruker DMX-400 Avance spectrometer at the NMR Facility at Madison (NMRFAM). Mass spectrometry was performed with a Micromass LCT (electrospray ionization, ESI) mass spectrometer in the Mass Spectrometry Facility in the Department of Chemistry.

5.5.2 Synthesis of Compounds 5.5, 5.6, 5.8, 5.10, and 5.12

Fluorescein Diacetoxymethyl Ether (5.5); Method 1. Fluorescein (**5.1**, 724 mg, 2.18 mmol), bromomethyl acetate (**5.4**, 1.0 g, 6.54 mmol), anhydrous Ag_2CO_3 (1.44 g, 5.23 mmol), and 3-Å molecular sieves (2.0 g) were suspended in anhydrous CH_2Cl_2 (50 mL) and anhydrous THF (50 mL) under Ar(g) . *sym*-Collidine (693 μL , 5.23 mmol) was added dropwise and the reaction was stirred for 144 h. The reaction mixture was diluted with CH_2Cl_2 and filtered through a pad of celite. The solution was concentrated under reduced pressure and the residue was taken up in EtOAc. and washed with 10% v/v HCl(aq) , H_2O , 0.1 M $\text{Na}_2\text{S}_2\text{O}_3$, saturated $\text{NaHCO}_3\text{(aq)}$, H_2O , and saturated brine. The organics were dried over anhydrous $\text{Na}_2\text{SO}_4\text{(s)}$ and concentrated under reduced pressure to give an orange oil. Purification via column chromatography (silica gel, 20% v/v EtOAc in hexanes) to give compound **5.5** as an off-white crystalline solid (465 mg, 45%). ^1H NMR

(400 MHz, CDCl₃) δ (ppm): 8.03 (d, J = 7.3 Hz, 1H), 7.67 (ddd, J = 7.5, 7.4, 1.3 Hz, 1H), 7.64 (ddd, J = 7.5, 7.4, 1.1 Hz, 1H), 7.16 (d, J = 7.2 Hz, 1H), 6.97 (m, 2H), 6.74 (m, 4H), 5.78 (s, 4H), 2.14 (s, 6H). ¹³C NMR (100 MHz, CDCl₃) δ (ppm): 169.79, 169.24, 158.31, 152.91, 152.17, 135.13, 129.89, 129.39, 126.58, 125.15, 123.85, 113.23, 112.70, 103.43, 84.86, 82.41, 20.89. ESIMS [M+Na]⁺ calculated, 499.1005; found, 499.0989.

Fluorescein Bis(Acetoxymethyl Ether) (5.5); Method 2. Fluorescein (**5.1**, 332 mg, 1.00 mmol) and anhydrous K₂CO₃ (829 mg, 6.00 mmol) were dissolved in water (10 mL) to give a dark orange solution. Tetrabutylammonium bisulfate (679 mg, 2.00 mmol) was added in CH₂Cl₂ (5 mL) followed by bromomethyl acetate (**5.4**, 785 μ L, 8.00 mmol) in CH₂Cl₂ (5 mL), and the reaction was stirred at maximal stirring speed under ambient temperature for 48 h. The reaction mixture was diluted with H₂O and CH₂Cl₂ and the layers separated. The aqueous layer was extracted with CH₂Cl₂ and the combined organics were washed with H₂O and saturated brine. The organic layer was dried over anhydrous Na₂SO₄ and concentrated under reduced pressure to give a brown oil. Purification via column chromatography (silica gel, 25% v/v EtOAc in hexanes) to give compound **5.5** as a colorless solid (149 mg, 31%). Analytical data matched the material prepared using Method 1.

2',7'-Difluorofluorescein Diacetoxymethyl Ether (5.6). 2',7'-Difluorofluorescein (**5.3**, 200 mg, 0.543 mmol), bromomethyl acetate (**5.4**, 213 μ L, 2.17 mmol), anhydrous Ag₂CO₃ (449 mg, 1.63 mmol), and 3-Å molecular sieves (2.0 g) were suspended in anhydrous DMF (15 mL) under Ar(g). *sym*-Collidine (216 μ L, 1.63 mmol) was added dropwise and the reaction was stirred for 96 h. The reaction mixture was diluted with CHCl₃ and filtered through a pad of celite. The solution was concentrated under high

vacuum and the residue was taken up in CH_2Cl_2 and washed with 10% v/v $\text{HCl}(\text{aq})$, H_2O , 0.1 M $\text{Na}_2\text{S}_2\text{O}_3$, saturated $\text{NaHCO}_3(\text{aq})$, H_2O , and saturated brine. The organics were dried over anhydrous $\text{MgSO}_4(\text{s})$ and concentrated under reduced pressure to give an orange oil. Purification via column chromatography (silica gel, 20% v/v EtOAc in hexanes) to give compound **5.6** as an off-white crystalline solid (42 mg, 15%). ^1H NMR (400 MHz, CDCl_3) δ (ppm): 8.07 (d, $J = 7.6$ Hz, 1H), 7.5 (ddd, $J = 7.6, 7.4, 1.2$ Hz, 1H), 7.70 (ddd, $J = 7.5, 7.3, 1.0$ Hz, 1H), 7.19 (d, $J = 7.5$ Hz, 1H), 7.10 ($J = 7.0$ Hz, 2H), 6.52 (d, $J = 10.7$ Hz, 2H), 5.83 (ABq, $J = 6.4$ Hz, 4H), 2.19 (s, 6H). ^{13}C NMR (100 MHz, CDCl_3) δ (ppm): 169.50, 168.54, 151.86, 150.53, 148.08, 147.48, 146.65, 146.55, 135.51, 130.45, 126.21, 125.54, 123.75, 114.73, 114.53, 112.42, 112.36, 105.54, 85.61, 81.62, 20.85. ESIMS $[\text{M}+\text{Na}]^+$ calculated, 535.0812; found, 535.0820.

Tokyo Green Acetoxymethyl Ether (5.8). Tokyo Green (**5.7**, 50 mg, 0.15 mmol), bromomethyl acetate (**5.4**, 74 μL , 0.75 mmol), and Hünig's base (158 μL , 0.90 mmol), were dissolved in anhydrous DMF (2.0 mL) under $\text{Ar}(\text{g})$ and the reaction was stirred for 24 h. The reaction mixture was concentrated under high vacuum giving an orange solid. Purification via column chromatography (silica gel, first column: 50% v/v EtOAc in CH_2Cl_2 ; second column: 2→4% v/v MeOH in CH_2Cl_2) afforded compound **5.8** as an orange solid (48 mg, 79%). ^1H NMR (400 MHz, CDCl_3) δ (ppm): 7.11 (d, $J = 2.4$ Hz, 1H), 7.06 (d, $J = 8.2$ Hz, 1H), 7.05 (d, $J = 9.1$ Hz, 1H), 6.99 (d, $J = 9.9$ Hz, 1H), 6.93–6.87 (m, 2H), 6.85 (dd, $J = 9.1, 2.4$ Hz, 1H), 6.55 (dd, $J = 9.7, 1.9$ Hz, 1H), 6.42 (d, $J = 1.9$ Hz, 1H), 5.83 (s, 2H), 3.88 (s, 2H), 2.14 (s, 2H), 2.03 (s, 2H). ^{13}C NMR (100 MHz, CDCl_3) δ (ppm): 185.84, 169.52, 160.73, 160.38, 158.77, 154.05, 148.95, 137.81, 130.69,

130.34, 130.29, 129.74, 124.31, 119.44, 116.12, 116.01, 113.78, 111.56, 105.85, 102.71, 84.38, 55.33, 20.79, 19.95. ESIMS $[M+H]^+$ calculated, 405.1333; found, 405.1325.

Resorufin Acetoxymethyl Ether (5.10). Resorufin (**5.9**, 200 mg, 0.938 mmol), anhydrous Ag_2CO_3 (621 mg, 2.25 mmol), and powdered 4-Å molecular sieves (500 mg) were suspended in anhydrous CH_2Cl_2 (50 mL) and anhydrous THF (50 mL) under $Ar(g)$. Bromomethyl acetate (**5.4**, 276 μ L, 2.81 mmol) was added dropwise and the reaction was stirred for 96 h. The reaction mixture was diluted with $CHCl_3$ and filtered through a pad of celite. The solution was concentrated under reduced pressure to give an orange powder. Purification via column chromatography (silica gel, first column: 5:3:2→3:4:3 v/v/v hexanes:EtOAc: CH_2Cl_2 ; second column: 10% v/v CH_3CN in $CHCl_3$) to give compound **5.5** as a red solid (87 mg, 33%). 1H NMR (400 MHz, $CDCl_3$) δ (ppm): 7.74 (d, $J = 8.8$ Hz, 1H), 7.42 (d, $J = 9.7$ Hz, 1H), 7.04 (dd, $J = 8.9, 2.7$ Hz, 1H), 6.99 (d, $J = 2.7$ Hz, 1H), 6.84 (dd, $J = 9.7, 1.9$ Hz, 1H), 6.33 (d, $J = 1.9$ Hz, 1H), 5.84 (s, 2H), 2.16 (s, 3H). ^{13}C NMR (100 MHz, $CDCl_3$) δ (ppm): 186.30, 169.55, 160.13, 149.59, 146.70, 145.24, 134.74, 134.64, 131.71, 129.33, 114.33, 107.01, 102.52, 84.54, 20.84. ESIMS $[M+H]^+$ calculated, 286.0710; found, 286.0712.

4-Carboxyresorufin Acetoxymethyl Ether, Acetoxymethyl Ester (5.12).

4-Carboxyresorufin (**5.11**, 110 mg, 0.428 mmol), bromomethyl acetate (**5.4**, 167 μ L, 1.71 mmol), and Hünig's base (100 μ L), were dissolved in anhydrous DMF (900 μ L) and the reaction was stirred for 96 h under $Ar(g)$. The reaction mixture was concentrated under high vacuum and the residue was taken up in CH_2Cl_2 and washed with 10% v/v $HCl(aq)$, H_2O , saturated $NaHCO_3(aq)$, H_2O , and saturated brine. The organics were dried over anhydrous $Na_2SO_4(s)$ and concentrated under reduced pressure to give a brown oil.

Purification via column chromatography (silica gel, 0→30% v/v EtOAc in CH₂Cl₂) to give compound **5.6** as a red solid (21 mg, 12%). ¹H NMR (400 MHz, CDCl₃) δ (ppm): 7.83 (d, *J* = 8.7 Hz, 1H), 7.50 (d, *J* = 10 Hz, 1H), 7.17–7.10 (m, 2H), 6.90 (d, *J* = 10 Hz, 1H), 6.03 (s, 2H), 5.87 (s, 2H), 2.22 (s, 3H), 2.19 (s, 3H). ¹³C NMR (100 MHz, CDCl₃) δ (ppm): 181.40, 169.60, 169.39, 161.91, 160.80, 147.73, 144.87, 144.68, 134.71, 134.28, 131.99, 129.34, 115.75, 110.90, 102.60, 84.54, 79.91, 20.75. ESIMS [M+Na]⁺ calculated, 424.0640; found, 424.0631.

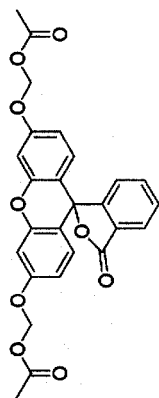
5.5.3 Materials and Methods: Biochemistry

Dulbecco's phosphate-buffered saline (DPBS), Dulbecco's modified Eagle's medium (DMEM) and fetal bovine serum (FBS) were from Invitrogen. All other reagents were from Sigma–Aldrich or Fisher Scientific. Phosphate-buffered saline, pH 7.4 (PBS) contained (in 1.00 liter) KCl (0.20 g), KH₂PO₄ (0.20 g), NaCl (8.0 g), and Na₂HPO₄·7H₂O (2.16 g). All measurements were recorded at ambient temperature (23 ± 2 °C) and buffers were not degassed prior to measurements. Fluorometric measurements were made using fluorescence grade quartz or glass cuvettes from Starna Cells and a QuantaMaster1 photon-counting spectrofluorometer from Photon Technology International equipped with sample stirring. Compounds were prepared as stock solutions in DMSO and diluted such that the DMSO concentration did not exceed 1% v/v. Porcine liver esterase (PLE, MW = 163 kDa (Horgan *et al.*, 1969)) was obtained from Sigma Chemical (product number E2884) as a suspension in 3.2 M (NH₄)₂SO₄, and was diluted to appropriate concentrations in PBS before use. Graphs were manipulated and parameters were calculated with Microsoft Excel 2003 and GraphPad Prism 4.

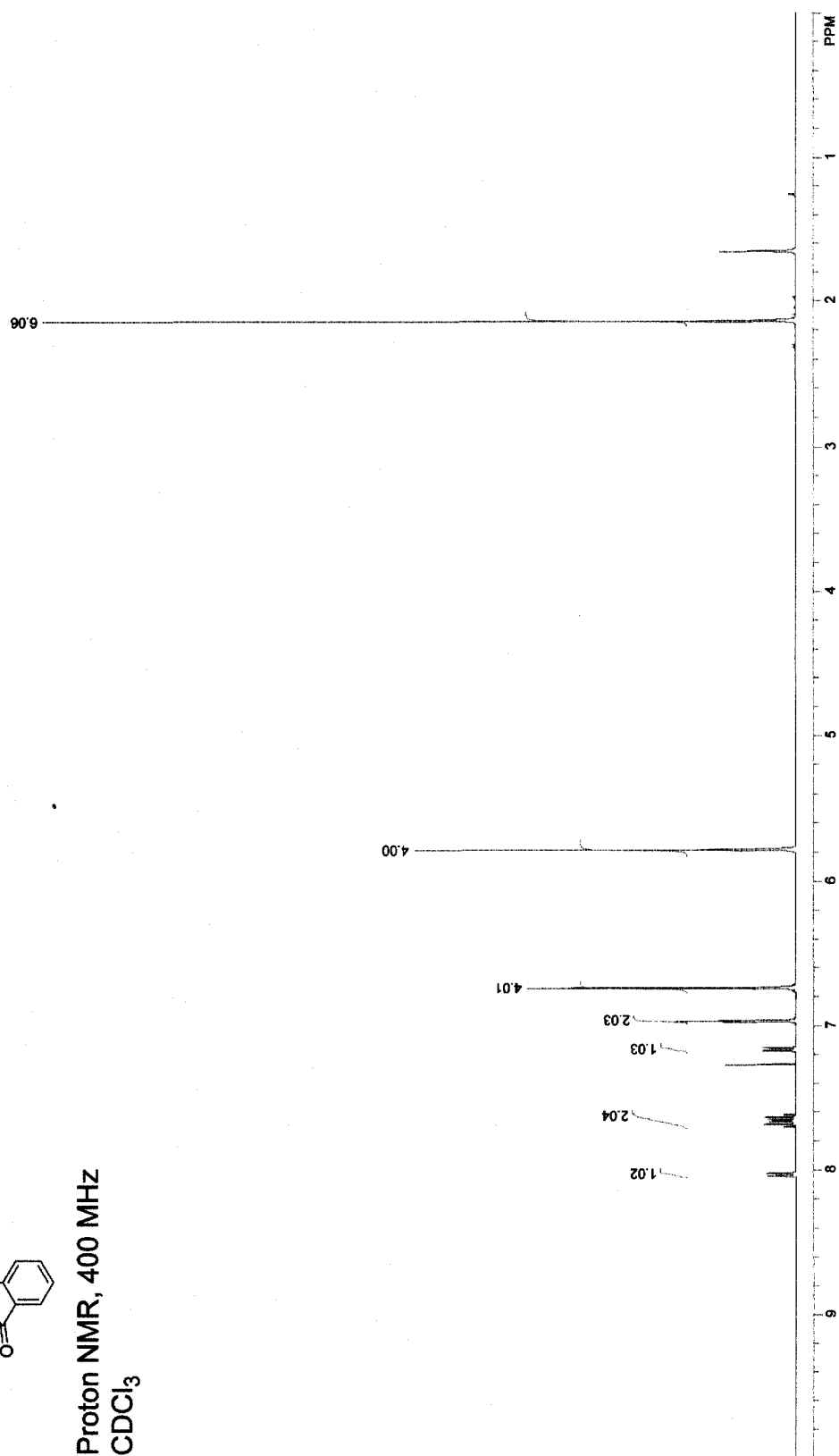
5.5.4 Cell Preparation and Imaging

HeLa cells were plated on Nunc Lab-Tek II 8-well Chamber Coverglass (Fisher Scientific) and grown to 70–80% confluence at 37 °C in DMEM containing FBS (10% v/v). For imaging, cells were first washed with Dulbecco's phosphate-buffered saline (DPBS, Invitrogen). Cells were then incubated with substrates **5.5**, **5.6**, **5.8**, **5.10**, or **5.12** (2 or 10 μ M) for 20 min or 1 h at 37 °C prior to imaging. Nuclear staining was accomplished by addition of Hoechst 33342 (2 μ g/mL) for the final 5 min of incubation. Cells were imaged on a Nikon Eclipse TE2000-U confocal microscope equipped with a Zeiss AxioCam digital camera, unless indicated otherwise. Excitation at 408 nm was provided by a blue-diode laser, and emission light was passed through a filter centered at 450 nm with a 35-nm band-pass. Excitation at 488 nm was provided by an argon-ion laser and emission light was passed through a filter centered at 515 nm with a 40-nm band-pass. Excitation at 543 nm was provided by a HeNe laser, and emission light was passed through a filter centered at 605 nm with a 75-nm band-pass.

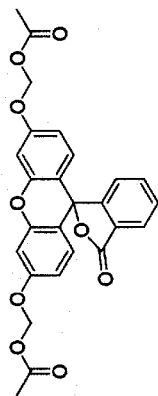
5.5



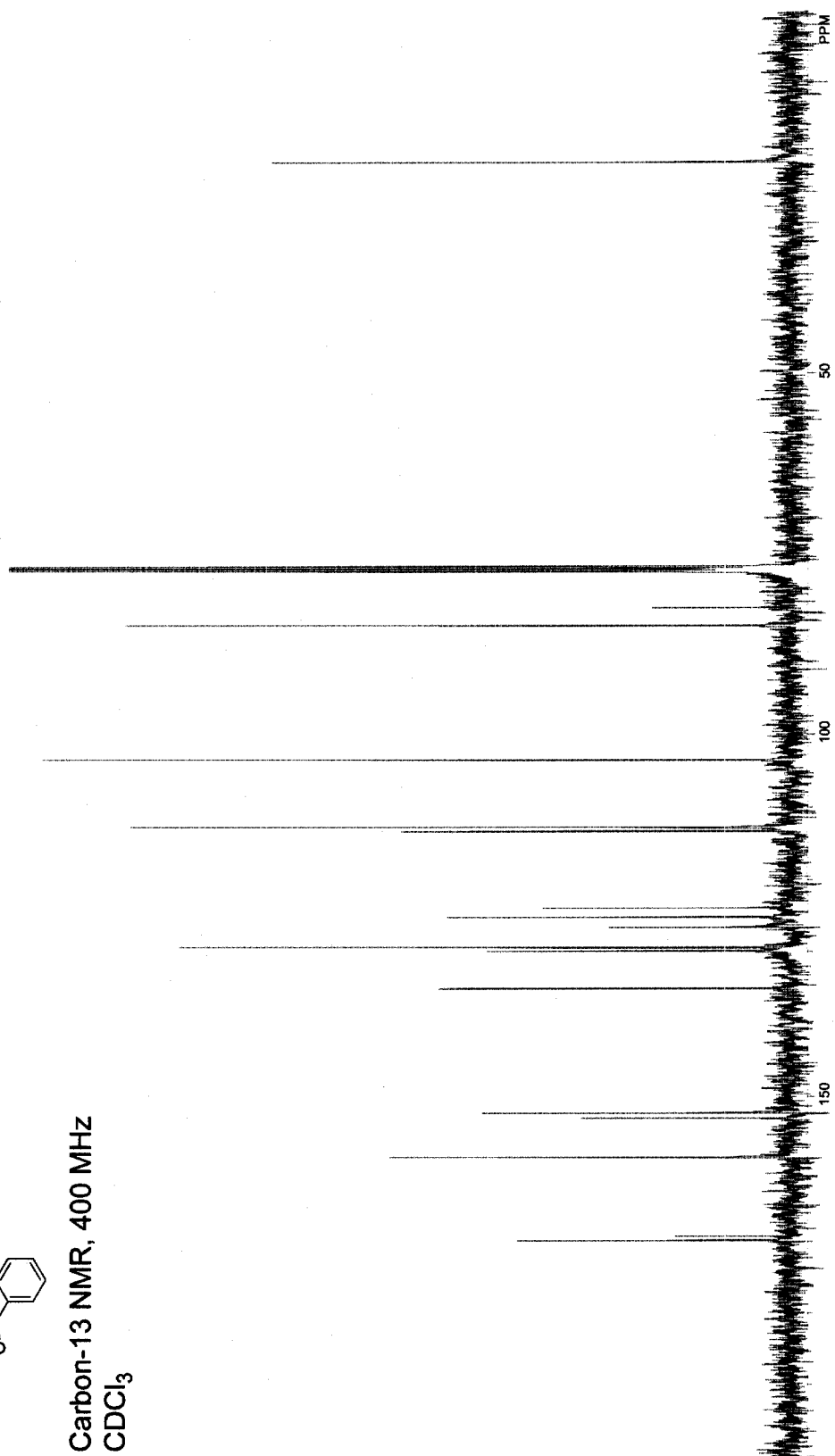
Proton NMR, 400 MHz
CDCl₃

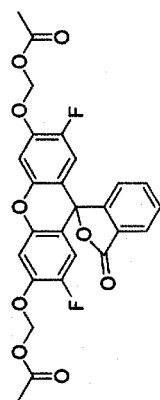


5.5

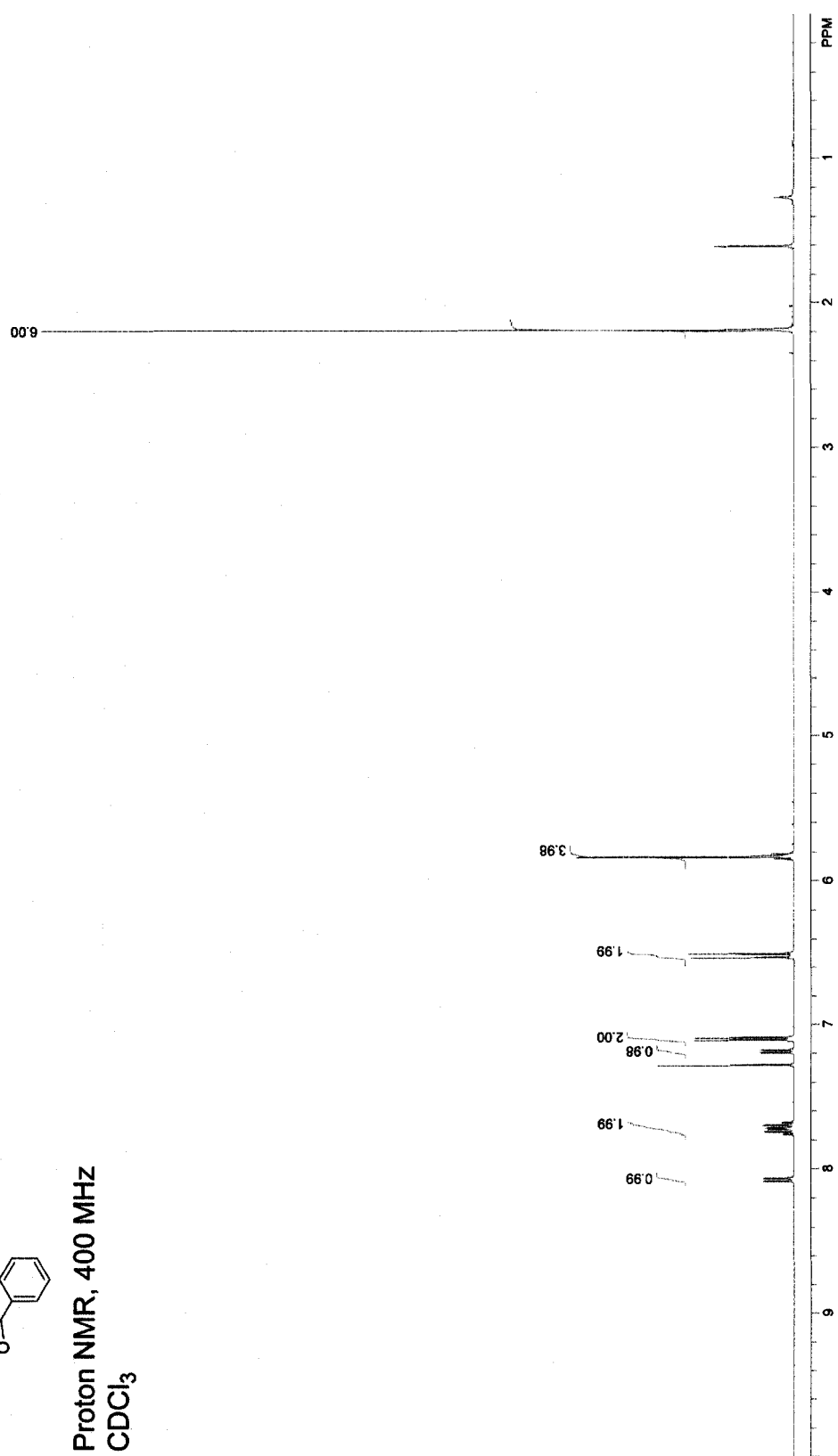


Carbon-13 NMR, 400 MHz
CDCl₃

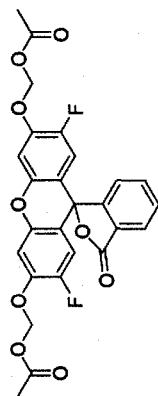


5.6

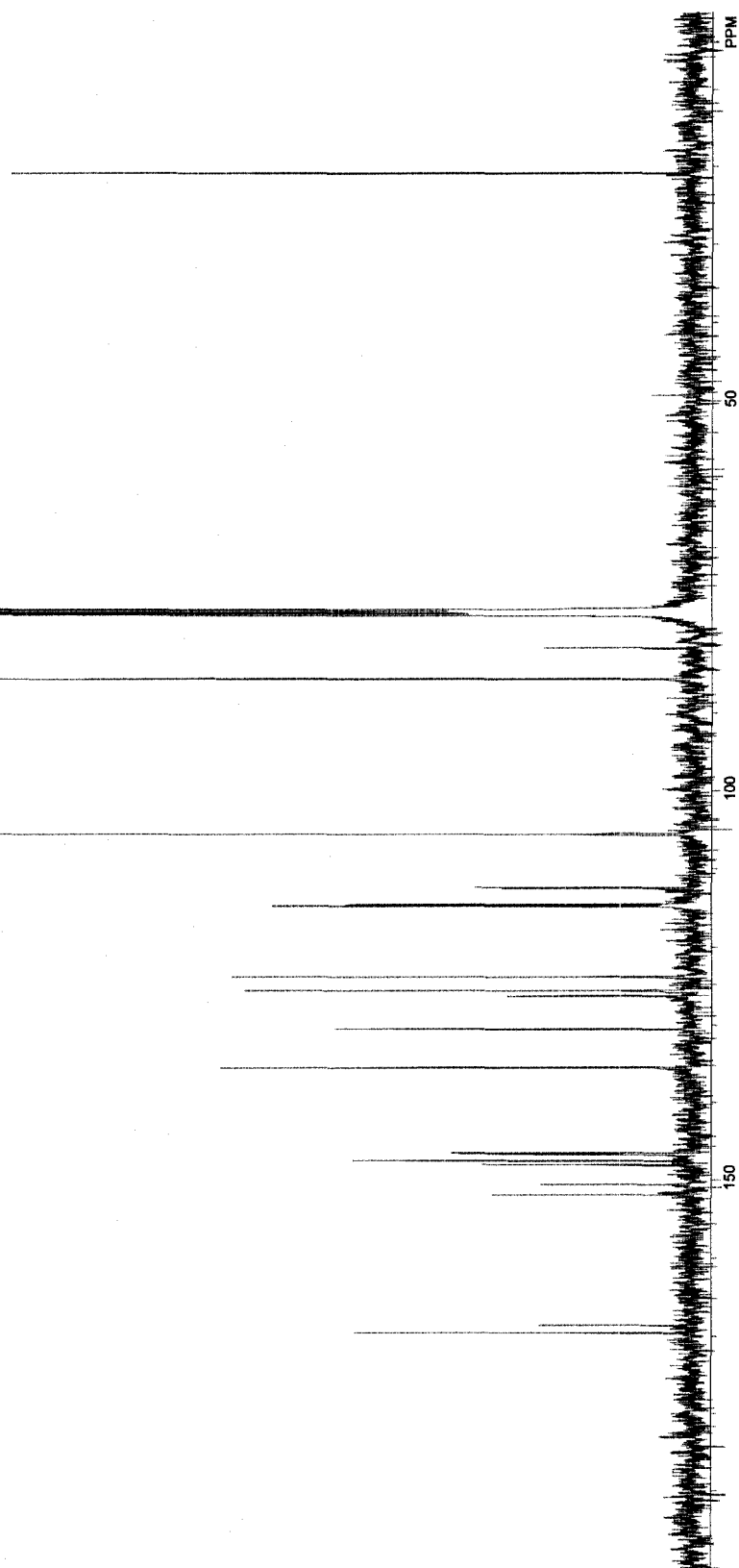
Proton NMR, 400 MHz
CDCl₃



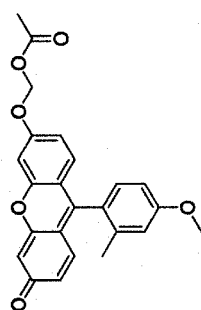
5.6



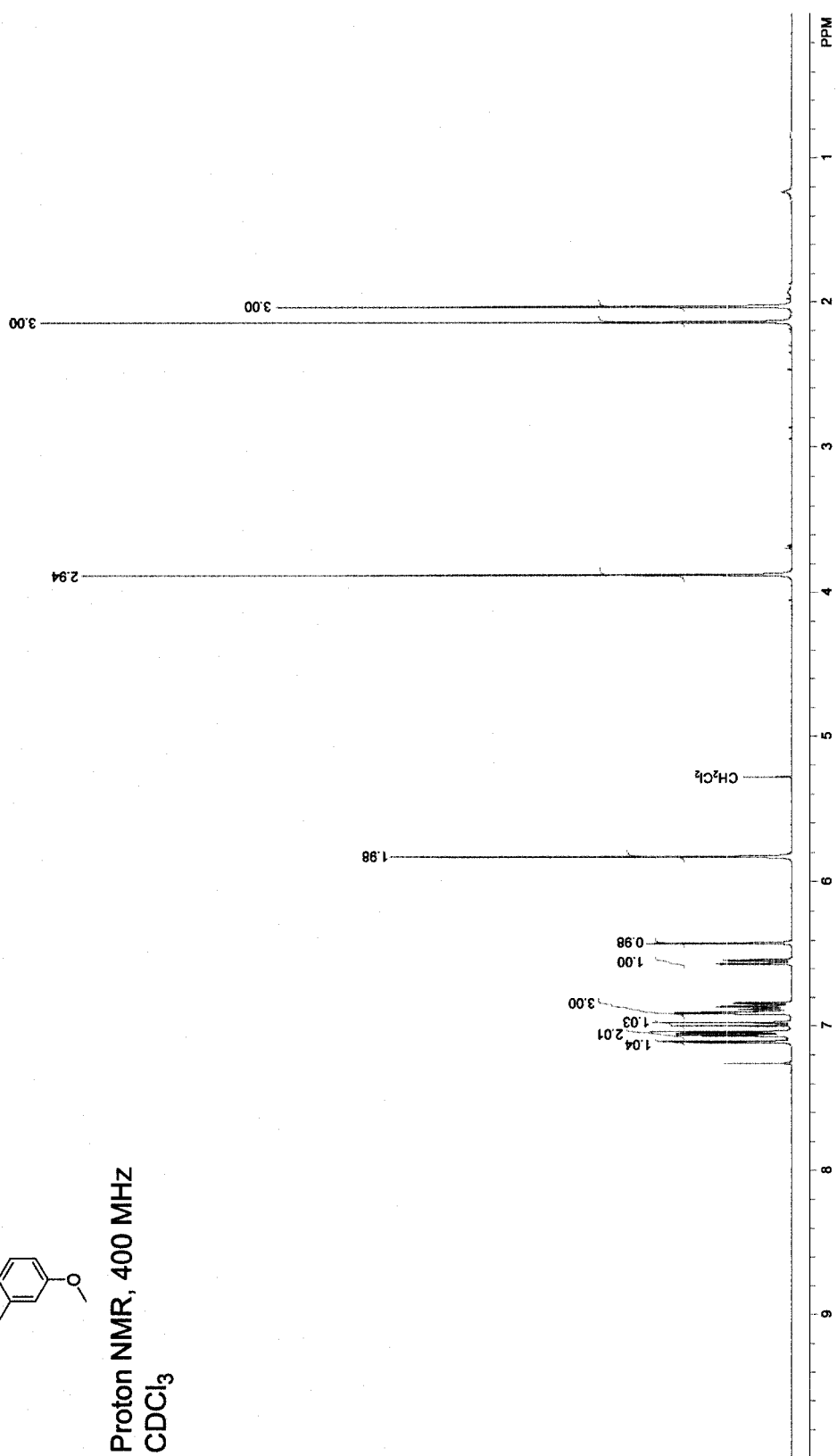
Carbon-13 NMR, 400 MHz
CDCl₃



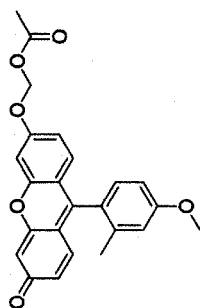
5.8



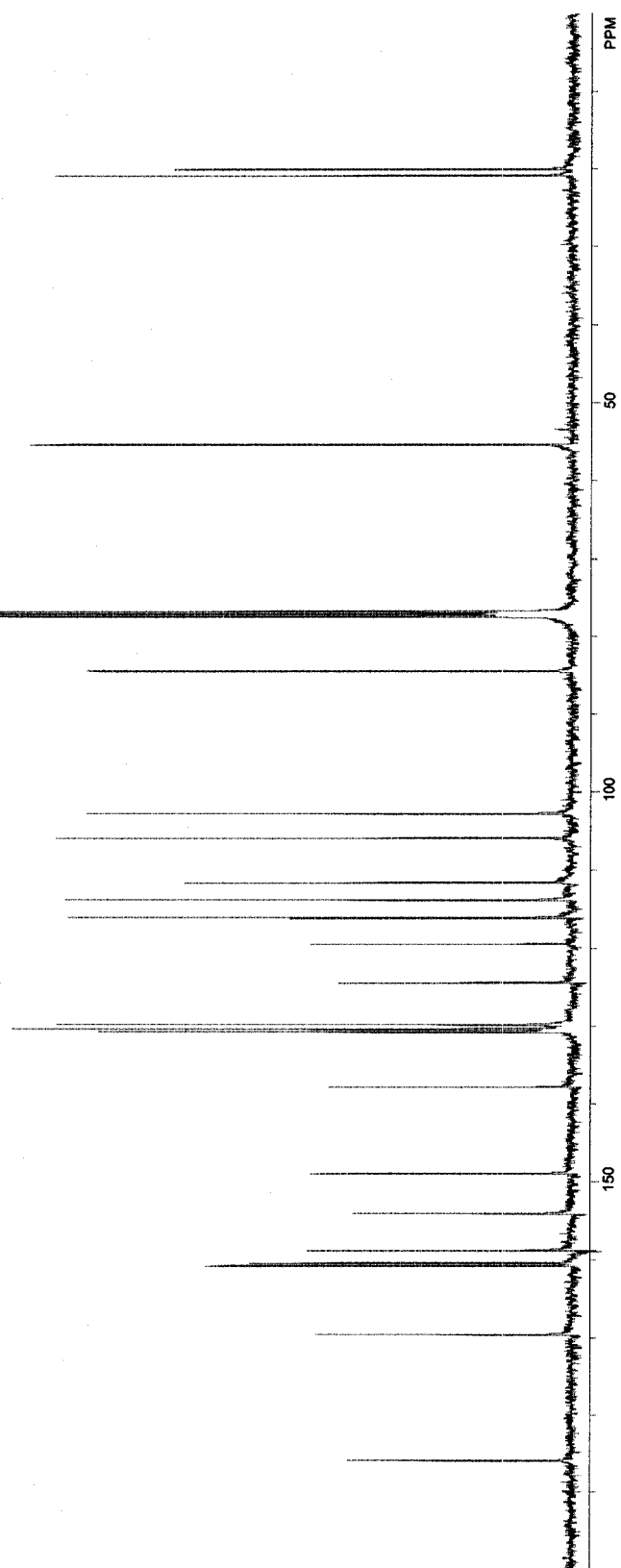
Proton NMR, 400 MHz
CDCl₃



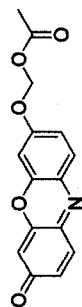
5.8



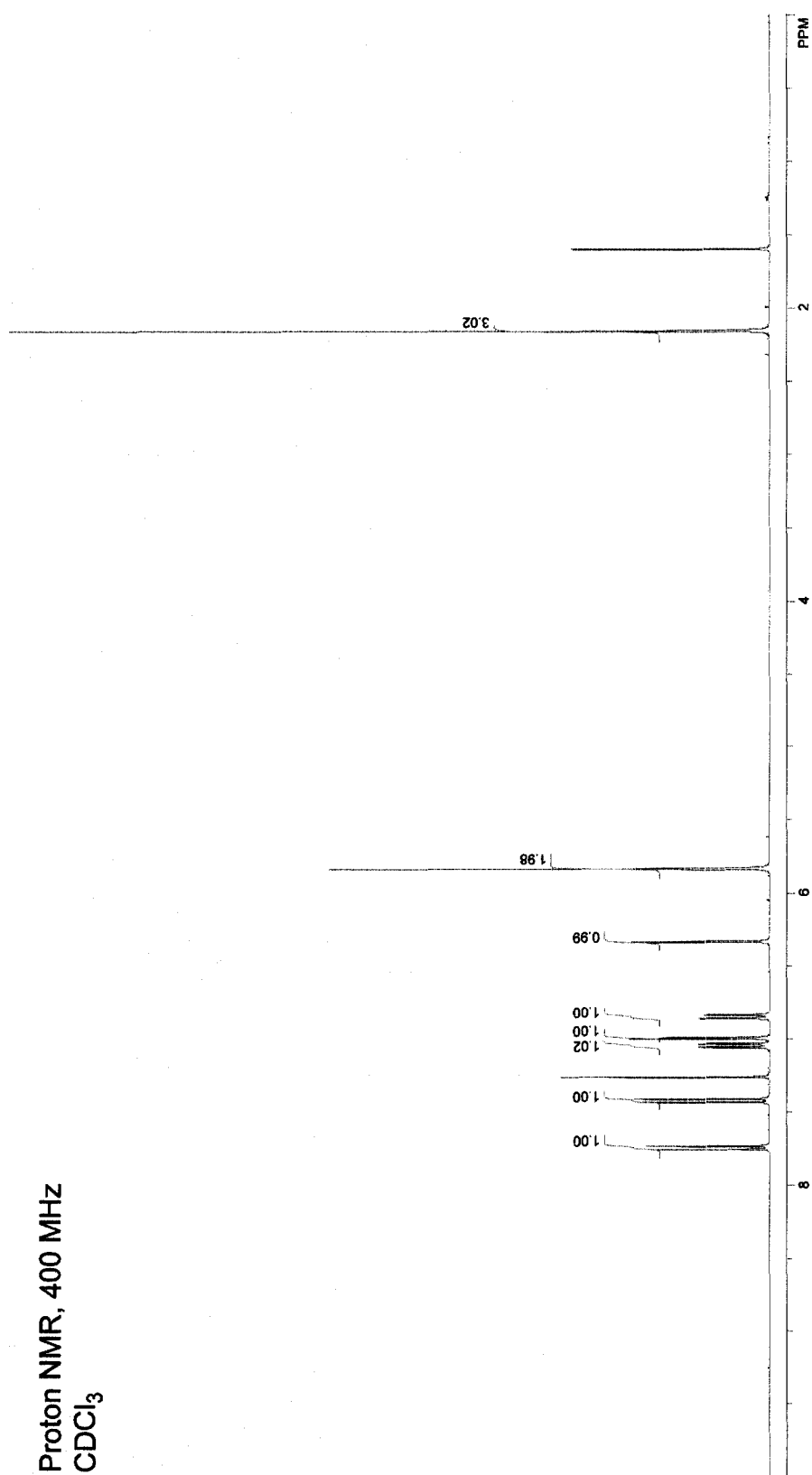
Carbon-13 NMR, 400 MHz
CDCl₃



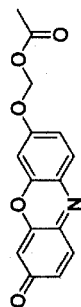
5.10



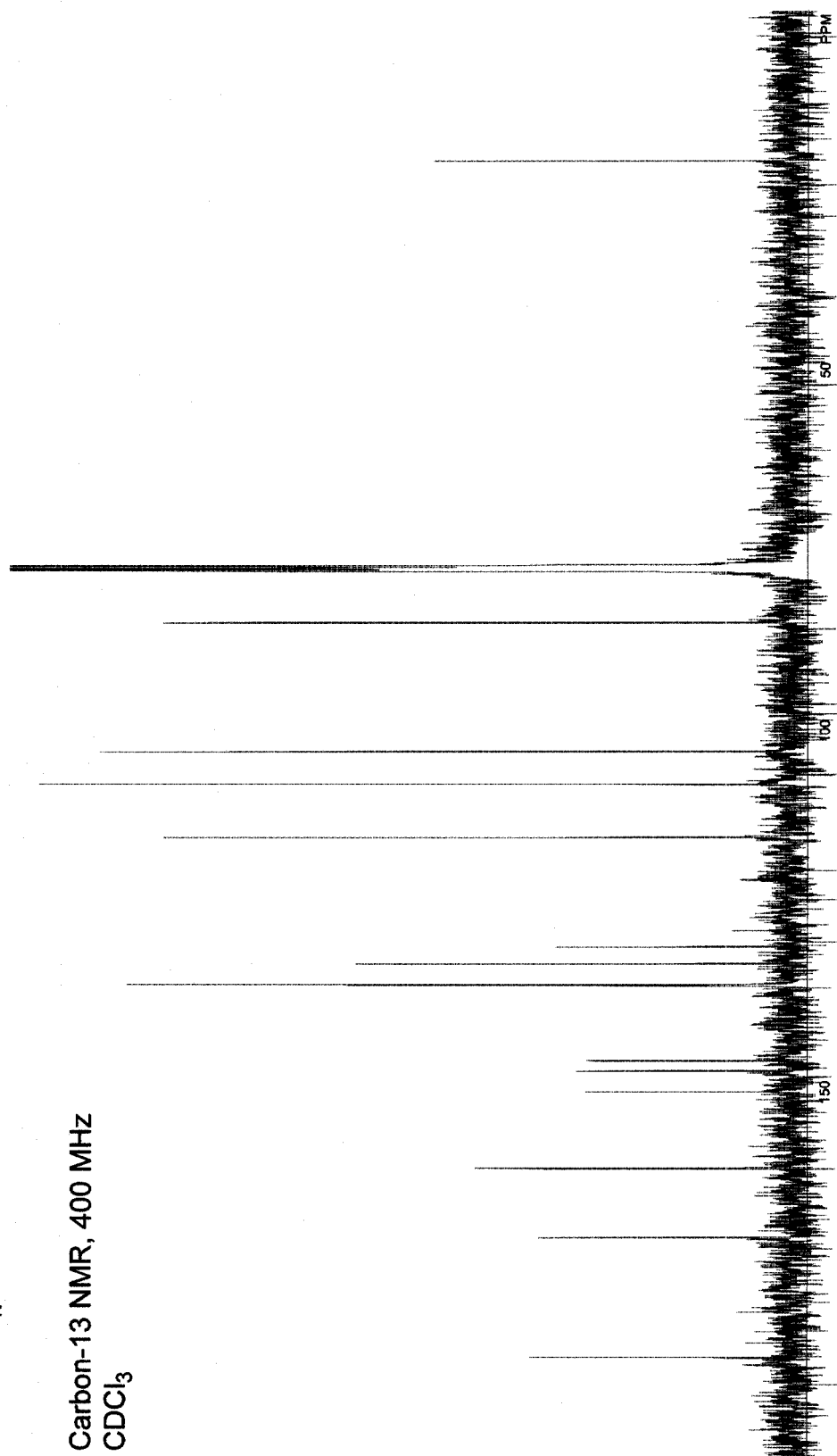
Proton NMR, 400 MHz
CDCl₃

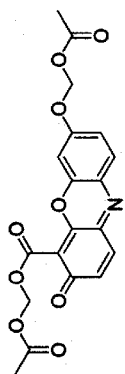


5.10

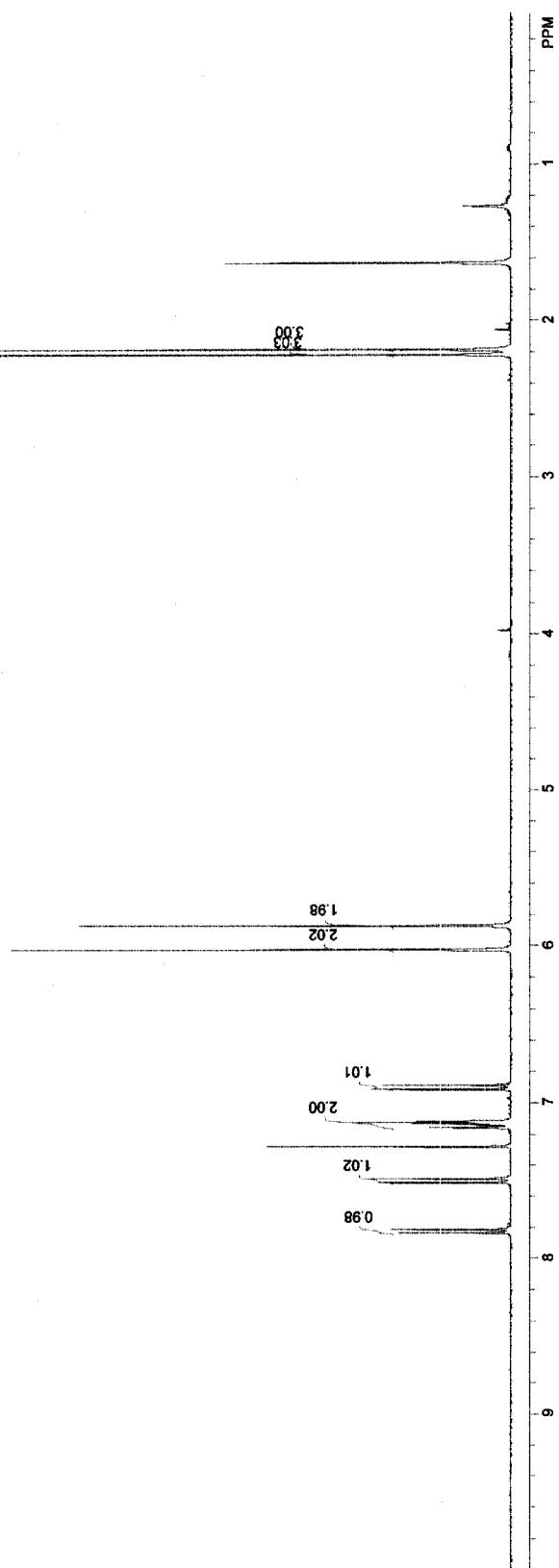


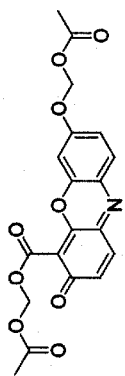
Carbon-13 NMR, 400 MHz
CDCl₃



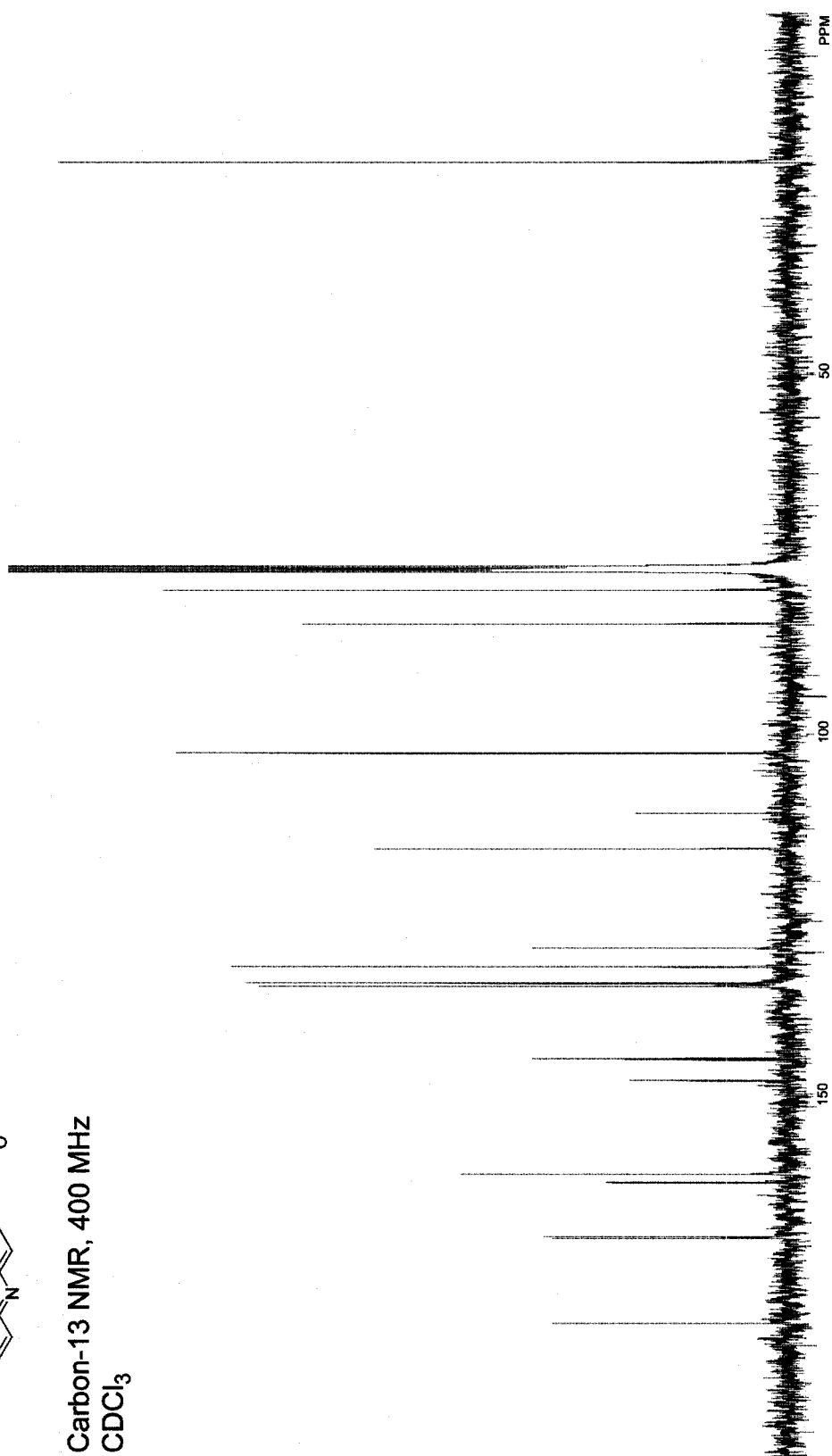
5.12

Proton NMR, 400 MHz
CDCl₃



5.12

Carbon-13 NMR, 400 MHz
CDCl₃



CHAPTER 6*

TUNING THE pK_a OF FLUORESCCEIN TO OPTIMIZE BINDING ASSAYS

Contribution: Chemical synthesis and characterization, determination of fluorescent properties, a portion of the pK_a determination and *in vitro* binding assays, assay miniaturization, composition of manuscript, and preparation of figure drafts. Protein conjugation and a portion of pK_a determination and *in vitro* assays were performed by T. J. Rutkoski.

*This chapter has been published, in part, under the same title. Reference: Lavis, L. D., Rutkoski, T. J., and Raines, R. T. (2007). *Anal. Chem.* **79**, 6775–6782.

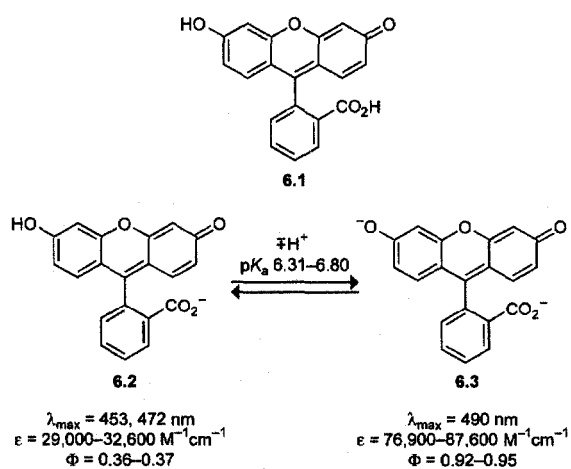
Abstract: The phenolic pK_a of fluorescein varies depending on its environment. The fluorescence of the dye varies likewise. Accordingly, a change in fluorescence can report on the association of a fluorescein-conjugate to another molecule. Here, we demonstrate how to optimize this process with chemical synthesis. The fluorescence of fluorescein-labeled model protein, bovine pancreatic ribonuclease (RNase A), decreases upon binding to its cognate inhibitor protein (RI). Free and RI-bound fluorescein–RNase A have pK_a values of 6.35 and 6.70, respectively, leaving the fluorescein moiety largely unprotonated at physiological pH and thus limiting the sensitivity of the assay. To increase the fluorescein pK_a and, hence, the assay sensitivity, we installed an electron-donating alkyl group *ortho* to each phenol group. 2',7'-Diethylfluorescein (DEF) has spectral properties similar to those of fluorescein but a higher phenolic pK_a . Most importantly, free and RI-bound DEF–RNase A have pK_a values of 6.68 and 7.29, respectively, resulting in a substantial increase in the sensitivity of the assay. Using the conjugate DEF–RNase A rather than fluorescein–RNase A in a microplate assay at pH 7.12 increased the *Z'*-factor from –0.17 to 0.69. We propose that synthetic “tuning” of the pK_a of fluorescein and other pH-sensitive fluorophores provides a general means to optimize binding assays.

6.1 Introduction

The xanthene dye fluorescein (**6.1**) was first synthesized by Baeyer in 1871 (Baeyer, 1871). Despite its antiquity, fluorescein remains one of the most widely utilized fluorophores in modern biochemical, biological, and medicinal research. This persistence can be attributed to the excellent spectral properties of fluorescein and the established synthetic chemistry of the dye. Fluorescein serves as a modular scaffold that is well-suited for elaboration to create various molecular tools, including ion indicators, fluorogenic enzyme substrates, and fluorescent labels for biomolecules (Haugland *et al.*, 2005; Urano *et al.*, 2005).

An important (and underappreciated) property of fluorescein is its complex acid–base equilibria in aqueous solution. Fluorescein can exist in seven prototropic forms. The determination of the distinct properties of each of these molecular forms has been the subject of numerous studies (Zanker and Peter, 1958; Lindqvist, 1960; Martin and Lindqvist, 1975; Chen *et al.*, 1979; Mchedlov-Petrosyan, 1979; Diehl, 1989; Diehl and Markuszewski, 1989; Sjoback *et al.*, 1995; Klonis and Sawyer, 1996; Lakowicz, 1999; Magde *et al.*, 2002; Smith and Pretorius, 2002; Krol *et al.*, 2006). The monoanion **6.2** and dianion **6.3** are the principal ground-state species under biologically-relevant conditions. Scheme 6.1 shows these two forms of fluorescein with the ranges of reported phenolic pK_a values and other spectral properties in aqueous solution. The dianionic form **6.3** is responsible for the characteristic strong visible absorption band and potent fluorescence emission. The absorbance of the monoionic form **6.2** is less intense, and the maxima are blue-shifted relative to **6.3**. The quantum yield of the monoanion is also significantly lower than that of the dianion. Because of the dissimilar optical properties of **6.2** and **6.3**

and the proximity of the pK_a value to physiological pH, special care must be taken when using fluorescein and fluorescein-labeled conjugates in biological experiments. To circumvent this pH-sensitivity problem, fluorescein derivatives have been developed that employ the electron-withdrawing nature of chlorine (Mchedlov-Petrosyan *et al.*, 1992; Sparano *et al.*, 2004) or fluorine (Sun *et al.*, 1997) substituents to shift this phenolic pK_a to a lower value, thereby suppressing the heterogeneity of the protonation state of this phenolic group at physiologically relevant pH values.

Scheme 6.1 Prototropic forms of fluorescein and corresponding photophysical values

The sensitivity of the fluorescence of fluorescein to its chemical environment has been exploited in assays of biological processes. Because of the proximity of the phenolic pK_a to biologically relevant pH values, small-molecule fluorescein derivatives have been employed as pH sensors (Thomas *et al.*, 1979; Paradiso *et al.*, 1984; Graber *et al.*, 1986; Nedergaard *et al.*, 1990; Liu *et al.*, 1997; Wu *et al.*, 2000; Schroder *et al.*, 2005). In addition, the pK_a value itself is sensitive to the electrostatic environment around the fluorescein molecule (Stanton *et al.*, 1984; Thelen *et al.*, 1984; Omelyanenko *et al.*, 1993; Griep and Mesman, 1995; Agi and Walt, 1997). Thus, the phenolic pK_a of a fluorescein label attached to a protein, for example, can be perturbed depending on the status of the biomolecule. The difference in pK_a value translates to an alteration in fluorescent intensity at constant pH. This environmentally-sensitive fluorescence variation has been used as an index to monitor changes in proteins (Garel, 1976; Labhardt *et al.*, 1983; Griep and Mchenry, 1990; Goldberg and Baldwin, 1998a; Goldberg and Baldwin, 1998b; Goldberg and Baldwin, 1999) and nucleic acids (Friedrich and Woolley, 1988; Friedrich *et al.*, 1988). Studies of protein–protein interactions, in particular, can benefit from assays relying on the pK_a shift of a fluorescein label. Such assays circumvent the double-label requirement of Förster resonance energy transfer (FRET) (Sapsford *et al.*, 2006), and the size limitations of fluorescence polarization (FP) (Owicki, 2000).

Although binding assays relying on the pK_a shift of fluorescein are prevalent, the development of such assays is largely empirical. The effects of minor modifications to the fluorescein label remain unexplored. We were especially interested in discerning whether altering the pK_a of the dye would have a significant effect on assay performance. Our interest stems from a fluorescence-based assay developed in our laboratory (Abel *et*

al., 2002; Rutkoski *et al.*, 2005) for the determination of equilibrium dissociation constants for variants of bovine pancreatic ribonuclease (RNase A (Raines, 1998)) and its homologues in complex with the ribonuclease inhibitor protein (RI (Dickson *et al.*, 2005)). The ability of these pancreatic-type ribonucleases to evade RI is a prerequisite for their toxic activity toward cancer cells (Rutkoski *et al.*, 2005). Our assay is based on the decrease in fluorescence (~10–20%) of a fluorescein-labeled ribonuclease variant once bound by RI (Abel *et al.*, 2002). Competitive binding of RI by unlabeled ribonuclease variants restores fluorescence intensity, allowing accurate determination of equilibrium dissociation constants. Although the assay has proven to be useful, the low dynamic range requires a laborious, cuvette-based assay using sensitive instrumentation and large assay volumes. Expansion of the utility of this assay to a miniaturized, high-throughput system (*e.g.*, microplate format) requires an increase in the fluorescence change without severe modification of other assay parameters.

Here, we describe a general means to improve binding assays through the synthesis and use of a “tuned” fluorescein derivative. As a model system, we use the RI–RNase A interaction, which allows for assays to be performed over a wide range of pH. First, we determine the pK_a values of the original fluorescein-labeled RNase A variant in the absence and presence of excess RI. From this analysis, we confirm a shift in the pK_a value of the fluorescein label upon complex formation, and surmise that tuning the pK_a to a higher value could lead to an improved dynamic range in our assay. Then, we synthesize and evaluate 2',7'-diethylfluorescein (DEF), which contains an electron-donating ethyl group proximal to each hydroxyl group. We find that DEF displays a higher phenolic pK_a than does fluorescein, making it a more useful probe. Next, we

synthesize a novel thiol-reactive derivative of DEF for bioconjugation, 2',7'-diethylfluorescein-5-iodoacetamide (DEFIA), and determine pK_a values of a DEF-labeled RNase A in the absence and presence of RI. We observe a substantial increase in assay dynamic range near neutral pH, and show that the diethylfluorescein derivative is a near-optimal probe for this binding assay at our target pH. Lastly, we adapt this improved assay to a microplate format and use this simple, robust system to measure the dissociation constants of several complexes containing RI and variants of RNase A. These findings herald a new and comprehensive strategy for facilitating the analysis of biomolecular interactions.

6.2 Results and Discussion

6.2.1 pK_a Values of Bound and Free Fluorescein-Labeled RNase A

Our binding assay utilizes the A19C/G88R variant of RNase A. Ala19 resides in a solvent-exposed loop that is not within the interface of the RI-RNase A complex (Kobe and Deisenhofer, 1996). Introduction of a thiol group at this position allows site-specific labeling that does not perturb other properties of the protein, such as enzymatic activity or binding to RI (Abel *et al.*, 2002). The fluorescein label is attached covalently by reaction of the free thiol-containing protein with 5-iodoacetamidofluorescein (5-IAF) to give fluorescein-labeled RNase A (fluorescein-RNase A). The RI-RNase A complex exhibits extremely tight binding ($K_d = 44$ fM (Lee *et al.*, 1989a)). Substitution at position 88 attenuates the binding constant of the complex by more than four orders of magnitude ($K_d = 1.4$ nM (Rutkoski *et al.*, 2005)) and thus allows for effective competition by other ribonucleases with K_d values at or above the nanomolar range. Our assay is typically

performed in commercial Dulbecco's phosphate-buffered saline (DPBS) (Dulbecco and Vogt, 1954) at pH 7.12, which defines the target pH for assay optimization.

In the original report (Abel *et al.*, 2002) of this assay system, we noted that the cause of the fluorescence change of the fluorescein conjugate of A19C/G88R RNase A (herein, fluorescein–RNase A) upon binding to RI was unclear, but we hypothesized that it arose from a shift in the pK_a of the fluorescein label. To test this premise, and gain insight for assay optimization, we measured the pK_a values of both bound and free fluorescein–RNase A. A series of buffers were prepared from pH 4 to 10, and the fluorescence intensity of the conjugate in the absence and presence of a 7-fold molar excess of RI was measured and plotted against pH. This surfeit of RI is sufficient to bind >99.5% of the labeled ribonuclease based on the K_d value of 1.4 nM (Rutkoski *et al.*, 2005). The difference between the curves was also calculated, and the resulting data are shown in Figure 6.1a.

The data in Figure 6.1a conform to a model for pK_a shifts of fluorescein–protein conjugates described by Garel (Garel, 1976), including the bell-shaped difference trace. We note that at high pH values, complex formation causes only a minor decrease (<5%) in fluorescence intensity. The inhibition of the catalytic activity of RNase A by RI is known to be similar in solutions of different pH (Lee *et al.*, 1989a), indicating that complex formation is unaffected by pH. Thus, the traces in Figure 6.1a suggest that the pK_a shift of fluorescein upon RI binding is the primary cause for the fluorescence modulation. The phenolic pK_a value of the free fluorescein–RNase A is 6.35 ± 0.03 , and the pK_a value for bound fluorescein–RNase A is 6.70 ± 0.02 . The maximal difference is at pH 6.5, making that the solution pH at which our assay is most sensitive. Interestingly,

the pK_a values for the free and RI-bound conjugates are both higher than our measured pK_a value for free fluorescein of 6.30 ± 0.03 (*vide infra*).

The phenolic pK_a value of fluorescein can change dramatically upon conjugation to a biomolecule (Klonis *et al.*, 1998), and it remains difficult to predict how the local environment around the label will affect the pK_a of the dye. Nonetheless, the shift in pK_a value upon binding of fluorescein–RNase A by RI is intuitive, based on the net macromolecular charge of the two proteins. RNase A is a cationic protein ($pI = 9.33$ (Ui, 1971)), creating an electropositive field in which the ionization of fluorescein is relatively favorable. Binding of RNase A to the comparatively anionic RI ($pI = 4.7$ (Blackburn *et al.*, 1977)) can neutralize much of this field (Lee *et al.*, 1989a), leading to an increased phenolic pK_a value for the fluorescein label.

The data in Figure 6.1a suggested to us an optimization strategy that involved “tuning” the phenolic pK_a value of the label through chemical synthesis. Changing the pK_a of fluorescein would, in effect, shift the pK_a curves of the free and RI-bound conjugate either higher or lower along the abscissa, causing the maximal difference between these two curves to align more closely with the desired assay pH. Such a shift could lead to a higher assay dynamic range at the preferred pH. Prior attempts to adjust the pK_a of fluorescein labels have focused on decreasing this value as much as possible to abolish pH sensitivity (Mchedlov-Petrosyan *et al.*, 1992; Sun *et al.*, 1997; Haugland *et al.*, 2005). Conversely, our goal was to *increase* the pK_a so as to maximize the fluorescence change at the assay pH.

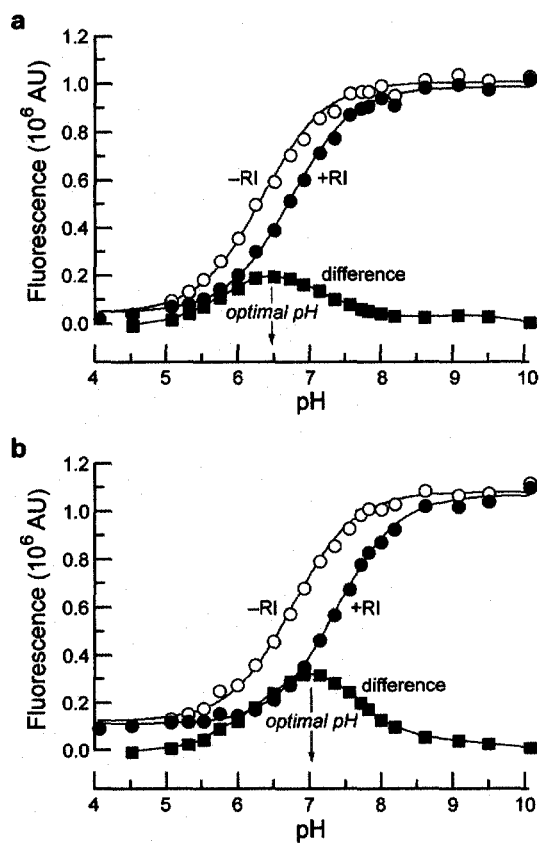


Figure 6.1 Effect of pH on the fluorescence ($\lambda_{\text{ex}} = 493$ nm, $\lambda_{\text{em}} = 515$ nm) of fluorophore-labeled RNase A (50 nM) in the absence (○) or presence (●) of excess RI (350 nM), and the difference (■). (a) Fluorescein-RNase A. (b) DEF-RNase A.

6.2.2 Design and Synthesis of 2',7'-Diethylfluorescein

The proximity of the pK_a value of fluorescein to biologically relevant pH values allows its use as fluorescent pH indicator in certain experiments (Thomas *et al.*, 1979; Graber *et al.*, 1986; Wu *et al.*, 2000). Alkyl substitution on the xanthenyl portion of fluorescein can increase the phenolic pK_a of fluorescein, making it more sensitive to changes in pH near neutrality. Such substitution was exploited by Tsien and coworkers to prepare the widely used pH indicator 2',7'-bis-carboxyethyl-5(6)-carboxyfluorescein (BCECF) that possesses a pK_a near 7.0 (Paradiso *et al.*, 1984; Graber *et al.*, 1986). Hexyl-substituted fluoresceins also show an increase in the phenolic pK_a making them useful fluorescent pH sensors (Schroder *et al.*, 2005). Although these compounds show the desired increase in pK_a value, the relatively large appendages could cause unnecessary disruption of the protein if incorporated into a fluorescent label. Substitution with smaller, ethyl groups at the 2' and 7' positions can also increase the pK_a of fluorescein (Diwu *et al.*, 2004). We reasoned that the negligible perturbation of the fluorescein structure from such ethyl substituents would preserve its utility as a label.

To evaluate the effect of ethyl-group substitution, we synthesized 2',7'-diethylfluorescein (DEF) by the route shown in Scheme 6.2. This compound was reported in the 1930's by Novelli in research directed toward the development of fluorescein-based antiseptics (Novelli, 1932; Novelli, 1933). We used a more contemporary route, taking advantage of the commercial availability of 4-ethylresorcinol (**6.4**). This compound was condensed with phthalic anhydride (**6.5**) in methanesulfonic acid (Sun *et al.*, 1997) to afford crude DEF. This material was acetylated with acetic anhydride in pyridine, and the resulting diacetate **6.6** was purified via crystallization. We

found that suspension of the crude **6.6** in cold EtOH prior to crystallization removed a significant amount of polar impurities, thereby improving the yield. Hydrolysis of the ester groups with base followed by acidification gave DEF (**6.7**).

6.2.3 Spectral Properties of 2',7'-Diethylfluorescein

Both fluorescein and 2',7'-diethylfluorescein were evaluated to confirm the anticipated effect of alkylation on the pK_a value and to compare other spectral properties of these dyes in aqueous solution. The measured parameters are listed in Table 6.1. The pK_a values for both fluorescein and DEF were determined in the same buffer system used for the fluorescein–RNase A conjugate (Figure 6.2). The extinction coefficients and quantum yields of fluorescein and DEF were determined in 0.1 M NaOH to isolate the properties of the dianionic dye form.

The spectral values determined for the diethyl variant of fluorescein are close to those reported for other dialkyl derivatives (Schroder *et al.*, 2005). The electron-donating character of the ethyl substituents increases the pK_a from 6.30 to 6.61. Our pK_a value for free fluorescein is slightly lower than the reported range of values (Mchedlov-Petrosyan, 1979; Diehl, 1989; Diehl and Markuszewski, 1989; Sjoback *et al.*, 1995; Klonis and Sawyer, 1996; Smith and Pretorius, 2002) because of the relatively high ionic strength of our buffer system (Sjoback *et al.*, 1995). The alkyl substitution also elicits bathochromic shifts of 10 nm for both absorption and emission maxima relative to fluorescein as shown in Figure 6.3. The extinction coefficient at maximal absorption of DEF under basic conditions (0.1 M NaOH) is about 10% higher than the absorptivity of fluorescein. The quantum yield of diethylfluorescein is slightly lower than that of fluorescein, again in

agreement with other reported dialkylfluorescein derivatives (Schroder *et al.*, 2005).

Overall, the ethyl group substitution confers the desired increase in pK_a value while causing only minor differences in absorption and fluorescence properties. This similarity of optical characteristics of the two dyes allows for the use of standard fluorescein excitation and emission wavelengths for both dyes and their conjugates.

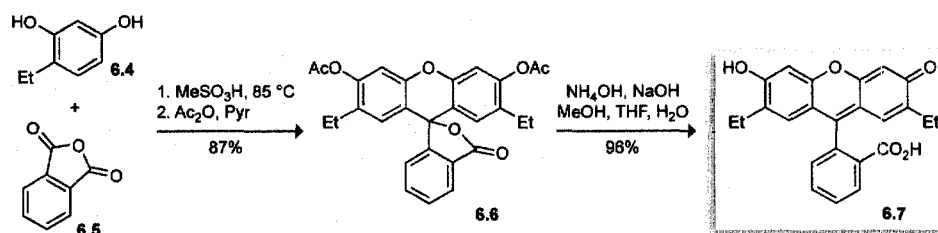
Scheme 6.2 Synthesis of 2',7'-diethylfluorescein

Table 6.1 Spectroscopic parameters of fluorescein and DEF

	Fluorescein	Diethylfluorescein
pK_a	6.30 ± 0.02	6.61 ± 0.03
λ_{\max} (nm)	491	501
ϵ ($M^{-1}cm^{-1}$)	$89,800 \pm 400$	$98,500 \pm 400$
λ_{em} (nm)	510	520
Φ	0.95 ± 0.03 (Lakowicz, 1999)	0.89 ± 0.03

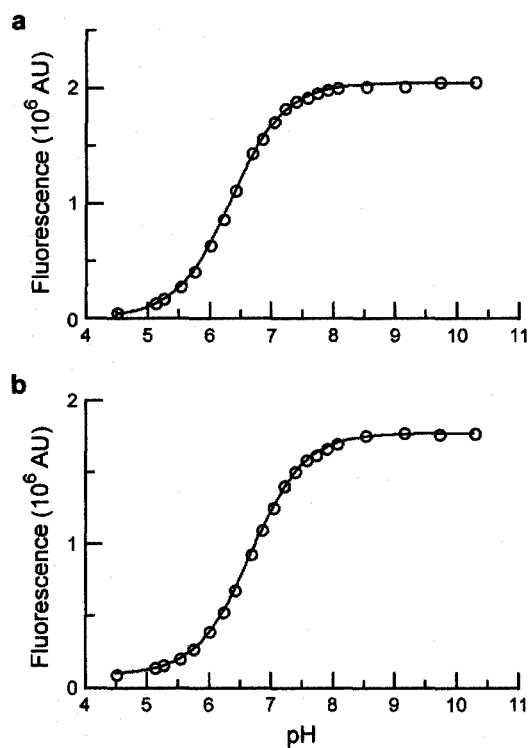


Figure 6.2 (a) pH-Dependence of the fluorescence of fluorescein (6.1).

(b) pH-Dependence of the fluorescence of 2',7'-diethylfluorescein (6.7).

Values of pK_a were found to be 6.30 ± 0.02 for 6.1, and 6.61 ± 0.03 for 6.7

($\lambda_{ex} = 493$ nm, $\lambda_{em} = 515$ nm).

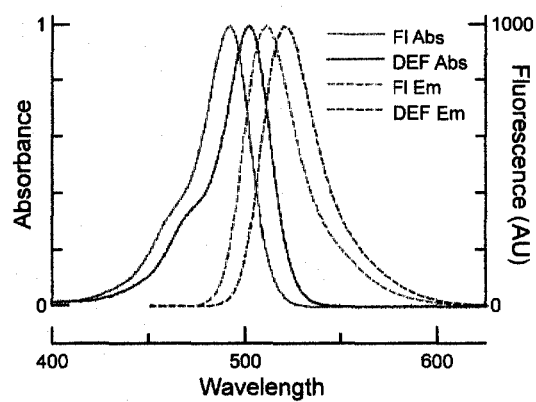


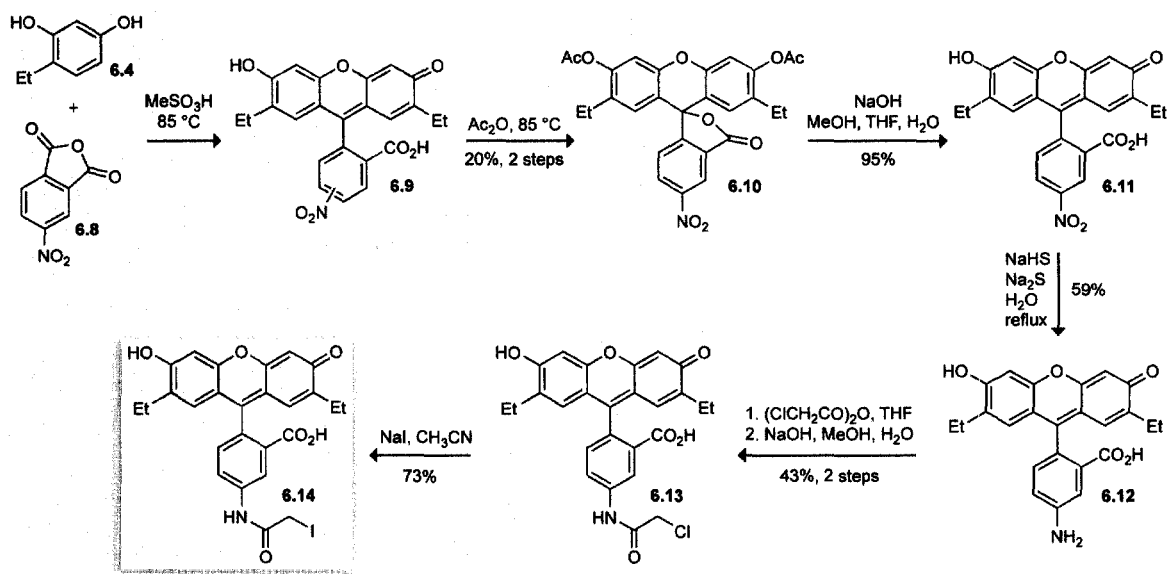
Figure 6.3 Normalized absorption and emission spectra of fluorescein (6.1) and 2',7'-diethylfluorescein (6.7) in 0.1 M NaOH.

6.2.4 Synthesis of 2',7'-Diethylfluorescein-5-iodoacetamide (DEFIA)

Having confirmed the elevated pK_a values of DEF, we next sought to prepare a thiol-reactive derivative for bioconjugation. To ensure an accurate comparison between fluorescein-labeled and DEF-labeled proteins, we designed an analogue of 5-IAF in which introduction of the ethyl groups was the only structural perturbation, thereby eliminating effects due to different linker lengths or conjugation chemistries. The synthesis of 5-aminofluorescein is well documented because of its intermediacy in the preparation of the widely-used fluorescent label: fluorescein-isothiocyanate (FITC) (Coons and Kaplan, 1950; McKinney *et al.*, 1962; Steinbach, 1974). We were pleased to discover that this established chemistry is sufficiently pliable to allow for introduction of the desired ethyl substituents without dramatic changes in yield. To our knowledge, this is the first example of a fluorescein-derived label in which the phenolic pK_a is tuned to a higher rather than a lower value. In addition, this synthesis adds to the sparse reports in the primary scientific literature describing iodoacetamide derivatives of xanthene dyes (Krafft *et al.*, 1988; Corrie and Craik, 1994).

The scheme for the synthesis of 2',7'-diethylfluorescein-5-iodoacetamide (DEFIA) is shown in Scheme 6.3. Condensation of 4-ethylresorcinol (**6.4**) with commercially available 4-nitrophthalic anhydride (**6.8**) gave fluorescein **6.9** as a mixture of 5- and 6-nitro isomers. This material could be acetylated with acetic anhydride to yield a diacetate. Separation of the two isomers via recrystallization (Coons and Kaplan, 1950) afforded the single 5-nitro isomer **6.10**. Hydrolysis of this diacetate with base gave free 5-nitro-2',7'-diethylfluorescein (**6.11**). Reduction of the nitro group with sulfide (Steinbach, 1974) followed by crystallization from aqueous HCl gave the

5-aminofluorescein as the HCl salt. Dissolving this intermediate HCl salt in basic solution followed by precipitation of the free amine with acetic acid (McKinney *et al.*, 1962) afforded the 5-amino-2',7'-diethylfluorescein (**6.12**). This material was treated with chloroacetic anhydride to give an intermediate 5-amidofluorescein diester. Hydrolysis of the ester groups using NaOH in the same pot gave chloroacetamide **13**, which was taken on to DEFIA (**6.14**) via reaction with NaI in acetone.

Scheme 6.3 Synthesis of 2',7'-diethylfluorescein-5-iodoacetamide (DEFIA)

6.2.5 pK_a Values of Free and RI-Bound DEF-Labeled A19C/G88R RNase A

Thiol-containing A19C/G88R RNase A variant was reacted with DEFIA, and the resulting conjugate was purified with cation-exchange chromatography. The fluorescence intensity of the resulting 2',7'-diethylfluorescein conjugate of A19C/G88R RNase A (herein, DEF–RNase A) was measured in the absence and presence of RI in buffered aqueous solution over a pH range of 4–10, as with the fluorescein–RNase A conjugate. The fluorescence values and fluorescence difference were plotted against pH as shown in Figure 6.1b. The pK_a values of the free and RI-bound DEF–RNase A were calculated to be 6.68 ± 0.03 and 7.29 ± 0.03 , respectively. As with the fluorescein system, these values are higher than those measured for unliganded DEF ($pK_a = 6.61 \pm 0.03$). This shift in pK_a values increases the maximum of the fluorescence difference to above 7.0.

The bound and free DEFIA conjugates exhibit a larger ΔpK_a value than did the fluorescein-labeled protein. This larger difference in pK_a likely arises from structural rather than electronic consequences of the two ethyl groups. For example, the DEF label could exist in a different orientation than the fluorescein label such that its pK_a value is affected to a greater degree upon binding to RI.

6.2.6 Assay Comparison

A major goal of this work was to improve the assay performance and then investigate the utility of the enhanced system in a microplate format. To quantify the assay improvement, we first determined the maximum dynamic range by measuring the change in fluorescence upon RI binding under typical assay conditions. Addition of excess RI to fluorescein–RNase A elicits a 15% decrease in fluorescence, whereas the change in

fluorescence intensity of the DEF–RNase A conjugate is a significantly larger 38% as shown in Figure 6.4.

Having confirmed the enhancement of the assay, we then evaluated the utility of this assay in a microplate format. A common quantification of plate-based assay performance is the *Z'*-factor which uses the standard deviation of controls and the dynamic range to assign a numerical value to assay utility (Zhang *et al.*, 1999). We measured the *Z'*-factor using microplates containing the labeled conjugate and RI. The positive control also contained excess RNase A to liberate fully the fluorophore-labeled protein. As shown in Figure 6.5, the fluorescein system had *Z'*-factor = -0.17 , signifying an overlap of the $\mu \pm 3\sigma$ levels for the positive and negative controls. In stark contrast, the diethylfluorescein system had a *Z'*-factor of 0.69 . An assay system with a *Z'*-factor >0.5 is considered to be “excellent” and therefore highly useful in microplate systems, including high-throughput screening (HTS) assays. Thus, in addition to improving assay performance, this new diethylfluorescein label could allow HTS to identify compounds that disrupt the RI–ribonuclease interaction.

6.2.7 Microplate-Based Determination of K_d Values

The increase in assay dynamic range and superb *Z'*-factor prompted us to validate this microplate system to measure RI-ribonuclease dissociation constants. Pancreatic-type ribonucleases are cationic proteins that can enter cells via endocytosis (Haigis and Raines, 2003). The ubiquitous ribonuclease inhibitor has a high cytosolic concentration ($4\ \mu\text{M}$) and can therefore protect cellular RNA from degradation by invading ribonucleases (Haigis *et al.*, 2003). Amino acid substitutions that disrupt the RI–

ribonuclease interface can endow an otherwise benign ribonuclease with cytotoxic activity (Rutkoski *et al.*, 2005). Thus, the K_d value of a RI-ribonuclease complex is helpful in predicting the cytotoxicity of a novel ribonuclease variant.

We first determined the affinity of DEF-RNase A for RI by direct titration (Abel *et al.*, 2002) and found that the ethyl groups did not cause any significant change in binding constant between the labeled protein and RI (data not shown). We then determined the K_d values for other variants of RNase A using DEF-RNase A in microplates (Figure 6.6). These values (\pm SE), which are listed in Table 6.2, are in gratifying agreement with those determined previously using the cuvette assay (Rutkoski *et al.*, 2005). The new system proved extremely facile and economical, requiring 5% of the protein and significantly less time compared to the original assay format.

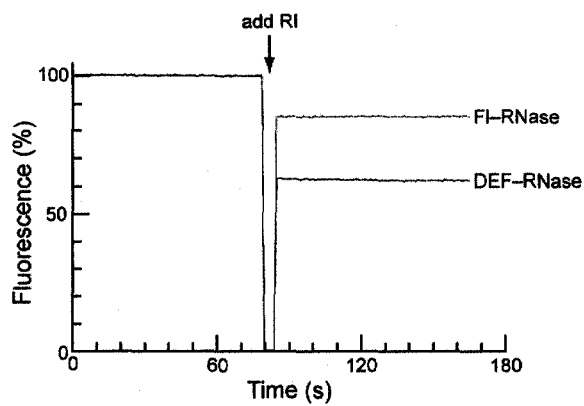


Figure 6.4 Comparison of the fluorescence change of FI-RNase (red) and DEF-RNase (blue) upon addition of excess RI ($\lambda_{\text{ex}} = 493 \text{ nm}$, $\lambda_{\text{em}} = 515 \text{ nm}$) in DPBS containing BSA ($2 \mu\text{g/mL}$). .

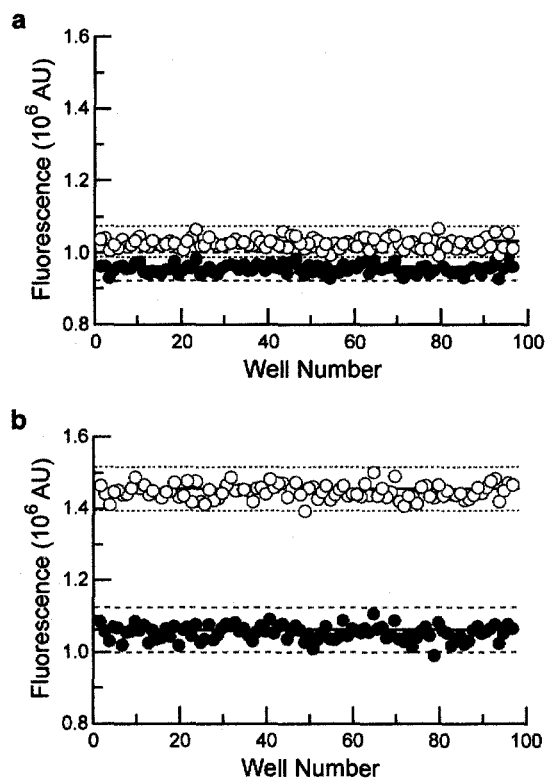


Figure 6.5 *Z'*-factor determination. Fluorescence in microplate wells containing a fluorophore-labeled ribonuclease (50 nM) and RI (50 nM) in the absence (○) or presence (●) of excess RNase A (5 μ M) at pH 7.12. Horizontal solid lines indicate the mean value; horizontal dashed lines indicate the range ($\pm 3\sigma$) of values. (a) Fluorescein–RNase A (*Z'*-factor -0.17). (b) DEF–RNase A (*Z'*-factor 0.69).

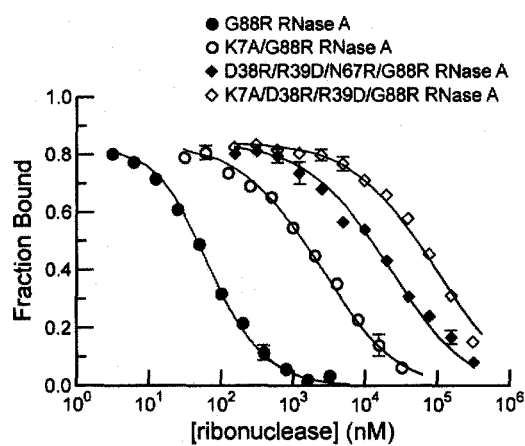


Figure 6.6 Data from microplate assays for determination of the K_d values of RI-ribonuclease complexes in DPBS containing BSA (0.1 mg/mL)..

Table 6.2 Values of K_d for RI-ribonuclease complexes

Ribonuclease Variant	K_d
G88R RNase A	1.3 ± 0.2 nM
K7A/G88R RNase A	80 ± 5 nM
D38R/R39D/N67R/G88R RNase A	730 ± 40 nM
K7A/D38R/R39D/G88R RNase A	3.1 ± 0.2 μ M

6.3 Conclusions

The ubiquity of fluorescein in biochemical, biological, and medicinal research demands a detailed grasp of the acid–base equilibria of this dye in aqueous solution. Our results show that a thorough understanding and application of the nuances of fluorescein can be useful in the optimization of assays. Shifts in the phenolic pK_a are a significant causal force behind many of the fluorescence modulations observed with fluorescein conjugates. Tuning this pK_a through chemical synthesis can have dramatic effects on assay dynamic range, leading to significant improvement in throughput and requisite sample volume.

This work could inspire the expansion of the current spectrum of fluorescent labels. A palette of reactive dyes with tuned pK_a values could prove useful in the development of new binding assays. In addition to fluorescein, other classes of fluorescent dyes are sensitive to pH and thus could be evaluated and optimized in a similar manner. Of particular interest are dye systems that exhibit a large spectral shift upon protonation (Whitaker *et al.*, 1991b; Liu *et al.*, 2001). Use of these fluorophores could permit ratiometric measurement of binding events. Overall, properly tuned fluorescent labels hold the potential to improve existing systems and aid in the development of new assays for characterizing protein–protein interactions and other important biomolecular processes.

6.4 Acknowledgments

We are grateful to C. Schilling for initial synthetic studies, K. J. Kolonko for assistance with NMR spectroscopy, and Z.J. Diwu, B.D. Smith, R.J. Johnson, G.A. Ellis,

and S.M. Fuchs for contributive discussions. L.D.L was supported by Biotechnology Training Grant 08349 (NIH) and an ACS Division of Organic Chemistry Graduate Fellowship sponsored by the Genentech Foundation. T.J.R was supported by Biotechnology Training Grant 08349 (NIH) and a William R. & Dorothy E. Sullivan Wisconsin Distinguished Graduate Fellowship. This work was supported by grant CA73808 (NIH). Biophysics Instrumentation Facility was established with grants BIR-9512577 (NSF) and S10 RR13790 (NIH). The Keck Center for Chemical Genomics was established with a grant from the W.M. Keck Foundation. NMRFAM was supported by grant P41 RR02301 (NIH). The MRF was supported by grants CHE-9709065 (NSF), CHE-9208463 (NSF), and S10 RR08389 (NIH).

6.5 Experimental Section

6.5.1 General Experimental: Chemical Synthesis

4-Nitrophthalic anhydride was from TCI America (Portland, OR). Dimethylformamide (DMF), tetrahydrofuran (THF), and dichloromethane (CH_2Cl_2) were drawn from a Baker CYCLE-TAINER solvent delivery system. All other reagents were obtained from Aldrich Chemical (Milwaukee, WI) or Fisher Scientific (Hanover Park, IL) and used without further purification. $\text{NaHS} \cdot \text{H}_2\text{O}$ was obtained as “sodium hydrosulfide hydrate” (Aldrich; Product 161527). HCl(aq) was prepared by dilution of concentrated HCl(aq) into H_2O in the indicated proportions.

Thin-layer chromatography was performed using aluminum-backed plates coated with silica gel containing F_{254} phosphor and visualized by UV illumination or staining with I_2 , ceric ammonium molybdate, or phosphomolybdic acid. Flash chromatography was

performed by using open columns loaded with silica gel-60 (230–400 mesh), or on a FlashMaster Solo system (Argonaut Inc., Redwood City, CA) with Isolute Flash Si II columns (International Sorbent Technology Ltd., Hengoed, Mid Glamorgan, UK). The term “high vacuum” refers to a vacuum (≤ 1 mm Hg) achieved by a mechanical belt-drive oil pump. The term “concentrated under reduced pressure” refers to the removal of solvents and other volatile materials using a rotary evaporator at water-aspirator pressure (< 20 mm Hg) while maintaining the water-bath temperature below 40 °C. The term “concentrated under high vacuum” refers to the removal of solvents and other volatile materials using a rotary evaporator at high vacuum while maintaining the water-bath temperature below 40 °C.

NMR spectra were obtained with a Bruker DMX-400 Avance spectrometer in the National Magnetic Resonance Facility at Madison (NMRFAM), or with Bruker AC-300 or Avance-360 spectrometers in the Magnetic Resonance Facility (MRF) in the Department of Chemistry. Mass spectrometry was performed with a Micromass LCT (electrospray ionization, ESI) mass spectrometer in the Mass Spectrometry Facility in the Department of Chemistry. Analytical HPLC was performed on a system from Waters (Milford, MA) with an 250×4.6 mm C-18 Microsorb column from Varian (Palo Alto, CA) using a linear gradient of CH₃CN (20–60% v/v) in H₂O. HPLC solvents contained TFA (0.1% v/v).

6.5.2 Synthesis of Compounds 6.6, 6.7, and 6.10–6.14

2',7'-Diethylfluorescein Diacetate (6.6) 4-Ethylresorcinol (**6.4**, 5.00 g, 36.2 mmol) and phthalic anhydride (**6.5**, 2.68 g, 18.09 mmol) were dissolved in methanesulfonic acid

(40 mL). The reaction mixture was stirred at 85 °C for 48 h. The dark brown solution was poured into ice water (250 mL), and the yellow-brown precipitate was collected by filtration and air dried. This material was dissolved in acetic anhydride (80 mL) and pyridine (80 mL), and stirred at 85 °C for 4 h. The reaction mixture was concentrated under high vacuum, and the brown residue was dissolved into CH₂Cl₂. This solution was washed with HCl(aq) (5% v/v), water, and saturated brine. The organic layer was then dried over anhydrous MgSO₄(s) and concentrated under reduced pressure. The brown residue was suspended in cold EtOH (300 mL), and the resulting pale brown solid was collected by filtration. This material was purified further by crystallization from CHCl₃/MeCN (1:1) and the crystals were washed with cold EtOH (excluded from the mother liquor). The mother liquor was concentrated under reduced pressure and a second crop of crystals was obtained by crystallization from acetic anhydride. The combined crystals were dried under high vacuum. Compound **6.6** was isolated as a pale yellow crystalline solid (7.41 g, 87%). ¹H NMR (400 MHz, CDCl₃) δ (ppm): 8.05 (d, *J* = 7.1 Hz, 1H), 7.69 (ddd, *J* = 7.6, 7.1, 1.6 Hz, 1H), 7.64 (ddd, *J* = 7.6, 7.5, 1.2 Hz, 1H), 7.19 (d, *J* = 7.4 Hz, 1H), 7.01 (s, 2H), 6.64 (s, 2H), 2.39 (m, 4H), 2.33 (s, 6H), 1.01 (t, *J* = 7.8 Hz, 6H). ¹³C NMR (100 MHz, CDCl₃) δ (ppm): 169.46, 168.88 (2C), 153.23, 150.11 (2C), 149.64 (2C), 135.20 (2C), 131.96, 129.87, 128.07 (2C), 125.93, 125.13 (2C), 124.09, 116.57, 110.87 (2C), 82.09, 22.94 (2C), 20.84 (2C), 14.02 (2C). HRMS (ESI): *m/z* 495.1417 (MNa⁺ [C₂₈H₂₄O₇Na] = 495.1420).

2',7'-Diethylfluorescein (6.7). 2',7'-Diethylfluorescein diacetate (**6.6**, 2.00 g, 4.23 mmol) was dissolved in THF (20 mL) and MeOH (20 mL). To this solution was added 29% w/w NH₄OH(aq) (5.12 mL, 42.2 mmol), and the mixture was stirred at ambient

temperature for 2 h. NaOH (1.69 g, 42.2 mmol) was added as a solution in H₂O (20 mL) and MeOH (5 mL), and the reaction mixture stirred for an additional 1 h at ambient temperature. The mixture was diluted with 200 mL of H₂O, and concentrated under reduced pressure to remove the organic solvents. The dark brown solution was filtered and then acidified with HCl(aq) (10% v/v) to pH ~3. The resulting yellow-orange precipitate was collected by filtration, washed with H₂O, and dried under high vacuum. Compound **6.7** was isolated as an orange solid (1.57 g, 96%). An analytical sample was prepared by column chromatography (silica gel, EtOAc). ¹H NMR (400 MHz, DMSO-*d*₆) δ (ppm): 10.09 (bs, 2H), 8.00 (d, *J* = 7.8 Hz, 1H), 7.78 (ddd, *J* = 7.5, 7.4, 1.2 Hz, 1H), 7.71 (ddd, *J* = 7.5, 7.4, 1.0 Hz, 1H), 7.24 (d, *J* = 7.4 Hz, 1H), 6.71 (s, 2H), 6.34 (s, 2H), 2.35 (m, 4H), 0.92 (t, *J* = 7.6 Hz, 6H). ¹³C NMR (100 MHz, DMSO-*d*₆) δ (ppm): 168.83, 157.11 (2C), 152.62, 149.95 (2C), 135.53, 130.01, 127.23 (2C), 127.12 (2C), 126.21, 124.55, 124.00, 109.02 (2C), 101.73 (2C), 83.55, 22.35 (2C), 14.10 (2C). HRMS (ESI): *m/z* 387.1219 (M-H [C₂₄H₁₉O₅] = 387.1232).

5(6)-Nitro-2',7'-Diethylfluorescein (6.9). 4-Ethylresorcinol (**6.4**, 5.00 g, 36.2 mmol) and 4-nitrophthalic anhydride (**6.8**, 3.49 g, 18.1 mmol) were dissolved in methanesulfonic acid (40 mL). The reaction mixture was stirred at 85 °C for 48 h. The dark brown solution was poured into ice water (250 mL), and the yellow-brown precipitate was collected by filtration. This material was washed with H₂O and air dried. Crude compound **6.9** was isolated as a yellow-brown solid and used in the next step without further purification.

5-Nitro-2',7'-diethylfluorescein Diacetate (6.10). Crude 5(6)-nitro-2',7'-diethylfluorescein (**6.9**) from the previous step was dissolved in acetic anhydride (30 mL)

and stirred at reflux for 2 h. This solution was placed at 4 °C for 48 h and the resulting tan crystals (2.61 g, 28%) were collected by filtration and washed with cold acetic anhydride. The mother liquor was concentrated under high vacuum and the residue was dissolved in acetic anhydride (15 mL). This solution was incubated at 4 °C for 48 h after which additional tan crystals formed (1.53 g, 16%). These crystals were isolated by filtration and washed with cold acetic anhydride. The combined crystals were purified further by crystallization twice from acetic anhydride and dried under high vacuum. Compound **6.10** was isolated as an off-white solid (1.91 g, 20%, two steps). ¹H NMR (400 MHz, DMSO-*d*₆) δ (ppm): 8.73 (d, *J* = 1.7 Hz, 1H), 8.59 (dd, *J* = 8.4, 2.3, 1H), 7.72 (d, *J* = 8.4 Hz, 1H), 7.27 (s, 2H), 6.86 (s, 2H), 2.37 (m, 4H), 2.33 (s, 6H), 0.94 (t, *J* = 7.6 Hz, 6H). ¹³C NMR (100 MHz, DMSO-*d*₆) δ (ppm): 168.92, 166.53, 156.73, 150.48, 149.26, 148.95, 132.53, 130.62, 128.53, 127.35, 125.95, 120.83, 115.09, 111.21, 81.88, 22.17, 20.63, 14.42. HRMS (ESI): *m/z* 518.1441 (MH⁺ [C₂₈H₂₄NO₉] = 518.1451).

5-Nitro-2',7'-diethylfluorescein (6.11). 5-Nitro-2',7'-diethylfluorescein diacetate (**6.10**, 1.00 g, 1.93 mmol) was dissolved in THF (35 mL). This solution was diluted with MeOH (35 mL) and H₂O (20 mL). To the resulting solution was added NaOH (1.55 g, 38.6 mmol), and the mixture was stirred at 0 °C for 1 h and then at ambient temperature for 1 h. This was concentrated under reduced pressure to remove the organic solvents, and the residue was diluted with 50 mL of H₂O and filtered. The resulting dark brown solution was acidified with HCl(aq) (10% v/v) to pH ~3, and the resulting yellow-orange precipitate was collected by filtration, washed with H₂O and dried under high vacuum. Compound **6.11** was isolated as an orange solid (0.797 g, 95%). ¹H NMR (400 MHz, DMSO-*d*₆) δ (ppm): 10.16 (bs, 2H), 8.66 (d, *J* = 1.7 Hz, 1H), 8.56 (dd, *J* = 8.4, 2.3 Hz,

1H), 7.53 (d, $J = 8.4$ Hz, 1H), 6.71 (s, 2H), 6.48 (s, 2H), 2.36 (m, 4H), 0.94 (t, $J = 7.5$ Hz, 6H). ^{13}C NMR (100 MHz, DMSO- d_6) δ (ppm): 166.78, 157.53 (3C), 150.01 (2C), 149.00, 130.20, 127.85, 127.64 (4C), 125.90, 120.41, 107.81 (2C), 101.88 (2C), 84.34, 22.41 (2C), 14.18 (2C). HRMS (ESI): m/z 432.1075 ($\text{M}-\text{H}$ [$\text{C}_{24}\text{H}_{18}\text{NO}_7$] = 432.1084).

5-Amino-2',7'-Diethylfluorescein (6.12). $\text{Na}_2\text{S}\cdot 9(\text{H}_2\text{O})$ (5.54 g, 23.1 mmol) was dissolved in H_2O (75 mL). 5-Nitro-2',7'-diethylfluorescein (**6.11**, 2.50 g, 5.77 mmol) was added, and the resulting solution was stirred at ambient temperature for 10 min. Then, to this solution was added $\text{NaHS}\cdot\text{H}_2\text{O}$ (2.59 g, 46.1 mmol), and the mixture was stirred at reflux for 24 h. The solution was carefully acidified with glacial acetic acid, and the resulting dark red precipitate was collected by filtration. This solid was dissolved in 175 mL of $\text{HCl}(\text{aq})$ (6% v/v), heated to reflux, and filtered while hot to remove elemental sulfur. The solution was incubated at 4 °C for 48 h, and the resulting red solid was collected by filtration. This solid was dissolved in 120 mL of $\text{HCl}(\text{aq})$ (6% v/v) and, as before, filtered while hot and incubated at 4 °C for 48 h. The solid was collected by filtration and taken up into 210 mL of $\text{NaOH}(\text{aq})$ (0.5% w/v) to give a dark red solution. Glacial acetic acid (4.2 mL) was added dropwise, and the resulting red precipitate was collected via filtration and dried under high vacuum. Compound **6.12** was isolated as an red-orange solid (1.92 g, 82%). ^1H NMR (400 MHz, DMSO- d_6) δ (ppm): 7.24 (d, $J = 2.1$ Hz, 1H), 7.05 (dd, $J = 8.3, 2.2$ Hz, 1H), 6.92 (d, $J = 8.2$ Hz, 1H), 6.62 (s, 2H), 6.61 (s, 2H), 2.46 (m, 4H), 1.03 (t, $J = 7.5$ Hz, 6H). ^{13}C NMR (100 MHz, DMSO- d_6) δ (ppm): 169.52, 156.84 (2C), 150.32 (2C), 150.04 (2C), 139.83, 127.51, 127.26 (2C), 126.85, 124.16, 121.73, 110.16 (2C), 106.16, 101.62 (2C), 83.23, 22.43 (2C), 14.18 (2C). HRMS (ESI): m/z 403.1509 (MH^+ [$\text{C}_{24}\text{H}_{22}\text{NO}_5$] = 403.1498).

2',7'-Diethylfluorescein-5-chloroacetamide (6.13). 5-Amino-2',7'-diethylfluorescein (**6.12**, 157 mg, 0.389 mmol) was dissolved in THF (5.0 mL). To this solution was added chloroacetyl chloride (382 μ L, 3.89 mmol), and the mixture was stirred at reflux for 1 h. The reaction mixture was cooled to 0 °C, and MeOH (5.0 mL) was added, followed by NaOH (311 mg, 7.78 mmol) dissolved in H₂O (5.0 mL). The resulting dark orange solution was stirred at 0 °C for 2 h. The reaction was concentrated under reduced pressure to remove the organic solvents, and the resulting dark red solution was acidified with HCl(aq) (10% v/v) to pH ~3. The yellow-orange precipitate was collected by filtration, washed with H₂O, and air-dried. Purification by column chromatography (silica gel, linear gradient of CHCl₃/MeOH/AcOH, 100:5:1–100:8:1 v/v/v) afforded compound **6.13** as an orange solid (182 mg, 97%). ¹H NMR (400 MHz, DMSO-*d*₆) δ (ppm): 10.82 (s, 1H), 10.27 (bs, 2H), 8.33 (s, 1H), 7.84 (dd, *J* = 8.3, 1.9 Hz, 1H), 7.22 (d, *J* = 8.3 Hz, 1H), 6.67 (s, 2H), 6.41 (s, 2H), 4.34 (s, 2H), 2.36 (m, 4H), 0.93 (t, *J* = 7.6, 6H). ¹³C NMR (100 MHz, DMSO-*d*₆) δ (ppm): 168.60, 165.37, 157.26 (2C), 150.05 (2C), 147.36, 139.97, 127.32 (5C), 126.39, 124.71, 109.09, 101.75 (2C), 83.85 (2C), 43.54, 22.39 (2C), 14.19 (2C). HRMS (ESI): *m/z* 480.1208 (MH⁺ [C₂₆H₂₃ClNO₆] = 480.1214).

2',7'-Diethylfluorescein-5-iodoacetamide (6.14, DEFIA). 2',7'-Diethylfluorescein-5-chloroacetamide (**6.13**, 72 mg, 0.150 mmol) was dissolved in acetone (10 mL). To this solution was added NaI (225 mg, 1.50 mmol), and the mixture was stirred at reflux for 24 h. The reaction was concentrated under reduced pressure and the residue was purified by column chromatography (silica gel, CHCl₃/MeOH/AcOH, 100:5:1 v/v/v). The purification afforded compound **14** as an orange solid (62 mg, 73%). An analytical sample was prepared by crystallization from CHCl₃/MeOH (9:1). ¹H NMR (300 MHz,

DMSO- d_6) δ (ppm): 10.81 (s, 1H), 10.08 (bs, 2H), 8.31 (d, $J = 1.6$ Hz, 1H), 7.78 (dd, $J = 8.4, 1.8$ Hz, 1H), 7.21 (d, $J = 8.3$ Hz, 1H), 6.68 (s, 2H), 6.39 (s, 2H), 3.88 (s, 2H), 2.36 (m, 4H), 0.93 (t, $J = 7.5$, 6H). ^{13}C NMR (100 MHz, DMSO- d_6) δ (ppm): 169.01, 167.85, 157.54 (2C), 150.38 (2C), 147.69, 140.73, 127.78 (3C), 127.60 (2C), 126.58, 125.03, 113.78, 109.43 (2C), 102.15 (2C), 84.04, 22.81 (2C), 14.62 (2C), 1.45. HPLC: 97% purity at $\lambda_{\text{abs}} = 449, 254$ nm. HRMS (ESI): m/z 572.0592 (MH^+ [$\text{C}_{26}\text{H}_{23}\text{INO}_6$] = 572.0570).

6.5.3 General Experimental: Biochemistry and Spectroscopy

Fluorescein (reference standard grade) and 5-iodoacetamidofluorescein (5-IAF) were from Molecular Probes (Eugene, OR). Dulbecco's phosphate-buffered saline (Dulbecco and Vogt, 1954) (DPBS; Gibco) was from Invitrogen (Carlsbad, CA). Dithiothreitol (DTT) and *tris*-(hydroxymethyl)-aminomethane (TRIS) were from Research Products International (Mount Prospect, IL). All other chemicals were from Fisher Scientific (Hanover Park, IL) or Sigma–Aldrich (Milwaukee, WI). Bovine serum albumin (BSA) was obtained as a 20 mg/mL solution (Sigma; Product B8667). 2-(*N*-Morpholino)-ethanesulfonic acid (MES) was purified as described previously (Smith *et al.*, 2003) to eliminate oligo(vinylsulfonic acid) contamination. MALDI–TOF mass spectra were obtained with a Perkin–Elmer Voyager mass spectrometer in the Biophysics Instrumentation Facility (BIF) at the University of Wisconsin–Madison.

6.5.4 Preparation of Ribonuclease Inhibitor and Labeled Ribonucleases

Human ribonuclease inhibitor (RI), K7A/G88R RNase A, D38R/R39D/N67R/G88R RNase A, and K7A/D38R/R39D/G88R RNase A were prepared as described previously (Rutkoski *et al.*, 2005). The G88R and A19C/G88R variants of RNase A and the fluorescein-labeled conjugate (fluorescein–RNase A) were prepared as described previously (Abel *et al.*, 2002) with the following change: the proteins were refolded for ≥ 4 days under an inert atmosphere of $N_2(g)$. The DEFIA–protein conjugate (DEF–RNase A) was prepared by reaction of A19C/G88R RNase A with ten-fold excess of DEFIA (6.14) for 2.5 h at ambient temperature and then 16 h at 4 °C. Purification using a HiTrap SP HP cation-exchange column (GE Healthcare, Uppsala, Sweden) afforded the desired conjugate; MS (MALDI): m/z 14,261.00 (expected = 14,258.46). Protein concentration was determined by UV absorption or a bicinchoninic acid (BCA) assay kit from Pierce (Rockford, IL) using wild-type RNase A as a standard.

6.5.5 UV–Visible and Fluorescence Spectroscopy

Absorption spectra were recorded in methacrylate cuvettes having 1-cm path length and 1.5-mL volume from Fisher Scientific on a Cary Model 50 spectrometer from Varian (Sugar Land, TX). Fluorometric measurements were made by using 4.5-mL methacrylate cuvettes from VWR or 4.5-mL glass cuvettes from Starna Cells (Atascadero, CA) and a QuantaMaster1 photon-counting spectrofluorometer from Photon Technology International (South Brunswick, NJ) equipped with sample stirring. All measurements were recorded at ambient temperature (23 ± 2 °C) and buffers were not degassed prior to measurements. Compounds were prepared as stock solutions in DMSO and diluted such

that the DMSO concentration did not exceed 1% v/v. The pH was measured with a Beckmann glass electrode that was calibrated prior to each use. Microplate-based experiments were performed in Costar 96-well NBS microplates (Product #3650) from Corning Life Sciences (Acton, MA). The fluorescence intensity was recorded using a Perkin–Elmer EnVision 2100 Plate Reader and an FITC filter set (excitation at 485 nm with 14-nm bandwidth; emission at 535 nm with 25-nm bandwidth; dichroic mirror cutoff at 505 nm) in the Keck Center for Chemical Genomics at the University of Wisconsin–Madison. Graphs were manipulated and parameters were calculated with the programs Microsoft Excel 2003 and GraphPad Prism 4.

6.5.6 Determination of pK_a Values

The fluorescein acid–base equilibrium between phenol **6.2** and phenolate **6.3** is shown in eq 6.1:



The observed fluorescence intensity (I) at a given excitation and emission wavelength is given by eq 6.2:

$$I = f_{6.2}I_{6.2} + f_{6.3}I_{6.3} \quad (6.2)$$

where f_2 and f_3 are the fractions of the phenol and phenolate form of fluorescein, respectively, and I_2 and I_3 are the phenol and phenolate fluorescence intensities. (Lee *et*

al., 1989a) The pK_a of this acid–base equilibrium can be estimated by measuring the fluorescence intensity as a function of pH and fitting the data to eq 6.3:

$$I = I_{6.2} + \frac{I_{6.3} - I_{6.2}}{1 + 10^{pK_a - pH}} \quad (6.3)$$

which is derived from eq 6.2 and the Henderson–Hasselbalch equation.

Buffers contained NaCl (138 mM), DTT (1 mM), and NaOAc, MES, NaH_2PO_4 , TRIS, and NaHCO_3 (10 mM each). The pH of the buffered solutions was adjusted with 1.0 M NaOH or 1.0 M HCl. All experiments were performed in cuvettes using $\lambda_{\text{ex}} = 493$ nm and $\lambda_{\text{em}} = 515$ nm. The pK_a values of the free dyes were determined at a final dye concentration of 50 nM. For determination of the pK_a of the protein labels, fluorescein–RNase A or DEF–RNase A was added to the buffer solution at a final concentration of 50 nM, and the initial fluorescence was measured. RI was then added to a final concentration of 350 nM, and the resulting fluorescence intensity was measured. The average pK_a values were determined from triplicate experiments involving separate buffer preparations.

6.5.7 Spectral Properties of Free Dyes

The extinction coefficient (ϵ) of fluorescein and 2',7'-diethylfluorescein was determined with solutions in 0.1 M NaOH ($A < 1.0$). The absorbance of a series of fluorescein and DEF concentrations were plotted against concentration, and the extinction coefficient was calculated by linear regression using Beer's Law. The quantum

yield of DEF was determined by using dilute samples ($A < 0.1$) in 0.1 M NaOH. These values were obtained by the comparison of the integrated area of the emission spectrum of the samples with that of fluorescein in 0.1 M NaOH, which has a quantum efficiency of 0.95 ± 0.03 (Lakowicz, 1999). The concentration of the fluorescein reference was adjusted to match the absorbance of the test sample at the excitation wavelength. Under these conditions, the quantum yield (Φ) was calculated with eq 6.4.

$$\Phi_{\text{sample}} = \Phi_{\text{standard}} (\int F_{\text{em, sample}} / \int F_{\text{em, standard}}) \quad (6.4)$$

6.5.8 Assay Comparison and Z'-factor Determination

Comparison of the gross dynamic range of the two protein conjugates was made using a cuvette format in DPBS containing BSA (2 $\mu\text{g/mL}$). The fluorescent protein conjugate (fluorescein–RNase A or DEF–RNase A) was added to a final concentration of 50 nM. RI was then added to a final concentration of 350 nM, and the resulting fluorescence change recorded. The *Z'*-factor was determined by preparing 96-well plates with 50 μL per well of DPBS containing fluorescein–RNase A or DEF–RNase A (100 nM; 2 \times) and BSA (0.1 mg/mL). The positive control plates also contained RNase A (10 μM ; 2 \times). To these plates were added 50 μL per well of DPBS containing BSA (0.1 mg/mL), DTT (10 mM; 2 \times), and RI (100 nM; 2 \times). The fluorescence of each well was quantified after incubation at ambient temperature for 30 min. The *Z'*-factor was determined with eq 6.5 where σ^+ and σ^- are the standard deviations of the positive and negative controls, respectively, and μ^+ and μ^- are the means of the positive and negative controls (Zhang *et al.*, 1999).

$$Z' - factor = 1 - 3 \frac{(\sigma^+ + \sigma^-)}{|\mu^+ - \mu^-|} \quad (6.5)$$

6.5.9 Determination of K_d Values

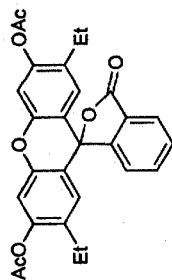
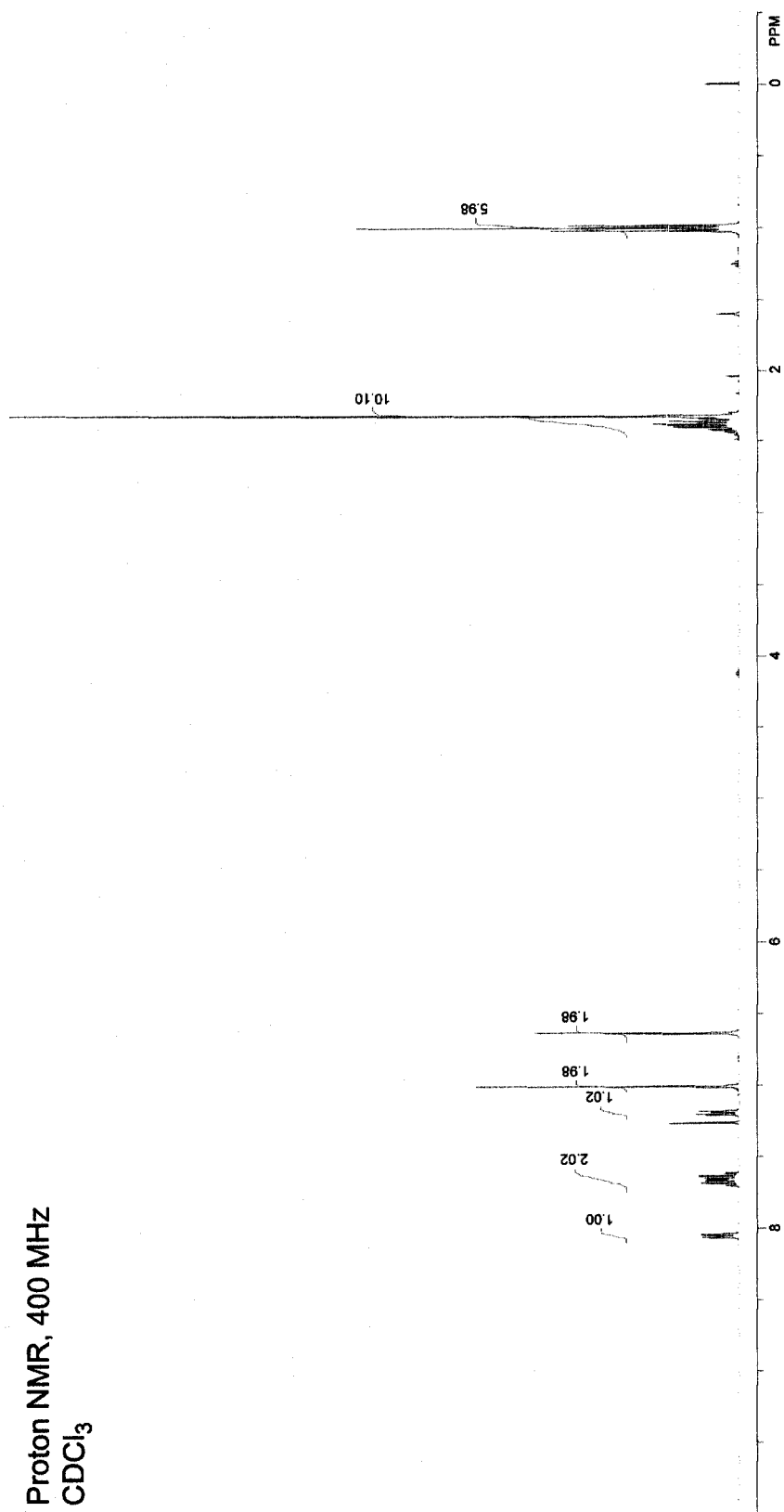
A serial dilution (2×) of the ribonuclease A variant in DPBS with BSA (0.1 mg/mL) was prepared in Eppendorf Protein LoBind Tubes (Fisher Scientific). An aliquot (50 µL) of these serial dilutions was added to the wells of a 96-well plate. A solution (50 µL) of DEF–RNase A (100 nM; 2×) and RI (100 nM; 2×) in DPBS containing DTT (10 mM; 2×) and BSA (0.1 mg/mL) was then added to each well. The negative control contained no ribonuclease and the positive control contained excess RNase A (5 µM). The plate was incubated for 30 min at ambient temperature after which the fluorescence intensity was measured. The observed fluorescence intensity (I) is described by eq 6.6:

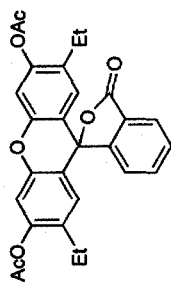
$$I = f_F I_F + f_B I_B \quad (6.6)$$

where f_F and f_B are the fractions of the free and RI-bound form of the fluorescent conjugate, respectively, and I_F and I_B are the fluorescence intensities of the free and RI-bound states, respectively. The value of I_B was determined via linear regression using the intensities of the positive and negative controls, which represent 0% and 84.6% bound respectively based on a K_d value of 1.4 nM for the fluorophore-labeled G88R variant of RNase A (Rutkoski *et al.*, 2005). The fraction bound (f_B) was then calculated using eq 6.7:

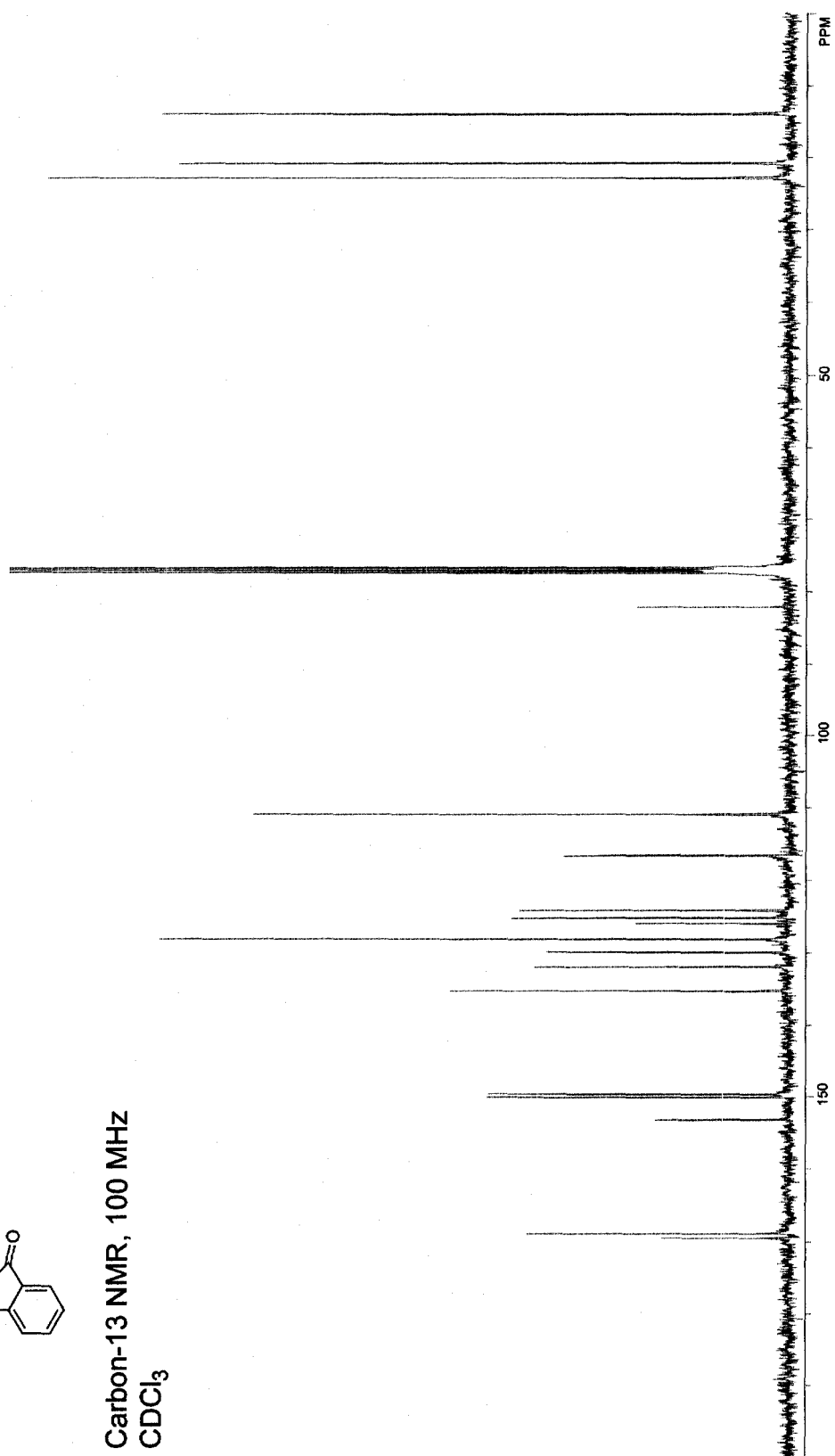
$$f_B = \frac{I - I_F}{I_B - I_F} \quad (6.7)$$

The value of K_d was calculated by plotting f_B against the concentration of competing ribonuclease and fitting the data to the mathematical expression for complete competitive binding of two different ligands (Wang, 1995; Roehrl *et al.*, 2004).

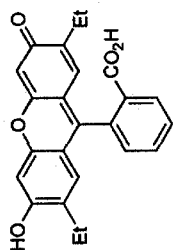
Proton NMR, 400 MHz
CDCl₃



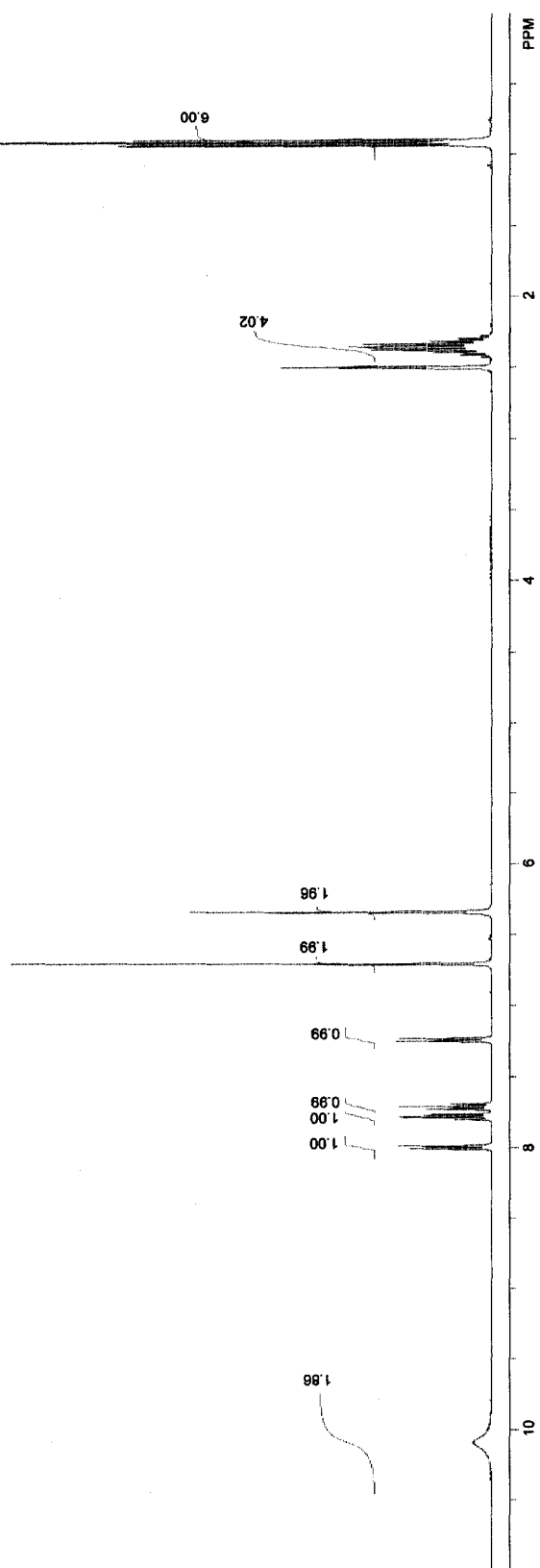
Carbon-13 NMR, 100 MHz
CDCl₃



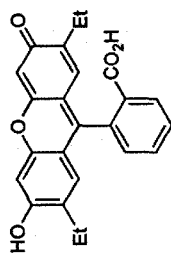
6.7



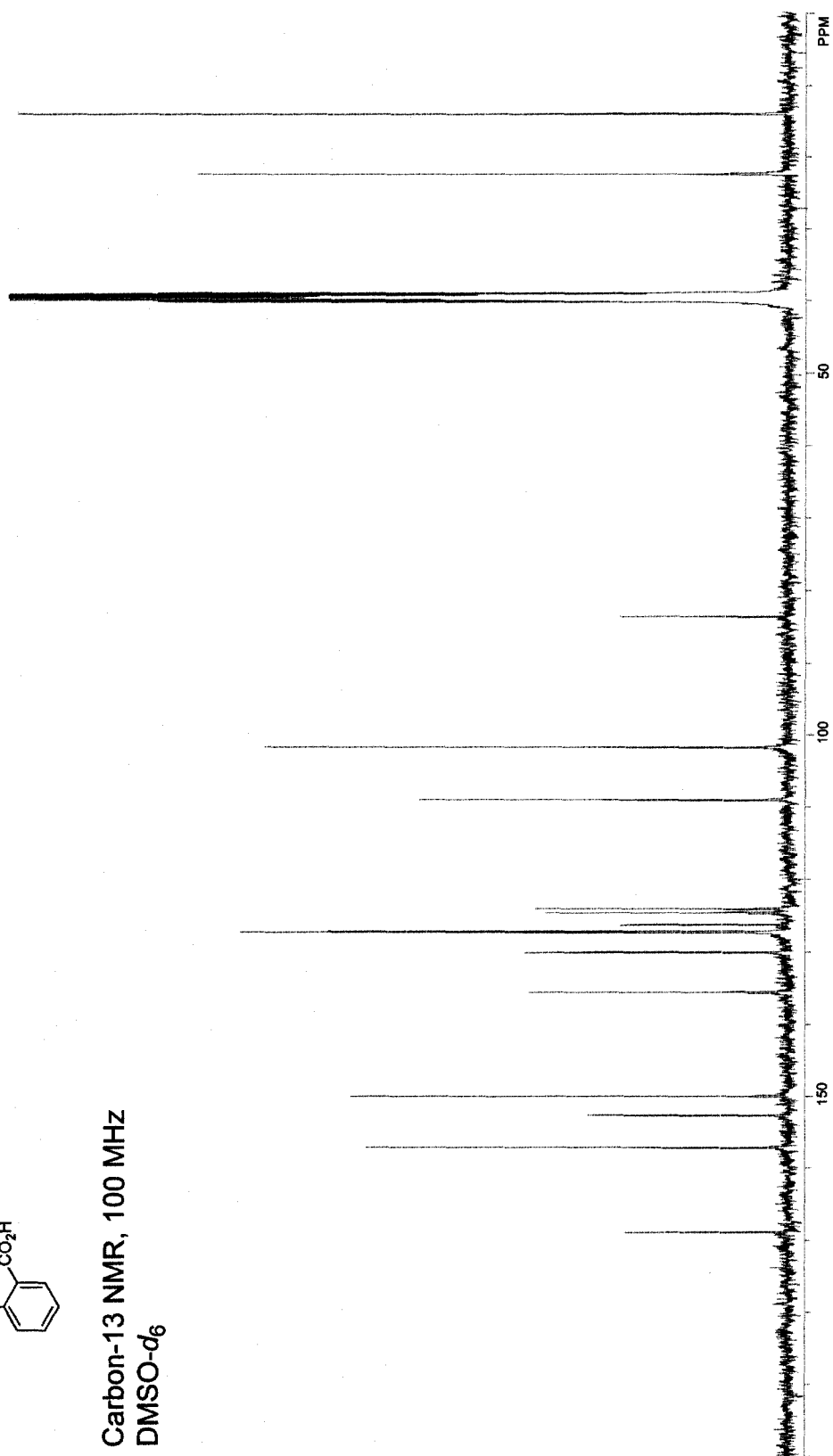
Proton NMR, 400 MHz
DMSO- d_6

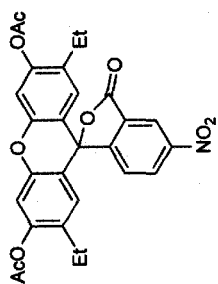


6.7

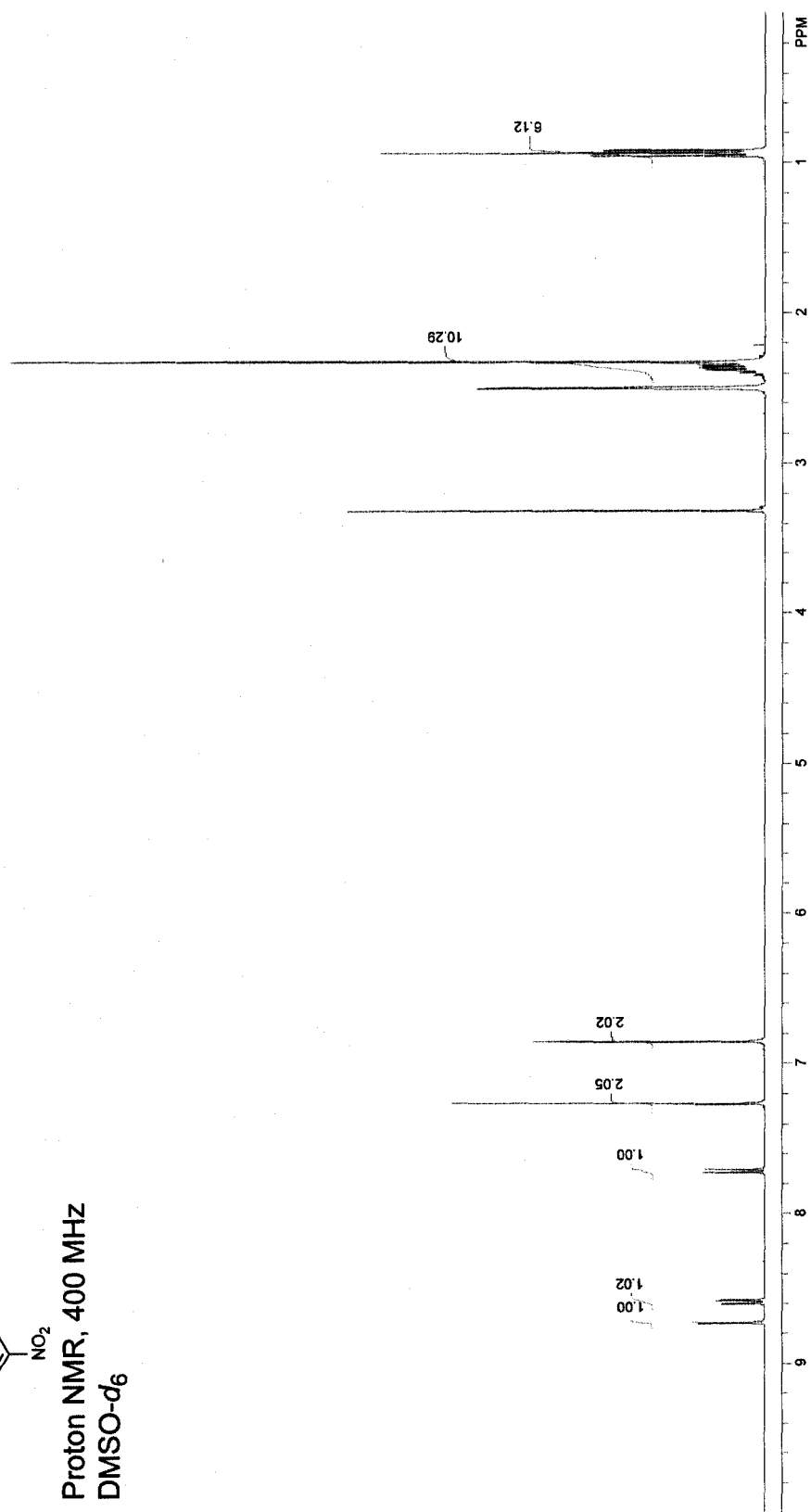


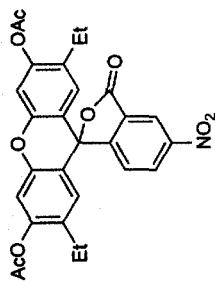
Carbon-13 NMR, 100 MHz
DMSO- d_6



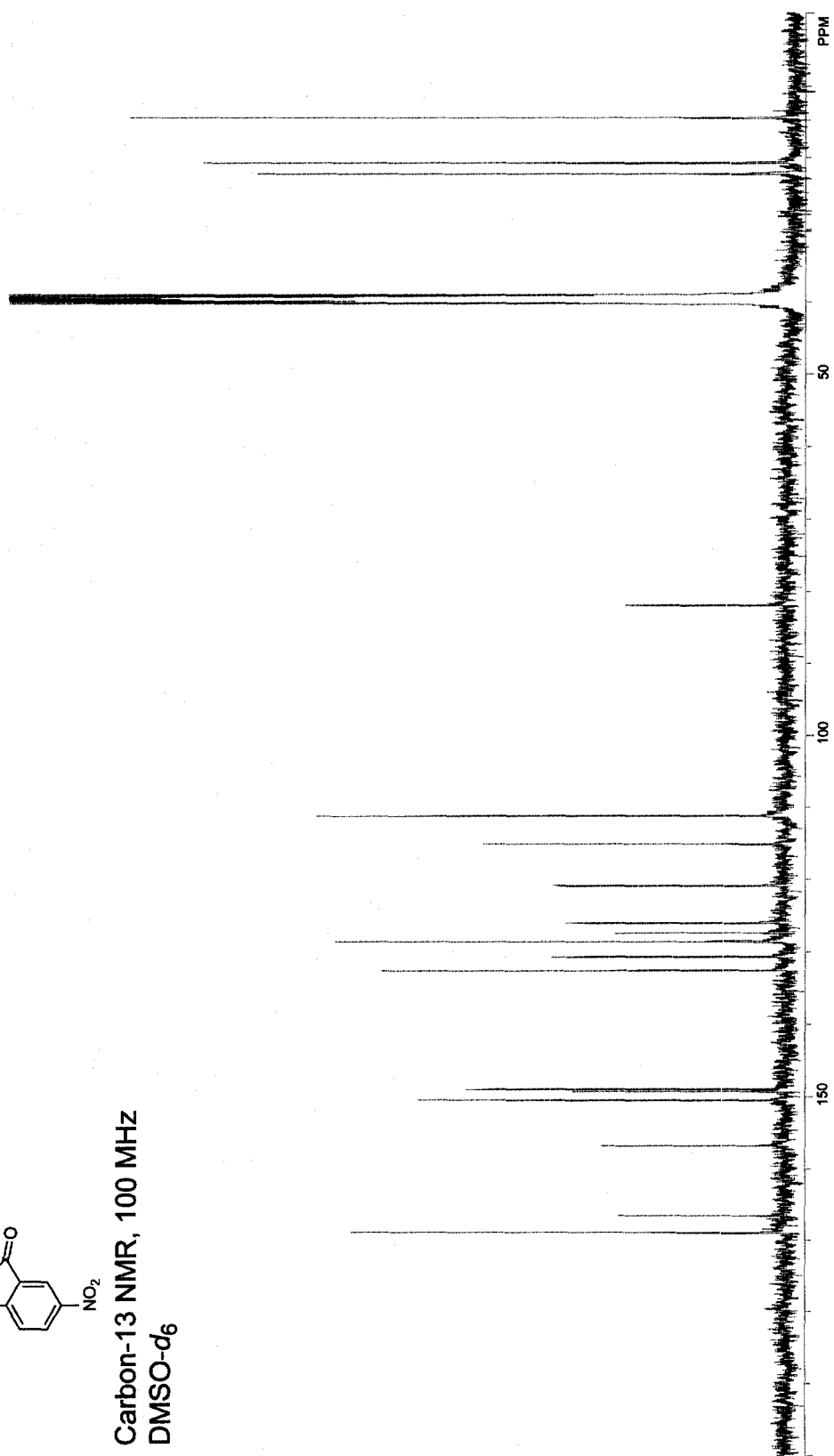
6.10

Proton NMR, 400 MHz
DMSO-*d*₆

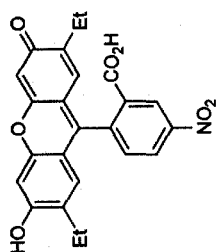


6.10

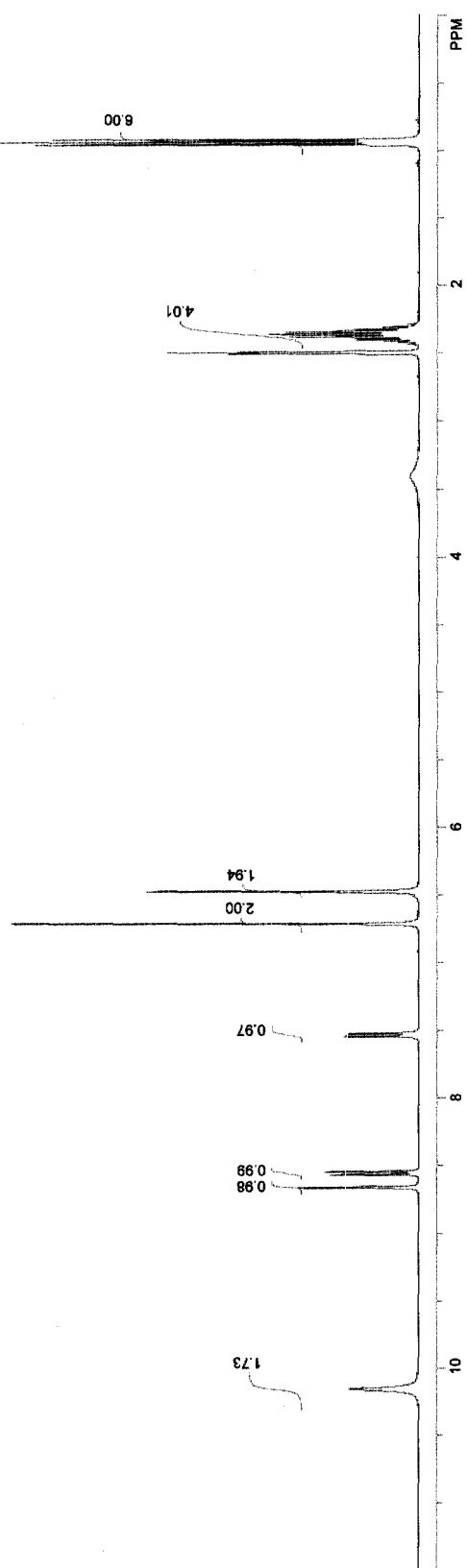
Carbon-13 NMR, 100 MHz
DMSO-*d*₆



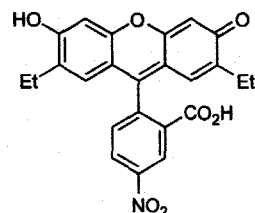
6.11



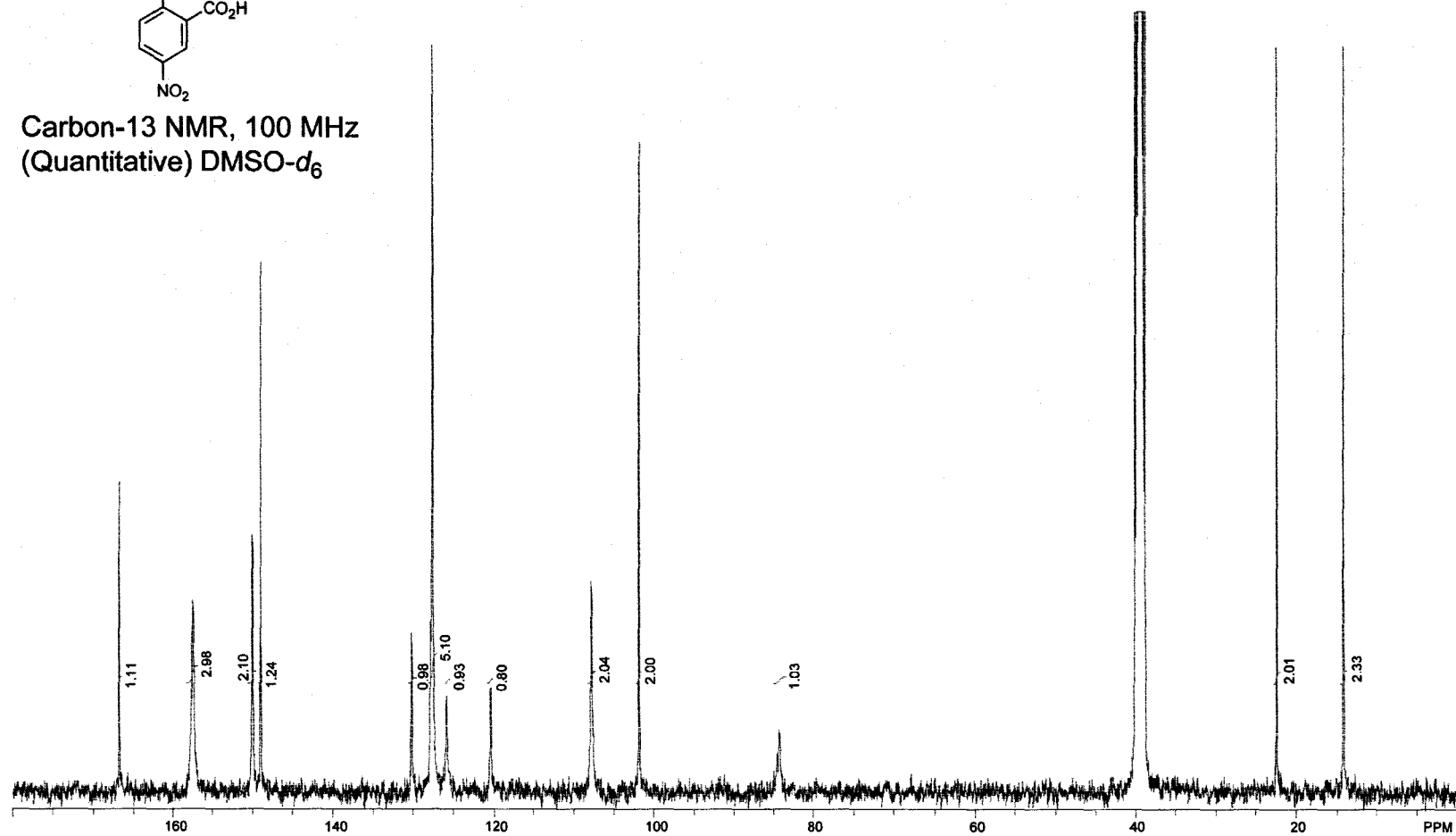
Proton NMR, 400 MHz
DMSO- d_6



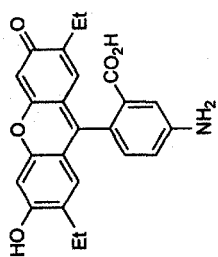
6.11



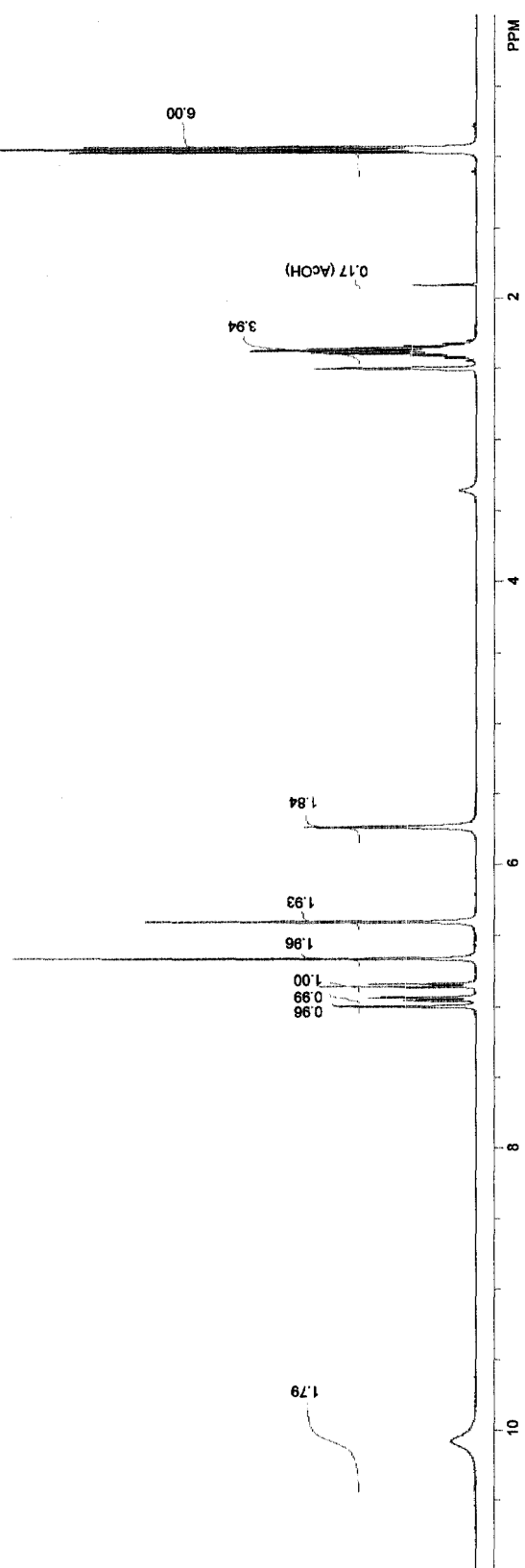
Carbon-13 NMR, 100 MHz
(Quantitative) DMSO-*d*₆

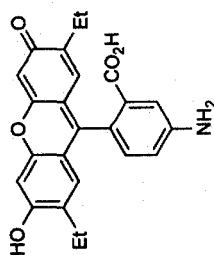


6.12

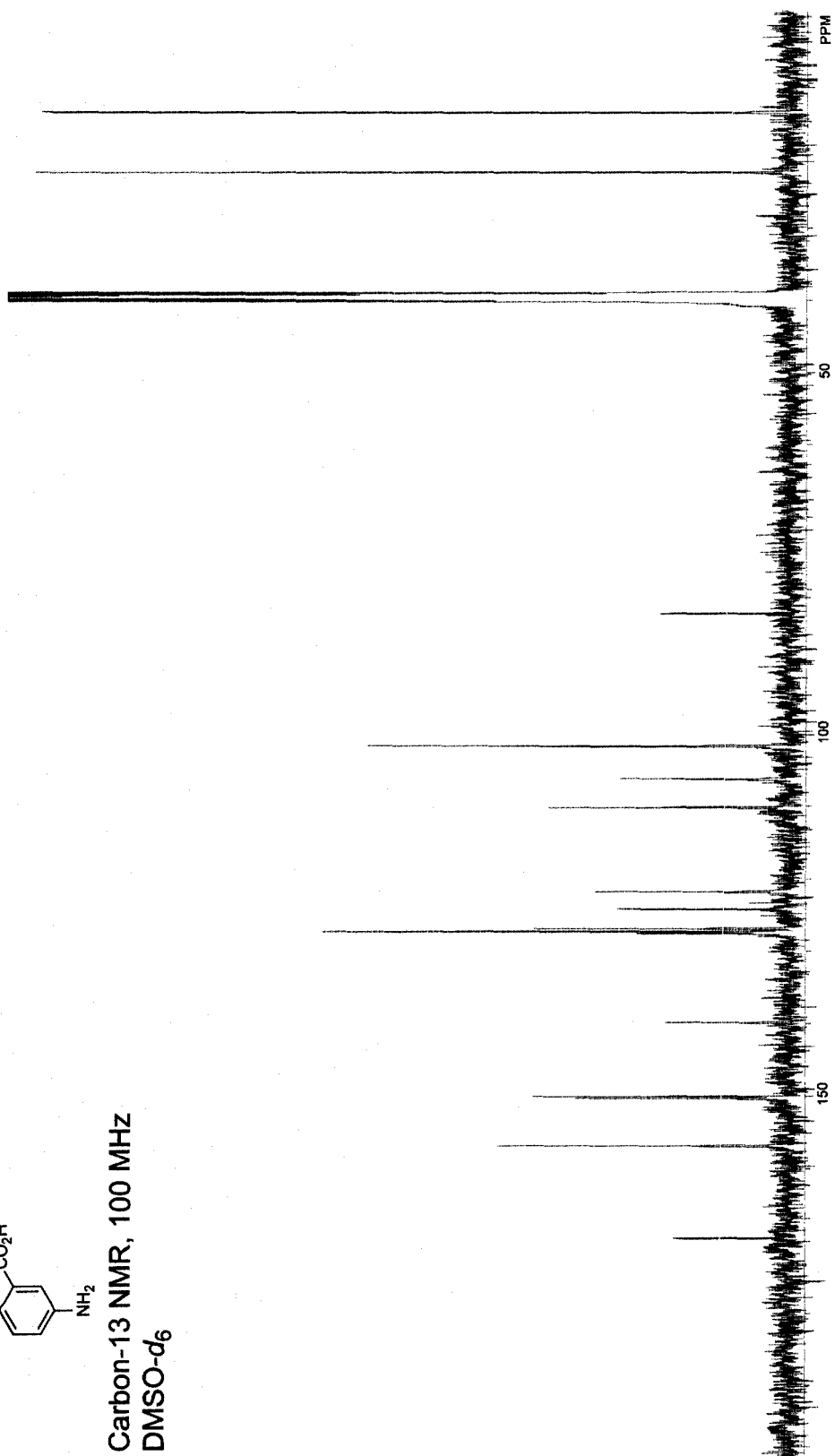


Proton NMR, 400 MHz
DMSO- d_6

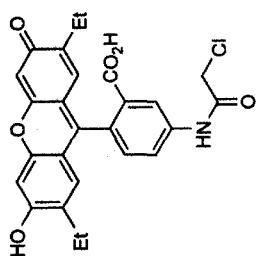




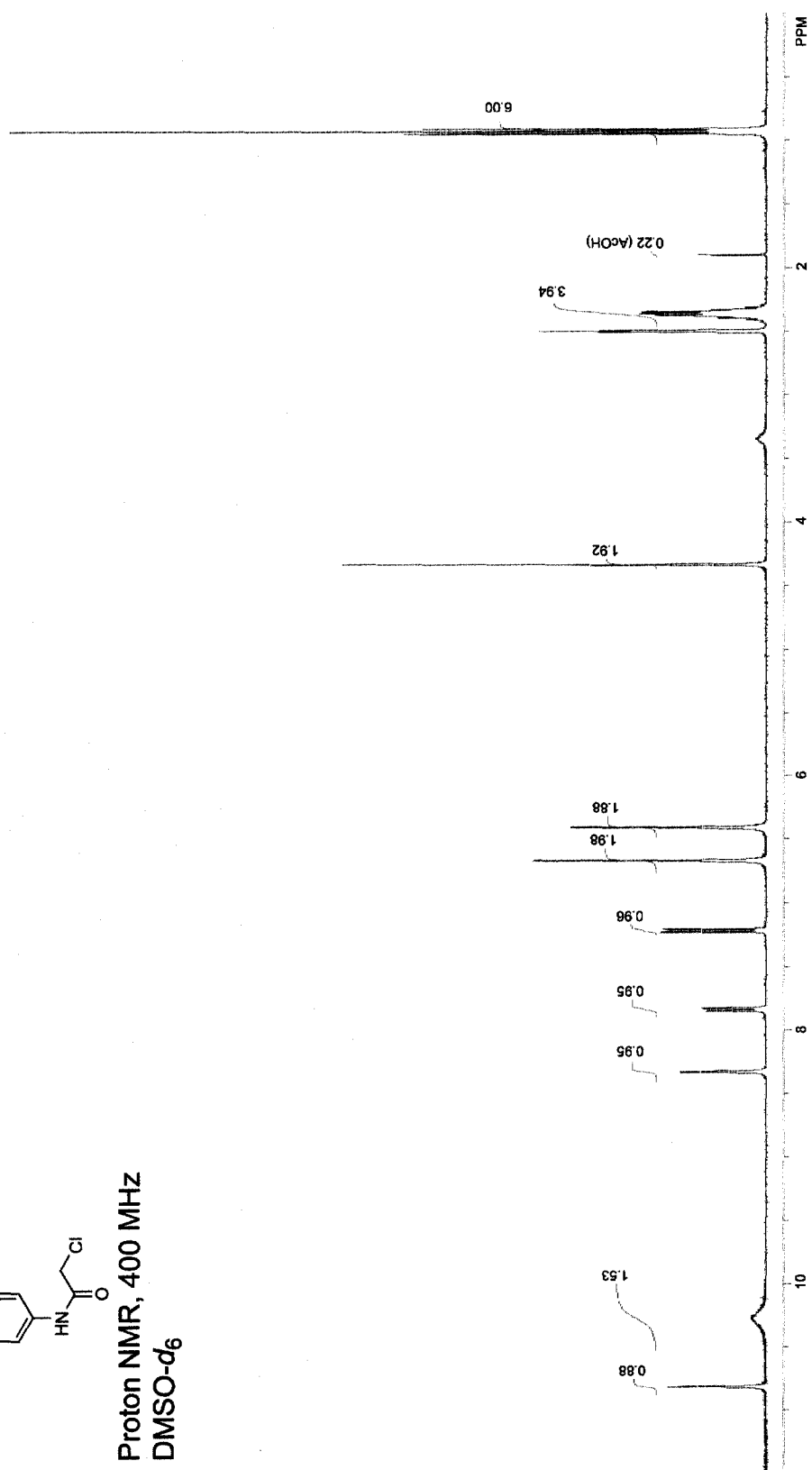
Carbon-13 NMR, 100 MHz
DMSO-*d*₆

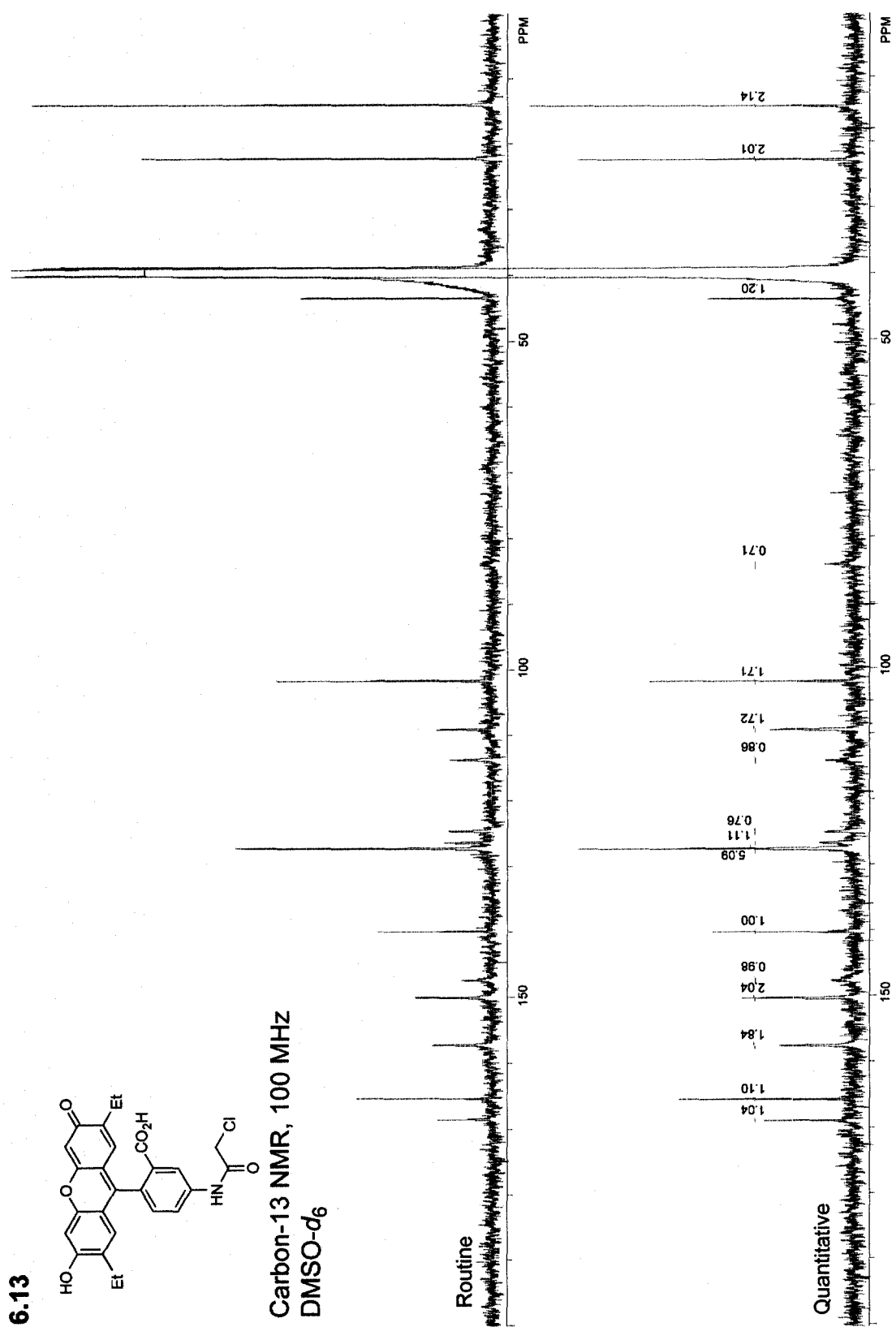


6.13

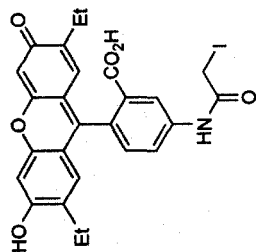


Proton NMR, 400 MHz
DMSO- d_6

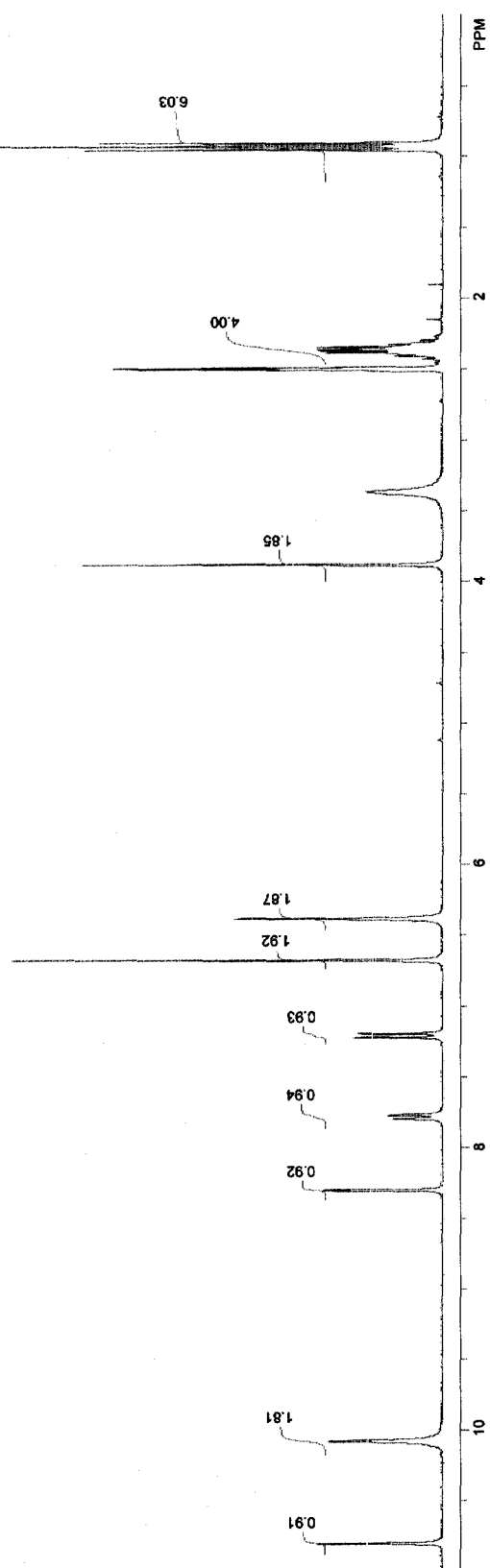


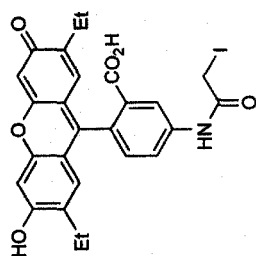


6.14

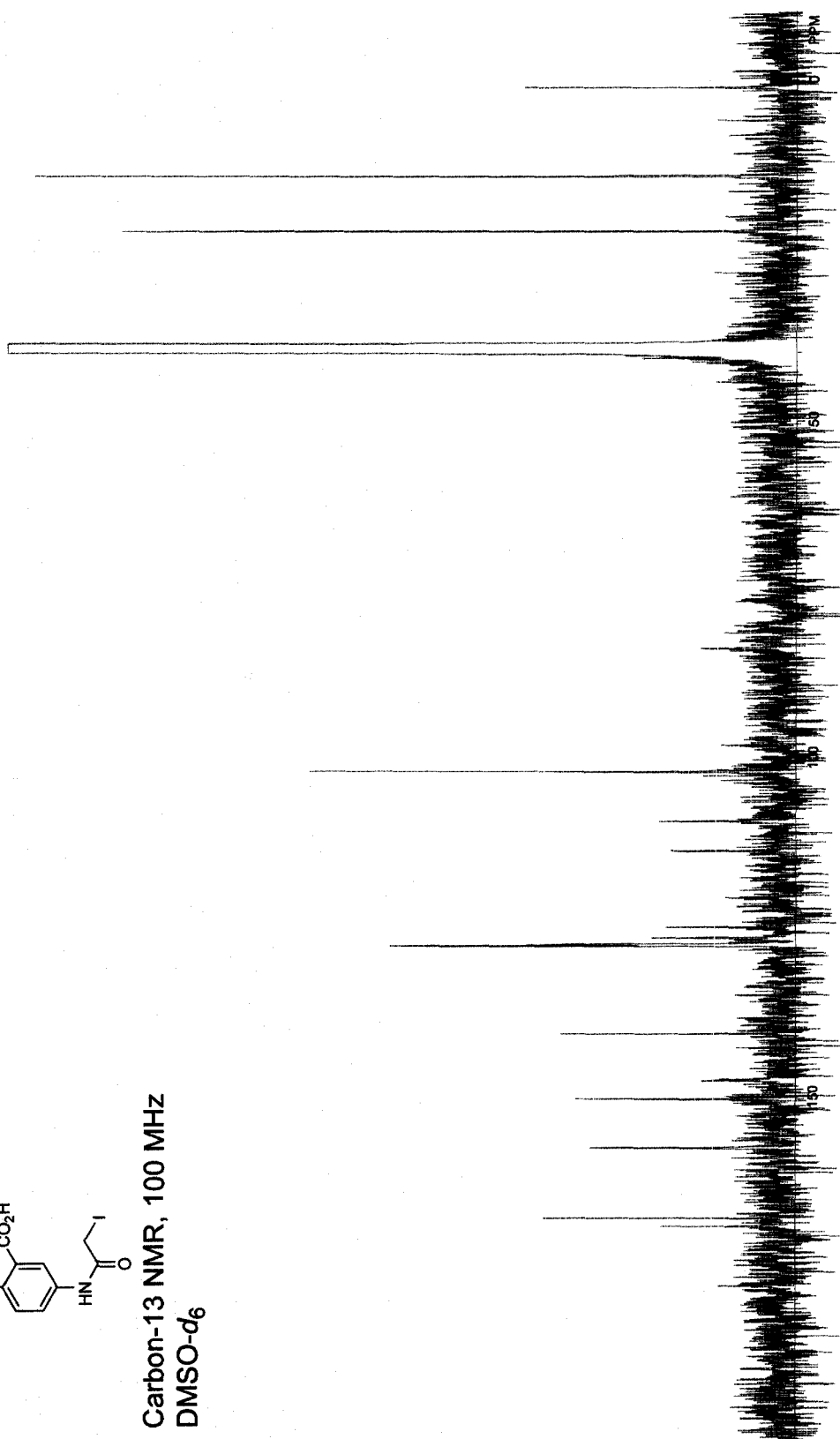


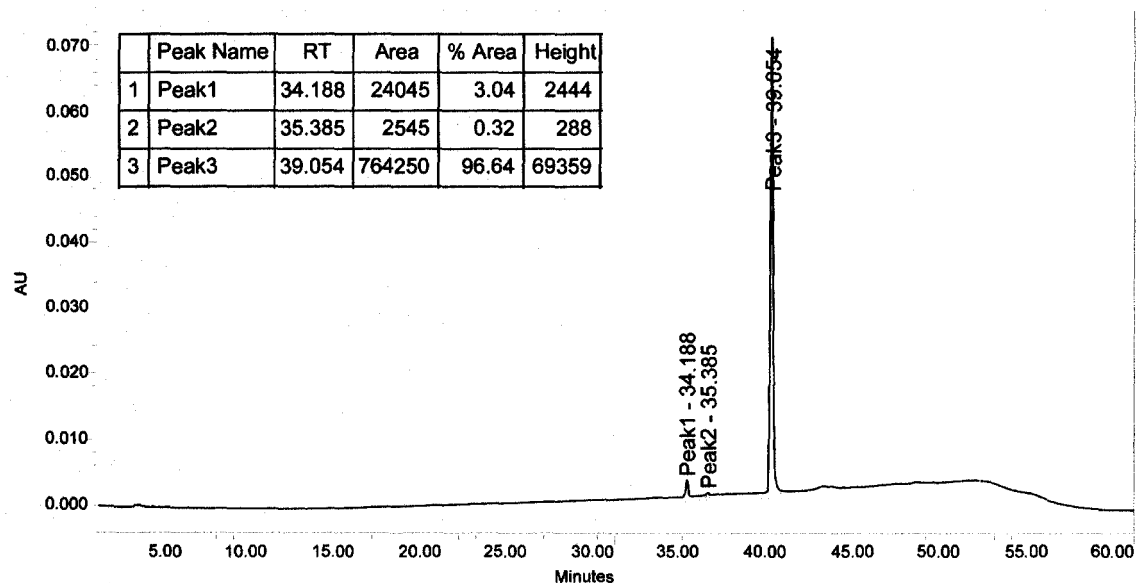
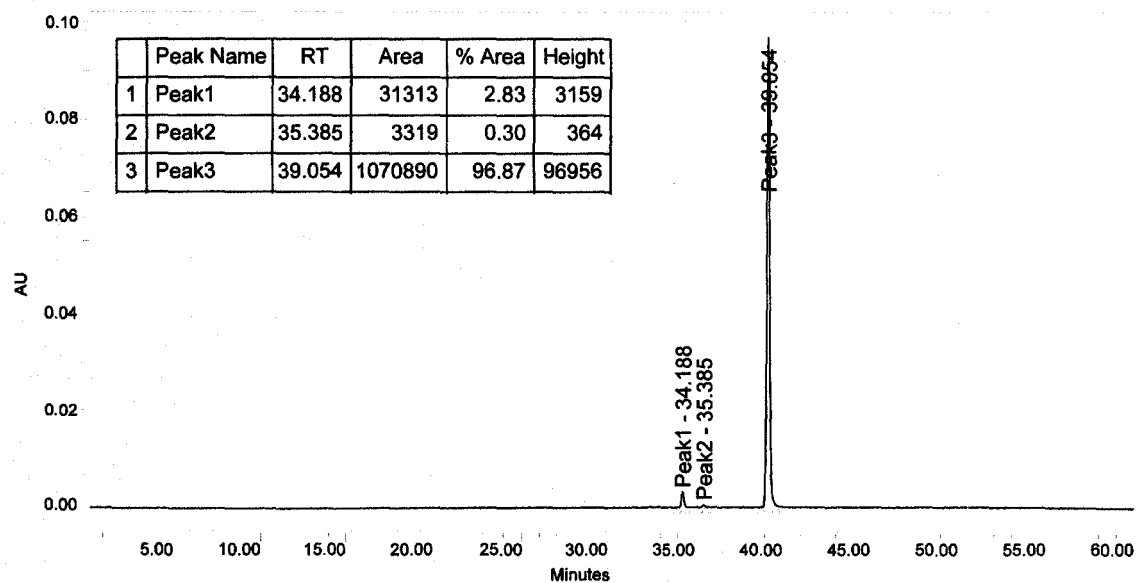
Proton NMR, 400 MHz
DMSO- d_6



6.14

Carbon-13 NMR, 100 MHz
DMSO- d_6



HPLC chromatogram for compound **6.14** ($\lambda = 254$ nm)HPLC chromatogram for compound **6.14** ($\lambda = 449$ nm)

CHAPTER 7

FUTURE DIRECTIONS

7.1 Latent Fluorophores Based on the Trimethyl Lock

In Chapters 2 and 3 (Lavis *et al.*, 2006a; Lavis *et al.*, 2006b) we described the construction of “profluorophores” based on the trimethyl lock (TML) prodrug strategy. The inherent modularity of the trimethyl lock system was exploited to mask fluorophores with different spectral characteristics and chemical functionalities (e.g., compounds **2.2**, **2.4**, and **3.8**). In these studies, the substrate moiety attached to the TML remained invariant as an acetate ester. Opportunities remain to “swap out” the substrate moiety with other functionalities to prepare substrates that are unmasked by different enzymes.

Work has already begun on phosphoryl-containing TML profluorophores, which show good chemical stability compared to analogous fluorescein-based phosphatase substrates (M.N. Levine). Incorporation of ethers is another avenue under exploration. Methoxy- and ethoxy-substituted trimethyl lock fluorophores show good reactivity with cytochrome P450 enzymes *in vitro* and can show induction of enzyme activity *in cellulo* (M. Yatzeck; T.-Y. Chao; L.D. Lavis). Attachment of a cephalosporin moiety to the trimethyl lock is being pursued (M.N. Levine; L.D. Lavis) and could provide a truly bioorthogonal fluorogenic label (*vide infra*). Incorporation of sulfate groups, although difficult, could also yield useful substrates for arylsulfatase enzymes (T. Baumann; L.D. Lavis). These ether- and sulfate-containing substrates represent an extension of the trimethyl lock beyond the systems explored in the prodrug literature, perhaps inspiring new uses of this system to mask and deliver drugs.

Another module that can be explored is the reactive group in compound **3.13**. We utilized the thiol-reactive maleimide group to allow efficient and site-specific coupling to thiol-containing protein variants. The incorporation of the urea moiety into the rhodamine

dye utilizes a Curtius rearrangement that begins ultimately from a simple carboxylic acid. This synthetic route can therefore be used to prepare urea–rhodamines with disparate chemical functionalities. Carboxylic acid-containing urea groups have been constructed to prepare amine-reactive fluorogenic labels (L.D. Lavis; V. Kung). In addition, the Kiessling group (University of Wisconsin–Madison) has used this synthetic strategy to prepare alkyne-containing fluorogenic labels that can be ligated to azide-containing multivalent polymers via the Huisgen 1,3-dipolar cycloaddition. A variety of different chemical functionalities could be incorporated into this fluorogenic label system and our modular synthetic route could facilitate the preparation of these compounds.

7.2 Bioorthogonal Fluorogenic Labels

The fluorogenic label unmasked by β -galactosidase (compound **4.2**) showed promising initial results, but did not allow rigorous quantitative assessment due to high fluorescence background resulting from native glycohydrolase activity in the endosomal/lysosomal pathway. A redeeming feature of this label is its hydrophilicity due to the numerous hydroxyl groups. Thus, label **4.2** could be useful for measuring the biomolecular trafficking of smaller molecules to the cytosol where a lipophilic fluorogenic label such as compound **3.13** could affect greatly the molecular character of the conjugate. In addition, monomeric β -galactosidase constructs could provide more efficient unmasking of a fluorogenic label conjugate.

Fluorogenic labels unmasked by different enzymes could also alleviate background problems. In particular, fluorogenic labels that are unmasked by β -lactamase could be very useful for examining the translocation of ribonucleases into the cytosol (*vide supra*).

Even with such advances, however, the measurement of cytosolic ribonucleases via a fluorogenic label strategy remains difficult. For example, translocation from the endosome to the cytosol with an efficiency of 1% will negate an increase in fluorescence intensity of two orders of magnitude. The best fluorogenic substrates exhibit $\sim 10^3$ increases in fluorescence intensity. Thus, in a flow cytometry experiment, we expect a simple fluorogenic label would give ~ 10 -fold increase in fluorescence intensity under ideal circumstances. Additional strategies might be required to attain good measurements of the translocation of ribonuclease variants with low background. For example, one could express a fluorescent protein–RI fusion and utilize FRET to distinguish labeled ribonucleases in the cytosol. Alternatively, a fluorogenic label could be designed that better exploits the difference in pH or redox potential between the endosomal/lysosomal pathway and the cytosol, thereby bolstering the change in fluorescence resulting from enzyme activity.

7.3 Fluorophore Acetoxymethyl (AM) Ethers

Additional work is required to improve the syntheses of AM ethers. A comprehensive examination of the promising experimental conditions would identify the most efficient synthetic route to the AM ethers of each fluorophore. In addition to completing the *in vitro* enzyme assays, the utility of these fluorophores in cell proliferation assays should be examined. In particular, compound **5.12** could be used in multicolor imaging to stain the cytosol.

Another interesting set of compounds would be the AM ether of resazurin, the *N*-oxide of resorufin. This profluorophore could be prepared using phase-transfer

conditions. 4-Carboxyresazurin, an intermediate in the published synthesis of **5.11**, could also succumb to these reaction conditions. These probes could also be interesting dyes in cell proliferation assays as simple resazurin is used extensively to measure cell number (O'Brien *et al.*, 2000). The AM ether derivatives could allow the use of lower concentrations and furnish lower fluorescence background.

7.4 Tuning the pK_a of Fluorophore Labels

The synthesis of DEFIA (**6.14**; (Lavis *et al.*, 2007)) showcased the effect of “tuning” the pK_a of a fluorophore label to improve the dynamic range of a binding assay. This assay has been improved further by changing the position of the label and by synthesizing pH-sensitive resorufin-based labels (G.A. Ellis; L.D. Lavis; T.J. Rutkoski). Opportunities remain to improve this assay by using dyes that exhibit different excitation and/or emission wavelengths depending on the protonation state of the dye (Liu *et al.*, 2001; Shynkar *et al.*, 2007). This would allow ratiometric measurement of protein–protein interactions perhaps resulting in greater dynamic range and better behavior in high-throughput screening assays. Overall, the concept of tuning would remain essential, as adjustments to the pK_a of such dyes would be necessary to optimize the assay.

APPENDIX A

FLUOROGENIC HISTONE DEACETYLASE SUBSTRATES WITH IMPROVED SPECIFICITY

Contribution: Design and synthesis of compounds in collaboration with B.C. Smith (Denu laboratory, Biomolecular Chemistry, UW–Madison).

A.1 Introduction

Histone deacetylases (HDACs) are currently of great interest due to the role of lysine acetylation/deacetylation in protein function (Kouzarides, 2000; Glozak *et al.*, 2005). Inhibition of these enzymes has proven useful in the treatment of cancer (Marks and Breslow, 2007; Piekarz *et al.*, 2007) and could provide relief from many other diseases, including diabetes and neurological disorders (Butler and Bates, 2006; Haigis and Guarente, 2006). The ongoing search for inhibitors of deacetylase activity in both the academic and industrial sector could benefit from the development of improved and class-specific fluorogenic substrates for these enzymes.

Current fluorogenic substrates for deacetylases employ 7-amino-4-methylcoumarin. This dye exhibits UV excitation ($\lambda_{\text{ex}} = 351 \text{ nm}$) and emission in the blue region of the spectrum ($\lambda_{\text{em}} = 430 \text{ nm}$). Useful protease substrates can be constructed from this fluorophore (Morita *et al.*, 1977; Zimmerman *et al.*, 1977). Such compounds rely on the hypsochromic shift in absorption and emission wavelengths and decrease in quantum yield upon amidation of the aniline moiety. This protease assay has elaborated to measure deacetylase activity as shown in Figure A.1 (Wegener *et al.*, 2003). Here, an acetylated peptide-AMC molecule is first subjected to a deacetylase where enzymatic activity results in free lysine side chains. The substrate is then “developed” by adding trypsin, which cleaves preferentially after the deacetylated lysine. Thus, fluorescence intensity correlates with deacetylase activity, albeit in a discontinuous fashion.

The deacetylase enzymes are divided into classes I–IV based on sequence homology. These enzymes can also be segregated by deacetylation mechanism (Hodawadekar and Marmorstein, 2007) as shown in Figure A.2. With the class I, II, and IV HDAC enzymes,

the carbonyl group of the acetylated lysine acts as an electrophile. These enzymes utilize a mechanism analogous to a metalloprotease where an active-site Zn^{2+} mediates attack of a water molecule on the amide leading to hydrolysis. In contrast, the class III HDAC enzymes, called “sirtuins” due to homology to the yeast Sir2 protein, employ different chemistry where the acetylated lysine is a nucleophile. Here, the oxygen of the carbonyl carbon attacks NAD^+ to give an alkylamidate intermediate that decomposes ultimately to the free lysine residue and an acetylated ADP ribose (Smith and Denu, 2007).

These disparate chemical mechanisms make possible the creation of class-specific enzyme substrates by attenuating the electronic character of the acetyl carbonyl group (Smith and Denu, 2007). Electron-poor, electrophilic carbonyl groups favor nucleophilic attack by water, making them excellent substrates for some class I, II, and IV HDACs. In contrast, electron-rich carbonyl groups could better attack NAD^+ and prove superior substrates for the sirtuins (*i.e.*, class III HDACs).

Here, we undertook the syntheses of novel fluorogenic substrate cores for deacetylases based on the fluorophore AMC and different acetylated lysine analogues. With the synthesis of these compounds, we are poised to test the activity of different HDACs with various acetylated lysine mimics, the end goal being the discovery of class-specific substrate motifs. Further derivatization and evaluation in bioassays will be performed in collaboration with Brian Smith in the laboratory of John Denu (Biomolecular Chemistry, UW–Madison).

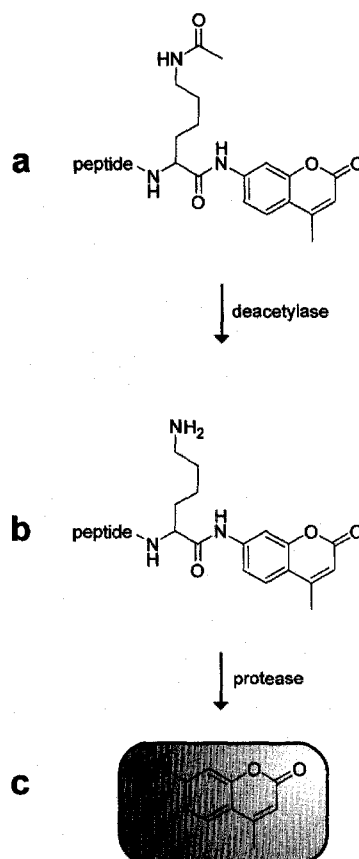


Figure A.1 Fluorescent histone deacetylase assay. (a) Peptide-AMC derivative exhibits low fluorescence. (b) Incubation of substrate with deacetylase-containing sample removes acetyl group. (c) Treatment with protease cleaves amide bond in deacetylated substrate, releasing AMC fluorophore.

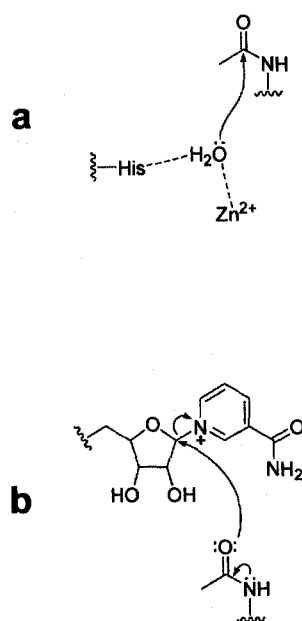


Figure A.2 Disparate histone deacetylase mechanisms. (a) Class I, II, and IV HDACs: Zn²⁺-Activation of a water molecule. (b) Class III HDACs (sirtuins): Attack of acetyl oxygen on NAD⁺ to form alkylamidate intermediate.

A.2 Results and Discussion

We prepared the acetylated lysine analogue–AMC derivatives **A.8–A.13** as shown in Scheme A.1. The synthesis was effected by simple incubation of Boc-protected lysine analogue with AMC (**A.1**) in the presence of Boc₂O and pyridine in anhydrous THF (Hamze *et al.*, 2004). In particular, this route proved useful for synthesis of the Fmoc–lysine–AMC derivative **A.13**. This compound was prepared to allow further elaboration to other acetylated lysine analogues. Overall, this facile synthesis gave the desired compounds in moderate yields.

A.3 Conclusions and Future Directions

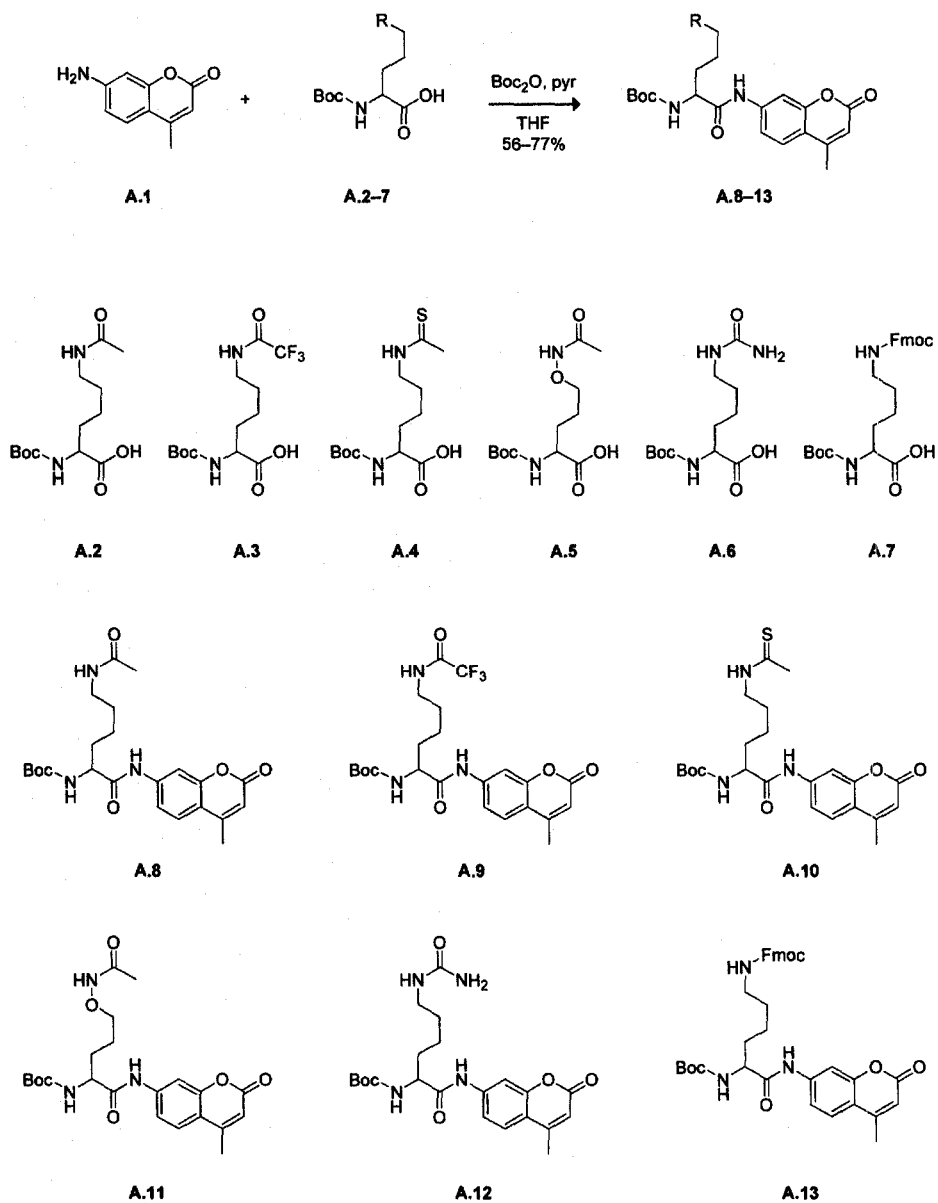
The synthesis of substrate cores **A.8–A.13** proved simple and should allow the construction of a variety of fluorogenic substrates for assaying HDAC activity. The resulting peptide–AMC substrates can be screened against available HDAC isoforms to test for specificity among the different classes of this important enzyme.

In addition to AMC-based substrates, other fluorophores could be used in this strategy. For example, rhodamine 110-based substrates can also be used as HDAC substrates in similar fashion to the AMC derivatives (Borra *et al.*, 2005). We propose that oxazine dyes displaying red-shifted wavelengths could also be used in this assay, based on their utility in protease substrates (Boonacker *et al.*, 2003). After identification of selective substrate motifs using the simple AMC derivatives, the same peptide sequences and acetylated lysine analogues could be incorporated into these longer-wavelength fluorophores. Such compounds could allow simultaneous measurement of multiple

HDACs in the same assay. Overall, these compounds should facilitate the high-throughput measurement of HDAC activity.

A.4 Acknowledgements

We are grateful to Brian Smith for the lysine analogues **A.4** and **A.5**. L.D.L was supported by Biotechnology Training Grant 08349 (NIH) and an ACS Division of Organic Chemistry Fellowship sponsored by the Genentech Foundation. This work was supported by grant CA73808 (NIH). NMRFAM was supported by grant P41 RR02301 (NIH).

Scheme A.1 Synthesis of intermediates **A.8–13**

A.5 Experimental Section

A.5.1 General Experimental

7-Amino-4-methylcoumarin (AMC; **A.1**; i.e., coumarin 440) was from Exciton (Dayton, OH). Amino acid derivatives **A.4** and **A.5** were a generous gift from B. Smith and J. Denu (University of Wisconsin–Madison). Other lysine derivatives were purchased from Chem-Impex (Wood Dale, IL) or EMD Chemicals (Novabiochem, San Diego, CA). Dimethylformamide (DMF), tetrahydrofuran (THF), and dichloromethane (CH_2Cl_2) were drawn from a Baker CYCLE-TAINER solvent delivery system. All other reagents were obtained from Aldrich Chemical (Milwaukee, WI) or Fisher Scientific (Hanover Park, IL) and used without further purification.

Thin-layer chromatography was performed using aluminum-backed plates coated with silica gel containing F_{254} phosphor and visualized by UV illumination or staining with I_2 , ceric ammonium molybdate, or phosphomolybdic acid. Flash chromatography was performed by using open columns loaded with silica gel-60 (230–400 mesh), or on a FlashMaster Solo system (Argonaut Inc., Redwood City, CA) with Isolute Flash Si II columns (International Sorbent Technology Ltd., Hengoed, Mid Glamorgan, UK). The term “high vacuum” refers to a vacuum (≤ 1 mm Hg) achieved by a mechanical belt-drive oil pump. The term “concentrated under reduced pressure” refers to the removal of solvents and other volatile materials using a rotary evaporator at water-aspirator pressure (< 20 mm Hg) while maintaining the water-bath temperature below 40°C . The term “concentrated under high vacuum” refers to the removal of solvents and other volatile materials using a rotary evaporator at high vacuum while maintaining the water-bath temperature below 40°C .

NMR spectra were obtained with a Bruker DMX-400 Avance spectrometer at the NMR Facility at Madison (NMRFAM). Mass spectrometry was performed with a Micromass LCT (electrospray ionization, ESI) mass spectrometer in the Mass Spectrometry Facility in the Department of Chemistry.

A.5.2 Synthesis of compounds A.8–A.13

Boc-Lys[Ac]-AMC (A.8). AMC (A.1, 30 mg, 0.17 mmol) and Boc-Lys[Ac]-OH (A.2, 41 mg, 0.14 mmol) were dissolved in THF (0.50 mL). Pyridine (12 μ L, 0.14 mmol) was added, followed by Boc₂O (37 mg, 0.17 mmol). The reaction mixture was stirred at ambient temperature for 48 h. The yellow gelatinous mixture was concentrated under reduced pressure and purified column chromatography (silica gel, first column: 50→100% v/v gradient of EtOAc in hexanes, second column: 0→8% v/v gradient of MeOH in CH₂Cl₂). Compound A.8 was isolated as a white solid (44 mg, 69%). ¹H NMR (400 MHz, CDCl₃) δ (ppm): 9.61 (bs, 1H), 7.69 (s, 1H), 7.46 (d, J = 8.8 Hz, 1H), 7.38 (d, J = 7.8 Hz, 1H), 6.14 (bs, 2H), 5.62 (d, J = 7.2 Hz, 1H), 4.35 (bs, 1H), 3.26 (m, 2H), 2.39 (s, 3H), 2.07–1.86 (m, 4H), 1.76 (m, 1H), 1.68–1.32 (m, 13H). HRMS (ESI): m/z 468.2132 (MNa⁺ [C₂₃H₃₁N₃O₆Na] = 468.2111).

Boc-Lys[TFA]-AMC (A.9). AMC (A.1, 50 mg, 0.29 mmol) and Boc-Lys[TFA]-OH (A.3, 82 mg, 0.24 mmol) were dissolved in THF (1.0 mL). Pyridine (19 μ L, 0.24 mmol) was added, followed by Boc₂O (62 mg, 0.29 mmol). The reaction mixture was stirred at ambient temperature for 24 h. The yellow gelatinous mixture was concentrated under reduced pressure and purified by column chromatography (silica gel, 25→50% v/v gradient of EtOAc in hexanes). Compound A.9 was isolated as a white solid (68 mg,

57%). ^1H NMR (400 MHz, acetone- d_6) δ (ppm): 9.67 (bs, 1H), 8.47 (bs, 1H), 7.83 (d, $J = 1.6$ Hz, 1H), 7.69 (d, $J = 8.5$ Hz, 1H), 7.51 (d, $J = 8.4$ Hz, 1H), 6.28 (d, $J = 7.0$ Hz, 1H), 6.18 (d, $J = 1.0$ Hz, 1H), 4.23 (m, 1H), 3.35 (m, 2H), 2.44 (d, $J = 1.2$ Hz, 3H), 1.90 (m, 1H), 1.77 (m, 1H), 1.64 (m, 2H), 1.59–1.32 (m, 11H). HRMS (ESI): m/z 500.2010 (MH^+ [$\text{C}_{23}\text{H}_{29}\text{F}_3\text{N}_3\text{O}_6$] = 500.2008).

Boc-Lys[Thioacetyl]-AMC (A.10). AMC (A.1, 30 mg, 0.17 mmol) and Boc-Lys[Thioacetyl]-OH (A.4, 43 mg, 0.14 mmol) were dissolved in THF (500 μL). Pyridine (12 μL , 0.14 mmol) was added, followed by Boc_2O (37 mg, 0.17 mmol). The reaction mixture was stirred at ambient temperature for 24 h. The reaction mixture was concentrated under reduced pressure and purified by column chromatography (silica gel, 25→75% v/v gradient of EtOAc in hexanes). Compound A.10 was isolated as an off-white solid (36 mg, 56%). ^1H NMR (400 MHz, CDCl_3) δ (ppm): 9.19 (bs, 1H), 7.87 (bs, 1H), 7.70 (s, 1H), 7.48 (d, $J = 8.2$ Hz, 1H), 7.37 (d, $J = 8.2$ Hz, 1H), 6.17 (s, 1H), 5.43 (d, $J = 7.7$ Hz, 1H), 4.35 (m, 1H), 3.69 (m, 2H), 2.55 (s, 3H), 2.40 (s, 3H), 1.96 (m, 1H), 2.05–1.71 (m, 4H), 1.66–1.34 (m, 11H). HRMS (ESI): m/z 484.1898 (MNa^+ [$\text{C}_{23}\text{H}_{31}\text{N}_3\text{O}_5\text{SNa}$] = 484.1882).

Boc-Homocanaline[Ac]-AMC (A.11). AMC (A.1, 30 mg, 0.17 mmol) and Boc-Homocanaline[Ac]-OH (A.5, 41 mg, 0.14 mmol) were dissolved in THF (500 μL). Pyridine (12 μL , 0.14 mmol) was added, followed by Boc_2O (37 mg, 0.17 mmol). The reaction mixture was stirred at ambient temperature for 120 h. The reaction mixture was concentrated under reduced pressure and purified by column chromatography (silica gel, 50→100% v/v gradient of EtOAc in hexanes). Compound A.11 was isolated as an off-white solid (44 mg, 70%). ^1H NMR (400 MHz, CDCl_3) δ (ppm): 9.97 (bs, 1H), 9.07

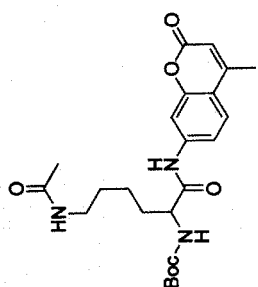
(bs, 1H), 7.74 (d, $J = 8.8$ Hz, 1H), 7.71 (s, 1H), 7.52 (d, $J = 8.7$ Hz, 1H), 6.18 (s, 1H), 5.43 (d, $J = 9.1$ Hz, 1H), 4.70 (m, 1H), 4.16 (m, 1H), 4.05 (m, 1H), 2.41 (s, 3H), 2.29 (m, 1H), 2.00 (s, 3H), 1.78 (m, 3H), 1.45 (s, 9H). HRMS (ESI): m/z 470.1909 (MNa^+ [$\text{C}_{22}\text{H}_{29}\text{N}_3\text{O}_7\text{Na}$] = 470.1903).

Boc-Homocitruline-AMC (A.12). AMC (A.1, 100 mg, 0.57 mmol) and Boc-Homocitruline-OH (A.6, 138 mg, 0.48 mmol) were dissolved in THF (1.0 mL). Pyridine (39 μL , 0.48 mmol) was added, followed by Boc_2O (125 mg, 0.57 mmol). The reaction mixture was stirred at ambient temperature for 24 h. The reaction mixture was concentrated under reduced pressure and purified by column chromatography (silica gel, 0 \rightarrow 10% v/v gradient of MeOH in CH_2Cl_2). Compound A.12 was isolated as an off-white solid (162 mg, 77%). ^1H NMR (400 MHz, $\text{DMSO}-d_6$) δ (ppm): 10.42 (bs, 1H), 7.77 (d, $J = 1.7$ Hz, 1H), 7.72 (d, $J = 8.6$ Hz, 1H), 7.49 (dd, $J = 8.5, 1.0$ Hz, 1H), 7.13 (d, $J = 7.5$ Hz, 1H), 6.26 (s, 1H), 5.91 (t, $J = 5.5$ Hz, 1H), 5.35 (bs, 2H), 4.04 (m, 1H), 2.93 (m, 2H), 2.40 (s, 3H), 1.81–1.29 (m, 15H). HRMS (ESI): m/z 469.2078 (MNa^+ [$\text{C}_{22}\text{H}_{30}\text{N}_4\text{O}_6\text{Na}$] = 469.2063).

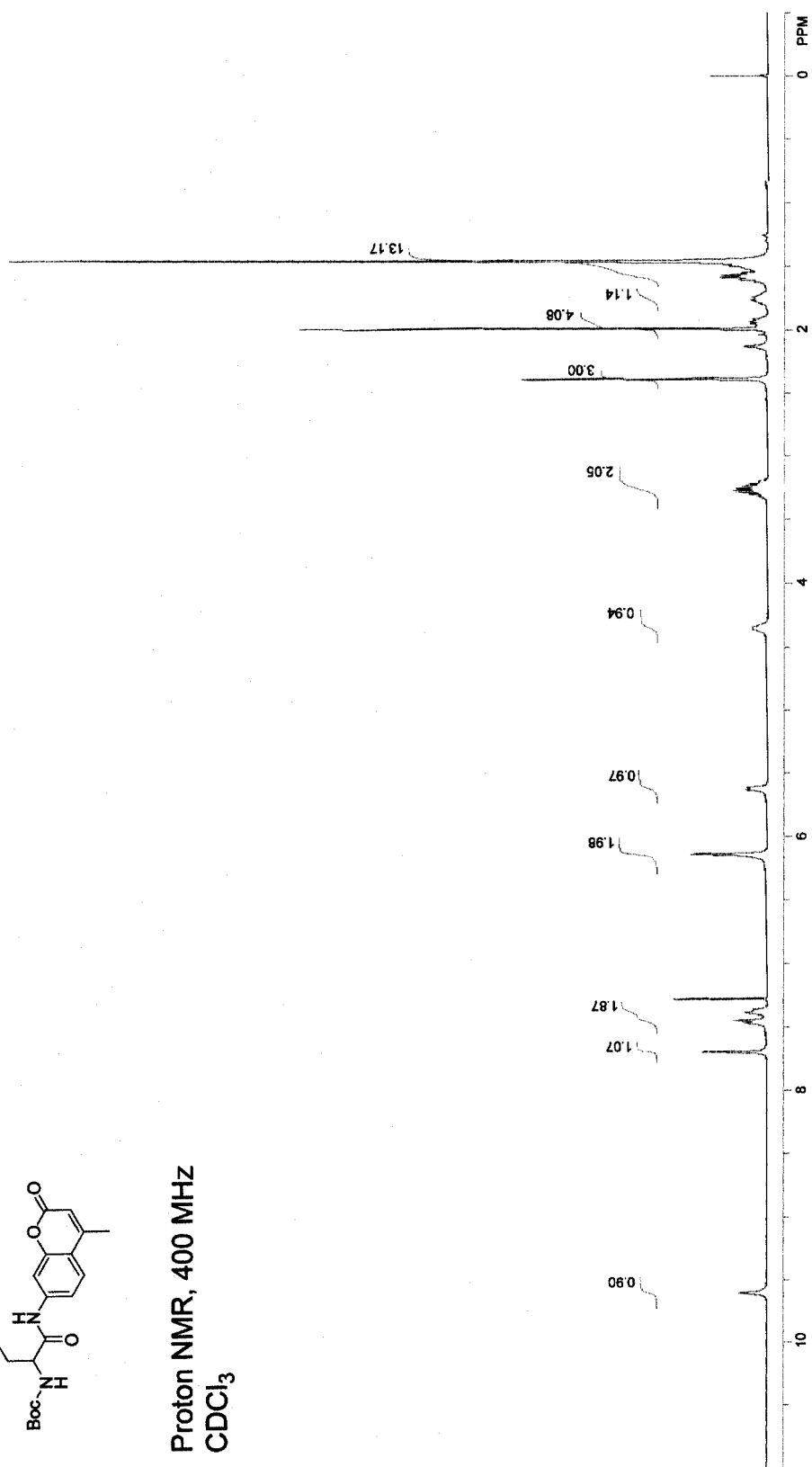
Boc-Lys[Fmoc]-AMC (A.13). AMC (A.1, 30 mg, 0.17 mmol) and Boc-Lys[Fmoc]-OH (A.7, 67 mg, 0.14 mmol) were dissolved in THF (500 μL). Pyridine (12 μL , 0.14 mmol) was added, followed by Boc_2O (37 mg, 0.17 mmol). The reaction mixture was stirred at ambient temperature for 24 h. The reaction mixture was concentrated under reduced pressure and purified by column chromatography (silica gel, 50% v/v EtOAc in hexanes). Compound A.13 was isolated as a white crystalline solid (50 mg, 56%). ^1H NMR (400 MHz, CDCl_3) δ (ppm): 9.29 (bs, 1H), 7.73 (d, $J = 7.7$ Hz, 2H), 7.68 (s, 1H), 7.55 (dd, $J = 7.0, 1.3$ Hz, 2H), 7.34–7.14 (m, 6H), 6.10 (bs, 1H), 5.45 (d, $J = 7.4$ Hz, 1H),

4.98 (m, 1H), 4.51–4.24 (m, 3H), 4.15 (d, $J = 7.1$ Hz, 1H), 3.20 (m, 2H), 2.33 (s, 3H),
1.91 (m, 1H), 1.74 (m, 1H), 1.65–1.34 (m, 13H). HRMS (ESI): m/z 648.2708 (MNa^+
[$\text{C}_{36}\text{H}_{39}\text{N}_3\text{O}_7\text{Na}$] = 648.2686).

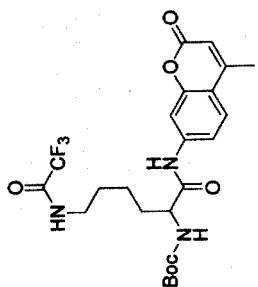
A.8



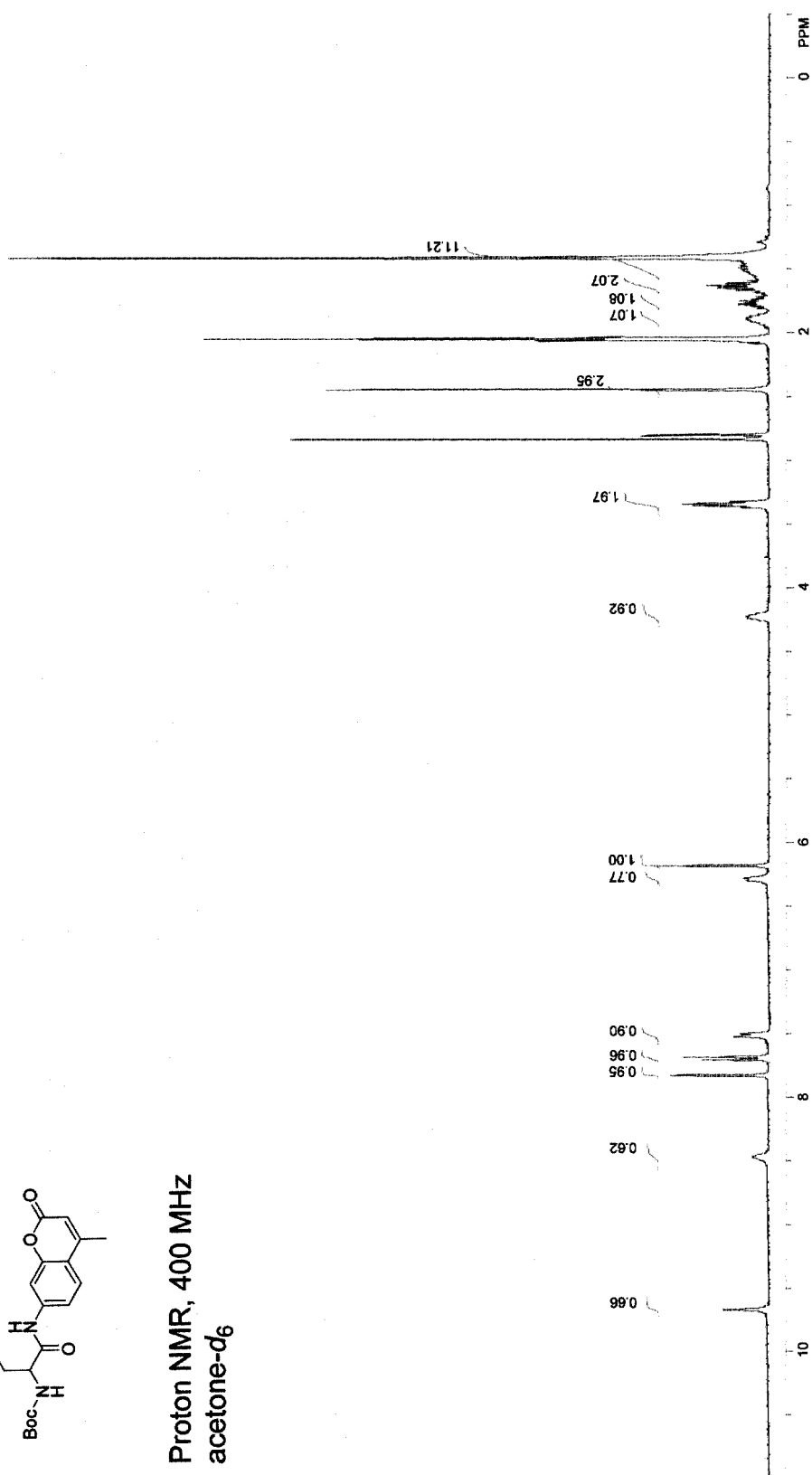
Proton NMR, 400 MHz
CDCl₃



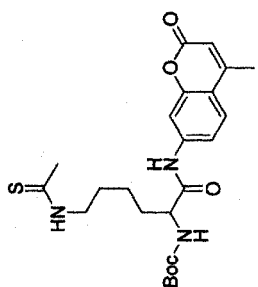
A.9



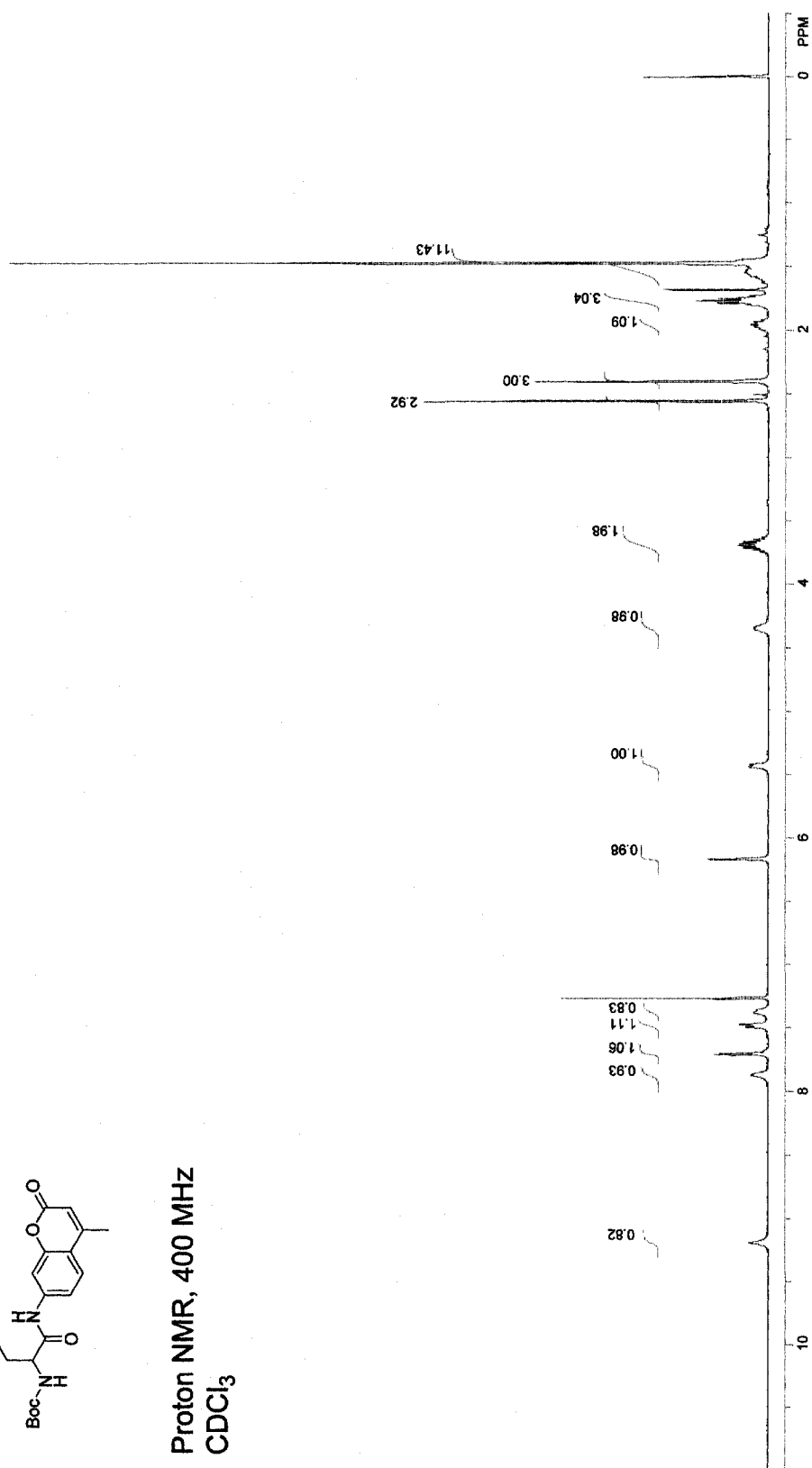
Proton NMR, 400 MHz
acetone-*d*₆

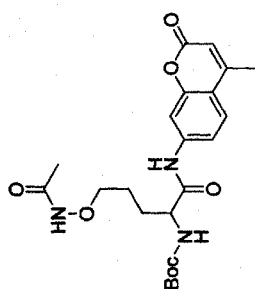


A.10

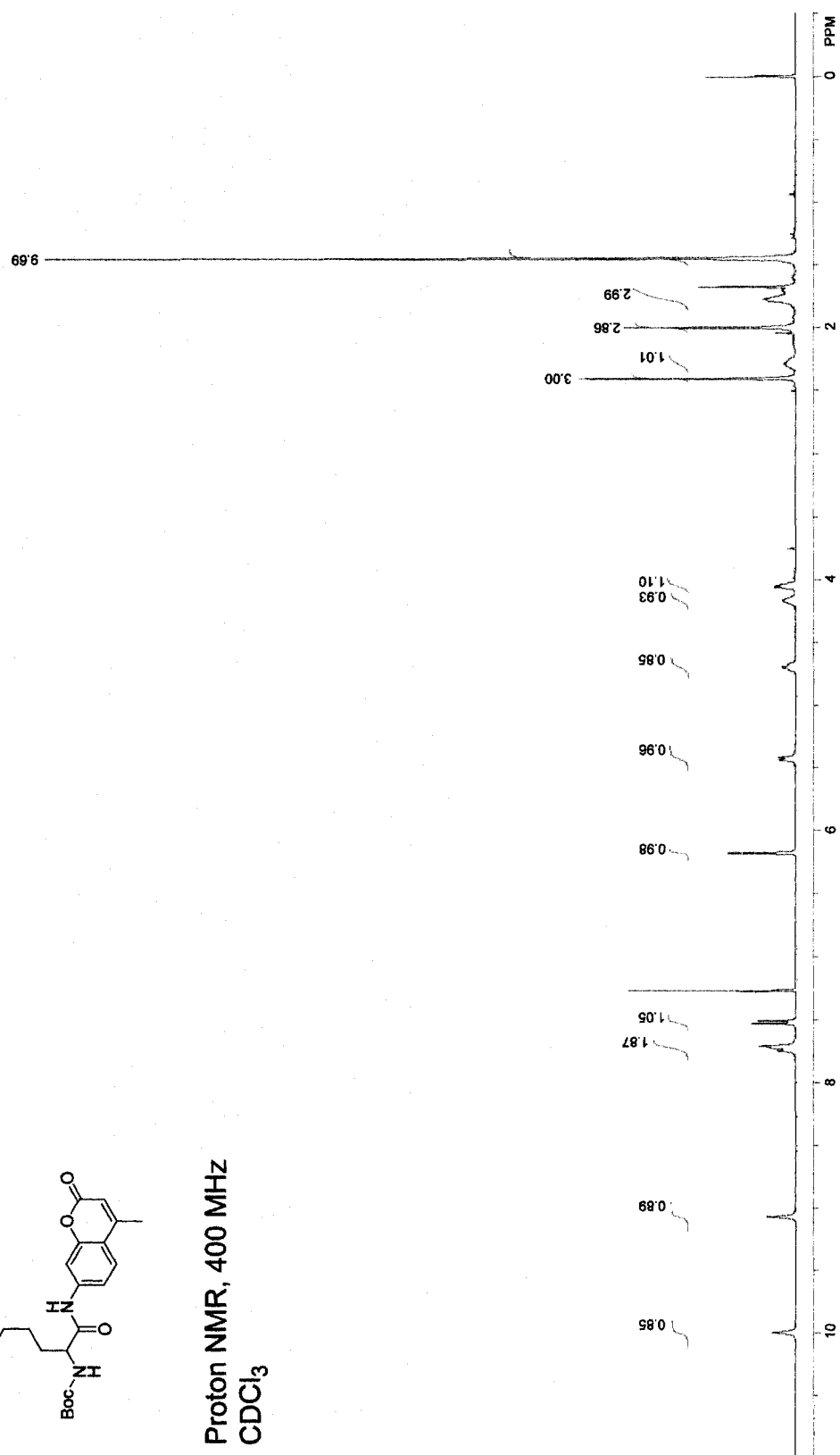


Proton NMR, 400 MHz
CDCl₃

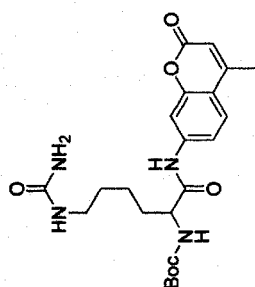


A.11

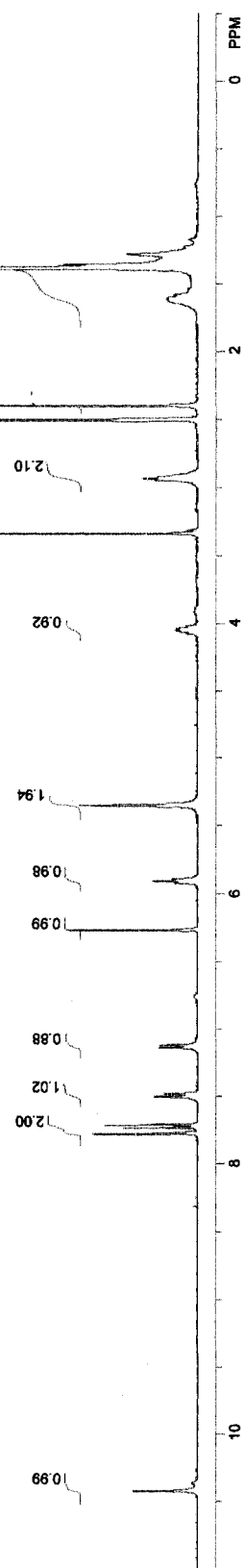
Proton NMR, 400 MHz
CDCl₃



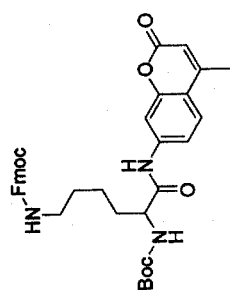
A.12



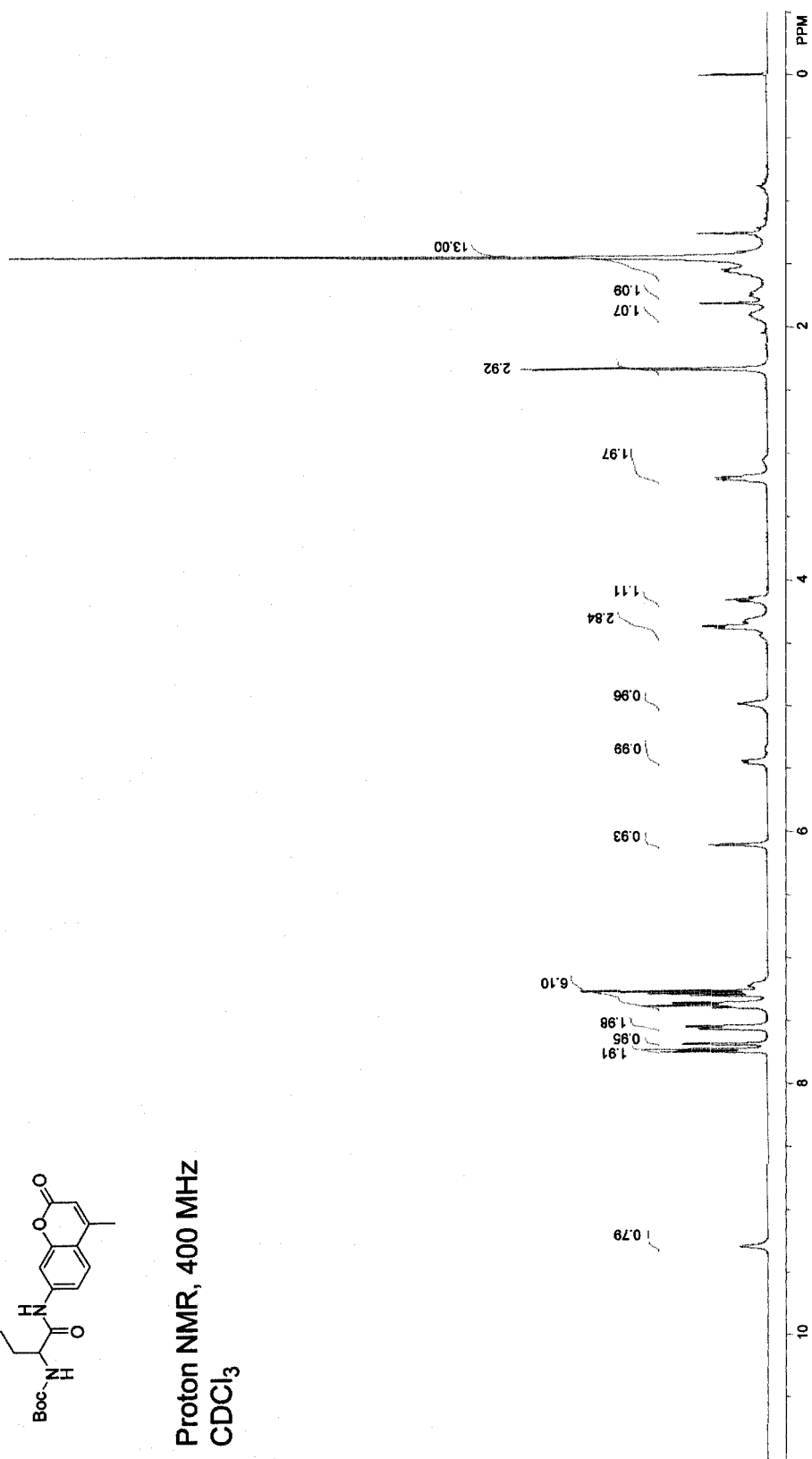
Proton NMR, 400 MHz
DMSO- d_6



A.13



Proton NMR, 400 MHz
CDCl₃



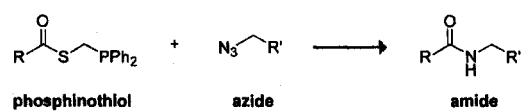
APPENDIX B**LIGHT-CONTROLLED STAUDINGER LIGATION**

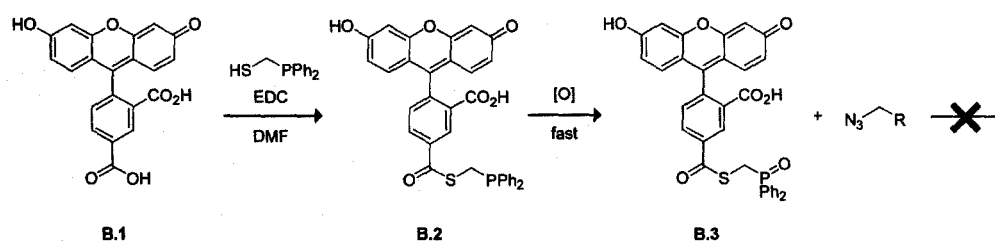
Contribution: All experiments and proposal.

B.1 Introduction

The Raines–Kiessling–Staudinger ligation is a reaction that forms an amide bond from an azide and phosphinothioester (Scheme B.1; (Nilsson *et al.*, 2000; Koehn and Breinbauer, 2004)). The utility of this reaction has been shown in a number of environments, including organic solvents (Soellner *et al.*, 2006), aqueous media (Tam *et al.*, 2007), and on surfaces (Soellner *et al.*, 2003). An obvious application of this ligation strategy would involve formation of a stable amide bond between small-molecule tags, such as fluorophores, and biomolecules. Indeed, this technology has also been used to ligate an azide-containing fluorescein, to a phosphinothioester-containing protein produced via expressed protein ligation (Tam *et al.*, 2007).

Another useful manifestation of this technology would involve production of fluorophores containing the phosphinothiol ester moiety. In principle, this could allow selective and site-specific labeling of azide moieties incorporated into biomolecules *in vitro* or even *in cellulo* (Saxon *et al.*, 2002). As shown in Scheme B.2, however, attempts to transform 5-carboxyfluorescein (**B.1**) to phosphinothioester (**B.2**) were fraught with rampant oxidation to the phosphine oxide (**B.3**), rendering the molecule inactive in a Raines–Kiessling–Staudinger ligation reaction (Kalia, J., Soellner, M.B., Lavis, L.D., and Raines, R.T., unpublished results). This rapid oxidation of the diarylmonoalkylphosphine was not observed with analogous phosphinothioester derivatives of amino acids. We hypothesized that the fluorophoric portion of the molecule sensitized singlet oxygen formation, leading to the rapid oxidation of the phosphine (Figure B.1). Here, we test this hypothesis using model compounds, and present a potential use of this phenomenon in the patterning of surfaces.

Scheme B.1 The Raines–Kiessling–Staudinger ligation

Scheme B.2 Attempted synthesis of fluorescein–phosphinothioester **B.2**

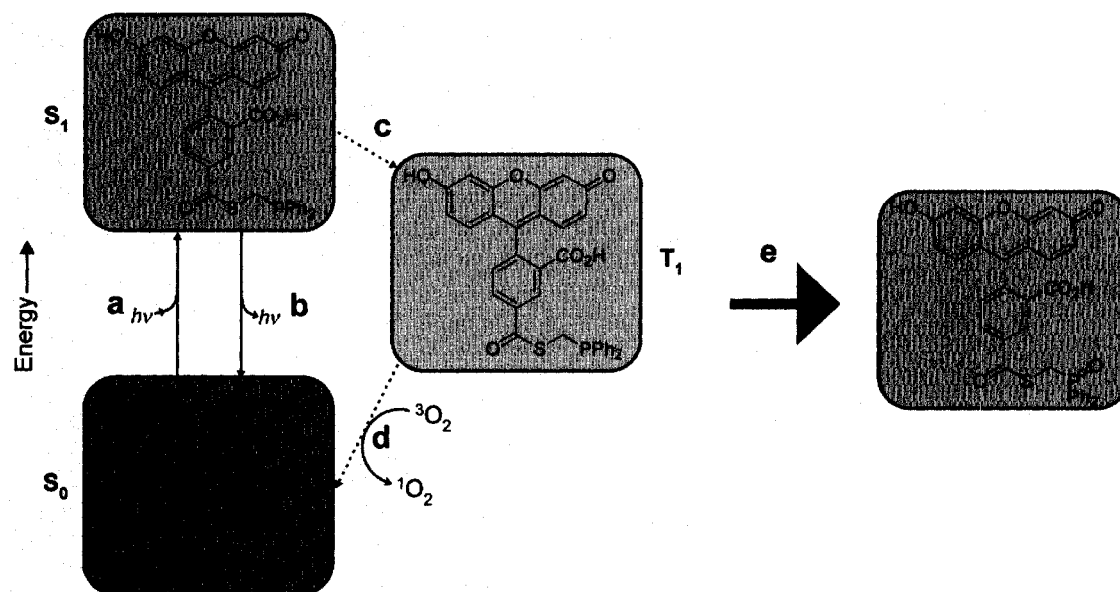


Figure B.1 Proposed mechanism for oxidation of phosphinothiol **B.2**. (a) Photon absorption gives a singlet excited state (S_1). (b) Relaxation via photon emission (fluorescence). (c) A small fraction of the molecules in the excited state undergo intersystem crossing (ITC) to a triplet excited state (T_1). (d) Sensitization of singlet oxygen (1O_2). (e) Oxidation of the phosphine by 1O_2 gives inactivated phosphine oxide product.

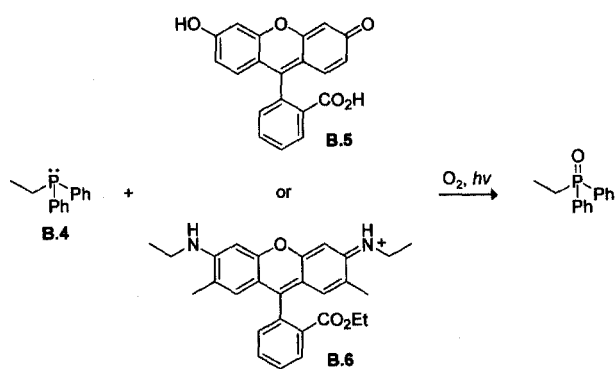
A.2 Results and Discussion

We hypothesized that the rapid oxidation of the phosphine in compound was due to singlet oxygen ($^1\text{O}_2$) photosensitization by the dye moiety (Figure B.1). Excited states of xanthene dyes such as fluorescein and rhodamine typically show low intersystem crossing (ITC) to the triplet state with efficiencies around 1% (Stracke *et al.*, 1999). Still, these fluorophores are able to sensitize singlet oxygen production to a measurable extent (Stracke *et al.*, 1999; Yamaguchi and Sasaki, 2001). The reaction between phosphines and $^1\text{O}_2$ occurs readily, however, and singlet oxygen can oxidize bulky triarylphosphines that withstand treatment with $^3\text{O}_2$ (Gao *et al.*, 2001; Ho *et al.*, 2003). Thus, we expect oxidation could occur rapidly given the high reactivity of $^1\text{O}_2$ with phosphines, despite the low intersystem crossing efficiency in xanthene dyes.

To test this hypothesis, we incubated a model phosphine, ethyldiphenylphosphine (EDPP; **B.4**), with rhodamine 6G (R6G; **B.5**) or fluorescein (**B.6**) dyes in DMF–water mixtures, and exposed the resulting solutions to ambient sunlight for 6 h (Scheme B.3). The ^{31}P NMR traces from these experiments are shown in Figure B.2. Incubation of a solution containing phosphine **B.4** *sans* dye led to no oxidation (Figure B.2a). Addition of fluorescein (**B.4**) or rhodamine 6G (**B.5**) dyes induced oxidation only in the presence of light (Figures B.2b–e). The new peak at ~26 PPM with the dark fluorescein experiment (Figure B.2b) is due perhaps to an unexplored side reaction of the phosphine with the oxygen-containing dye. Purging of the solution with dry $\text{N}_2(\text{g})$ to remove dissolved molecular oxygen prevented oxidation (Figure B.2f). Exposing this degassed solution to atmospheric O_2 , however, again shows oxidation of the phosphine (Figure B.2g). In

short, these data demonstrate the oxidation of the phosphine occurs only when light, dye, and molecular oxygen were applied to the solution.

Oxidation of trisubstituted phosphines in the presence of R6G has been reported previously in oxygen-free solution in ~25% yield after illumination from a xenon arc lamp for 7 h. The proposed mechanism involves single-electron transfer from the phosphine to the triplet state (T_1) of the rhodamine dye and subsequent reaction of the phosphine radical cation with water (Yasui *et al.*, 2000). We failed to observe any oxidation in our degassed experiment with R6G (Figure B.2f), due likely to the use of ambient light rather than a high-output lamp.

Scheme B.3 Photoinduced oxidation experiments

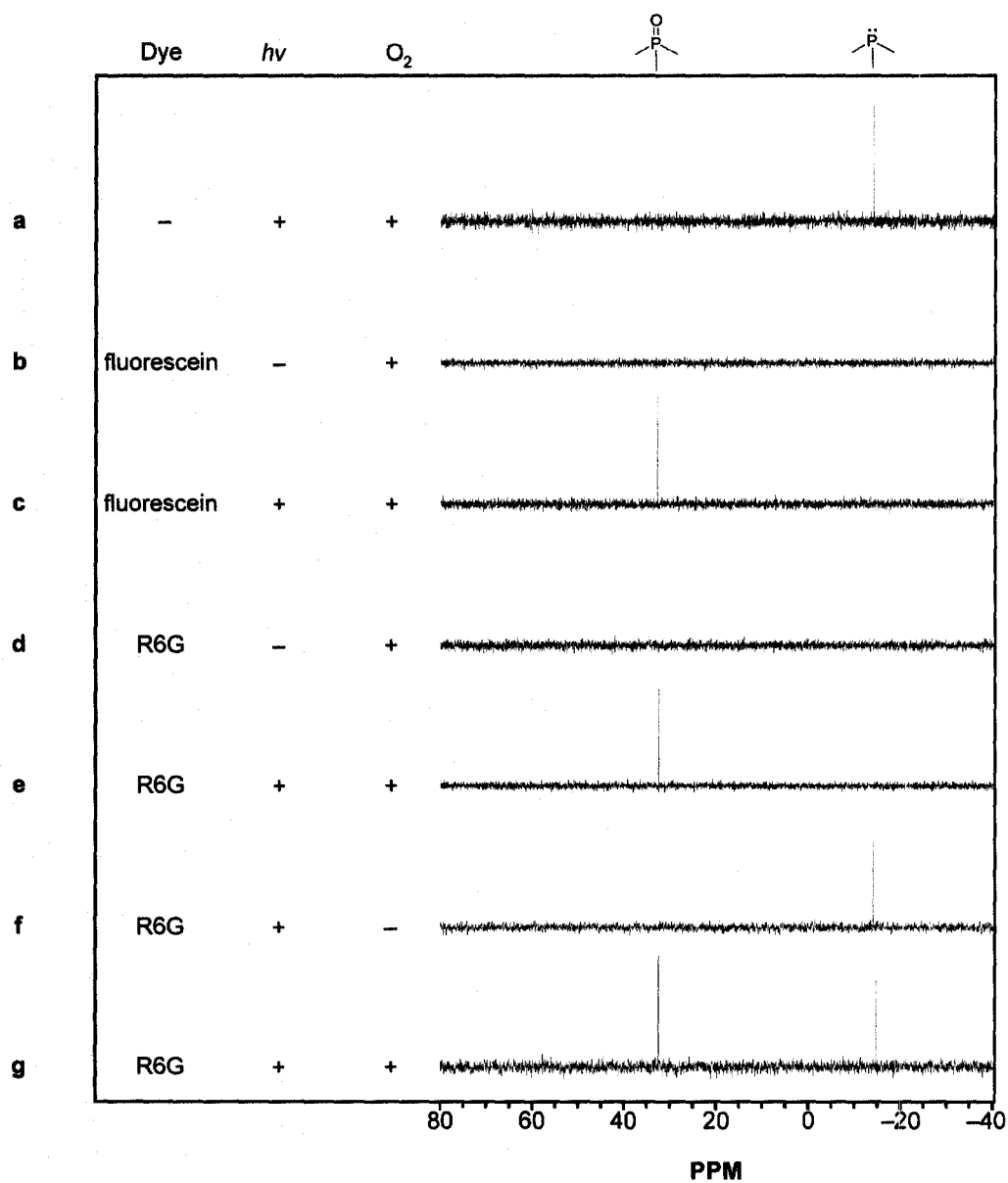


Figure B.2 Photoinduced oxidation experiments.

B.3 Conclusions and Future Directions

We have shown that phosphines are susceptible to oxidation in the presence of common fluorophores, atmospheric molecular oxygen, and ambient light. This instability causes the synthesis and preservation of fluorophore-containing phosphinothiols difficult, requiring rigorous protection from stray O₂ and photons. While this phenomenon precludes the use of such compounds in many biological experiments, it also inspires a way to control the Raines–Kiessling–Staudinger ligation using light.

We envision the selective deactivation of surface-bound Staudinger Ligation reagents using light as shown in Figure B.3. Formation of the phosphinothioester on a carboxyl-coated surface (Figure B.3a) has precedence (Soellner *et al.*, 2003). Application of a solution of a sensitizing dye and O₂ to the surface (Figure B.3b) followed by selective illumination of the surface (Figure B.3c) should oxidize the Staudinger ligation reagent only in areas where light is applied (Figure B.3d). To limit diffusion of ¹O₂ (and potential “blurring” of the ablation pattern) we could add a tertiary amine such as 1,4-diazabicyclo[2.2.2]octane (DABCO) quench singlet O₂ (Ouannes and Wilson, 1968; Young and Martin, 1972). Addition of an azide substrate should elicit ligation at remaining reduced phosphines where light was not applied (Figure B.3e). After ligation, there remains a second opportunity where phosphine oxide thioesters could react with nucleophilic hydrazine moieties (Kalia and Raines, 2006) to allow attachment of a another ligand to the surface (Figure B.3f).

An obvious technology to enable this proposal is the Maskless Array Synthesizer (MAS) developed originally to facilitate DNA synthesis (Singh-Gasson *et al.*, 1999). This technology can also be used to produce arrays of different biologically-relevant

molecules (Shaginian *et al.*, 2004). Candidates for sensitizing dyes include tetraphenylporphine (TPP; (DeRosa and Crutchley, 2002)) and terthiophene (Sease and Zechmeister, 1947; Boch *et al.*, 1996). Both dyes are well-known photosensitizing dyes with absorption maxima matching the common light sources used in MAS instruments. Initial experiments could involve attachment of biotin to the surface (via an azide-containing biotin molecule) and the pattern would be “developed” using fluorescently-labeled avidin. Overall, this technology could augment or supplant various strategies that use light to direct the attachment of biomolecules to surfaces (Min and Mrksich, 2004; Lee and Shin, 2005; Sun *et al.*, 2006).

B.4 Acknowledgements

We thank M.B. Soellner for contributive discussions. L.D.L was supported by Biotechnology Training Grant 08349 (NIH) and an ACS Division of Organic Chemistry Fellowship sponsored by the Genentech Foundation. This work was supported by grant CA73808 (NIH). NMRFAM was supported by grant P41 RR02301 (NIH).

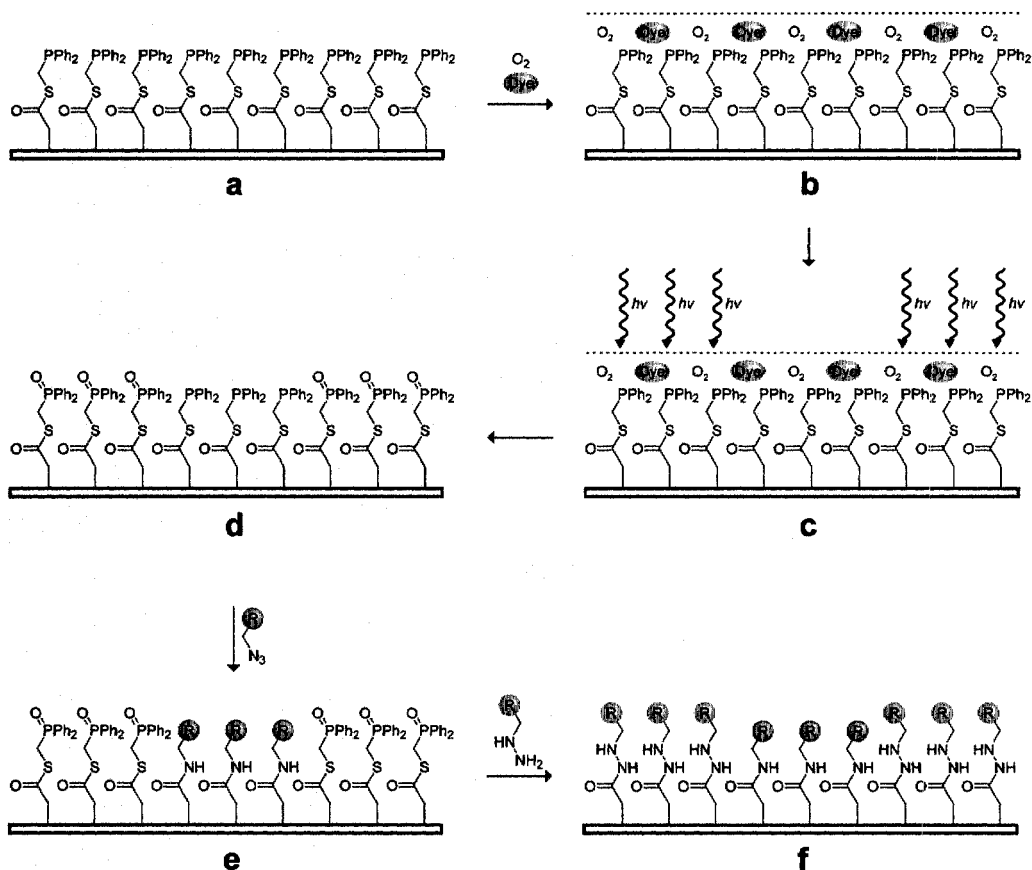


Figure B.3 Proposed photopatterning via light-induced oxidation. (a) Formation of phosphinothioester on surface. (b) Incubation of oxygenated solution containing photosensitizing dye. (c) Spatially-controlled application of light. (d) Resulting phosphine oxide formation. (e) First incubation with azide ligand. (f) Second incubation with hydrazine ligand.

B.5 Experimental Section

B.5.1 General Experimental

Ethyldiphenylphosphine (EDPP; **B.4**), fluorescein (**B.5**), and rhodamine 6G (**B.6**) were from Aldrich Chemical (Milwaukee, WI). Deuterated DMF (DMF- d_7) was from Cambridge Isotope Laboratories. Dimethylformamide (DMF) was drawn from a Baker CYCLE-TAINER solvent delivery system. DMF, DMF- d_7 , and H₂O were equilibrated with atmospheric O₂ for at least 24 h prior to experiment. NMR spectra were obtained with a Bruker DMX-400 Avance spectrometer at the NMR Facility at Madison (NMRFAM).

B.5.2 Photoinduced Oxidation Experiments

Clear glass vials were equipped with Teflon-lined caps and charged with solutions of EDPP (10.0 mM; 2×) in DMF containing 10% v/v H₂O and 10% v/v DMF- d_7 . An equal volume of fluorescein (10.0 mM; 2×), rhodamine 6G (10.0 mM; 2×), or a no-dye control in DMF containing 10% v/v H₂O and 10% v/v DMF- d_7 was added and the reaction was placed in ambient sunlight for 6 h. Removal of O₂ for control vials was accomplished by sparging of the DMF–DMF- d_7 –H₂O solution with dry N₂(g) for 1 h prior to the experiment and ambient O₂ was excluded by sealing with Parafilm. Reintroduction of O₂ after degassing involved unsealing the vial during incubation in sunlight. ³¹P NMR spectra were obtained using undiluted samples.

APPENDIX C***LETTER TO THE EDITOR OF THE NEW ENGLAND JOURNAL OF MEDICINE**

This letter was submitted to the New England Journal of Medicine in response to a published image showing fluorescent urine from a patient suffering from ethylene glycol poisoning. The editor did not choose to publish this letter (see: Figure C.2)

To the Editor:

The recently submitted image (McStay and Gordon, 2007) shows obvious fluorescence of a urine sample obtained from a patient who ingested ethylene glycol. The blue fluorescence of the urine is attributed to the dye fluorescein, which is a common additive in commercial antifreeze. The use of urine fluorescence as a diagnostic for ethylene glycol poisoning has been evaluated previously (Casavant *et al.*, 2001; Parsa *et al.*, 2005). The authors of these studies found that urine samples from most normal subjects exhibit considerable blue fluorescence that could potentially obscure the signal from ingested fluorescein. Casavant and co-workers later challenged critics to check their own urine for any visible fluorescence (Sharma *et al.*, 2002). Indeed, samples of our own urine fluoresced bright blue upon UV excitation (Figure C.1). Moreover, fluorescein and its monoglucuronide metabolite emit in the yellow-green portion of the visible spectrum (Grotte *et al.*, 1983) whereas the fluorescence in the image is blue. It is likely that the fluorescent signal shown in the image is not due to fluorescein, but to some other common component of urine with intrinsic fluorescence.

-Luke D. Lavis, Department of Chemistry, University of Wisconsin–Madison

-Thomas J. Rutkoski, Department of Biochemistry, University of Wisconsin–Madison

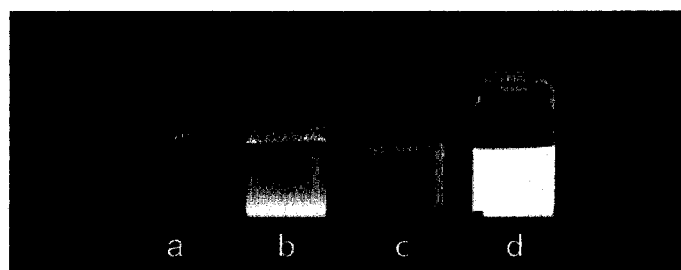


Figure C.1 Fluorescence of solutions under long-wave UV illumination ($\lambda = 366$ nm):
(a) deionized H₂O (b) undiluted urine (c) phosphate-buffered saline (d)
fluorescein in phosphate-buffered saline.

Luke D. Lavis

From: Letter [letter@nejm.org]
Sent: Thursday, March 15, 2007 9:46 AM
To: lavis@chem.wisc.edu
Subject: RE: NEJM Correspondence #: 07-0644

Dear Mr. Lavis,

I am sorry that we will not be able to print your recent letter to the editor. The space available for correspondence is very limited, and we must use our judgment to present a representative selection of the material received. Many worthwhile communications must be declined simply for lack of space.

Sincerely yours,

Lindsey R. Baden, M.D.
Deputy Editor
New England Journal of Medicine

Figure C.2 Response to letter to the editor submission.

REFERENCES

- Abel, R. L., Haigis, M. C., Park, C., and Raines, R. T. (2002). Fluorescence assay for the binding of ribonuclease A to the ribonuclease inhibitor protein. *Anal. Biochem.* **306**, 100-107.
- Adamczyk, M., Fishpaugh, J. R., and Heuser, K. J. (1997). Preparation of succinimidyl and pentafluorophenyl active esters of 5- and 6-carboxyfluorescein. *Bioconjugate Chem.* **8**, 253-255.
- Agi, Y., and Walt, D. R. (1997). Fluorescence monitoring of the microenvironmental pH of highly charged polymers. *J. Polym. Sci., Part A: Polym. Chem.* **35**, 2105-2110.
- Amsberry, K. L., Gerstenberger, A. E., and Borchardt, R. T. (1991). Amine prodrugs which utilize hydroxy amide lactonization. II. A potential esterase-sensitive amide prodrug. *Pharm. Res.* **8**, 455-461.
- Anderson, M. T., Baumgarth, N., Haugland, R. P., Gerstein, R. M., Tjioe, T., Herzenberg, L. A., and Herzenberg, L. A. (1998). Pairs of violet-light-excited fluorochromes for flow cytometric analysis. *Cytometry* **33**, 435-444.
- Andrews, J. L., Ghosh, P., Ternai, B., and Whitehouse, M. W. (1982). Ammonium 4-chloro-7-sulfobenzofurazan: A new fluorogenic [*sic*] thiol-specific reagent. *Arch. Biochem. Biophys.* **214**, 386-396.
- Arano, Y., Uezono, T., Akizawa, H., Ono, M., Wakisaka, K., Nakayama, M., Sakahara, H., Konishi, J., and Yokoyama, A. (1996). Reassessment of diethylenetriaminepentaacetic acid (DTPA) as a chelating agent for indium-111

labeling of polypeptides using a newly synthesized monoreactive DTPA derivative. *J. Med. Chem.* **39**, 3451-3460.

Aslam, M., and Dent, A. (1998). "Bioconjugation: Protein Coupling Techniques for the Biomedical Sciences." Macmillan Reference, London.

Aubin, J. E. (1979). Autofluorescence of viable cultured mammalian cells. *J. Histochem. Cytochem.* **27**, 36-43.

Babiak, P., and Reymond, J.-L. (2005). A high-throughput, low-volume enzyme assay on solid support. *Anal. Chem.* **77**, 373-377.

Baeyer, A. (1871). Ueber eine neue Klasse von Farbstoffen. *Ber. Dtsch. Chem. Ges.* **4**, 555-558.

Ballou, B., Ernst, L. A., and Waggoner, A. S. (2005). Fluorescence imaging of tumors in vivo. *Curr. Med. Chem.* **12**, 795-805.

Banks, P., Gosselin, M., and Prystay, L. (2000). Impact of a red-shifted dye label for high throughput fluorescence polarization assays of G protein-coupled receptors. *J. Biomol. Screen.* **5**, 329-334.

Banny, T. M., and Clark, G. (1950). The new domestic cresyl echt violet. *Stain Technol.* **25**, 195-196.

Bates, M., Huang, B., Dempsey, G. T., and Zhuang, X. (2007). Multicolor super-resolution imaging with photo-switchable fluorescent probes. *Science* **317**, 1749-1753.

- Bednar, R. A. (1990). Reactivity and pH dependence of thiol conjugation to *N*-ethylmaleimide: Detection of a conformational change in chalcone isomerase. *Biochemistry* **29**, 3684-3690.
- Beechem, J. M., and Brand, L. (1985). Time-resolved fluorescence of proteins. *Annu. Rev. Biochem.* **54**, 43-71.
- Bensel, N., Reymond, M. T., and Reymond, J.-L. (2001). Pivalase catalytic antibodies: towards abzymatic activation of prodrugs. *Chem. Eur. J.* **7**, 4604-4612.
- Bergsdorf, C., Beyer, C., Umansky, V., Werr, M., and Sapp, M. (2003). Highly efficient transport of carboxyfluorescein diacetate succinimidyl ester into COS7 cells using human papillomavirus-like particles. *FEBS Lett.* **536**, 120-124.
- Berlier, J. E., Rothe, A., Buller, G., Bradford, J., Gray, D. R., Filanoski, B. J., Telford, W. G., Yue, S., Liu, J., Cheung, C.-Y., Chang, W., Hirsch, J. D., Beechem, J. M., Haugland, R. P., and Haugland, R. P. (2003). Quantitative comparison of long-wavelength Alexa Fluor dyes to CyDyes: Fluorescence of the dyes and their bioconjugates. *J. Histochem. Cytochem.* **51**, 1699-1712.
- Bernstein, S., and Conrow, R. B. (1971). Steroid conjugates. VI. Improved Koenigs-Knorr synthesis of aryl glucuronides using cadmium carbonate, a new and effective catalyst. *J. Org. Chem.* **36**, 863-870.
- Blackburn, P., Wilson, G., and Moore, S. (1977). Ribonuclease inhibitor from human placenta: Purification and properties. *J. Biol. Chem.* **252**, 5904-5910.

- Boch, R., Mehta, B., Connolly, T., Durst, T., Arnason, J. T., Redmond, R. W., and Scaiano, J. C. (1996). Singlet oxygen photosensitizing properties of bithiophene and terthiophene derivatives. *J. Photochem. Photobiol., A* **93**, 39-47.
- Bodor, N., Sloan, K. B., Kaminski, J. J., Shih, C., and Pogany, S. (1983). A convenient synthesis of (acyloxy)alkyl α -ethers of phenols. *J. Org. Chem.* **48**, 5280-5284.
- Boonacker, E., Elferink, S., Bardai, A., Fleischer, B., and Van Noorden, C. J. F. (2003). Fluorogenic substrate [Ala-Pro]2-cresyl violet but not Ala-Pro-rhodamine 110 is cleaved specifically by DPPIV activity: A study in living Jurkat cells and CD26/DPPIV-transfected Jurkat cells. *J. Histochem. Cytochem.* **51**, 959-968.
- Boonacker, E., and Van Noorden, C. J. F. (2001). Enzyme cytochemical techniques for metabolic mapping in living cells, with special reference to proteolysis. *J. Histochem. Cytochem.* **49**, 1473-1486.
- Borchardt, R. T., and Cohen, L. A. (1972a). Stereopopulation control. II. Rate enhancement of intramolecular nucleophilic displacement. *J. Am. Chem. Soc.* **94**, 9166-9174.
- Borchardt, R. T., and Cohen, L. A. (1972b). Stereopopulation control. III. Facilitation of intramolecular conjugate addition of the carboxyl group. *J. Am. Chem. Soc.* **94**, 9175-9182.
- Borra, M. T., Smith, B. C., and Denu, J. M. (2005). Mechanism of human SIRT1 activation by resveratrol. *J. Biol. Chem.* **280**, 17187-17195.

- Bosch, M., Benito, A., Ribo, M., Puig, T., Beaumelle, B., and Vilanova, M. (2004). A nuclear localization sequence endows human pancreatic ribonuclease with cytotoxic activity. *Biochemistry* **43**, 2167-2177.
- Bräse, S., Gil, C., Knepper, K., and Zimmermann, V. (2005). Organic azides: An exploding diversity of a unique class of compounds. *Angew. Chem. Int. Ed. Engl.* **44**, 5188-5240.
- Bright, F. V., and Munson, C. A. (2003). Time-resolved fluorescence spectroscopy for illuminating complex systems. *Anal. Chim. Acta* **500**, 71-104.
- Brinkley, M. (1992). A brief survey of methods for preparing protein conjugates with dyes, haptens, and cross-linking reagents. *Bioconjugate Chem.* **3**, 2-13.
- Brustugun, O. T., Mellgren, G., Gjertsen, B. T., Bjerkvig, R., and Doskeland, S. O. (1995). Sensitive and rapid detection of β -galactosidase expression in intact cells by microinjection of fluorescent substrate. *Exp. Cell Res.* **219**, 372-378.
- Bueno, C., Villegas, M. L., Bertolotti, S. G., Previtali, C. M., Neumann, M. G., and Encinas, M. V. (2002). The excited-state interaction of resazurin and resorufin with amines in aqueous solutions. Photophysics and photochemical reaction. *Photochem. Photobiol.* **76**, 385-390.
- Burdette, S. C., and Lippard, S. J. (2002). The rhodafluor family. An initial study of potential ratiometric fluorescent sensors for Zn^{2+} . *Inorg. Chem.* **41**, 6816-6823.
- Burke, M. D., Thompson, S., Weaver, R. J., Wolf, C. R., and Mayer, R. T. (1994). Cytochrome P450 specificities of alkoxyresorufin *O*-dealkylation in human and rat liver. *Biochem. Pharmacol.* **48**, 923-936.

- Buschmann, V., Weston, K. D., and Sauer, M. (2003). Spectroscopic study and evaluation of red-absorbing fluorescent dyes. *Bioconjugate Chem.* **14**, 195-204.
- Butler, R., and Bates, G. P. (2006). Histone deacetylase inhibitors as therapeutics for polyglutamine disorders. *Nat. Rev. Neurosci.* **7**, 784-796.
- Cai, S. X., Zhang, H.-Z., Guastella, J., Drewe, J., Yang, W., and Weber, E. (2001). Design and synthesis of rhodamine 110 derivative and caspase-3 substrate for enzyme and cell-based fluorescent assay. *Bioorg. Med. Chem. Lett.* **11**, 39-42.
- Casavant, M. J., Shah, M. N., and Battels, R. (2001). Does fluorescent urine indicate antifreeze ingestion by children? *Pediatrics* **107**, 113-114.
- Cavaluzzi, M. J., and Borer, P. N. (2004). Revised UV extinction coefficients for nucleoside-5'-monophosphates and unpaired DNA and RNA. *Nucleic Acids Res.* **32**, e13.
- Chandran, S. S., Dickson, K. A., and Raines, R. T. (2005). Latent fluorophore based on the trimethyl lock. *J. Am. Chem. Soc.* **127**, 1652-1653.
- Chang, C. J., Jaworski, J., Nolan, E. M., Sheng, M., and Lippard, S. J. (2004). A tautomeric zinc sensor for ratiometric fluorescence imaging: Application to nitric oxide-induced release of intracellular zinc. *Proc. Natl. Acad. Sci. U.S.A.* **101**, 1129-1134.
- Chattopadhyay, A. (1990). Chemistry and biology of *N*-(7-nitrobenz-2-oxa-1,3-diazol-4-yl)-labeled lipids: Fluorescent probes of biological and model membranes. *Chem. Phys. Lipids* **53**, 1-15.

- Chen, S. C., Nakamura, H., and Tamura, Z. (1979). Supplemental studies on relationship between structure and spectrum of fluorescein. *Chem. Pharm. Bull.* **27**, 475-479.
- Chilvers, K. F., Perry, J. D., James, A. L., and Reed, R. H. (2001). Synthesis and evaluation of novel fluorogenic substrates for the detection of bacterial β -galactosidase. *J. Appl. Microbiol.* **91**, 1118-1130.
- Christie, R. M. (2001). "Colour Chemistry." Royal Society of Chemistry, Cambridge, UK.
- Christoph, S., and Meyer-Almes, F. J. (2003). Novel fluorescence based receptor binding assay method for receptors lacking ligand conjugates with preserved affinity: Study on estrogen receptor α . *Biopolymers* **72**, 256-263.
- Cohen, B. E., Pralle, A., Yao, X., Swaminath, G., Gandhi, C. S., Jan, Y. N., Kobilka, B. K., Isacoff, E. Y., and Jan, L. Y. (2005). A fluorescent probe designed for studying protein conformational change. *Proc. Natl. Acad. Sci. U.S.A.* **102**, 965-970.
- Coons, A. H., and Kaplan, M. H. (1950). Localization of antigen in tissue cells. II. Improvements in a method for the detection of antigen by means of fluorescent antibody. *J. Exp. Med.* **91**, 1-13.
- Corrie, J. E. T., and Craik, J. S. (1994). Synthesis and characterization of pure isomers of iodoacetamidotetramethylrhodamine. *J. Chem. Soc., Perkin Trans. 1*, 2967-2973.
- Corrie, J. E. T., Craik, J. S., and Munasinghe, V. R. N. (1998). A homobifunctional rhodamine for labeling proteins with defined orientations of a fluorophore. *Bioconjugate Chem.* **9**, 160-167.

- Cosa, G., Focsaneanu, K. S., McLean, J. R. N., McNamee, J. P., and Scaiano, J. C. (2001). Photophysical properties of fluorescent DNA-dyes bound to single- and double-stranded DNA in aqueous buffered solution. *Photochem. Photobiol.* **73**, 585-599.
- Crissman, H. A., and Hirons, G. T. (1994). Staining of DNA in live and fixed cells. *Methods Cell Biol.* **41**, 195-209.
- Culling, C. F. A., Allison, R. T., and Barr, W. T. (1985). "Cellular Pathology Technique." Butterworths, Boston.
- Curtius, T. (1890). Ueber Stickstoffwasserstoffsäure (Azoimid) N_3H . *Ber. Dtsch. Chem. Ges.* **23**, 3023-3033.
- Curtius, T. (1894). Hydrazide und Azide organischer Säuren. *J. Prakt. Chem.* **50**, 275-294.
- Dai, Z., Dulyaninova, N. G., Kumar, S., Bresnick, A. R., and Lawrence, D. S. (2007). Visual snapshots of intracellular kinase activity at the onset of mitosis. *Chem. Biol.* **14**, 1254-1260.
- Daniel, E., and Weber, G. (1966). Cooperative effects in binding by bovine serum albumin. I. The binding of 1-anilino-8-naphthalenesulfonate. Fluorimetric titrations. *Biochemistry* **5**, 1893-1900.
- Darzynkiewicz, Z., Bruno, S., Del Bino, G., Gorczyca, W., Hotz, M. A., Lassota, P., and Traganos, F. (1992). Features of apoptotic cells measured by flow cytometry. *Cytometry* **13**, 795-808.

- Davenport, L., Shen, B., Joseph, T. W., and Straher, M. P. (2001). A novel fluorescent coronenyl-phospholipid analogue for investigations of submicrosecond lipid fluctuations. *Chem. Phys. Lipids* **109**, 145-156.
- Dawson, W. R., and Windsor, M. W. (1968). Fluorescence yields of aromatic compounds. *J. Phys. Chem.* **72**, 3251-3260.
- de Silva, A. P., Gunaratne, H. Q. N., Gunnlaugsson, T., Huxley, A. J. M., McCoy, C. P., Rademacher, J. T., and Rice, T. E. (1997). Signaling recognition events with fluorescent sensors and switches. *Chem. Rev.* **97**, 1515-1566.
- Demchenko, A. P. (1986). "Ultraviolet Spectroscopy of Proteins." Springer-Verlag, Berlin.
- DeRosa, M. C., and Crutchley, R. J. (2002). Photosensitized singlet oxygen and its applications. *Coord. Chem. Rev.* **233**, 351-371.
- Descalzo, A. B., Rurack, K., Weisshoff, H., Martinex-Manez, R., Marcos, M. D., Amoros, P., Hoffmann, K., and Soto, J. (2005). Rational design of a chromo- and fluorogenic hybrid chemosensor material for the detection of long-chain carboxylates. *J. Am. Chem. Soc.* **127**, 184-200.
- Dickson, K. A., Haigis, M. C., and Raines, R. T. (2005). Ribonuclease inhibitor: Structure and function. *Prog. Nucleic Acid Res. Mol. Biol.* **80**, 349-374.
- Diehl, H. (1989). Studies on fluorescein-VI: Absorbance of the various prototropic forms of yellow fluorescein in aqueous solution. *Talanta* **36**, 413.

- Diehl, H., and Markuszewski, R. (1989). Studies on fluorescein-VII: The fluorescence of fluorescein as a function of pH. *Talanta* **36**, 416.
- Diwu, Z., Chen, C. S., Zhang, C., Klaubert, D. H., and Haugland, R. P. (1999). A novel acidotropic pH indicator and its potential application in labeling acidic organelles of live cells. *Chem. Biol.* **6**, 411-418.
- Diwu, Z., Liao, J., and Wang, Z. (2003) Preparation of rhodamine peptide derivatives as luminogenic protease substrates. WO Patent Application 2003099780.
- Diwu, Z., Twu, J. J., Yi, G., Lavis, L. D., Chen, Y.-W., and Cassutt, K. J. (2004) Fluorescent pH indicators for intracellular assays. U.S. Patent 6,800,765.
- Diwu, Z., Zhang, C., Klaubert, D. H., and Haugland, R. P. (2000). Fluorescent molecular probes VI: The spectral properties and potential biological applications of water-soluble DapoxylTM sulfonic acid. *J. Photochem. Photobiol., A* **131**, 95-100.
- Drexhage, K. H. (1977). Structure and properties of laser dyes. In "Dye Lasers" (F. P. Schäfer, Ed.), pp. 144-193. Springer-Verlag, Berlin; New York.
- Drobni, P., Mistry, N., McMillan, N., and Evander, M. (2003). Carboxy-fluorescein diacetate, succinimidyl ester labeled papillomavirus virus-like particles fluoresce after internalization and interact with heparan sulfate for binding and entry. *Virology* **310**, 163-172.
- Dulbecco, R., and Vogt, M. (1954). Plaque formation and isolation of pure lines with poliomyelitis viruses. *J. Exp. Med.* **99**, 167-182.

Eaton, D. F. (1988). Reference materials for fluorescence measurement. *Pure Appl. Chem.* **60**, 1107-1114.

Ferres, H. (1980). Pro-drugs of β -lactam antibiotics. *Chem. Ind.*, 435-440.

Fickling, M. M., Fischer, A., Mann, B. R., Packer, J., and Vaughan, J. (1959). Hammett substituent constants for electron-withdrawing substituents: Dissociation of phenols, anilinium ions and dimethylanilinium ions. *J. Am. Chem. Soc.* **81**, 4226-4230.

Fiering, S. N., Roederer, M., Nolan, G. P., Micklem, D. R., Parks, D. R., and Herzenberg, L. A. (1991). Improved FACS-Gal: Flow cytometric analysis and sorting of viable eukaryotic cells expressing reporter gene constructs. *Cytometry* **12**, 291-301.

Fieser, L. F., and Fieser, M. (1967). "Reagents for Organic Synthesis, Volume 1." Wiley, New York.

Fleming, G. R., Knight, A. W. E., Morris, J. M., Morrison, R. J. S., and Robinson, G. W. (1977). Picosecond fluorescence studies of xanthene dyes. *J. Am. Chem. Soc.* **99**, 4306-4311.

Foster, L. J., de Hoog, C. L., Zhang, Y., Zhang, Y., Xie, X., Mootha, V. K., and Mann, M. (2006). A mammalian organelle map by protein correlation profiling. *Cell* **125**, 187-199.

Frangioni, J. V. (2003). In vivo near-infrared fluorescence imaging. *Curr. Opin. Chem. Biol.* **7**, 626-634.

- Friedrich, K., and Woolley, P. (1988). Electrostatic potential of macromolecules measured by pK_a shift of a fluorophore 1. The 3' terminus of 16S RNA. *Eur. J. Biochem.* **173**, 227-231.
- Friedrich, K., Woolley, P., and Steinhauser, K. G. (1988). Electrostatic potential of macromolecules measured by pK_a shift of a fluorophore 2. Transfer RNA. *Eur. J. Biochem.* **173**, 233-239.
- Gabe, Y., Urano, Y., Kikuchi, K., Kojima, H., and Nagano, T. (2004). Highly sensitive fluorescence probes for nitric oxide based on boron dipyrromethene chromophore—rational design of potentially useful bioimaging fluorescence probe. *J. Am. Chem. Soc.* **126**, 3357-3367.
- Gacoin, P., and Flamant, P. (1972). High efficiency cresyl violet laser. *Optics Commun.* **5**, 351-353.
- Gao, R., Ho, D. G., Dong, T., Khuu, D., Franco, N., Sezer, O., and Selke, M. (2001). Reaction of arylphosphines with singlet oxygen: Intra- vs intermolecular oxidation. *Org. Lett.* **3**, 3719-3722.
- Gao, W., Xing, B., Tsien, R. Y., and Rao, J. (2003). Novel fluorogenic substrates for imaging β -lactamase gene expression. *J. Am. Chem. Soc.* **125**, 11146–11147.
- Garel, J. R. (1976). pK changes of ionizable reporter groups as an index of conformational changes in proteins: A study of fluorescein-labelled ribonuclease A. *Eur. J. Biochem.* **70**, 179-189.
- Garfield, S. (2001). "Mauve: How One Man Invented a Color that Changed the World." W.W. Norton & Co., New York.

- Gee, K. R. (1999). Novel fluorogenic substrates for acid phosphatase. *Bioorg. Med. Chem. Lett.* **9**, 1395-1396.
- Gee, K. R., Sun, W.-C., Bhalgat, M. K., Upson, R. H., Klaubert, D. H., Latham, K. A., and Haugland, R. P. (1999). Fluorogenic substrates based on fluorinated umbelliferones for continuous assays of phosphatases and β -galactosidases. *Anal. Biochem.* **273**, 41-48.
- Ghosh, P. B., and Whitehouse, M. W. (1968). 7-Chloro-4-nitrobenzo-2-oxa-1,3-diazole: A new fluorogenic reagent for amino acids and other amines. *Biochem. J.* **108**, 155-156.
- Giepmans, B. N. G., Adams, S. R., Ellisman, M. H., and Tsien, R. Y. (2006). The fluorescent toolbox for assessing protein location and function. *Science* **312**, 217-224.
- Glozak, M. A., Sengupta, N., Zhang, X., and Seto, E. (2005). Acetylation and deacetylation of non-histone proteins. *Gene* **363**, 15-23.
- Goddard, J.-P., and Reymond, J.-L. (2004a). Enzyme assays for high-throughput screening. *Curr. Opin. Biotechnol.* **15**, 314.
- Goddard, J.-P., and Reymond, J.-L. (2004b). Recent advances in enzyme assays. *Trends Biotechnol.* **22**, 363.
- Goldberg, J. M., and Baldwin, R. L. (1998a). Kinetic mechanism of a partial folding reaction. 1. Properties of the reaction and effects of denaturants. *Biochemistry* **37**, 2546-2555.

- Goldberg, J. M., and Baldwin, R. L. (1998b). Kinetic mechanism of a partial folding reaction. 2. Nature of the transition state. *Biochemistry* **37**, 2556-2563.
- Goldberg, J. M., and Baldwin, R. L. (1999). A specific transition state for S-peptide combining with folded S-protein and then refolding. *Proc. Natl. Acad. Sci. U.S.A.* **96**, 2019-2024.
- Graber, M. L., Dilillo, D. C., Friedman, B. L., and Pastorizamunoz, E. (1986). Characteristics of fluoroprobes for measuring intracellular pH. *Anal. Biochem.* **156**, 202-212.
- Grandberg, I. I., Denisov, L. K., and Popova, O. A. (1987). 7-Aminocoumarins. *Chem. Heterocycl. Compd. (N.Y.)* **23**, 117-142.
- Griep, M. A., and Mchenry, C. S. (1990). Dissociation of the DNA polymerase III holoenzyme β_2 subunits is accompanied by conformational change at distal cysteines 333. *J. Biol. Chem.* **265**, 20356-20363.
- Griep, M. A., and Mesman, T. N. (1995). Fluorescent labeling of cysteine-39 on *Escherichia coli* primase places the dye near an active site. *Bioconjugate Chem.* **6**, 673-682.
- Grotte, D., Mattox, V., and Brubaker, R. F. (1983). Fluorescein glucuronide: Can this metabolite interfere with fluorescein tracer studies? *Trans. Am. Ophthalmol. Soc.* **81**, 125-129.
- Gruber, H. J., Hahn, C. D., Kada, G., Riener, C. K., Harms, G. S., Ahrer, W., Dax, T. G., and Knaus, H. G. (2000). Anomalous fluorescence enhancement of Cy3 and

Cy3.5 versus anomalous fluorescence loss of Cy5 and Cy7 upon covalent linking to IgG and noncovalent binding to avidin. *Bioconjugate Chem.* **11**, 696-704.

Grynkiewicz, G., Poenie, M., and Tsien, R. Y. (1985). A new generation of Ca^{2+} indicators with greatly improved fluorescence properties. *J. Biol. Chem.* **260**, 3440-3450.

Gunnlaugsson, T., Glynn, M., Tocci, G. M., Kruger, P. E., and Pfeffer, F. M. (2006). Anion recognition and sensing in organic and aqueous media using luminescent and colorimetric sensors. *Coord. Chem. Rev.* **250**, 3094-3117.

Guzikowski, A. P., Naleway, J. J., Shipp, C. T., and Schutte, R. C. (2000). Synthesis of a macrocyclic rhodamine 110 enzyme substrate as an intracellular probe for caspase 3 activity. *Tetrahedron Lett.* **41**, 4733-4735.

Haigis, M. C., and Guarente, L. P. (2006). Mammalian sirtuins—emerging roles in physiology, aging, and calorie restriction. *Genes Dev.* **20**, 2913-2921.

Haigis, M. C., Kurten, E. L., and Raines, R. T. (2003). Ribonuclease inhibitor as an intracellular sentry. *Nucleic Acids Res.* **31**, 1024-1032.

Haigis, M. C., and Raines, R. T. (2003). Secretory ribonucleases are internalized by a dynamin-independent endocytic pathway. *J. Cell Sci.* **116**, 313-324.

Hamze, A., Martinez, J., and Hernandez, J. F. (2004). Solid-phase synthesis of arginine-containing peptides and fluorogenic substrates using a side-chain anchoring approach. *J. Org. Chem.* **69**, 8394-8402.

- Hansch, C., Leo, A., and Taft, R. W. (1991). A survey of Hammett substituent constants and resonance and field parameters. *Chem. Rev.* **91**, 165-195.
- Haugland, R. P., Naleway, J. J., and Zhang, Y.-Z. (1990) Lipophilic fluorescent glycosidase substrates. U.S. Patent 5,208,148.
- Haugland, R. P., Spence, M. T. Z., Johnson, I. D., and Basey, A. (2005). "The Handbook: A Guide to Fluorescent Probes and Labeling Technologies, 10th ed." Molecular Probes, Eugene, OR.
- Hemmilä, I. A. (1991). "Applications of Fluorescence in Immunoassays." Wiley, New York.
- Herschel, J. F. W. (1845). On a case of superficial colour presented by a homogeneous liquid internally colourless. *Phil. Trans. R. Soc. London* **135**, 143-145.
- Herzig, J., Nudelman, A., Gottlieb, H. E., and Fischer, B. (1986). Studies in sugar chemistry. 2. A simple method for O-deacylation of polyacylated sugars. *J. Org. Chem.* **51**, 727-730.
- Ho, D. G., Gao, R., Celaje, J., Chung, H.-Y., and Selke, M. (2003). Phosphadioxirane: A peroxide from an *ortho*-substituted arylphosphine and singlet dioxygen. *Science* **302**, 259-262.
- Ho, N. H., Weissleder, R., and Tung, C. H. (2007). A self-immolative reporter for β -galactosidase sensing. *ChemBioChem* **8**, 560-566.

- Hodawadekar, S. C., and Marmorstein, R. (2007). Chemistry of acetyl transfer by histone modifying enzymes: Structure, mechanism and implications for effector design. *Oncogene* **26**, 5528-5540.
- Hofmann, J., and Sernetz, M. (1983). A kinetic study on the enzymatic hydrolysis of fluoresceindiacetate and fluorescein-di- β -D-galactopyranoside. *Anal. Biochem.* **131**, 180-186.
- Hofmann, J., and Sernetz, M. (1984). Immobilized enzyme kinetics analyzed by flow-through microfluorimetry: Resorufin- β -galactopyranoside as a new fluorogenic substrate for β -galactosidase. *Anal. Chim. Acta* **163**, 67-72.
- Hoogeveen, A. T., Verheijen, F. W., and Galjaard, H. (1983). The relation between human lysosomal β -galactosidase and its protective protein. *J. Biol. Chem.* **258**, 12143-12146.
- Horecker, B. L., and Kornberg, A. (1948). The extinction coefficients of the reduced band of pyridine nucleotides. *J. Biol. Chem.* **175**, 385-390.
- Horgan, D. J., Dunstone, J. R., Stoops, J. K., Webb, E. C., and Zerner, B. (1969). Carboxylesterases (EC 3.1.1.). The molecular weight and equivalent weight of pig liver carboxylesterase. *Biochemistry* **8**, 2006-2013.
- Hornick, C. A., Thouron, C., Delamatre, J. G., and Huang, J. (1992). Triacylglycerol hydrolysis in isolated hepatic endosomes. *J. Biol. Chem.* **267**, 3396-3401.
- Huang, Z., Wang, Q. P., Ly, H. D., Gorvindarajan, A., Scheigetz, J., Zamboni, R., Desmarais, S., and Ramachandran, C. (1999). 3,4-Fluorescein diphosphate: A

sensitive fluorogenic and chromogenic substrate for protein tyrosine phosphatases. *J. Biomol. Screen.* **4**, 327-334.

Hudson, E. N., and Weber, G. (1973). Synthesis and characterization of two fluorescent sulfhydryl reagents. *Biochemistry* **12**, 4154-4161.

Hyatt, J. L., Stacy, V., Wadkins, R. M., Yoon, K. J. P., Wierdl, M., Edwards, C. C., Zeller, M., Hunter, A. D., Danks, M. K., Crundwell, G., and Potter, P. M. (2005). Inhibition of carboxylesterases by benzil (diphenylethane-1,2-dione) and heterocyclic analogues is dependent upon the aromaticity of the ring and the flexibility of the dione moiety. *J. Med. Chem.* **48**, 5543-5550.

Inglese, J., Johnson, R. L., Simeonov, A., Xia, M., Zheng, W., Austin, C. P., and Auld, D. S. (2007). High-throughput screening assays for the identification of chemical probes. *Nat. Chem. Biol.* **3**, 466-479.

Ioffe, I. S., and Otten, V. F. (1965a). Rhodamine dyes and related compounds. XII. Diacetyl derivatives of rhodamine and rhodol; structure of colorless forms of fluoran dyes. *Zh. Obshch. Khim.* **1**, 336-339.

Ioffe, I. S., and Otten, V. F. (1965b). Rhodamine dyes and related compounds. XIV. Mutual conversions of colorless and colored forms of rhodamine and rhodol. *Zh. Obshch. Khim.* **1**, 343-346.

Ishii, Y., and Lehrer, S. S. (1986). Effects of the state of succinimido-ring on the fluorescence and structural properties of pyrene maleimide-labeled alpha-alpha-tropomyosin. *Biophys. J.* **50**, 75-80.

- Jansen, A. B., and Russell, T. J. (1965). Some Novel Penicillin Derivatives. *J. Chem. Soc.* **65**, 2127-2132.
- Jayaraman, S., and Verkman, A. S. (2000). Quenching mechanism of quinolinium-type chloride-sensitive fluorescent indicators. *Biophys. Chem.* **85**, 49-57.
- Ji, T. H. (1983). Bifunctional reagents. *Methods Enzymol.* **91**, 580-609.
- Jiao, G. S., Han, J. W., and Burgess, K. (2003). Syntheses of regioisomerically pure 5- and 6-halogenated fluoresceins. *J. Org. Chem.* **68**, 8264-8267.
- Johnson, I. (1998). Fluorescent probes for living cells. *Histochem. J.* **30**, 123-140.
- Johnson, R. J., Chao, T. Y., Lavis, L. D., and Raines, R. T. (2007). Cytotoxic ribonucleases: The dichotomy of Coulombic forces. *Biochemistry* **46**, 10308-10316.
- Johnsson, N., and Johnsson, K. (2007). Chemical tools for biomolecular imaging. *ACS Chem. Biol.* **2**, 31-38.
- Juergens, D. H., Jacobson, R. H., Wigley, D., Zhang, X., Huber, R. E., Tronrud, D. E., and Matthews, B. W. (2000). High resolution refinement of β -galactosidase in a new crystal form reveals multiple metal-binding sites and provides a structural basis for α -complementation. *Protein Sci.* **9**, 1685-1699.
- Kalia, J., and Raines, R. T. (2006). Reactivity of intein thioesters: Appending a functional group to a protein. *ChemBioChem* **7**, 1375-1383.

- Kamal, A., Ramulu, P., Srinivas, O., Ramesh, G., and Kumar, P. P. (2004). Synthesis of C8-linked pyrrolo[2,1-*c*][1,4]benzodiazepine–benzimidazole conjugates with remarkable DNA-binding affinity. *Bioorg. Med. Chem. Lett.* **14**, 4791-4794.
- Kamiya, M., Kobayashi, H., Hama, Y., Koyama, Y., Bernardo, M., Nagano, T., Choyke, P. L., and Urano, Y. (2007). An enzymatically activated fluorescence probe for targeted tumor imaging. *J. Am. Chem. Soc.* **129**, 3918-3929.
- Kano, K., and Fendler, J. H. (1978). Pyranine as a sensitive pH probe for liposome interiors and surfaces. pH gradients across phospholipid vesicles. *Biochim. Biophys. Acta* **509**, 289-299.
- Karolin, J., Johansson, L. B. A., Strandberg, L., and Ny, T. (1994). Fluorescence and absorption spectroscopic properties of dipyrrometheneboron difluoride (BODIPY) derivatives in liquids, lipid membranes, and proteins. *J. Am. Chem. Soc.* **116**, 7801-7806.
- Karpovich, D. S., and Blanchard, G. J. (1995). Relating the polarity-dependent fluorescence response of pyrene to vibronic coupling. Achieving a fundamental understanding of the *py* polarity scale. *J. Phys. Chem.* **99**, 3951-3958.
- Karstens, T., and Kobs, K. (1980). Rhodamine B and rhodamine 101 as reference substances for fluorescence quantum yield measurements. *J. Phys. Chem.* **84**, 1871-1872.
- Kasai, K., Uchida, R., and Yamaji, N. (1993). Glycosides having chromophores as substrates for sensitive enzyme analysis. IV. Synthesis of N-acetyl- β -D-glucosaminides of fluorescein derivatives and their application to the rate-assay of N-acetyl- β -D-glucosaminidase. *Chem. Pharm. Bull.* **41**, 314-318.

- Kaufman, T. S., and Rúveda, E. A. (2005). The quest for quinine: Those who won the battles and those who won the war. *Angew. Chem., Int. Ed.* **44**, 854-885.
- Kikuchi, K., Komatsu, K., and Nagano, T. (2004). Zinc sensing for cellular application. *Curr. Opin. Chem. Biol.* **8**, 182-191.
- Kim, J. S., and Raines, R. T. (1995). Dibromobimane as a fluorescent crosslinking reagent. *Anal. Biochem.* **225**, 174-176.
- Kislinger, T., Cox, B., Kannan, A., Chung, C., Hu, P., Ignatchenko, A., Scott, M. S., Gramolini, A. O., Morris, Q., Hallett, M. T., Rossant, J., Hughes, T. R., Frey, B., and Emili, A. (2006). Global survey of organ and organelle protein expression in mouse: Combined proteomic and transcriptomic profiling. *Cell* **125**, 173-186.
- Kitson, T. M. (1996). Comparison of resorufin acetate and *p*-nitrophenyl acetate as substrates for chymotrypsin. *Bioorg. Chem.* **24**, 331-339.
- Klein, C., Batz, H.-G., and Herrmann, R. (1990) Resorufin derivatives. U.S. Patent 6,800,765.
- Klonis, N., Clayton, A. H. A., Voss, E. W., Jr., and Sawyer, W. H. (1998). Spectral properties of fluorescein in solvent-water mixtures: Applications as a probe of hydrogen bonding environments in biological systems. *Photochem. Photobiol.* **67**, 500-510.
- Klonis, N., and Sawyer, W. H. (1996). Spectral properties of the prototropic forms of fluorescein in aqueous solution. *J. Fluoresc.* **6**, 147-157.

- Kobayashi, T., Urano, Y., Kamiya, M., Ueno, T., Kojima, H., and Nagano, T. (2007). Highly activatable and rapidly releasable caged fluorescein derivatives. *J. Am. Chem. Soc.* **129**, 6696-6697.
- Kobe, B., and Deisenhofer, J. (1996). Mechanism of ribonuclease inhibition by ribonuclease inhibitor protein based on the crystal structure of its complex with ribonuclease A. *J. Mol. Biol.* **264**, 1028-1043.
- Koehn, M., and Breinbauer, R. (2004). The Staudinger ligation—a gift to chemical biology. *Angew. Chem., Int. Ed.* **43**, 3106-3116.
- Koenigs, W., and Knorr, E. (1901). Ueber einige Derivate des Traubenzuckers und der Galactose. *Ber. Dtsch. Chem. Ges.* **34**, 957-981.
- Kohl, C., Weil, T., Qu, J., and Müllen, K. (2004). Towards highly fluorescent and water-soluble perylene dyes. *Chem.—Eur. J.* **10**, 5297-5310.
- Koide, Y., Urano, Y., Kenmoku, S., Kojima, H., and Nagano, T. (2007). Design and synthesis of fluorescent probes for selective detection of highly reactive oxygen species in mitochondria of living cells. *J. Am. Chem. Soc.* **129**, 10324-10325.
- Kosower, N. S., Kosower, E. M., Newton, G. L., and Ranney, H. M. (1979). Bimane fluorescent labels: Labeling of normal human red cells under physiological conditions. *Proc. Natl. Acad. Sci. U.S.A.* **76**, 3382-3386.
- Kouzarides, T. (2000). Acetylation: A regulatory modification to rival phosphorylation? *EMBO J.* **19**, 1176-1179.

- Krafft, G. A., Sutton, W. R., and Cummings, R. T. (1988). Photoactivable fluorophores. 3. Synthesis and photoactivation of fluorogenic difunctionalized fluoresceins. *J. Am. Chem. Soc.* **110**, 301-303.
- Krol, M., Wrona, M., Page, C. S., and Bates, P. A. (2006). Macroscopic pK_a calculations for fluorescein and its derivatives. *J. Chem. Theory Comput.* **2**, 1520-1529.
- Kupcho, K., Hsiao, K., Bulleit, B., and Goueli, S. A. (2004). A homogeneous, nonradioactive high-throughput fluorogenic protein phosphatase assay. *J. Biomol. Screen.* **9**, 223-231.
- Kwart, H., and King, K. (1968). The reverse Diels–Alder or retrodiene reaction. *Chem. Rev.* **68**, 415-447.
- Labhardt, A. M., Ridge, J. A., Lindquist, R. N., and Baldwin, R. L. (1983). Measurement of the refolding combination reaction between S-peptide and S-protein. *Biochemistry* **22**, 321-327.
- Lakowicz, J. R. (1999). "Principles of Fluorescence Spectroscopy." Kluwer Academic/Plenum, New York.
- Lakowicz, J. R. (2006). "Principles of Fluorescence Spectroscopy." Springer, New York.
- Lampson, L. A., Lampson, M. A., and Dunne, A. D. (1993). Exploiting the *lacZ* reporter gene for quantitative analysis of disseminated tumor growth within the brain: Use of the *lacZ* gene product as a tumor antigen, for evaluation of antigenic modulation, and to facilitate image analysis of tumor growth in situ. *Cancer Res.* **53**, 176-182.

- Larsen, T. A., Goodsell, D. S., Cascio, D., Grzeskowiak, K., and Dickerson, R. E. (1989). The structure of DAPI bound to DNA. *J. Biomol. Struct. Dyn.* **7**, 477-491.
- Laurent, A., Debart, F., Lamb, N., and Rayner, B. (1997). Esterase-triggered fluorescence of fluorogenic oligonucleotides. *Bioconjugate Chem.* **8**, 856-861.
- Lavis, L. D., Chao, T.-Y., and Raines, R. T. (2006a). Fluorogenic label for biomolecular imaging. *ACS Chem. Biol.* **1**, 252-260.
- Lavis, L. D., Chao, T. Y., and Raines, R. T. (2006b). Latent blue and red fluorophores based on the trimethyl lock. *ChemBioChem* **7**, 1151-1154.
- Lavis, L. D., Rutkoski, T. J., and Raines, R. T. (2007). Tuning the pK_a of fluorescein to optimize binding assays. *Anal. Chem.* **79**, 6775-6782.
- Lee, B. W., Johnson, G. L., Hed, S. A., Darzynkiewicz, Z., Talhouk, J. W., and Mehrotra, S. (2003). DEVDase detection in intact apoptotic cells using the cell permeant fluorogenic substrate, (Z-DEVD)₂-cresyl violet. *BioTechniques* **35**, 1080-1085.
- Lee, F. S., Shapiro, R., and Vallee, B. L. (1989a). Tight-binding inhibition of angiogenin and ribonuclease A by placental ribonuclease inhibitor. *Biochemistry* **28**, 225-230.
- Lee, L. G., Berry, G. M., and Chen, C.-H. (1989b). Vita Blue: A new 633-nm excitable fluorescent dye for cell analysis. *Cytometry* **10**, 151-164.
- Lee, L. G., Spurgeon, S. L., Heiner, C. R., Benson, S. C., Rosenblum, B. B., Menchen, S. M., Graham, R. J., Constantinescu, A., Upadhyya, K. G., and Cassel, J. M. (1997). New energy transfer dyes for DNA sequencing. *Nucl. Acids Res.* **25**, 2816-2822.

- Lee, M. R., and Shin, I. (2005). Fabrication of chemical microarrays by efficient immobilization of hydrazide-linked substances on epoxide-coated glass surfaces. *Angew. Chem., Int. Ed.* **44**, 2881–2884.
- Leinweber, F.-J. (1987). Possible physiological roles of carboxylic ester hydrolases. *Drug Metab. Rev.* **18**, 379-439.
- Leland, P. A., and Raines, R. T. (2001). Cancer chemotherapy—ribonucleases to the rescue. *Chem. Biol* **8**, 405-413.
- Leroy, E., Bense, N., and Reymond, J.-L. (2003). A low background high-throughput screening (HTS) fluorescence assay for lipases and esterases using acyloxymethylethers of umbelliferone. *Bioorg. Med. Chem. Lett.* **13**, 2105-2108.
- Levi, J., Cheng, Z., Gheysens, O., Patel, M., Chan, C. T., Wang, Y., Namavari, M., and Gambhir, S. S. (2007). Fluorescent fructose derivatives for imaging breast cancer cells. *Bioconjugate Chem.* **18**, 628-634.
- Lewis, G. N., and Calvin, M. (1939). The color of organic substances. *Chem. Rev.* **25**, 273-328.
- Leytus, S. P., Melhado, L. L., and Mangel, W. F. (1983a). Rhodamine-based compounds as fluorogenic substrates for serine proteinases. *Biochem. J.* **209**, 299-307.
- Leytus, S. P., Patterson, W. L., and Mangel, W. F. (1983b). New class of sensitive and selective fluorogenic substrates for serine proteinases. Amino acid and dipeptide derivatives of rhodamine. *Biochem. J.* **215**, 253-260.

- Lim, M. H., and Lippard, S. J. (2007). Metal-based turn-on fluorescent probes for sensing nitric oxide. *Acc. Chem. Res.* **40**, 41-51.
- Lin, S., and Struve, W. S. (1991). Time-resolved fluorescence of nitrobenzoxadiazole aminohexanoic acid: Effect of intermolecular hydrogen-bonding on nonradiative decay. *Photochem. Photobiol.* **54**, 361-365.
- Lindqvist, L. (1960). A flash photolysis study of fluorescein. *Ark. Kemi* **16**, 79-138.
- Liu, J., Bhalgat, M., Zhang, C., Diwu, Z., Hoyland, B., and Klaubert, D. H. (1999). Fluorescent molecular probes V: A sensitive caspase-3 substrate for fluorometric assays. *Bioorg. Med. Chem. Lett.* **9**, 3231-3236.
- Liu, J., Diwu, Z., and Leung, W.-Y. (2001). Synthesis and photophysical properties of new fluorinated benzo[*c*]xanthene dyes as intracellular pH indicators. *Bioorg. Med. Chem. Lett.* **11**, 2903-2905.
- Liu, J. X., Diwu, Z. J., and Klaubert, D. H. (1997). Fluorescent molecular probes III. 2',7'-bis-(3-carboxypropyl)-5-(and-6)-carboxyfluorescein (BCPCF): A new polar dual-excitation and dual-emission pH indicator with a pK_a of 7.0. *Bioorg. Med. Chem. Lett.* **7**, 3069-3072.
- Liu, J. X., Diwu, Z. J., Leung, W. Y., Lu, Y. X., Patch, B., and Haugland, R. P. (2003). Rational design and synthesis of a novel class of highly fluorescent rhodamine dyes that have strong absorption at long wavelengths. *Tetrahedron Lett.* **44**, 4355-4359.

Liu, W., Jensen, T. J., Fronczek, F. R., Hammer, R. P., Smith, K. M., and Vicente, G. H. (2005). Synthesis and cellular studies of nonaggregated water-soluble phthalocyanines. *J. Med. Chem.* **48**, 1033-1041.

López Arbeloa, F., López Arbeloa, T., Tapia Estevez, M. J., and López Arbeloa, I. (1991). Photophysics of rhodamines: Molecular structure and solvent effects. *J. Phys. Chem.* **95**, 2203-2208.

López Arbeloa, F., Urrecha Aguirresacona, I., and López Arbeloa, I. (1989). Influence of the molecular structure and the nature of the solvent on the absorption and fluorescence characteristics of rhodamines. *Chem. Phys.* **130**, 371-378.

López Arbeloa, T., López Arbeloa, F., Hernández Bartolomé, P., and López Arbeloa, I. (1992). On the mechanism of radiationless deactivation of rhodamines. *Chem. Phys.* **160**, 123-130.

Lorey, S., Faust, J., Mrestani-Klaus, C., Kaehne, T., Ansorge, S., Neubert, K., and Buehling, F. (2002). Transcellular proteolysis demonstrated by novel cell surface-associated substrates of dipeptidyl peptidase IV (CD26). *J. Biol. Chem.* **277**, 33170-33177.

Lumbierres, M., Palomo, J. M., Kragol, G., Roehrs, S., Müller, O., and Waldmann, H. (2005). Solid-phase synthesis of lipidated peptides. *Chem.—Eur. J.* **11**, 7405-7415.

MacGregor, G. R., Nolan, G. P., Fiering, S., Roederer, M., and Herzenberg, L. A. (1991). Use of *E. coli lacZ* (β -galactosidase) as a reporter gene. *Methods Mol. Biol.* **7**, 217-235.

- Magde, D., Wong, R., and Seybold, P. G. (2002). Fluorescence quantum yields and their relation to lifetimes of rhodamine 6G and fluorescein in nine solvents: Improved absolute standards for quantum yields. *Photochem. Photobiol.* **75**, 327-334.
- Maggiore, L. L., Smith, C. W., and Zhang, Z. Y. (1992). A general method for the preparation of internally quenched fluorogenic protease substrates using solid-phase peptide synthesis. *J. Med. Chem.* **35**, 3727-3730.
- Mantovani, G., Lecolley, F., Tao, L., Haddleton, D. M., Clerx, J., Cornelissen, J. J. L. M., and Velonia, K. (2005). Design and synthesis of *N*-maleimido-functionalized hydrophilic polymers via copper-mediated living radical polymerization: A suitable alternative to PEGylation chemistry. *J. Am. Chem. Soc.* **127**, 2966-2973.
- Marks, P. A., and Breslow, R. (2007). Dimethyl sulfoxide to vorinostat: Development of this histone deacetylase inhibitor as an anticancer drug. *Nat. Biotechnol.* **25**, 84-90.
- Marmé, N., Knemeyer, J.-P., Wolfrum, J., and Sauer, M. (2004). Highly sensitive protease assay using fluorescence quenching of peptide probes based on photoinduced electron transfer. *Angew. Chem., Int. Ed.* **43**, 3798-3801.
- Martin, M. M., and Lindqvist, L. (1975). The pH dependence of fluorescein fluorescence. *J. Lumin.* **10**, 381.
- Martin, V. V., Rothe, A., Diwu, Z., and Gee, K. R. (2004). Fluorescent sodium ion indicators based on the 1,7-diaza-15-crown-5 system. *Bioorg. Med. Chem. Lett.* **14**, 5313-5316.

- Martin, V. V., Rothe, A., and Gee, K. R. (2005). Fluorescent metal ion indicators based on benzoannelated crown systems: A green fluorescent indicator for intracellular sodium ions. *Bioorg. Med. Chem. Lett.* **15**, 1851-1855.
- Maxfield, F. R., and McGraw, T. E. (2004). Endocytic recycling. *Nat. Rev. Mol. Cell Biol.* **5**, 121-132.
- McElhanon, J. R., and Wheeler, D. R. (2001). Thermally responsive dendrons and dendrimers based on reversible furan–maleimide Diels–Alder adducts. *Org. Lett.* **3**, 2681-2683.
- McElhanon, J. R., Zifer, T., Kline, S. R., Wheeler, D. R., Loy, D. A., Jamison, G. M., Long, T. M., Rahimian, K., and Simmons, B. A. (2005). Thermally cleavable surfactants based on furan–maleimide Diels–Alder adducts. *Langmuir* **21**, 3259-3266.
- McGlynn, S. P., Daigre, J., and Smith, F. J. (1963). External heavy-atom spin–orbital coupling effect. IV. Intersystem crossing. *J. Chem. Phys.* **39**, 675-679.
- Mchedlov-Petrosyan, N. O., Rubtsov, M. I., and Lukatskaya, L. L. (1992). Ionization and tautomerism of chloro-derivatives of fluorescein in water and aqueous acetone. *Dyes Pigm.* **18**, 179-198.
- Mchedlov-Petrosyan, N. O. (1979). Ionization constants of fluorescein. *Zh. Anal. Khim.* **34**, 1055-1059.
- McKinney, R. M., Spillane, J. T., and Pearce, G. W. (1962). Amino- and nitrofluorescein derivatives. *J. Org. Chem.* **27**, 3986-3988.

- McStay, C. M., and Gordon, P. E. (2007). Urine fluorescence in ethylene glycol poisoning. *New Engl. J. Med.* **356**, 611.
- Meunier, F., and Wilkinson, K. J. (2002). Nonperturbing fluorescent labeling of polysaccharides. *Biomacromolecules* **3**, 857-864.
- Mikulski, S. M., Costanzi, J. J., Vogelzang, N. J., McCachren, S., Taub, R. N., Chun, H., Mittelman, A., Panella, T., Puccio, C., and Fine, R. (2002). Phase II trial of a single weekly intravenous dose of ranpirnase in patients with unresectable malignant mesothelioma. *J. Clin. Oncol.* **20**, 274.
- Miller, E. W., Bian, S. X., and Chang, C. J. (2007). A fluorescent sensor for imaging reversible redox cycles in living cells. *J. Am. Chem. Soc.* **129**, 3458-3459.
- Milstein, S., and Cohen, L. A. (1972). Stereopopulation control. I. Rate enhancement in the lactonizations of *o*-hydroxyhydrocinnamic acids. *J. Am. Chem. Soc.* **94**, 9158-9165.
- Min, D. H., and Mrksich, M. (2004). Peptide arrays: Towards routine implementation. *Curr. Opin. Chem. Biol.* **8**, 554-558.
- Minta, A., Kao, J. P., and Tsien, R. Y. (1989). Fluorescent indicators for cytosolic calcium based on rhodamine and fluorescein chromophores. *J. Biol. Chem.* **264**, 8171-8178.
- Mislow, K. (1951). Optically active phenylmethylcarbinyl ethers. *J. Am. Chem. Soc.* **73**, 4043-4044.

- Mitchison, T. J., Sawin, K. E., Theriot, J. A., Gee, K., Mallavarapu, A., and Gerard, M. (1998). Caged fluorescent probes. *Methods Enzymol.* **291**, 63-78.
- Morita, T., Kato, H., Iwanaga, S., Takada, K., and Kimura, T. (1977). New fluorogenic substrates for alpha-thrombin, factor Xa, kallikreins, and urokinase. *J. Biochem. (Tokyo)* **82**, 1495-1498.
- Morreau, H., Galjart, N. J., Gillemans, N., Willemsen, R., van der Horst, G. T., and d'Azzo, A. (1989). Alternative splicing of β -galactosidase mRNA generates the classic lysosomal enzyme and a β -galactosidase-related protein. *J. Biol. Chem.* **264**, 20655-20663.
- Mozdziak, P. E., Pulvermacher, P. M., Schultz, E., and Schell, K. (2000). Hoechst fluorescence intensity can be used to separate viable bromodeoxyuridine-labeled cells from viable non-bromodeoxyuridine-labeled cells. *Cytometry* **41**, 89-95.
- Mujumdar, R. B., Ernst, L. A., Mujumdar, S. R., Lewis, C. J., and Waggoner, A. S. (1993). Cyanine dye labeling reagents: Sulfoindocyanine succinimidyl esters. *Bioconjugate Chem.* **4**, 105-111.
- Mujumdar, S. R., Mujumdar, R. B., Grant, C. M., and Waggoner, A. S. (1996). Cyanine-labeling reagents: Sulfobenzindocyanine succinimidyl esters. *Bioconjugate Chem.* **7**, 356-362.
- Nathans, J. (1987). Molecular biology of visual pigments. *Annu. Rev. Neurosci.* **10**, 163-194.

- Nedergaard, M., Desai, S., and Pulsinelli, W. (1990). Dicarboxy-dichlorofluorescein: A new fluorescent probe for measuring acidic intracellular pH. *Anal. Biochem.* **187**, 109.
- Nilsson, B. L., Kiessling, L. L., and Raines, R. T. (2000). Staudinger ligation: A peptide from a thioester and azide. *Org. Lett.* **2**, 1939-1941.
- Nolan, G. P., Fiering, S., Nicolas, J. F., and Herzenberg, L. A. (1988). Fluorescence-activated cell analysis and sorting of viable mammalian cells based on β -D-galactosidase activity after transduction of *Escherichia coli lacZ*. *Proc. Natl. Acad. Sci U.S.A.* **85**, 2603-2607.
- Novelli, A. (1932). Alkyl fluoresceins. *Anales Farm. Bioquim.* **3**, 112-120.
- Novelli, A. (1933). Antiseptics. Mercury salts of alkylfluoresceins. *Anales Farm. Bioquim.* **4**, 29-35.
- O'Brien, J., Wilson, I., Orton, T., and Pognan, F. (2000). Investigation of the Alamar Blue (resazurin) fluorescent dye for the assessment of mammalian cell cytotoxicity. *Eur. J. Biochem.* **267**, 5421-5426.
- Omelyanenko, V. G., Jiskoot, W., and Herron, J. N. (1993). Role of electrostatic interactions in the binding of fluorescein by antifluorescein antibody 4-4-20. *Biochemistry* **32**, 10423-10429.
- Ouannes, C., and Wilson, T. (1968). Quenching of singlet oxygen by tertiary aliphatic amines. Effect of DABCO. *J. Am. Chem. Soc* **90**, 6527-6528.

- Ouyang, H., Borchardt, R. T., and Siahaan, T. J. (2002). Steric hindrance is a key factor in the coupling reaction of (acyloxy) alkyl- α -halides with phenols to make a new promoiety for prodrugs. *Tetrahedron Lett.* **43**, 577-579.
- Owicki, J. C. (2000). Fluorescence polarization and anisotropy in high throughput screening: Perspectives and primer. *J. Biomol. Screen.* **5**, 297-306.
- Panchuk-Voloshina, N., Haugland, R. P., Bishop-Stewart, J., Bhalgat, M. K., Millard, P. J., Mao, F., Leung, W.-Y., and Haugland, R. P. (1999). Alexa Dyes, a series of new fluorescent dyes that yield exceptionally bright, photostable conjugates. *J. Histochem. Cytochem.* **47**, 1179-1188.
- Paradiso, A. M., Tsien, R. Y., and Machen, T. E. (1984). Na^+ - H^+ exchange in gastric glands as measured with a cytoplasmic-trapped, fluorescent pH indicator. *Proc. Natl. Acad. Sci. U.S.A.* **81**, 7436-7440.
- Parsa, T., Cunningham, S. J., Wall, S. P., Almo, S. C., and Crain, E. F. (2005). The usefulness of urine fluorescence for suspected antifreeze ingestion in children. *Am. J. Emerg. Med.* **23**, 787-792.
- Paulsen, H. (1982). Advances in selective chemical syntheses of complex oligosaccharides. *Angew. Chem. Int. Ed. Engl.* **21**, 155-173.
- Peng, X., Draney, D. R., Volcheck, W. M., Bashford, G. R., Lamb, D. T., Grone, D. L., Zhang, Y., and Johnson, C. M. (2006). Phthalocyanine dye as an extremely photostable and highly fluorescent near-infrared labeling reagent. *Proc. SPIE-Int. Soc. Opt. Eng.* **6097E**, 1-12.

- Petit, J.-M., Denis-Gay, M., and Ratinaud, M.-H. (1993). Assessment of fluorochromes for cellular structure and function studies by flow cytometry. *Biol. Cell* **78**, 1-13.
- Piekarz, R. L., Sackett, D. L., and Bates, S. E. (2007). Histone deacetylase inhibitors and demethylating agents: Clinical development of histone deacetylase inhibitors for cancer therapy. *Cancer J.* **13**, 30-39.
- Plasek, J., and Sigler, K. (1996). Slow fluorescent indicators of membrane potential: A survey of different approaches to probe response analysis. *J. Photochem. Photobiol., B* **33**, 101-124.
- Pontrello, J. K., Allen, M. J., Underbakke, E. S., and Kiessling, L. L. (2005). Solid-phase synthesis of polymers using the ring-opening metathesis polymerization. *J. Am. Chem. Soc.* **127**, 14536-14537.
- Poot, M., and Arttamangkul, S. (1997). Verapamil inhibition of enzymatic product efflux leads to improved detection of β -galactosidase activity in *lacZ*-transfected cells. *Cytometry* **28**, 36-41.
- Raines, R. T. (1998). Ribonuclease A. *Chem. Rev.* **98**, 1045-1065.
- Rakhmanova, V. A., and MacDonald, R. C. (1998). A microplate fluorimetric assay for transfection of the β -galactosidase reporter gene. *Anal. Biochem.* **257**, 234-237.
- Roehrl, M. H., Wang, J. Y., and Wagner, G. (2004). A general framework for development and data analysis of competitive high-throughput screens for small-molecule inhibitors of protein-protein interactions by fluorescence polarization. *Biochemistry* **43**, 16056-16066.

- Rondelez, Y., Tresset, G., Tabata, K. V., Arata, H., Fujita, H., Takeuchi, S., and Noji, H. (2005). Microfabricated arrays of femtoliter chambers allow single molecule enzymology. *Nat. Biotech.* **23**, 361-365.
- Rotman, B., and Papermaster, B. W. (1966). Membrane properties of living mammalian cells as studied by enzymatic hydrolysis of fluorogenic esters. *Proc. Natl. Acad. Sci U.S.A.* **55**, 134-141.
- Rotman, B., Zderic, J. A., and Edelstein, M. (1963). Fluorogenic substrates for β -D-galactosidases and phosphatases derived from fluorescein (3,6-dihydroxyfluoran) and its monomethylether. *Proc. Natl. Acad. Sci U.S.A.* **50**, 1-6.
- Runquist, E. A., and Havel, R. J. (1991). Acid hydrolases in early and late endosome fractions from rat liver. *J. Biol. Chem.* **266**, 22557-22563.
- Rutkoski, T. J., Kurten, E. L., Mitchell, J. C., and Raines, R. T. (2005). Disruption of shape-complementarity markers to create cytotoxic variants of ribonuclease A. *J. Mol. Biol.*
- Sadaghiani, A. M., Verhelst, S. H. L., and Boggyo, M. (2007). Tagging and detection strategies for activity-based proteomics. *Curr. Opin. Chem. Biol.* **11**, 20-28.
- Sahoo, D., Narayanaswami, V., Kay, C. M., and Ryan, R. O. (2000). Pyrene excimer fluorescence: A spatially sensitive probe to monitor lipid-induced helical rearrangement of apolipoprotein III. *Biochemistry* **39**, 6594-6601.
- Salisbury, C. M., Maly, D. J., and Ellman, J. A. (2002). Peptide microarrays for the determination of protease substrate specificity. *J. Am. Chem. Soc.* **124**, 14868-14870.

- Sapsford, K. E., Berti, L., and Medintz, I. L. (2006). Materials for fluorescence resonance energy transfer analysis: Beyond traditional donor–acceptor combinations. *Angew. Chem., Int. Ed.* **45**, 4562-4588.
- Sarpara, G. H., Hu, S. J., Palmer, D. A., French, M. T., Evans, M., and Miller, J. N. (1999). A new long-wavelength fluorogenic substrate for alkaline phosphatase: Synthesis and characterisation. *Anal. Commun.* **36**, 19-20.
- Saxon, E., Luchansky, S. J., Hang, H. C., Yu, C., Lee, S. C., and Bertozzi, C. R. (2002). Investigating cellular metabolism of synthetic azidosugars with the Staudinger ligation. *J. Am. Chem. Soc.* **124**, 14893-14902.
- Schobel, U., Egelhaaf, H. J., Brecht, A., Oelkrug, D., and Gauglitz, G. (1999). New donor-acceptor pair for fluorescent immunoassays by energy transfer. *Bioconjugate Chem.* **10**, 1107-1114.
- Schroder, C. R., Weidgans, B. M., and Klimant, I. (2005). pH Fluorosensors for use in marine systems. *Analyst* **130**, 907-916.
- Schulman, S. G., Threatte, R. M., Capomacchia, A. C., and Paul, W. L. (1974). Fluorescence of 6-methoxyquinoline, quinine, and quinidine in aqueous media. *J. Pharm. Sci.* **63**, 876-880.
- Schultz, C., Vajanaphanich, M., Harootunian, A. T., Sammak, P. J., Barrett, K. E., and Tsien, R. Y. (1993). Acetoxymethyl esters of phosphates, enhancement of the permeability and potency of cAMP. *J. Biol. Chem.* **268**, 6316-6322.
- Scriven, E. F. V., and Turnbull, K. (1988). Azides: Their preparation and synthetic uses. *Chem. Rev.* **88**, 297-368.

- Sease, J. W., and Zechmeister, L. (1947). Chromatographic and spectral characteristics of some polythienyls. *J. Am. Chem. Soc.* **69**, 270-273.
- Seeman, J. I. (2007). The Woodward–Doering/Rabe–Kindler total synthesis of quinine: Setting the record straight. *Angew. Chem., Int. Ed.* **46**, 1378-1413.
- Shaginian, A., Patel, M., Li, M. H., Flickinger, S. T., Kim, C., Cerrina, F., and Belshaw, P. J. (2004). Light-directed radial combinatorial chemistry: Orthogonal safety-catch protecting groups for the synthesis of small molecule microarrays. *J. Am. Chem. Soc.* **126**, 16704-16705.
- Shan, D., Nicolaou, M. G., Borchardt, R. T., and Wang, B. (1997). Prodrug strategies based on intramolecular cyclization reactions. *J. Pharm. Sci.* **86**, 765-767.
- Sharma, A. N., O'Shaughnessy, P. M., Hoffman, R. S., Casavant, M. J., Shah, M. N., and Battels, R. (2002). Urine fluorescence: Is it a good test for ethylene glycol ingestion? *Pediatrics* **109**, 345.
- Shults, M. D., Carrico-Moniz, D., and Imperiali, B. (2006). Optimal Sox-based fluorescent chemosensor design for serine/threonine protein kinases. *Anal. Biochem.* **352**, 198-207.
- Shynkar, V. V., Klymchenko, A. S., Kunzelmann, C., Duportail, G., Muller, C. D., Demchenko, A. P., Freyssinet, J. M., and Mely, Y. (2007). Fluorescent biomembrane probe for ratiometric detection of apoptosis. *J. Am. Chem. Soc.* **129**, 2187-2193.
- Silhavy, T. J., and Beckwith, J. R. (1985). Uses of *lac* fusions for the study of biological problems. *Microbiol. Rev.* **49**, 398-418.

- Singh-Gasson, S., Green, R. D., Yue, Y., Nelson, C., Blattner, F., Sussman, M. R., and Cerrina, F. (1999). Maskless fabrication of light-directed oligonucleotide microarrays using a digital micromirror array. *Nat. Biotech.* **17**, 974-978.
- Sjoberg, R., Nygren, J., and Kubista, M. (1995). Absorption and fluorescence properties of fluorescein. *Spectrochim. Acta, Part A* **51**, L7-L21.
- Smalley, M. K., and Silverman, S. K. (2006). Fluorescence of covalently attached pyrene as a general RNA folding probe. *Nucleic Acids Res.* **34**, 152-166.
- Smith, B. C., and Denu, J. M. (2007). Acetyl-lysine analog peptides as mechanistic probes of protein deacetylases. *J. Biol. Chem.* **282**, 37256-37265.
- Smith, B. D., Soellner, M. B., and Raines, R. T. (2003). Potent inhibition of ribonuclease A by oligo(vinylsulfonic acid). *J. Biol. Chem.* **278**, 20934-20938.
- Smith, J. C. (1990). Potential-sensitive molecular probes in membranes of bioenergetic relevance. *Biochim. Biophys. Acta* **1016**, 1-28.
- Smith, S. A., and Pretorius, W. A. (2002). Spectrophotometric determination of pK_a values for fluorescein using activity coefficient corrections. *Water SA* **28**, 395-402.
- Soellner, M. B., Dickson, K. A., Nilsson, B. L., and Raines, R. T. (2003). Site-specific protein immobilization by Staudinger ligation. *J. Am. Chem. Soc.* **125**, 11790-11791.
- Soellner, M. B., Tam, A., and Raines, R. T. (2006). Staudinger ligation of peptides at non-glycyl residues. *J. Org. Chem.* **71**, 9824-9830.

- Song, F., Garner, A. L., and Koide, K. (2007). A highly sensitive fluorescent sensor for palladium based on the allylic oxidative insertion mechanism. *J. Am. Chem. Soc.* **129**, 12354-12355.
- Sparano, B. A., Shahi, S. P., and Koide, K. (2004). Effect of binding and conformation on fluorescence quenching in new 2',7'-dichlorofluorescein derivatives. *Org. Lett.* **6**, 1947-1949, and references therein.
- Stanton, S. G., Kantor, A. B., Petrossian, A., and Owicki, J. C. (1984). Location and dynamics of a membrane-bound fluorescent hapten: A spectroscopic study. *Biochim. Biophys. Acta* **776**, 228-236.
- Steinbach, G. (1974). Characterization of fluorescein isothiocyanate. Synthesis and testing methods for fluorescein isothiocyanate isomers. *Acta Histochem.* **50**, 19-34.
- Stewart, W. W. (1981). Synthesis of 3,6-disulfonated 4-aminonaphthalimides. *J. Am. Chem. Soc.* **103**, 7615-7620.
- Stokes, G. G. (1852). On the change of refrangibility of light. *Phil. Trans. R. Soc. London* **142**, 463-562.
- Stracke, F., Heupel, M., and Thiel, E. (1999). Singlet molecular oxygen photosensitized by rhodamine dyes: Correlation with photophysical properties of the sensitizers. *J. Photochem. Photobiol., A* **126**, 51-58.
- Streu, C., and Meggers, E. (2006). Ruthenium-induced allylcarbamate cleavage in living cells. *Angew. Chem., Int. Ed.* **45**, 5645-5648.

- Sun, W.-C., Gee, K. R., and Haugland, R. P. (1998). Synthesis of novel fluorinated coumarins: Excellent UV-light excitable fluorescent dyes. *Bioorg. Med. Chem. Lett.* **8**, 3107-3110.
- Sun, W.-C., Gee, K. R., Klaubert, D. H., and Haugland, R. P. (1997). Synthesis of fluorinated fluoresceins. *J. Org. Chem.* **62**, 6469-6475.
- Sun, X. L., Stabler, C. L., Cazalis, C. S., and Chaikof, E. L. (2006). Carbohydrate and protein immobilization onto solid surfaces by sequential Diels–Alder and azide–alkyne cycloadditions. *Bioconjugate Chem.* **17**, 52-57.
- Süßmeier, F., and Langhals, H. (2001). Novel fluorescence labels: The synthesis of perylene-3,4,9-tricarboxylic imides. *Eur. J. Org. Chem.* **2001**, 607-610.
- Svoboda, K., and Yasuda, R. (2006). Principles of two-photon excitation microscopy and its applications to neuroscience. *Neuron* **50**, 823-839.
- Szalai, M. L., McGrath, D. V., Wheeler, D. R., Zifer, T., and McElhanon, J. R. (2007). Dendrimers based on thermally reversible furan–maleimide Diels–Alder adducts. *Macromolecules* **40**, 818-823.
- Tam, A., Soellner, M. B., and Raines, R. T. (2007). Water-soluble phosphinothiols for traceless Staudinger ligation and integration with expressed protein ligation. *J. Am. Chem. Soc.* **129**, 11421-11430.
- Teale, F. W., and Weber, G. (1957). Ultraviolet fluorescence of the aromatic amino acids. *Biochem. J.* **65**, 476-482.

- Testa, B., and Mayer, J. M. (2003). "Hydrolysis in Drug and Prodrug Metabolism: Chemistry, Biochemistry, and Enzymology." Verlag Helvetica Chimica Acta, Zürich, Switzerland.
- Thelen, M., Petrone, G., Oshea, P. S., and Azzi, A. (1984). The use of fluorescein-dipalmitoylphosphatidylethanolamine for measuring pH-changes in the internal compartment of phospholipid vesicles. *Biochim. Biophys. Acta* **766**, 161-168.
- Thomas, J. A., Buchsbaum, R. N., Zimniak, A., and Racker, E. (1979). Intracellular pH measurements in Ehrlich ascites tumor cells utilizing spectroscopic probes generated in situ. *Biochemistry* **18**, 2210-2218.
- Thomas, J. D., and Sloan, K. B. (2007). Overcoming steric effects in the coupling reaction of alkyloxycarbonyloxymethyl (AOCOM) halides with phenols: An efficient synthesis of AOCOM phenolic prodrugs. *Tetrahedron Lett.* **48**, 109-112.
- Thompson, V. F., Saldaña, S., Cong, J., and Goll, D. E. (2000). A BODIPY fluorescent microplate assay for measuring activity of calpains and other proteases. *Anal. Biochem.* **279**, 170-178.
- Tsien, R. Y. (1980). New calcium indicators and buffers with high selectivity against magnesium and protons: Design, synthesis, and properties of prototype structures. *Biochemistry* **19**, 2396-2404.
- Tsien, R. Y. (1981). A non-disruptive technique for loading calcium buffers and indicators into cells. *Nature* **290**, 527-528.
- Tyagi, S., and Kramer, F. R. (1996). Molecular beacons: Probes that fluoresce upon hybridization. *Nat. Biotechnol.* **14**, 303-308.

- Udenfriend, S. (1995). Development of the spectrophotofluorometer and its commercialization. *Protein Sci.* **4**, 542-551.
- Ui, N. (1971). Isoelectric points and conformation of proteins. I. Effect of urea on the behavior of some proteins in isoelectric focusing. *Biochim. Biophys. Acta* **229**, 567-581.
- Urano, Y., Kamiya, M., Kanda, K., Ueno, T., Hirose, K., and Nagano, T. (2005). Evolution of fluorescein as a platform for finely tunable fluorescence probes. *J. Am. Chem. Soc.* **127**, 4888-4894.
- Valeur, B. (2002). "Molecular Fluorescence: Principles and Applications." Wiley-VCH, Weinheim.
- Van Noorden, C. J., Boonacker, E., Bissell, E. R., Meijer, A. J., van Marle, J., and Smith, R. E. (1997). Ala-Pro-cresyl violet, a synthetic fluorogenic substrate for the analysis of kinetic parameters of dipeptidyl peptidase IV (CD26) in individual living rat hepatocytes. *Anal. Biochem.* **252**, 71-77.
- Verschueren, W. G., Dierynck, I., Amssoms, K. I., Hu, L., Boonants, P. M., Pille, G. M., Daeyaert, F. F., Hertogs, K., Surleraux, D. L., and Wigerinck, P. B. (2005). Design and optimization of tricyclic phthalimide analogues as novel inhibitors of HIV-1 integrase. *J. Med. Chem* **48**, 1930-1940.
- Vogel, M., Rettig, W., Sens, R., and Drexhage, K. H. (1988). Structural relaxation of rhodamine dyes with different N-substitution patterns—A study of fluorescence decay times and quantum yields. *Chem. Phys. Lett.* **147**, 452-460.

- Waggoner, A. (2006). Fluorescent labels for proteomics and genomics. *Curr. Opin. Chem. Biol.* **10**, 62-66.
- Waggoner, A., and Kenneth, S. (1995). Covalent labeling of proteins and nucleic acids with fluorophores. *Methods Enzymol.* **246**, 362-373.
- Wainwright, M. (2003). The use of dyes in modern biomedicine. *Biotech. Histochem.* **78**, 147-155.
- Wang, Z.-Q., Liao, J., and Diwu, Z. (2005). N-DEVD-N'-morpholinecarbonyl-rhodamine 110: Novel caspase-3 fluorogenic substrates for cell-based apoptosis assay. *Bioorg. Med. Chem. Lett.* **15**, 2335-2338.
- Wang, Z.-X. (1995). An exact mathematical expression for describing competitive binding of two different ligands to a protein molecule. *FEBS Lett.* **360**, 111-114.
- Watson, P., Jones, A. T., and Stephens, D. J. (2005). Intracellular trafficking pathways and drug delivery: Fluorescence imaging of living and fixed cells. *Adv. Drug Deliv. Rev.* **57**, 1024-1032.
- Weber, G. (1952). Polarization of the fluorescence of macromolecules II. Fluorescent conjugates of ovalbumin and bovine serum albumin. *Biochem. J.* **51**, 155-167.
- Weber, G. (1957). Intramolecular transfer of electronic energy in dihydrodiphosphopyridine nucleotide. *Nature* **180**, 1409.
- Weber, G., and Farris, F. J. (1979). Synthesis and spectral properties of a hydrophobic fluorescent probe: 6-Propionyl-2-(dimethylamino)naphthalene. *Biochemistry* **18**, 3075-3078.

- Wegener, D., Wirsching, F., Riester, D., and Schwienhorst, A. (2003). A fluorogenic histone deacetylase assay well suited for high-throughput activity screening. *Chem. Biol.* **10**, 61-68.
- Whitaker, J. E., Haugland, R. P., Moore, P. L., Hewitt, P. C., Reese, M., and Haugland, R. P. (1991a). Cascade blue derivatives: Water soluble, reactive, blue emission dyes evaluated as fluorescent labels and tracers. *Anal. Biochem.* **198**, 119-130.
- Whitaker, J. E., Haugland, R. P., and Prendergast, F. G. (1991b). Spectral and photophysical studies of benzo[c]xanthene dyes: Dual emission pH sensors. *Anal. Biochem.* **194**, 330-344.
- Whitaker, J. E., Haugland, R. P., Ryan, D., Hewitt, P. C., Haugland, R. P., and Prendergast, F. G. (1992). Fluorescent rhodol derivatives: Versatile, photostable labels and tracers. *Anal. Biochem.* **207**, 267-279.
- Whitby, L. G. (1953). A new method for preparing flavin-adenine dinucleotide. *Biochem. J.* **54**, 437-442.
- Wolfbeis, O. S. (1985). The fluorescence of organic natural products. In "Molecular Luminescence Spectroscopy: Methods and Applications—Part 1" (S. G. Schulman, Ed.), Vol. Part 1, pp. 167-317. Wiley, New York.
- Wu, M. M., Llopis, J., Adams, S., McCaffery, J. M., Kulomaa, M. S., Machen, T. E., Moore, H. P., and Tsien, R. Y. (2000). Organelle pH studies using targeted avidin and fluorescein-biotin. *Chem. Biol.* **7**, 197-209.

- Xu, K., Tang, B., Huang, H., Yang, G., Chen, Z., Li, P., and An, L. (2005). Strong red fluorescent probes suitable for detecting hydrogen peroxide generated by mice peritoneal macrophages. *Chem. Commun.*, 5974-5976.
- Yamaguchi, S., and Sasaki, Y. (2001). Spectroscopic determination of very low quantum yield of singlet oxygen formation photosensitized by industrial dyes. *J. Photochem. Photobiol., A* **142**, 47-50.
- Yamazaki, H., Inoue, K., Mimura, M., Oda, Y., Guengerich, F. P., and Shimada, T. (1996). 7-Ethoxycoumarin *O*-deethylation catalyzed by cytochromes P450 1A2 and 2E1 in human liver microsomes. *Biochem. Pharmacol.* **51**, 313.
- Yang, X.-F., Ye, S.-J., Bai, Q., and Wang, X.-Q. (2007). A fluorescein-based fluorogenic probe for fluoride ion based on the fluoride-induced cleavage of *tert*-butyldimethylsilyl ether. *J. Fluoresc.* **17**, 81-87.
- Yang, Y. Z., Babiak, P., and Reymond, J. L. (2006). New monofunctionalized fluorescein derivatives for the efficient high-throughput screening of lipases and esterases in aqueous media. *Helv. Chim. Acta* **89**, 404-415.
- Yasui, S., Tsujimoto, M., Itoh, K., and Ohno, A. (2000). Quenching of a photosensitized dye through single-electron transfer from trivalent phosphorus compounds. *J. Org. Chem* **65**, 4715-4720.
- Yeh, R.-H., Yan, X., Cammer, M., Bresnick, A. R., and Lawrence, D. S. (2002). Real time visualization of protein kinase activity in living cells. *J. Biol. Chem.* **277**, 11527-11532.

- Yoon, S., Miller, E. W., He, Q., Do, P. H., and Chang, C. J. (2007). A bright and specific fluorescent sensor for mercury in water, cells, and tissue. *Angew. Chem., Int. Ed.* **46**, 6658-6661.
- Yoshitake, S., Yamada, Y., Ishikawa, E., and Masseyeff, R. (1979). Conjugation of glucose-oxidase from *Aspergillus niger* and rabbit antibodies using N-hydroxysuccinimide ester of N-(4-carboxycyclohexylmethyl)-maleimide. *Eur. J. Biochem.* **101**, 395-399.
- Young, R. H., and Martin, R. L. (1972). On the mechanism of quenching of singlet oxygen by amines. *J. Am. Chem. Soc.* **94**, 5183-5185.
- Zaikova, T. O., Rukavishnikov, A. V., Birrell, G. B., Griffith, O. H., and Keana, J. F. W. (2001). Synthesis of fluorogenic substrates for continuous assay of phosphatidylinositol-specific phospholipase C. *Bioconjugate Chem.* **12**, 307-313.
- Zanker, V., and Peter, W. (1958). Die prototropen Formen des Fluoresceins. *Ber. Dtsch. Chem. Ges.* **91**, 572-580.
- Zelent, B., Kusba, J., Gryczynski, I., Johnson, M. L., and Lakowicz, J. R. (1998). Time-resolved and steady-state fluorescence quenching of *N*-acetyl-tryptophanamide by acrylamide and iodide. *Biophys. Chem.* **73**, 53.
- Zhang, H.-Z., Cai, S. X., Drewe, J. A., and Yang, W. (2000) Novel fluorescence dyes and their applications for whole cell fluorescence screening assays for caspases, peptidases, proteases and other enzymes and the use thereof. WO Patent Application 2000004914.

- Zhang, H. Z., Kasibhatla, S., Guastella, J., Tseng, B., Drewe, J., and Cai, S. X. (2003). N-Ac-DEVD-N'-(polyfluorobenzoyl)-R110: Novel cell-permeable fluorogenic caspase substrates for the detection of caspase activity and apoptosis. *Bioconjugate Chem.* **14**, 458-463.
- Zhang, J., Campbell, R. E., Ting, A. Y., and Tsien, R. Y. (2002). Creating new fluorescent probes for cell biology. *Nat. Rev. Mol. Cell Biol.* **3**, 906-918.
- Zhang, J. H., Chung, T. D., and Oldenburg, K. R. (1999). A simple statistical parameter for use in evaluation and validation of high-throughput screening assays. *J. Biomol. Screen.* **4**, 67-73.
- Zhang, Y. Z., Naleway, J. J., Larison, K. D., Huang, Z. J., and Haugland, R. P. (1991). Detecting *lacZ* gene expression in living cells with new lipophilic, fluorogenic β -galactosidase substrates. *FASEB J.* **5**, 3108-3113.
- Zhou, M., Diwu, Z., Panchuk-Voloshina, N., and Haugland, R. P. (1997). A stable nonfluorescent derivative of resorufin for the fluorometric determination of trace hydrogen peroxide: Applications in detecting the activity of phagocyte NADPH oxidase and other oxidases. *Anal. Biochem.* **253**, 162-168.
- Zimmerman, M., Ashe, B., Yurewicz, E. C., and Patel, G. (1977). Sensitive assays for trypsin, elastase, and chymotrypsin using new fluorogenic substrates. *Anal. Biochem.* **78**, 47.
- Zimmerman, M., Yurewicz, E., and Patel, G. (1976). A new fluorogenic substrate for chymotrypsin. *Anal. Biochem.* **70**, 258-262.

Zlokarnik, G., Negulescu, P. A., Knapp, T. E., Mere, L., Burres, N., Feng, L., Whitney, M., Roemer, K., and Tsien, R. Y. (1998). Quantitation of transcription and clonal selection of single living cells with β -lactamase as reporter. *Science* **279**, 84-88.